5-2023

# Supraspinal reorganization after pediatric-onset spinal cord injury.

Luis R. Alvarado
*University of Louisville*

# SUPRASPINAL REORGANIZATION AFTER PEDIATRIC-ONSET SPINAL CORD INJURY

By

Luis R. Alvarado
B.S., University of California, Los Angeles, 2005
M.S., University of Louisville, 2017

A Dissertation
Submitted to the Faculty of the
School of Medicine of the University of Louisville
In Partial Fulfillment of the Requirements
for the Degree of

Doctor of Philosophy
in
Anatomical Sciences and Neurobiology

Department of Anatomical Sciences and Neurobiology
University of Louisville
Louisville, Kentucky

May 2023

# SUPRASPINAL REORGANIZATION AFTER PEDIATRIC-ONSET SPINAL CORD INJURY

By

Luis R. Alvarado
B.S., University of California, Los Angeles, 205
M.S., University of Louisville, 2017

A Dissertation Approved on

March 2nd, 2023

By the following Dissertation Committee:

_____
Andrea Behrman, Ph.D., PT
Dissertation Director

_____
Brendan E. Depue, Ph.D.

_____
Charles H. Hubscher, Ph.D.

_____
Maxwell Boakye, MD, MPH

_____
Doug Lorenz, Ph.D.

# DEDICATION

To my beloved wife and daughter,

You are a constant source of love and inspiration. Your love has brought so much joy into my life and made this journey all the more meaningful.

To my incredible wife, Dr. Alicia Fernandez, as I embark on the final stage toward completing this Ph.D., I cannot help but reflect on the love and support you have provided throughout this process. You have been my rock, confidant, and inspiration. Your unwavering belief in me has given me the courage to tackle this project and bring it to fruition. I am in awe of your selflessness, dedication, and the sacrifices you have made to ensure my success. I cannot fathom going through this experience without you. You have listened to me talk about my research highs and vent about the lows, always offering encouragement and fresh perspectives. You have sacrificed so much of your time and energy to ensure we complete this chapter of our lives. I am eternally grateful for your unwavering love and support. You have been my ***teammate*** in every sense of the word. You are my heart and soul, and I am blessed to have you by my side. I cannot wait to celebrate this achievement with you, my love.

To our precious daughter, Victoria, I am filled with pride and joy, knowing that someday you will comprehend the hard work and dedication invested in these pages. While you may not yet grasp the full extent of what I have done, I hope this

dissertation will serve as a testament to my love for you and the lengths I will go to ensure your future success and happiness. From the moment you entered this world, you filled our lives with laughter and love. Watching you grow and thrive has been the universe's most extraordinary gift, and I am so proud of your inquisitive brain, determined spirit, and adventurous nature. I aim to set the best example for you as you grow and pursue your own passions and dreams. Embodying intelligence, perseverance, kindness, strength, and beauty, you are truly extraordinary. Te amo mucho, mi ***persy!***

This dissertation is dedicated to you both. I love you more than words can express.

A mis madres y ñaño,

Estoy agradecido por el amor y la guía que me han brindado a lo largo de mi vida. Cada uno de ustedes ha desempeñado un papel único en formar la persona que soy hoy, y estoy eternamente agradecido por su apoyo y aliento.

A mi madre, Margarita Salvatierra, este logro académico es en buena parte gracias a tu amor y apoyo incondicional a lo largo de mi vida. Desde pequeño, me has enseñado el valor del esfuerzo y la dedicación. Tu sacrificio y dedicación son extraordinarios y una de las razones por la cual hoy puedo celebrar este logro.

A mi segunda madre, Emmita Salvatierra, gracias por despertar en mí el deseo de aprender y por ser mi segunda madre. Gracias a ti, he aprendido a amar la ciencia y descubrí mi pasión por la biología. Como mi profesora en el colegio, me enseñaste no solo los conceptos científicos, sino también el valor del trabajo duro y la dedicación. Eres una docente talentosa y abnegada. Tu amor por la ciencia es contagioso y me has motivado a seguir adelante en mi camino en ella.

A mi abuelita, Otilia Marmolejo, aunque ya no estás con nosotros, tu amor e influencia todavía me guían. Fuiste una verdadera madre para mí. Fuiste una fuente constante de sabiduría y consejos. Tu presencia en mi vida fue un regalo inestimable y siempre tendrás una parte importante de mi corazón. Te extraño.

A mi ñaño, Joshue Sandoval, me enorgullece tanto ver en el hombre en que te has convertido. Eres un padre maravilloso para Sebastián y un esposo amoroso y fiel para Kerly. Como hermano, has sido un apoyo incondicional en los momentos difíciles y has celebrado conmigo en los momentos de alegría. Tu amor y apoyo han sido clave en mi camino.

# ACKNOWLEDGMENTS

First and foremost, I would like to express my profound gratitude to my advisor, Dr. Andrea Behrman, for her guidance throughout this journey, as well as her invaluable support and direction. Dr. Behrman's passion for neurorehabilitation and commitment to her patients are truly inspiring. Her knowledge and experience have significantly influenced my research and fostered my growth as a scientist. In addition to her exceptional academic guidance, I am deeply touched by Dr. Behrman's genuine care for me as an individual beyond the scholarly realm. Her attentiveness to my overall well-being and proactive approach in helping me overcome obstacles on the path to completing my Ph.D. reflect her extraordinary empathy and compassion. She provided an unparalleled graduate experience, surpassing all my expectations for an advisor through her constant encouragement and patience. Completing this Ph.D. would not have been possible without her guidance and expertise. Dr. Behrman's professionalism, kindness, and generosity will continue to inspire me as I mentor future students.

I would also like to extend my gratitude to Dr. Brendan Depue, who played a crucial role in my training as a neuroscientist. Dr. Depue's expertise in neuroimaging and his passion for teaching were indispensable in completing this project. His patient and supportive approach to teaching helped me develop my

skills and understand the complexities of neuroimaging. I am so grateful to have had the opportunity to learn from him.

To each of the members of my committee, Dr. Boakye, Dr. Hubscher, and Dr. Lorenz, I am immensely grateful for your unwavering kindness and professionalism. Your generosity with your time and expertise has profoundly impacted this work and shaped my training in immeasurable ways. Your feedback and guidance have been priceless, and I will carry your example of excellence with me as I move forward in my career. I am deeply thankful for the lessons I have learned from each of you.

I am deeply grateful to the research subjects who participated in this study. Your willingness to generously share your time, experiences, and perspectives has been nothing short of remarkable. Your bravery, strength, and resilience in the face of challenges are inspiring, and I am grateful to have had the opportunity to work with you. Your contributions will have a lasting impact on the field, and I am deeply thankful for your trust. I would also like to acknowledge the sacrifices and dedication of the families and caregivers who have provided support and care for the participants. Your unwavering love and commitment to improving the lives of those you care for are truly inspiring.

To the current and former staff, technicians, and physical therapists who have been a part of the Pediatric NeuroRecovery family during the course of this research, thank you. Your hard work, dedication, and expertise have been instrumental in the success of this project. Your contributions are critical in the day-to-day operations of the lab. I am honored to have had the opportunity to work with

such a talented and passionate team. I would also like to acknowledge your unwavering commitment to advancing the field and improving the lives of those affected by spinal cord injuries. Your contributions will always be remembered and appreciated.

Finally, I would like to acknowledge the funding sources that made this research possible, including the Kosair for Kids Center for Pediatric NeuroRecovery, the Todd Crawford Foundation for Paralysis Cure, and the Crawford Scholar Fund. Their financial support was critical in bringing this project to fruition. Their contributions have been instrumental in advancing our understanding of the pediatric brain and spinal cord following injury, and I am deeply grateful for their support.

Thank you all for being a part of this journey. It truly takes a village, and I appreciate every one of you.

# ABSTRACT

SUPRASPINAL REORGANIZATION AFTER PEDIATRIC-ONSET SPINAL CORD INJURY

Luis R. Alvarado

March 2nd, 2023

Pediatric spinal cord injury (SCI) disrupts the efferent and afferent flow of the developing brain, leading to devastating functional impairments below the injury site, yet our understanding of its impact on the brain remains limited. This study examines supraspinal reorganization in children with SCI using electrophysiology and neuroimaging techniques to understand the relationship between residual spinal transmission and supraspinal reorganization. Chapter 2 discusses the development of a child-centric approach using 'learn, play, and practice' to foster a trusting relationship with each child and increase compliance with experimental protocols. Chapter 3 evaluates the residual neural transmission of three spinal pathways in children with SCI, revealing that supraspinal inputs onto spinal motor circuitry persist despite a clinical diagnosis of complete SCI. This finding supports the concept of discomplete injuries and suggests that clinical assessments may not fully capture the extent of residual sensorimotor function in this population. The neural conduction of the corticospinal tract (CST), the primary

mediator of volitional motor function, was assessed via functional neurophysiological assessment (FNPA). Reticulospinal tract (RST) activity, crucial for movement coordination, was evaluated using acoustic startle response (ASR). Finally, the functional transmission of the dorsal column-medial lemniscus (DCML) pathway, which conveys touch information from the periphery to the brain, was evaluated by analyzing somatosensory evoked potentials (SSEP). In Chapter 4, the impact of SCI on the pediatric brain was investigated using neuroimaging techniques. Analysis of 8 children with SCI and 18 age- and gender-matched typically developing controls showed reduced gray matter morphometry and functional connectivity in cortical and subcortical sensorimotor structures and lower CST microstructural integrity in the brains of children with SCI. Additional analysis reveals that higher cortical and subcortical neuroimaging measures were associated with a higher probability of volitional muscle activation, and higher RST activity levels were correlated with better measurements of subcortical morphometry and functional connectivity. These findings provide valuable insights into the effects of pediatric SCI on the brain and their underlying relationships to motor pathways activity, suggesting the potential of supraspinal neuroimaging to serve as biomarkers to assess recovery and track the efficacy of interventions targeting spinal translesional connectivity.

# TABLE OF CONTENTS

# LIST OF TABLES

PAGE

# LIST OF FIGURES

PAGE

# CHAPTER 1: GENERAL INTRODUCTION

## Background

Pediatric-onset spinal cord injury (SCI) derails the typical growth and development experienced during the first decades of life (Schottler et al., 2012; Vogel et al., 2012). Children with SCI have vastly divergent motor and sensory experiences from their typically developing (TD) peers during this crucial period of development (Atkinson et al., 2019; Howland et al., 2014; Singh et al., 2018). Paralysis and the disruption of sensory and motor flow to and from the brain after SCI may significantly reduce the influence of activity-dependent processes on the typical development of the brain (Delcour et al., 2018). This diminished flow of motor and sensory activity is frequently compounded by current standard-of-care treatments for children with SCI. Often, these children are prescribed braces and orthoses (Calhoun et al., 2013; Parent et al., 2010) that further restrict their mobility and sensory experiences. Common pharmaceutical interventions such as baclofen and botulinum toxin (Powell & Davidson, 2015; Vogel et al., 2012) may also diminish neural activity flow to and from the CNS. This disruption of sensory and motor activity may significantly impact neurodevelopment. Nevertheless, the impact of SCI on the developing pediatric brain has not yet been elucidated. Given

the void of studies investigating this question, patterns of supraspinal remodeling and any relationship to the severity of the injury remain speculative at best.

While the preponderance of pre-clinical and clinical SCI research has focused on the spinal cord at or below the injury site (Angeli et al., 2018; Harkema et al., 2018; Hubscher et al., 2018; Saksena et al., 2019), this dissertation focuses on the impact of SCI on the pediatric brain. To our knowledge, no other studies to date have endeavored to investigate the effects of SCI on the pediatric brain. In addition, there is a void of research examining possible associations between SCI-induced supraspinal neuroimaging changes and the electrophysiology status of the injured spinal cord. Aiming to address these gaps in the literature, this cross-sectional study implemented a child-centric approach that leveraged multiple neuroimaging and electrophysiological techniques (Chapter 2) to elucidate the residual electrophysiological integrity of motor and sensory spinal pathways after pediatric SCI (Chapter 3) and assess how these changes influence the anatomy and functional connectivity of the pediatric brain (Chapter 4).

The current chapter provides a focused review of the literature relevant to a) the overall arrangement of somatic sensory and motor systems in humans, b) how SCI affects the electrophysiology of spinal pathways, c) the consequences of significant sensory and motor deprivation in early childhood, and d) supraspinal changes that occur in adulthood as a result of SCI.

*General Organization of the Nervous System*

The human nervous system is responsible for an enormous number of sensory and motor functions. The anatomical study of this complex system has mainly been tackled from regional and functional perspectives. From a regional neuroanatomy perspective, one can study the spatial relations between neural structures within a specific portion of the nervous system (Haines, 2004a, 2004b). Within this framework, the nervous system is usually divided into central (CNS) and peripheral (PNS) divisions. The CNS consists of the brain and spinal cord. The brain is subdivided into cerebral hemispheres, diencephalon, brainstem, and cerebellum. The spinal cord starts inferior to the medulla oblongata of the brainstem and terminates at the level of the first and second lumbar vertebra within the spinal canal (Mancall, 2011a; Purves et al., 2001a).

The spinal cord is longitudinally organized into cervical (C), thoracic (T), lumbar (L), and sacral (S)/coccygeal regions. Cervical and lumbar engorgements are due to the large number of neurons needed in these regions to serve the upper and lower limbs, respectively. Cross-sectionally, the spinal cord is organized with a central butterfly-shaped area consisting of neuronal bodies collectively known as the central gray matter (GM). The ventral “wings” of the butterfly, referred to as ventral horns, contain alpha and gamma motor neurons and interneurons. The dorsal horns contain sensory neurons that receive sensory fibers from the dorsal root ganglia of each segmental spinal nerve. The lipid-rich myelinated axons within the spinal cord's white matter (WM) are organized as posterior, anterior, and lateral columns surrounding the central gray matter. These columns contain ascending

and descending pathways that ultimately connect the CNS with sensory receptors and motor effectors via the spinal nerves of the PNS (Cho, 2015; Mancall, 2011b).

Alternatively, functional neuroanatomy deals with structures across the nervous system that work together to accomplish a particular function. Functional systems, therefore, consist of intra- and interregional neural connections that form complex neural circuits (Haines, 2004c). Within this framework, the nervous system can be functionally organized into visceral and somatic divisions (Boezaart et al., 2021; Standring, 2021b), each with afferent and efferent components. The visceral nervous system is dedicated to the sensory surveilling and motor control of internal organs. The somatic nervous system, on the other hand, controls the body's voluntary movements and sensations. Ultimately, a synergistic overview of regional and functional neuroanatomy is fundamental for a comprehensive understanding of the nervous system. Here I present a brief review of the regional and functional anatomy of selected afferent and efferent somatic pathways—within the scope of this dissertation.

### *Visceral Nervous System*

The visceral nervous system consists of afferent fibers (Sanvictores & Tadi, 2022) carrying sensory information from the viscera and blood vessels into the CNS and efferent fibers (Cheng & Tadi, 2022) that provide autonomic motor innervation to smooth muscles, cardiac muscles, and secreting glands. Although of considerable interest, the neuroanatomy of the visceral nervous system and its subdivisions are beyond the scope of this work.

### *Somatic Nervous System*

The somatic nervous system consists of nerves that carry peripheral sensations to the CNS and neurons that exit the CNS to innervate skeletal muscles. This system allows us to interact with our environment. The afferent division is responsible for our conscious perception of external stimuli and body movements. Our reaction to those stimuli via the volitional control of skeletal muscles is mediated by the efferent division (Standring, 2021a, 2021c). An inherent characteristic of the somatic system is the topographical organization of their projections. The sensory and motor somatic systems maintain topographically organized maps of the corresponding sensory receptors and motor effectors throughout their neuroaxis (Guo et al., 2012; Huang & Sereno, 2018; Penfield & Boldrey, 1937; Penfield & Rasmussen, 1950).

#### *Afferent Division of the Somatic System*

The somatic afferent system conveys neural impulses, generated by the activation of receptors in the peripheral nervous system (PNS), to the spinal cord and ultimately the brain for conscious perception. Somatic sensory receptors are activated by stimuli from outside the body or by the movement of our muscles and joints. There are two types of somatic afferent modalities—special or general. The special somatic afferent (SSA) system employs specialized receptors confined within a specific organ (i.e., eye, inner ear, tongue, or nose) and sensitive to changes in the external environment (i.e., light, air pressure, taste, or odorants). SSA impulses are conducted by specific cranial nerves, which then project to the brainstem and cerebrum. The general somatic afferent (GSA) system transmits

information about discriminative touch, proprioception, pain, and temperature from peripheral receptors from the head (via selected cranial nerves) and from the surface of the body (via all spinal nerves) to the brainstem and spinal cord respectively.

In general, GSA pathways consist of a primary afferent neuron with a cell body situated within the peripheral ganglion of a spinal or cranial nerve (Purves et al., 2001b). These primary neurons are pseudounipolar, with a peripheral axon forming (in some cases innervating) receptors that transduce stimuli into action potentials and a central axon that synapses with secondary afferent neurons in the posterior horn of the spinal cord or within brainstem nuclei. These secondary neurons often cross the midline to the opposite side of the spinal cord or brainstem and ascend to synapse with tertiary afferent neurons in the thalamus. Tertiary thalamic neurons will then synapse in the cerebral cortex's primary somatosensory (S1) gyrus.

This afferent flow of information from the PNS to the CNS is organized to preserve topographical information about the location of the originating stimuli. For instance, information related to the lower part of the body travels in fibers located medially in the white matter of the spinal cord. In contrast, lateral white matter fibers carry neural transmission from the upper portions of the body. Within each somatosensory pathway, there is a map of the body in the spinal horns, white matter tracts, thalamus, and cortex. Due to this organization, each body region is represented in a specific area of the cortex (Catani, 2017; Penfield & Boldrey, 1937; Penfield & Rasmussen, 1950). Within this topographically organized cortical

map, known as the homunculus, the foot and leg are represented in the superior aspect of the contralateral primary motor cortex (M1) lateral to the medial longitudinal fissure. The trunk is represented lateral to the legs, followed by regions representing the fingers and hands. The most inferior and lateral segments of M1 mapped the lips and face (Roux et al., 2018).

In addition, sensory information is transmitted within different white matter pathways depending on the nature and location of the originating stimuli. For example, discriminative touch and proprioceptive information from the body travel to the brain via the posterior column-medial lemniscus system. In comparison, similar impulses originating from the face are transmitted to S1 via the trigeminal nerve. While crude touch, pain, and temperature stimuli from the body are carried via the spinothalamic pathway of the anterolateral system (ALS).

### *Dorsal Column-Medial Lemniscus (DCML) System*

The DCML system relays fine touch, vibration, and conscious proprioception information to S1. This system is composed of the dorsal columns of the spinal cord, the dorsal column nuclei (gracilis and cuneatus) in the medulla, medial lemniscus, thalamus, and primary sensory cortex of the brain (Al-Chalabi et al., 2022; Patestas, 2016). First-order neurons transmit discriminative touch and proprioception information from peripheral receptors to two distinct nuclei in the medulla. The cell bodies of these primary neurons are found in the dorsal root ganglion. Signals originating from the body caudal to the sixth spinal thoracic level (from lower limbs) enter the dorsal horn of the spinal cord and ascend in the ipsilateral medial subdivision of the dorsal column known as the fasciculus gracilis

and then synapse on the ipsilateral nucleus gracilis of the medulla. Touch and proprioception signals from the body above T6 travel ipsilaterally within the fasciculus cuneatus (the lateral portion of the dorsal column) to then synapse with secondary neurons within the ipsilateral nucleus cuneatus. Axons from second-order neurons of the medullary nuclei decussate and travel in the contralateral medial lemniscus bundle to reach the ventral posterolateral nucleus of the thalamus (Th). From here, third-order neurons ascend via the internal capsule to synapse with the primary somatosensory region of the brain cortex.

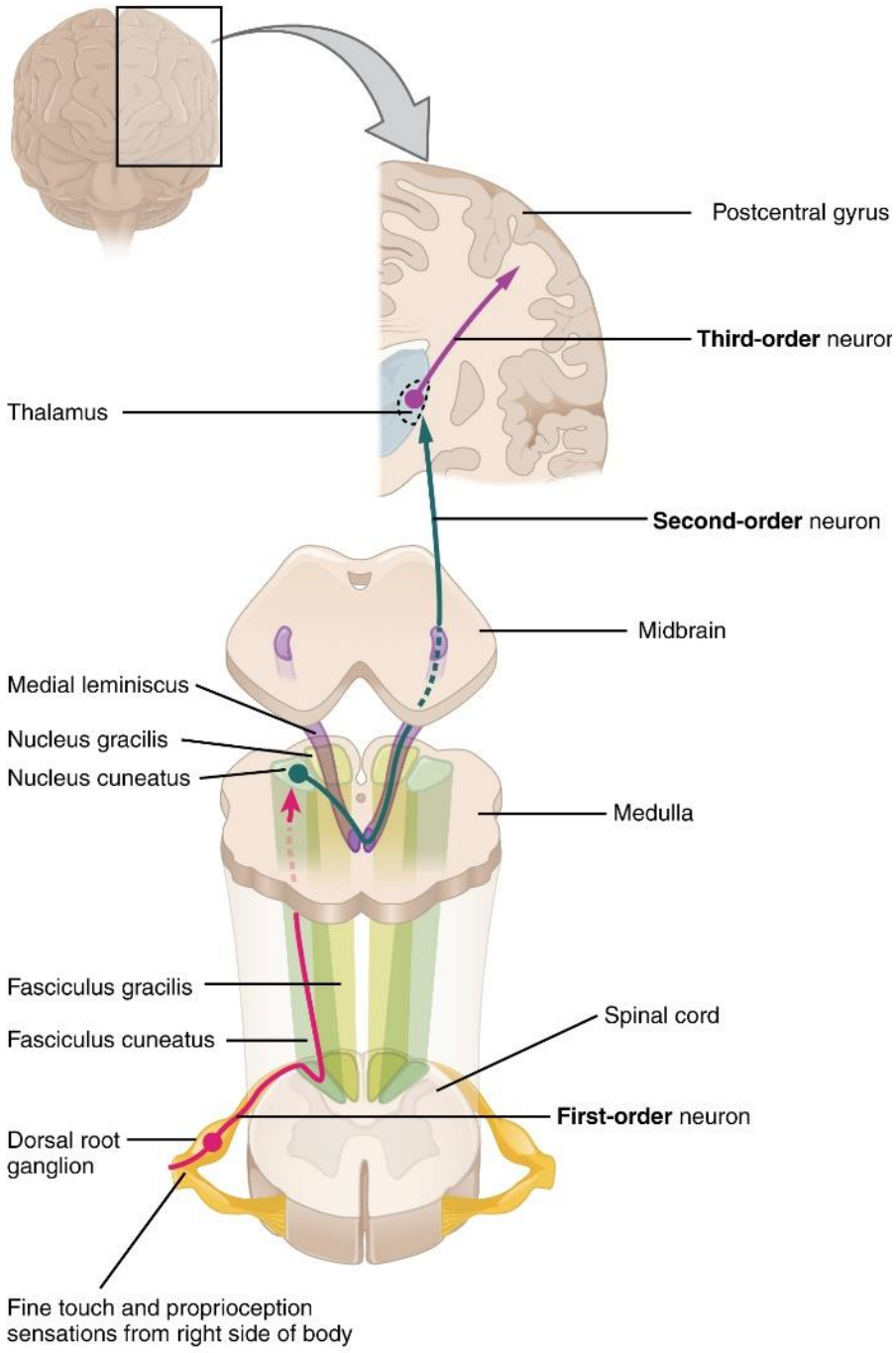


**Figure 1.1: Diagram of the dorsal column-medial lemniscus system.**

(Source: Anatomy & Physiology, Connexions Web site. http://cnx.org/content/col11496/1.6/, Jun 19, 2013. Image licensed under the Creative Commons Attribution 3.0 Unported (CC BY 3.0) license.)

### *Efferent Division of the Somatic System*

This system consists of descending tracts that relay neural signals caudally to skeletal muscles. Each descending tract is formed by two interconnecting neurons that create a pathway from supraspinal neural structures to the target effector muscles. The first neuron, known as the upper motor neuron (UMN), originates from the cortex or brainstem and descent to the spinal cord to synapse onto second-order neurons in the anterior gray horn. These lower motor neurons (LMN) then exit the spinal cord via spinal nerves to innervate skeletal muscles. Functional mapping and lesion studies have demonstrated the somatotopic organization of the primary motor cortex (Desmurget & Sirigu, 2015; Lemon, 1988; Roux et al., 2020). The two major tracts concerned with volitional control of lower motor neuron activity are the corticospinal tract and the reticulospinal tract.

#### *Corticospinal Tract (CST)*

The corticospinal tract, together with supraspinal motor structures (e.g., M1, supplementary motor area (SMA), premotor cortex (PM), and basal ganglia) and spinal motor networks, plays a significant role in controlling, planning, and coordinating movements in humans (Lemon, 2008). CST first-order neurons predominantly originate from M1, SMA, and other motor areas of the brain, with a minority of projections arising from the cingulate motor and parietal somatosensory cortex (Dum & Strick, 1991, 2002; Martin, 2005). These axons travel caudally through the brainstem via the cerebral peduncles before reaching the pyramids at the level of the medulla oblongata. Here about 90% of the CST fibers crossover to

the other side of the brainstem giving rise to the pyramidal decussation. These contralateral fibers enter the spinal cord in the lateral white matter column forming the lateral CST. The remaining 10% of the CST fibers do not decussate. They project caudally into the spinal cord within the ventral columns. The majority of these ventral CST will decussate within the spinal cord right before reaching their target LMN (Standring, 2021c). These lateral CST projections primarily control muscles of the arms and legs essential for skilled movements and hand dexterity. The ventral CST tract innervates axial muscles of the trunk involved in postural control.

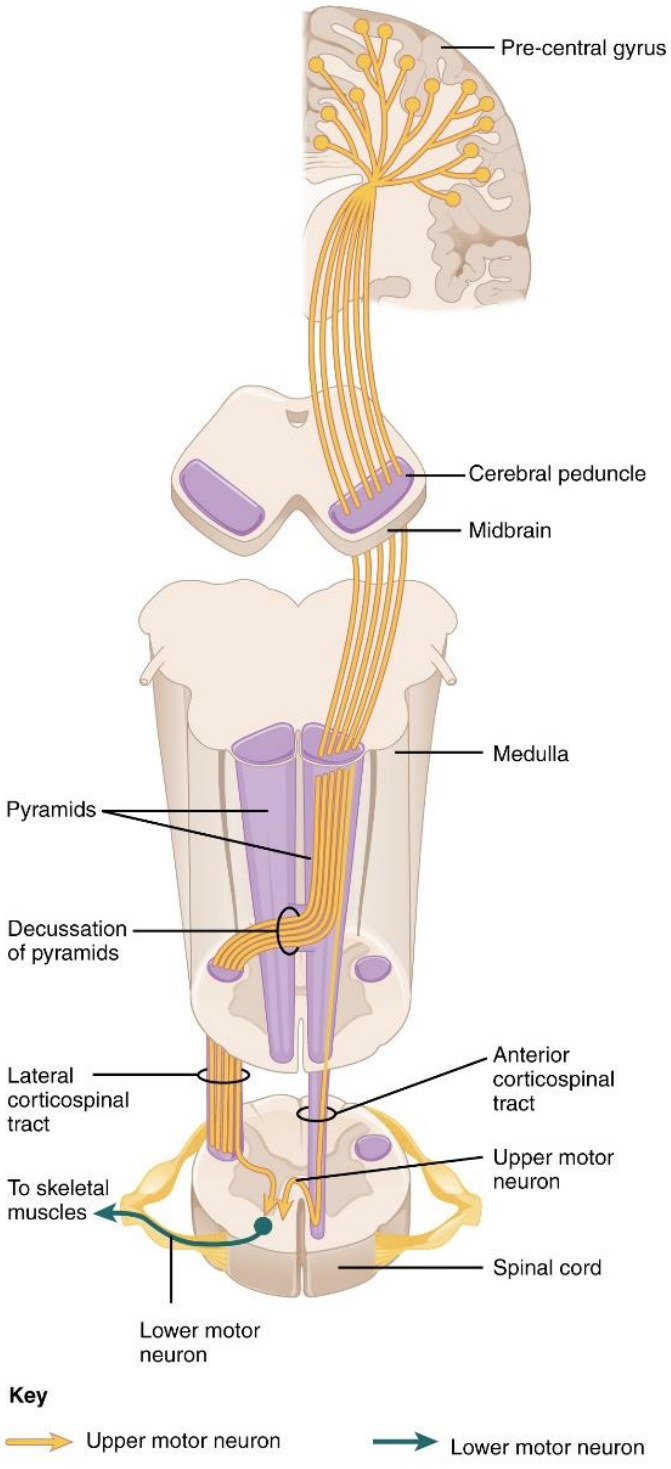


**Figure 1.2: Diagram of the corticospinal tract.**

(Source: Anatomy & Physiology, Connexions Web site. http://cnx.org/content/col11496/1.6/, Jun 19, 2013. Image licensed under the Creative Commons Attribution 3.0 Unported (CC BY 3.0) license.)

*Reticulospinal Tract (RST)*

RST fibers originate from large cells in the pontine or medullary reticular formation of the brainstem and descent ipsilaterally into the spinal cord to form synapses with interneurons and motoneurons in multiple spinal segments in order to drive muscle activation. (Brownstone & Chopek, 2018; Standring, 2021c). The distinction between these two tracts is poorly defined as they are typically scattered throughout the ventral and lateral columns (Nathan et al., 1996). It is worth mentioning that there is significant overlap in the termination of RST and CST projections to segmental interneurons (Lemon, 2008; Standring, 2021c). The RST influences the activity of the alpha and gamma motor neurons through these interneurons (Lemon, 2008).

In contrast to other descending systems, the RST contains excitatory and inhibitory projections (Brownstone & Chopek, 2018) that allow it to exert a diverse role in the modulation of motor activity depending on the integration and processing of the various inputs it receives. The medullary reticular formation serves as a control center for the initiation and stop of locomotion. On the other hand, the pontine reticular formation is involved in the modulation of locomotion speed and gait (Brownstone & Chopek, 2018).

Of particular interest to our scope, many reports have demonstrated the ability of intact and injured RST fibers to sprout new connections with target neurons of other tracts (Filli et al., 2014; May et al., 2017; Vavrek et al., 2007). Animal models of SCI have shown that the reticulospinal system can play a role in the recovery of motor function after corticospinal lesions (Baker, 2011). Given their

extensive overlap with CST, diffuse location within the white matter columns, ability to sprout collateral fibers, and diverse output, RST neuronal projections may play a critical role in the recovery of motor function after injury.

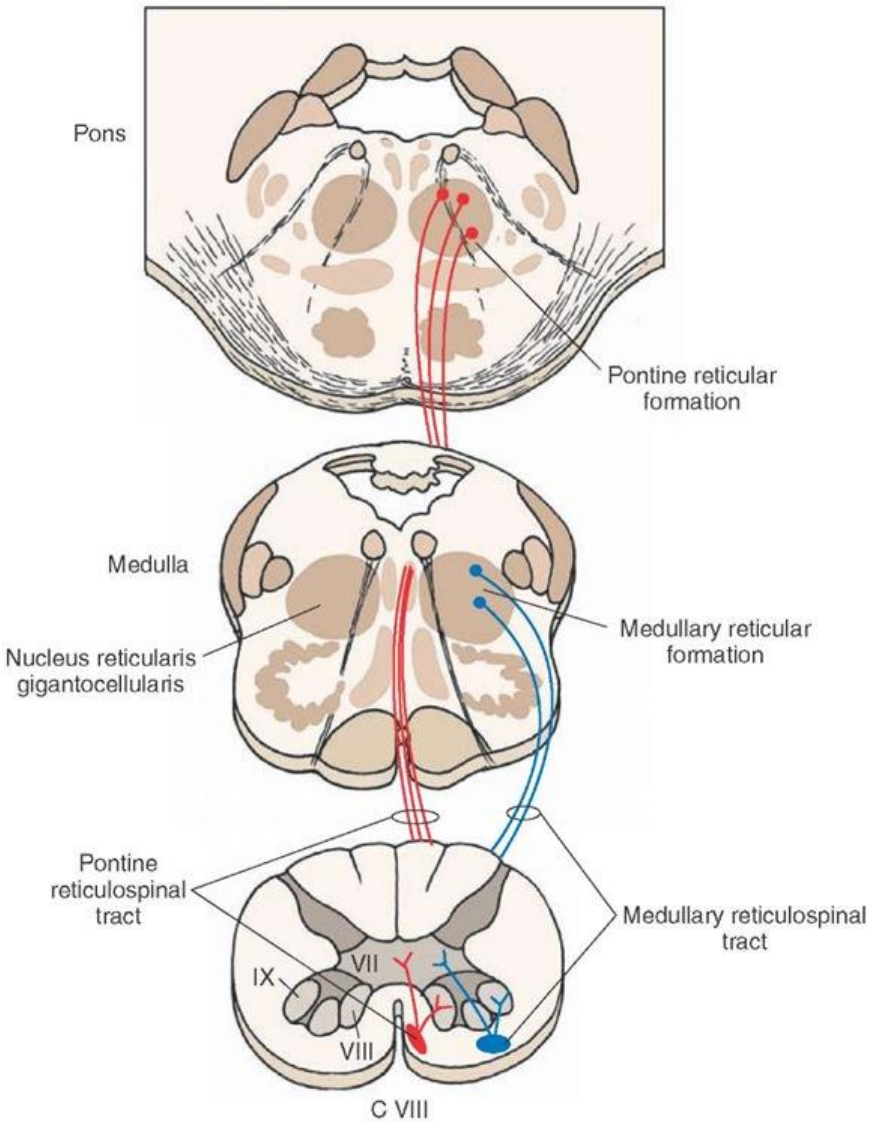


**Figure 1.3: Diagram of the reticulospinal tract**

The medullary (lateral) reticulospinal tract (shown in blue) arises from the nucleus gigantocellularis and projects bilaterally to all levels of the spinal cord (only ipsilateral projections are shown). The pontine (medial) reticulospinal tract (shown in red) arises from the pons and projects ipsilaterally to the entire extent of the spinal cord. (Source: Anatomy & Physiology, Connexions Web site. http://cnx.org/content/col11496/1.6/, Jun 19, 2013. Image licensed under the Creative Commons Attribution 3.0 Unported (CC BY 3.0) license.)

*Impact of SCI on Spinal Pathway Electrophysiology*

The impact of spinal cord injuries (SCI) on the electrophysiological transmission of spinal pathways has been well-studied in animal and adult human models. SCI can result from traumatic, nontraumatic, or congenital causes, with the most common traumatic causes being motor vehicle accidents, falls, and sports-related injuries. Nontraumatic causes may include tumors, infections, and certain genetic conditions. Injuries to the spinal cord can disrupt the normal neural transmission of spinal pathways, leading to changes in their electrophysiology, such as altered conduction velocities, increased excitability of spinal neurons, and changes in synaptic connectivity. The patterns of sensorimotor loss relate to the extent of damage or sparing of specific spinal pathways (Ahuja et al., 2017). For example, anterior cord syndrome causes complete motor paralysis and loss of pain and temperature sensation but preserves light-touch sensation and proprioception. In contrast, posterior cord syndrome leads to the loss of light touch and proprioception but preserves motor function, pain, and temperature sensation. However, it is worth noting that various imaging (Freund et al., 2019; Petersen et al., 2012; Vallotton et al., 2019), electrophysiological (Angeli et al., 2014; Dimitrijevic, 1988; Dimitrijevic et al., 1983; Sherwood et al., 1992), and anatomical (Kakulas & Kaelan, 2015) studies have revealed that even severe SCIs often leave regions of white matter intact.

This section of the dissertation will concentrate on the effect of SCI on the electrophysiological state of the CST, RST, and DCML as they are essential for the research presented in this work. Several previous studies have evaluated the

residual neural transmission of the CST after SCI using various established techniques, such as transcranial magnetic stimulation (TMS), which excites the motor cortex using a magnetic coil placed over the scalp. This stimulation elicits motor-evoked potentials (MEPs) in the muscles of the limbs, which can be measured using surface electromyography (EMG) electrodes (Barthelemy et al., 2015; Bjerkefors et al., 2015; McKay et al., 2005). Although TMS can be an effective means of directly assessing the CST circuitry, its use in pediatric populations is potentially limited by some drawbacks. For example, TMS may cause discomfort or pain in some children (Allen et al., 2017), leading to anxiety and resistance to the procedure, which can affect the reliability of the results. Additionally, differences in cortical excitability and brain size between children and adults may require higher stimulation intensities to elicit MEPs, increasing the risk of discomfort or adverse effects associated with TMS. These factors can limit the reliability of the results, particularly if the child is unable to tolerate the procedure or muscle fatigue affects the MEP responses.

In recent decades, researchers developed protocols to assess the neural transmission of supraspinal volitional control of muscle activation to measure motor capacity (Dimitrijevic et al., 1980; Li et al., 2012; McKay et al., 2004; Sherwood et al., 1996). This interest led to the development of the Functional NeuroPhysiological Assessment (FNPA), which systematically measures the EMG activity of multiple muscles during volitional attempts to perform standardized movements. This protocol was adapted to accommodate pediatric subjects by our group (Atkinson et al., 2019). The FNPA offers a sensitive evaluation of volitional

motor capacity and the potential to detect subclinical residual descending influence on spinal motor networks. However, as volitional muscle activation is mediated by multiple descending spinal pathways (e.g., CST and RST), EMG activity observed during FNPA experiments cannot be exclusively interpreted as the result of neural transmission of the CST.

Changes in the electrophysiology of the RST have been extensibility studied via acoustic startle response (ASR) experiments of adults (Blumenthal, 2015; Kiziltan et al., 2015; Ludewig et al., 2003) and children (Bakker, Boer, et al., 2009; Bakker, Tijssen, et al., 2009; Gregg & Scott, 2015; Klorman et al., 2003) in multiple disease models. In these experiments, the reflexive muscle activation in response to a startling auditory stimulus is recorded and examined. The startle reflex is a defense response generated in the brainstem that propagates down the spinal cord through the RST. Auditory startle responses are most prominent in the face, neck, and shoulders. Studies have reported that individuals with SCI exhibit increased probabilities of eliciting a response from all supralesional muscles when compared to neurological intact controls (Abanoz et al., 2018; Kumru, Kofler, et al., 2009; Kumru et al., 2008; Sangari & Perez, 2020), indicating that loss of descending inputs to the spinal cord may contribute to the development of exaggerated ASRs.

Somatosensory-evoked potentials (SSEPs) are a valuable tool for evaluating the residual neural transmission of the DCML pathway after SCI (Chabot et al., 1985; Curt & Ellaway, 2012; de Haan & Kalkman, 2001; Spiess et al., 2008). SSEPs measure the cortical electrical signals generated in response to

electrical stimulation of a peripheral nerve, allowing for a non-invasive and direct evaluation of DCML function. SSPEs have been well tolerated by adults and children (Azouz et al., 2019; Bockowski et al., 2010; Boor, Goebel, & Taylor, 1998; Boor et al., 2008). By measuring the amplitude and latency of these signals, researchers can assess the degree of DCML impairment and the severity of sensory loss in individuals with SCI (Li et al., 1990). Studies have shown that after SCI, SSEPs are often decreased in amplitude with prolonged latency, indicating reduced conduction velocity and processing of sensory information by the DCML. In cases of clinically incomplete injuries, individuals with SCI often have delayed cortical evoked potentials from stimulations below the level of injury, while cortical SSEPs are often absent in individuals with complete injuries. These changes in SSEPs are typically associated with the severity of sensory impairment.

Overall, the FNPA, ASR, and SSEP protocols have been established as valuable tools for evaluating the CST, RST, and DCML pathways. These techniques offer a precise and sensitive evaluation of motor and sensory functions in individuals with SCI. Moreover, they are well tolerated by pediatric subjects, allowing the assessment of residual neural transmission of these pathways in young patients. By utilizing these well-established techniques, researchers and clinicians can accurately evaluate the extent of damage to these neural pathways and their association with the resulting functional impairments.

### *Effects of Childhood Sensorimotor Deprivation on the Brain*

The English and Romanian Adoptees (ERA) study (Rutter et al., 2007) provided a suitable model to study the effects of sensorimotor deprivation during

the first years of life, a period of intense growth of the central nervous system. Neuroimaging studies of a sample of this cohort showed significant reductions in WM and GM volumes in the brains of orphaned Romanian children who experienced impoverished sensory environments and limited mobility during childhood (Mehta et al., 2009; Sheridan et al., 2012). Mehta et al. (2009) used magnetic resonance imaging (MRI) to measure GM and WM volumes of 14 previously institutionalized adolescents adopted from Romania to the United Kingdom and 11 never-institutionalized adoptees from the United Kingdom. The Romanian adoptees had significantly reduced brain GM and WM volumes compared with the control group. The average age of both groups was 16 years at the time of imaging.

Similarly, Sheridan et al. (2012) used structural MRI to examine the brain morphology of 20 typically developing Romanian children, 29 previously institutionalized children, and 25 children in a high-quality foster care intervention that was previously institutional. Children with a history of institutionalization had significantly smaller cortical GM and WM volumes than children in the control group. Of note, there was no statistically significant difference between the cortical WM of children placed in foster care and children that were never institutionalized. Children that stayed in the orphanage had significantly smaller WM volumes than the control group and the group randomized to foster care. The increase in white matter among children randomized to an improved rearing environment relative to children who remained in institutional care indicates the potential for

developmental “catch-up” in white matter growth, even after experiencing extreme environmental deprivation.

Eluvathingal et al. (2006) employed diffusion tensor imaging to examine structural connectivity in 7 children adopted from Romania to families in the United States, and 7 children born to North American families reported reduced apparent diffusion coefficients and fractional anisotropy across all white matter tracts in previously institutionalized children when compared to the control group, suggesting a general reduction of white matter tract integrity (Eluvathingal et al., 2006). Finally, Govindan et al. demonstrated that the extent of WM abnormalities was significantly correlated with the duration of the sensorimotor neglect (i.e., time in the orphanage) (Govindan et al., 2010).

In the absence of a direct examination of the effects of a SCI on the pediatric brain, these studies provide some insights into this question. The results from the study of these populations suggest a noteworthy association between diminished afferent and efferent activity flow and differences in supraspinal neural structures of children. In addition, these conclusions aligned well with numerous reports from the literature on adults with SCI.

*Effect of a Spinal Cord Injury on the Adult Brain*

Neuroimaging examination of the adult brain following SCI provides convincing evidence of significant anatomical, functional, and connectivity alterations of supraspinal structures (Freund et al., 2013; Guleria et al., 2008; Hawasli et al., 2018; Jurkiewicz et al., 2006; Lotze et al., 1999; Nardone et al., 2018; Pan et al., 2017; Solstrand Dahlberg et al., 2018; Wrigley et al., 2009).

Understanding these structural and functional supraspinal changes and defining their relationship to clinical outcomes may facilitate the development and validation of evidence-based rehabilitation therapies (Freund et al., 2019; Ziegler et al., 2018). Hence, there is a growing interest in developing non-invasive in-vivo neuroimaging biomarkers (Freund et al., 2019; Freund et al., 2013; Seif et al., 2018) that can reliably assess the extent of neural damage, elucidate the mechanisms of neural repair, and inform clinical outcomes after SCI. All these efforts, however, have been devoted to the adult-SCI population.

The adult SCI literature describes GM atrophy of both cortical and subcortical structures (Freund et al., 2013; Freund et al., 2011; Jurkiewicz et al., 2006; Wrigley et al., 2009). Cortical structures commonly reported as atrophied after SCI include the primary motor cortex (M1), primary sensory cortex (S1), supplementary motor area (SMA), and premotor area (PM). Affected subcortical structures included the thalamus (Th), striatum, and basal ganglia (BG) nuclei. In addition, several studies have established significant correlations between the degree of supraspinal reorganization and clinical outcomes. For instance, Freund et al. (Freund et al., 2013; Freund et al., 2011) reported a correlation between the chronicity of the injury and the severity of GM atrophy. In addition to GM atrophy, several elegant studies have reported WM atrophy, most prominently in various locations of the corticospinal tract (CST). The work of Guleria et al. (Guleria et al., 2008) and others (Freund, Schneider, et al., 2012; Freund, Wheeler-Kingshott, et al., 2012; Grabher et al., 2015) have shown WM atrophy in the pyramids, internal capsule, and cerebral peduncles of patients with SCI.

In a seminal study in the field, Freund et al. (Freund et al., 2013) longitudinally studied 13 patients with acute traumatic SCI and healthy controls. Subjects were assessed at baseline (within two months of the injury for subjects with SCI) and followed at 2, 6, and 12 months. The authors examined the interactions between MRI parameters and clinical progression. Results showed a rapid volumetric decrease of WM in the CST and GM in S1 and M1 during the first two months after SCI. In addition, the study revealed correlations between supraspinal changes and clinical outcomes with faster degenerative changes relating to poorer recovery. Similarly, Hou et al. (Hou et al., 2014) observed a significant negative correlation between bilateral atrophy of M1 and the total American Spinal Injury Association impairment scale (AIS) motor scores of 20 acute SCI patients (4 – 12 weeks after injury). These observations suggest that SCI causes significant structural supraspinal atrophy of the sensorimotor system and that these changes are associated with clinical outcomes.

Resting-state functional connectivity (rs-FC) changes have also been reported in the context of adult SCI. Spontaneous neural activity in the absence of goal-directed cognition or tasks can be studied using resting-state functional MRI (rs-fMRI). The strength of the correlation of these spontaneous activations between brain regions over time is defined as rs-FC (Biswal et al., 1995). This indirect measurement of brain connectivity allows the characterization of distinct functional networks. In a recent rs-fMRI study, Zhu et al. (Zhu et al., 2015) reported widespread rs-FC disruptions among the M1, S1, SMA, dorsolateral prefrontal cortex, brainstem, insula, and anterior cingulate cortex of adult patients with SCI.

These disruptions were negatively correlated with AIS motor scores, suggesting increased cortical reorganization is associated with greater severity of motor impairments. By contrast, rs-FC among areas not directly impacted by cortical deafferentation are preserved (Min, Chang, et al., 2015; Min, Park, et al., 2015). Changes in the rs-FC of adults with SCI have also correlated with clinical outcomes. In 2016, Hou et al. examined the rs-FC reorganization in SCI patients in the acute stage of the injury (< 9 weeks post-injury) and tracked their motor recovery during the first six months after injury. Patients were classified as good or bad recoverers. Patients that achieved an increase of at least one AIS grade after six months were classified as good recoverers. On the other hand, poor recoverers had no significant upward conversion of AIS grade at follow-up. Functional connectivity was reduced in the primary and association motor cortices in patients who had poor motor recovery after six months, whereas an opposite pattern of increased connectivity between these areas was observed in patients that achieved an upward conversion of their AIS grades (Hou et al., 2016).

## Objectives

While conclusions from the adult SCI literature cannot be directly extrapolated to a pediatric SCI population, it remains a valuable source of information for experimental design, methodology, and analysis. It is clear from this body of work that advances in the accuracy, affordability, and accessibility of magnetic resonance imaging (MRI) techniques have made them indispensable tools for investigating cortical and subcortical changes following SCI. These

methods were crucial in conducting our study on a pediatric SCI population. Many of these studies have expanded our understanding of supraspinal remodeling after adult-onset SCI by correlating it with anatomical features of the injured spinal cord, such as cross-sectional area and myelination. However, there is a lack of research examining the impact of residual neural transmission in the injured spinal cord on subsequent supraspinal reorganization following SCI. This research gap, coupled with the scarcity of pediatric-onset SCI studies, highlights the need for pediatric-specific research to examine the developing brain after SCI. Therefore, the primary objectives of this dissertation are twofold: first, to characterize the residual neural transmission in the pediatric spinal cord after SCI (Chapter 3), and second, to investigate the anatomy and functional connectivity of the brain in children with SCI, examining the relationship between supraspinal remodeling and injury severity (Chapter 4).

## Hypotheses

This study is grounded in several hypotheses across different chapters. Chapter 3 proposes that children with spinal cord injuries (SCI) will exhibit decreased neural transmission in the corticospinal (CST), reticulospinal (RST), and dorsal column-medial lemniscus (DCML) tracts when compared to normative data. Chapter 4 hypothesizes that children with SCI will show reduced gray matter (GM) morphometry in cortical and subcortical sensorimotor structures with somatotopic representation of the body below the injury, as well as white matter (WM) integrity of the CST and functional connectivity (FC) of the sensorimotor

intrinsic connectivity network, when compared to normative data. It was expected that these neuroimaging changes would correspond with the residual neural transmission of the injured spinal cord.

# CHAPTER 2: CHILD-CENTRIC RESEARCH APPROACH

## Governing Principles

To enhance compliance with the experimental protocols and minimize potential difficulties stemming from boredom, fatigue, and frustration, we designed a pediatric-centric approach for each facet of this study. From the first interaction during the consent/assent meeting to the final assessment, we aimed to engage each child as an actively invested partner in every experiment. The success of this approach hinged on fostering trusting relationships with the children. Building these positive relationships entailed the following strategy, adapted from Johnson et al. (2014) recommendations:

- Get to know every child by name.
- Allocate time for the child to ask questions about any aspect of the research.
- Answer each question truthfully and with age-appropriate language.
- Allow time for the child to understand each procedure and the materials that will be in direct contact with them.
- Learn about the child's day-to-day interests outside the research environment and share our interests with them (e.g., movies, books,

TV shows, comicbooks). This offers a glimpse into their personalities and opinions, which may prove useful in guiding decisions about protocol presentation.

- Provide clear feedback to the child, acknowledging their efforts and praising their achievements.
- Encourage the child to voice their opinions (Johnson et al., 2014).

Establishing and maintaining a strong rapport with each child was crucial to creating a positive research environment in which children felt safe, had fun, and were ultimately eager to return. To ensure each child was invested in the success of the data collection protocols, it was paramount for the child to have a clear, age-appropriate understanding of the purpose of each of our interactions.

To accomplish this, we started by creating an informational comicbook (Kelly, 2019; Lee, 2014) that concisely outlined all the experiments and described their purpose and procedures in a visually appealing, child-friendly manner (see Appendix B. Comicbook illustration of the study). This comicbook was introduced during the consent/assent meeting and frequently referenced during each experiment. In it, we explained how an MRI scanner functions like a camera to capture images of the brain and emphasized the importance of remaining as still as possible during the scans. The comicbook also explained how the brain controls muscles and how nerves can talk to our brains using a secret electric language. Learning about these messages piqued the children's interest to discover this electric language, allowing them to become more invested in obtaining good EMG and evoked potential signals. In turn, the research team leveraged this interest to

underscore the importance of the children's cooperation and adherence to experimental preparation and procedures.

We encouraged participants to ask questions and took the time to answer them in an age-appropriate manner. During each experiment, time was allowed for the child to experience what the materials felt like and how they were utilized. This strategy was particularly useful for easing any apprehension regarding discomfort caused by materials (i.e., markers, tape, or gel electrodes) in contact with hypersensitive skin regions of children with SCI. Figure 2.1 captures this strategy. In one example, a child is given the time to explore the materials involved in skin preparation and use them to clean the skin of the examiner (Figure 2.1-A). In another case, a child was given the opportunity to explore and perform specific parts of the preparation procedure (e.g., marking the scalp) onto the investigator (Figure 2.1-C). The child observed the investigator’s reaction to the procedure and asked questions about the experience. The few minutes invested in this activity helped lessen the anxiety expressed by the child about this part of the protocol.

Experimental data acquisition can be intimidating, especially MRI scans, which can be loud and overwhelming for children, potentially causing anxiety, frustration, and low compliance during acquisitions. To preempt this outcome, we scheduled an initial introductory visit to a mock MRI scanner before the first neuroimaging session to alleviate anxiety and familiarize the child with the environment. During this mock MRI session, the participant learned the importance of staying still during an MRI and practiced remaining motionless within the bore of the mock scanner. We enhanced participant comfort and engagement by

fostering a safe and playful environment during mock sessions (Pressdee et al., 1997; Raschle et al., 2012; Rosenberg et al., 1997).

A prevalent concern in pediatric neuroimaging is head movement during data acquisition. Head motion can introduce substantial artifacts to the images, potentially impacting the subsequent analysis. To minimize head movement artifacts, we utilized a mock MRI suite and implemented the following strategies:

1. Clarifying the importance of remaining still by employing a "blurry picture" analogy, helping children understand the consequences of movement during the scan.
2. Demonstrating the effects of motion by taking images of the child with and without movement, and then collaboratively reviewing the results to emphasize the importance of remaining still (Figure 2.2).
3. Engaging children with age-appropriate movies during the mock MRI session, with playback contingent on the absence of head motion, thus providing an incentive to stay still (Figure 2.3).

These strategies facilitated a positive research environment that fostered trust, understanding, and engagement. Consequently, children were more likely to comply with experimental protocols, resulting in higher-quality data acquisition and more reliable outcomes.

## Experimental Design

This work was conceived as a cross-sectional study designed to examine the residual electrophysiological integrity of the injured pediatric spinal cord, establish the impact of pediatric-onset SCI on the anatomy and functional connectivity of the brain, and elucidate correlations between the residual functional integrity of the spinal cord after injury and the degree of supraspinal changes secondary to SCI. To that end, we planned to conduct extensive brain neuroimaging and spinal electrophysiological assessments of 24 children (SCI=12 and TD=12). Given the unexpected global disruptions to socioeconomic, healthcare, and travel activities (Chams et al., 2020) during the worldwide coronavirus disease-2019 (COVID-19) pandemic caused by the sudden emergence of a novel coronavirus (severe acute respiratory syndrome coronavirus-2 (SARS-CoV-2) (Zhu et al., 2020)) in December 2019, recruitment and data collection for this work was severely affected. Sensible measures implemented federally and locally to mitigate the rapid transmission of SARS-CoV-2 led to the inability to recruit and enroll TD children throughout 2020 and well into 2021. We, however, were able to recruit and assess 9 children with SCI and 1 TD child.

### *Electrophysiological Assessments*

We utilized three non-invasive neurophysiological tests (described in detail in Chapter 3) to interrogate the electrophysiological integrity of the corticospinal (CST), reticulospinal (RST), and dorsal column-medial lemniscus (DCML) tracts.

The neural transmission integrity above and below the SCI level of motor pathways facilitating volitional movement was assessed by measuring the surface electromyography (EMG) activity of agonist and antagonist effector muscles during a modified functional neurophysiological assessment (FNPA) (Atkinson, 2016; Lee et al., 2004; Li et al., 2012). These efferent connections are primary CST fibers, but recent evidence demonstrated the involvement of the RST in volitional motor function (Baker & Perez, 2017; Brownstone & Chopek, 2018; Lemon, 2008). A more detailed picture of the RST integrity was obtained by measuring the probability of acoustic startle reflex (ASR) responses (Bakker, Boer, et al., 2009; Blumenthal et al., 2005; Brownstone & Chopek, 2018). Finally, the functional transmission of the DCML pathway was evaluated by analyzing somatosensory evoked potentials (SSEP) (Gilmore, 1992; Li et al., 1990; Singh, 2018) from the arms and legs.

To enhance compliance and understanding during electrophysiological experiments, we employed various child-centric strategies tailored to the unique needs of pediatric participants. These included allowing children to practice and learn about skin preparation by cleaning the skin of the examiner, which helped them gain a better understanding of what to expect and increased their confidence that the process would not be painful or uncomfortable. Additionally, we used role reversals to familiarize participants with procedures, such as wearing EEG caps and marking the scalp with a grease ink pen. These activities helped alleviate any concerns or apprehensions the child may have had about the procedure. Demonstrating the use of EEG caps, electrodes, and amplifiers, and explaining

their role in measuring brain activity ensured that participants understood the purpose of the experiment, the importance of their cooperation in recording accurate data, and ultimately improved compliance. Lastly, engaging participants' interest in the equipment and experiment processes by allowing them to explore and ask questions about the materials and procedures encouraged a sense of ownership and investment in the success of the experiment, fostering trust and confidence in the research environment.

By providing education, reassurance, and engagement, researchers fostered a positive and effective experience for the participants, contributing to the overall success of the electrophysiological experiments and the acquisition of more reliable and meaningful data.

*Neuroimaging Assessments*

Three neuroimaging modalities were utilized to investigate differences in the anatomy (GM and WM) and functional connectivity (at rest and during naturalistic viewing) among children with SCI and TD children from the HBN biobank and one local TD participant. The following neuroimaging scans (described in detail in Chapter 3) were collected using a Siemens Skyra 3 Tesla magnetic resonance imaging (MRI) scanner:

- T1-weighted: to provide information about the shape, size, and volume of gray and white matter structures in the brain.

- Diffusion-weighted imaging (DWI): to provide an indirect measurement of the architecture of white matter tracts connecting different areas of the brain.
- Resting-state fMRI (rs-fMRI): to provide a measure of functional connectivity among areas of the brain with synchronous low-frequency activation patterns.

We employed child-centric strategies that incorporated a mock MRI scanner, interactive activities, educational materials, and toys to help children understand the importance of remaining still during MRI scans, reduce anxiety, and foster a positive experience. These approaches improved image quality, reduced the need for repeat scans, and enhanced overall comfort for young participants, ultimately contributing to more meaningful research outcomes.

*MRI Training Session*

Before local MRI data collection, each child attended a mock MRI session to alleviate any anxiety, become familiar with the sights and sounds of the scanner, and help prevent motion-related artifacts (Durston et al., 2009; Suzuki et al., 2022). Children only were only scanned after a successful practice session. Each MRI training session consisted of three sections: learn, play, and practice.

**Learn:** In the first section of the training session, children learn that MRI scanners take pictures of the brain and that they are very safe. Young children watched an animated movie produced by the Pediatric Brain Tumor Foundation entitled “Imaginary Friend Society – What is an MRI?” (Link:

https://youtu.be/rMFbbsZOEv4) while preteen children watched a video “Are MRIs safe?” (Link: https://youtu.be/hlRpl_GMPPc) produced by Physics Girl in partnership with the PBS Digital Studios. These videos illustrate how MRI scanners work and emphasize the importance of remaining still during the acquisition.

**Play:** During the second portion, children play-rehearse the MRI protocol with the aid of a set of toys that included an MRI scanner, a wheelchair, and action figures. The rehearsal was designed to allow children to understand every part of the MRI scanning day. They played with the toys to learn about the roles of every person that would be present during the MRI scanning.

In addition, we encouraged the children to participate in a photo shoot as photographers and models to understand the importance of remaining motionless while taking a picture. Children took a set of pictures as they moved and then again while remaining very still. After reviewing the differences between the two pictures, we asked them to think about why the two pictures were so different and what role the movement of the model might have played in the quality of the pictures.

**Practice:** In the final section, we used a Vera MRI Simulator (Psychology Software Tools, Pittsburgh, PA) to help children practice remaining still during MRI scans. To monitor head movement, we used MoTrack motion tracking system (Psychology Software Tools, Pittsburgh, PA). Children were allowed to move their heads initially to get a feel for how the tracking system worked, while receiving instantaneous feedback on the position and motion of their heads via a video monitor from the MoTrack system. After getting familiar with the tracking system, children watched a video while trying to remain motionless while still being able to

breathe and communicate with the research team if necessary. We informed them that the continuous playback of the video was conditional on keeping their heads as motionless as possible. Children watched a video of their choosing for about 5 minutes to get comfortable with the motion-conditional playback. After 5 minutes, we introduced MRI-like sounds into the simulator room via the SimFX software (Psychology Software Tools, Pittsburgh, PA) for the remainder of the mock session. To mitigate head movement and provide comfort, we placed foam pads around the head and neck of the child during both the mock and actual MRI scanning sessions.

*MRI Scanning Session*

All local scans were conducted using a Siemens 3T Skyra MR scanner, equipped with a 20-channel head coil, at the University of Louisville School of Medicine's Department of Radiology. Participants wore MR-compatible earphones to receive instructions and listen to the video. Foam padding was used to restrict motion if there was extra space within the head coil. A trained research team member stayed with the child during the scan to ensure comfort and monitor for excessive movement.

The Child Mind Institute Healthy Brain Network MRI data in this study were obtained from two sites: the HBN Rutgers University Brain Imaging Center, which used a Siemens Trio Tim 3T scanner, and the HBN CitiGroup Cornell Brain Imaging Center, which employed a Siemens Prisma 3T scanner. Both sites followed identical scan parameters. Comprehensive information on the scan

parameters for the Healthy Brain Network project can be found online at http://fcon_1000.projects.nitrc.org/indi/cmi_healthy_brain_network/MRI%20Protocol.html.


**Figure 2.1: Preparing participants with SCI for electrophysiology experiments.**

Panels depicting the preparation process for electrophysiology experiments with pediatric participants. In **panel A**, a participant is practicing and learning about skin preparation by cleaning the skin of the examiner. By temporarily reversing the roles in the preparation procedure, the child can gain a better understanding of what to expect and can feel more confident that the process will not be painful or uncomfortable. In **panel B**, a participant and a research team member are shown

wearing EGG caps during the introduction and preparation for the experiment to help the participant feel more comfortable and at ease. In addition to helping the participant feel more comfortable and at ease, this activity also serves a practical purpose. By demonstrating how the cap works and how it is used to measure brain activity, we can ensure the participant understands the purpose of the experiment, the importance of their cooperation in recording accurate data, and ultimately improve compliance. In **panel C**, a participant is using a grease ink pen to mark the scalp of the examiner to help to alleviate any concerns or apprehensions that the participant may have had about the procedure. In **panel D**, a participant is exploring an EKG electrode and amplifier. He had shown an interest in interest in learning how the body signals can be read and recorded by the equipment. Taking the time to engage participants' interests allows them to develop a sense of ownership and investment in the success of the experiment. These activities are part of a larger effort to help our participants better understand and participate in our experiments. Through activities like this, participants can develop a greater sense of trust and confidence, which can ultimately lead to better outcomes and more meaningful research. By providing education, reassurance, and engagement, researchers can create a more positive and effective experience for the participants.

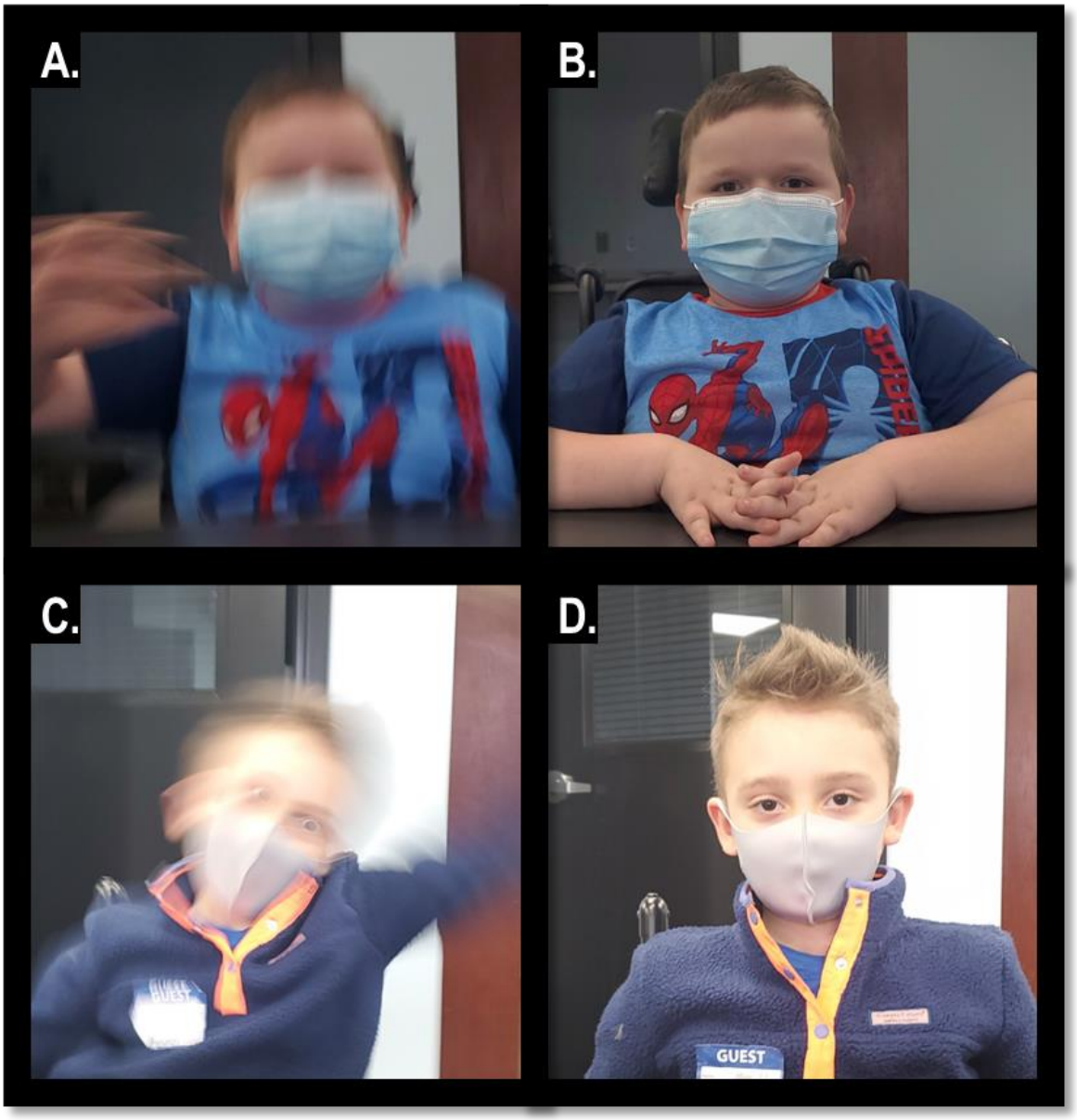


**Figure 2.2: Staying still for clear and accurate pictures.**

Panels illustrating the photoshoot section of the mock MRI session, which was meant to reinforce the importance of remaining still during MRI scans. **Panel A** shows a blurry picture of a child due to excessive movement, whereas **panel B** shows the same child in a focused picture because they remained still during the scan. Similarly, **panel C** shows another blurry picture of a child, whereas in **panel D** the same child is seen in focus, having remained still. During the mock MRI session, we asked all participants to move while taking the first picture and then to predict the quality of the picture. For the second picture, we asked participants to try to remain still and again predict the

quality of the picture. This quick interactive activity is a useful tool to help young children understand the importance of remaining still during imaging acquisition and its correlation to the accuracy and quality of the images. The activity uses the practical analogy of the MRI scanner working like a big camera. This analogy can help children understand the importance of remaining still during the scan, just like they would when taking a picture with a camera. By working with children to make the experience less intimidating and more understandable, we can obtain better quality imaging, reduce the need for repeat scans, and make the overall experience more comfortable for children.

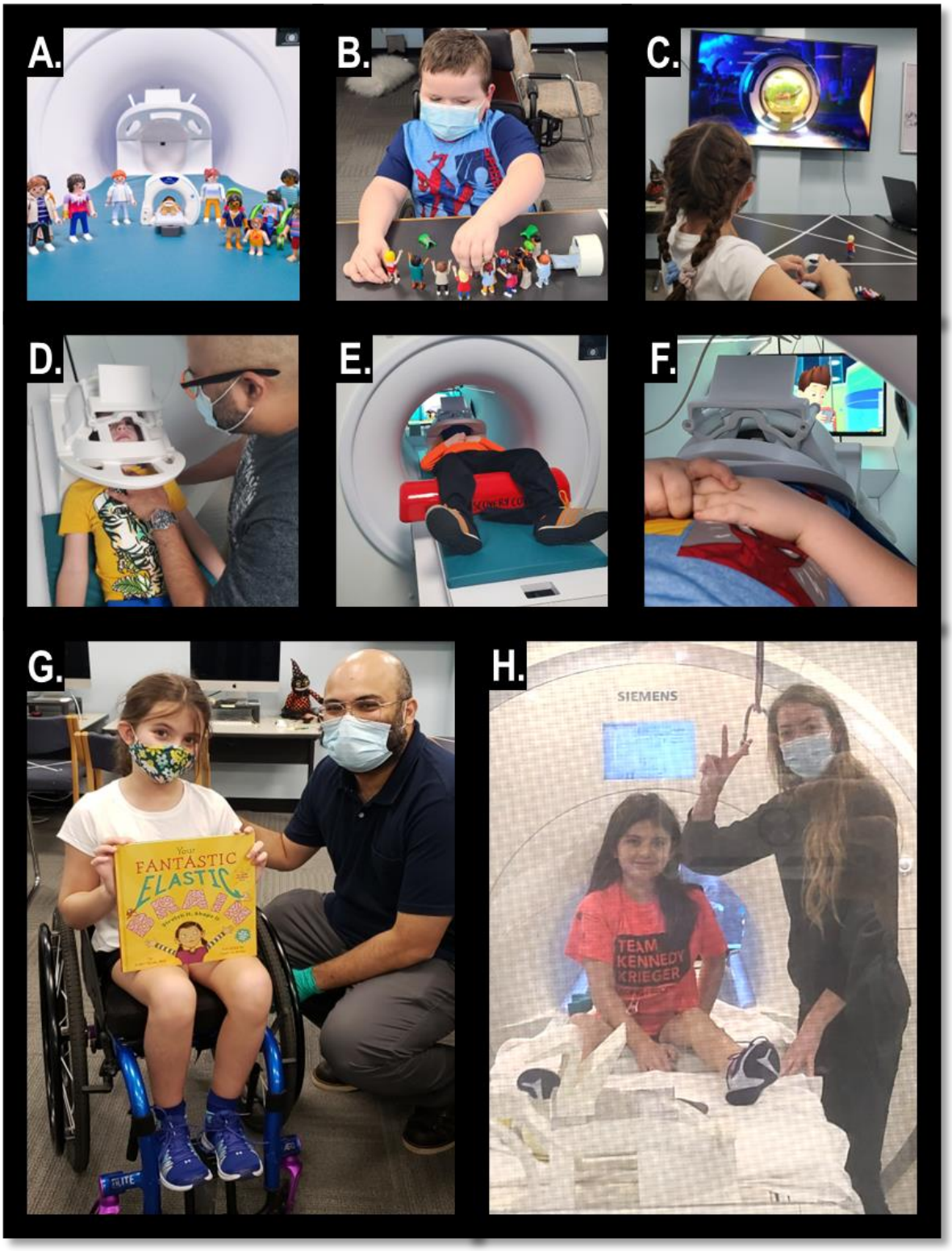


**Figure 2.3: Using games and interactive tools to prepare children for MRI scans.**

Tools and activities used to prepare children for MRI scans. The top row shows a Playmobil set **(Panel A)** that contains a toy MRI, a wheelchair, and figurines of a diverse group of adults and

children. The set was used for role-play activities **(Panel B)** to help children understand the safety concerns associated with bringing metal into the proximity of the magnetic field of the scanner. The toy set includes a wheelchair that is useful in demonstrating the potential consequences of bringing metal into the scanner. In addition to the Playmobil set, **panel C** shows a participant watching a cartoon explaining the MRI process. This provides an interactive and engaging way to help children understand what to expect during the scan. The next row shows the head coil **(Panel D)**, the bore of the mock MRI **(Panel E)**, and a media player with conditional playback activated by motion sensors **(Panel F)**. The mock scanner head coil and bore provided an opportunity for children to experience the physical space of the scanner before the actual scan, which can help reduce anxiety and fear. The media player with conditional playback allows us to control the audio and visual stimulation during the scan. Finally, the bottom row shows the end of the scanner session, where participants receive an educational book **(Panel G)** about the human brain in preparation for the real MRI **(Panel H)**. This provides a fun and informative way for children to learn more about the brain and how it functions. Overall, these different tools and activities help us prepare children for MRI scans and reduce anxiety and fear associated with the procedure. The use of the Playmobil set, informative cartoon, and interactive media player, in combination with the educational book, helped prepare children for the MRI scan and promote a positive experience.

# CHAPTER 3: ELECTROPHYSIOLOGICAL INTEGRITY OF THE PEDIATRIC SPINAL CORD AFTER SCI

## Introduction

Several neurophysiological assessments have been established and validated to provide objective evaluations of the supraspinal-spinal connectivity of spinal tracts (Boakye et al., 2012; Curt & Dietz, 1999; Curt & Ellaway, 2012; de Haan & Kalkman, 2001; Xie & Boakye, 2008). Here we utilized three non-invasive neurophysiological tests to interrogate the functional integrity of the corticospinal (CST), reticulospinal (RST), and dorsal column-medial lemniscus (DCML) pathways of children with spinal cord injuries (SCI).

The neural conduction of the CST and RST mediating volitional motor function (Baker & Perez, 2017; Brownstone & Chopek, 2018; Lemon, 2008) was assessed via functional neurophysiological assessment (FNPA) (Atkinson, 2016; Lee et al., 2004; Li et al., 2012). An acoustic startle response (ASR) (Bakker, Boer, et al., 2009; Blumenthal et al., 2005; Leitner et al., 1980) assessment tested the reflexive activity of the RST. Finally, the functional transmission of the DCML pathway was evaluated by analyzing somatosensory evoked potentials (SSEP) (Gilmore, 1992; Li et al., 1990; Singh, 2018).

All electrophysiological experiments discussed in this section included skin preparation with alcohol and occasional localized body-hair shaving to reduce impedance and increase signal fidelity. For the experiments collecting EMG data, electrodes were placed on the skin parallel to the long axis and on the belly of each muscle (Hermens et al., 2000). Instructions were provided in an age-appropriate manner, and short breaks were taken between events throughout the session. Video and audio recordings of each assessment were made to assist in preprocessing and data analysis. The maximum duration of each assessment, including preparation time, was limited to two hours.

## Ethics Statement

The studies included in this chapter were reviewed and approved by the University of Louisville Institutional Review Board (University of Louisville IRB #19.1281 and # 06.0647) in compliance with all federal and local regulations concerning the ethical use of human volunteers for research studies. The parent or legal guardian of all participants provided written informed consent to participate. Additionally, all participants older than seven gave written informed assents (University of Louisville IRB: 19.1281). To enhance the children's understanding of the study's procedures, an age-appropriate comicbook was created that detailed the experiment's purpose and protocols. The comicbook was introduced during the consent/assent meeting and frequently referenced during each experiment to ensure that the children had a clear, child-friendly understanding of the study's objectives.

## Participants

We recruited nine subjects with pediatric-onset SCI from the Human Locomotion Research Center's Potential Volunteer Database (University of Louisville IRB #06.0647), containing approximately 100 children with SCI. Families grant permission to enter their child's name and information into this approved research volunteer database and agree to be contacted by us. Potential volunteers were informed of the study and its purpose, and interested candidates were medically screened for eligibility by the study physician. The parents of candidates that met the inclusion criteria met with the investigators for an informed consent meeting.

The electrophysiological assessments described in this chapter involved nine children with SCI (7 males and 2 females; mean age = 8.8 ± 2.2 years old) and one typically developing female (7 years old). Based on the American Spinal of Injury Association (ASIA) Impairment Scale (AIS) assessment, five children had cervical injuries, and four had thoracic SCI. All SCI participants had bilateral spinal injuries, with a mean age at injury of 3.5 ± 1.8 years and a mean post-SCI period of 5.3 ± 1.8 years at the time of assessment. Table 3-1 provides clinical characteristics for each SCI participant, and Figure 3.1 presents details about motor and sensory injury levels.

### *Eligibility*

Children who fulfilled the following inclusion criteria were recruited to participate in this study:

- Children with SCI:
    - 4 and 12 years of age.
    - Acquired non-progressive SCI after they began walking, crawling, or cruising, as reported by their parent(s).
    - At least 1-year post-injury at the time of enrollment.
    - In stable medical condition without neurodevelopmental, cardiovascular, pulmonary, endocrine, or other major medical illness.
    - Discharged from inpatient rehabilitation.
    - Unable to stand, walk, or initiate steps.
- Local typically developing children:
    - 4 to 12 years old.
    - No history of SCI.
    - In stable medical condition.

We excluded participants who met any of the following exclusion criteria:

- All Participants:
    - Painful musculoskeletal dysfunction, unhealed fracture, or pressure sore.
    - Progressive neurological disease/condition.
    - Total ventilator-dependence.
    - Contraindications to MRI (e.g., metallic implants, implanted medical devices, metallic foreign bodies).

- Use of Botox, baclofen, or any other antispasmodic medication that affects the neuromuscular system's ability to respond within the past 3 months.

Basic demographic information was collected for all participants. For children with SCI, we adhered to the NINDS-CDE guidelines for children with SCI (Mulcahey et al., 2017) and documented their injury level, severity, etiology, onset age, and chronicity. Children with SCI who were over the age of six (Chafetz et al., 2009; Mulcahey et al., 2011) underwent a clinical examination and were scored on the International Standards for Neurological Classification of SCI (ISNCSCI) American Spinal Injury Association (ASIA) Impairment Scale (AIS) evaluation (Kirshblum et al., 2011) by an experienced pediatric physical therapist. Additionally, we recorded any history of previous rehabilitation interventions for children with SCI.

| | | | Injury | | | | | AIS Sensory | | AIS Motor | |
|---|---|---|---|---|---|---|---|---|---|---|---|
| ID | Sex | Age (years) | Mechanism | Age at Injury (years) | Duration (years) | AIS | AIS Level | Light Touch (max 56) R/L | Pinprick (max 56) R/L | UEMS (max 25) R/L | LEMS (max 25) R/L |
| P14 | M | 10.6 | Vehicle accident | 3.5 | 7.1 | A | C6 | 15/14 | 14/13 | 16/16 | 0/0 |
| P15 | F | 8.6 | Epidural abscess | 3.1 | 5.5 | A | T9 | 34/35 | 35/34 | 25/25 | 0/0 |
| P16 | M | 10.2 | Vehicle accident | 4.0 | 6.2 | D | C2 | 35/34 | 40/47 | 25/25 | 6/19 |
| P18 | F | 12.9 | Vehicle accident | 4.8 | 8.2 | A | T1 | 21/21 | 18/20 | 25/25 | 0/0 |
| P23 | M | 7.2 | Transverse myelitis | 2.3 | 4.8 | B | C1 | 3/2 | 3/4 | 3/3 | 0/0 |
| P24 | M | 5.8 | Spinal Hematoma | 0.9 | 4.9 | A | C1 | 22/22 | 30/27 | 23/25 | 0/0 |
| P34 | M | 6.3 | Spinal Tumor | 1.2 | 5.2 | A | C3 | 27/26 | 18/20 | 21/23 | 0/0 |
| P40 | M | 9.1 | Vehicle accident | 4.7 | 4.4 | A | T6 | 28/22 | 26/28 | 25/25 | 0/0 |
| P204 | M | 8.5 | Vehicle accident | 6.7 | 1.8 | A | T11 | 39/38 | 38/37 | 25/25 | 1/0 |

**Table 3-1: Spinal cord injury participants**

Neurologic levels are determined by sensory and motor scores on the American Spinal Injury Association Impairment Scale (AIS). AIS grades: A - complete loss of motor/sensory function below injury level; B - some sensation, no motor function; C - weak motor function; D - motor function against gravity; E - normal function. Light touch/pinprick scores range from 0-56 for each side. Arm and leg motor function scores range from 0-25 per limb. UEMS = upper extremity motor score, LEMS = lower extremity motor score. Vertebrae levels are represented by: C# = cervical vertebrae, T# = thoracic vertebrae, L# = lumbar vertebrae; F = female; M = male.

**P14 – A**

Motor Sensory

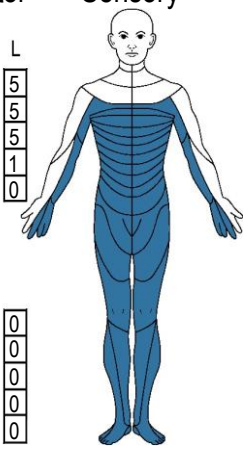

| | R | L |
|---|---|---|
| C5 | 5 | 5 |
| C6 | 5 | 5 |
| C7 | 5 | 5 |
| C8 | 0 | 1 |
| T1 | 1 | 0 |
| L2 | 0 | 0 |
| L3 | 0 | 0 |
| L4 | 0 | 0 |
| L5 | 0 | 0 |
| S1 | 0 | 0 |

**P15 – A**

Motor Sensory

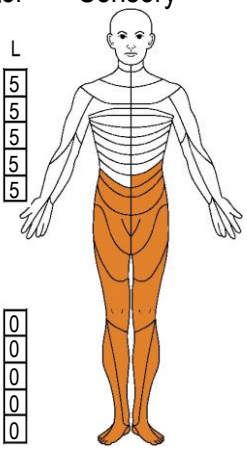

| | R | L |
|---|---|---|
| C5 | 5 | 5 |
| C6 | 5 | 5 |
| C7 | 5 | 5 |
| C8 | 5 | 5 |
| T1 | 5 | 5 |
| L2 | 0 | 0 |
| L3 | 0 | 0 |
| L4 | 0 | 0 |
| L5 | 0 | 0 |
| S1 | 0 | 0 |

**P16 – D**

Motor Sensory

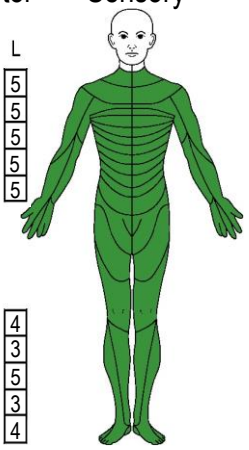

| | R | L |
|---|---|---|
| C5 | 5 | 5 |
| C6 | 5 | 5 |
| C7 | 5 | 5 |
| C8 | 5 | 5 |
| T1 | 5 | 5 |
| L2 | 2 | 4 |
| L3 | 3 | 3 |
| L4 | 0 | 5 |
| L5 | 0 | 3 |
| S1 | 0 | 4 |

**P18 – A**

Motor Sensory

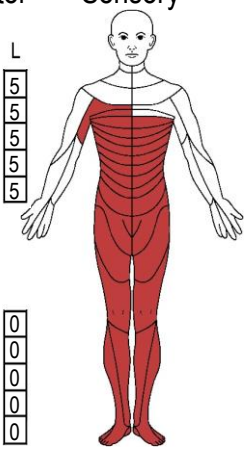

| | R | L |
|---|---|---|
| C5 | 5 | 5 |
| C6 | 5 | 5 |
| C7 | 5 | 5 |
| C8 | 5 | 5 |
| T1 | 5 | 5 |
| L2 | 0 | 0 |
| L3 | 0 | 0 |
| L4 | 0 | 0 |
| L5 | 0 | 0 |
| S1 | 0 | 0 |

**P23 – B**

Motor Sensory

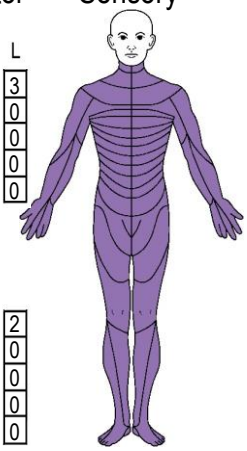

| | R | L |
|---|---|---|
| C5 | 3 | 3 |
| C6 | 0 | 0 |
| C7 | 0 | 0 |
| C8 | 0 | 0 |
| T1 | 0 | 0 |
| L2 | 0 | 2 |
| L3 | 0 | 0 |
| L4 | 0 | 0 |
| L5 | 0 | 0 |
| S1 | 0 | 0 |

**P24 – A**

Motor Sensory

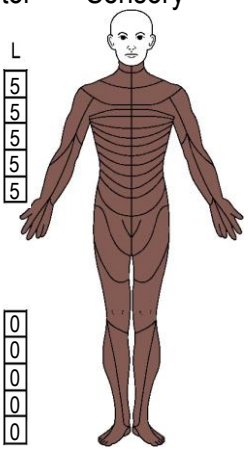

| | R | L |
|---|---|---|
| C5 | 5 | 5 |
| C6 | 5 | 5 |
| C7 | 5 | 5 |
| C8 | 5 | 5 |
| T1 | 3 | 5 |
| L2 | 0 | 0 |
| L3 | 0 | 0 |
| L4 | 0 | 0 |
| L5 | 0 | 0 |
| S1 | 0 | 0 |

**P34 – A**

Motor Sensory

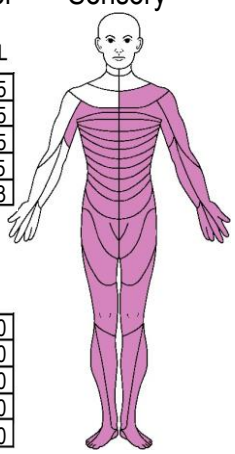

| | R | L |
|---|---|---|
| C5 | 5 | 5 |
| C6 | 5 | 5 |
| C7 | 5 | 5 |
| C8 | 3 | 5 |
| T1 | 3 | 3 |
| L2 | 0 | 0 |
| L3 | 0 | 0 |
| L4 | 0 | 0 |
| L5 | 0 | 0 |
| S1 | 0 | 0 |

**P40 – A**

Motor Sensory

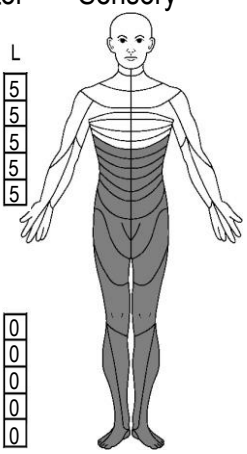

| | R | L |
|---|---|---|
| C5 | 5 | 5 |
| C6 | 5 | 5 |
| C7 | 5 | 5 |
| C8 | 5 | 5 |
| T1 | 5 | 5 |
| L2 | 0 | 0 |
| L3 | 0 | 0 |
| L4 | 0 | 0 |
| L5 | 0 | 0 |
| S1 | 0 | 0 |

**P204 – A**

Motor Sensory

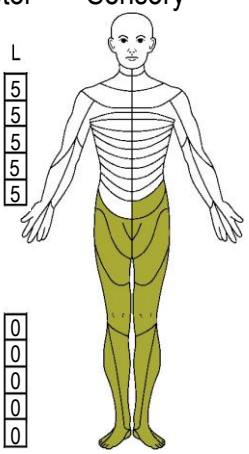

| | R | L |
|---|---|---|
| C5 | 5 | 5 |
| C6 | 5 | 5 |
| C7 | 5 | 5 |
| C8 | 5 | 5 |
| T1 | 5 | 5 |
| L2 | 1 | 0 |
| L3 | 0 | 0 |
| L4 | 0 | 0 |
| L5 | 0 | 0 |
| S1 | 0 | 0 |

**Figure 3.1: AIS motor and sensory injury levels.**

Individual panel represents the sensory and motor injury levels for each participant based on the American Spinal Injury Association Impairment Scale (AIS) standardized neurological examination. Each panel is titled with the **participant ID** and their **AIS grades**, where AIS A represents complete loss of motor and sensory function below the level of injury, AIS B represents some sensation but no motor function below the level of injury, AIS C indicates some motor function, but muscles are too weak to move against gravity, AIS D indicates some motor function with muscles strong enough to move against gravity, and AIS E represents normal motor and sensory function. **Dermatome diagrams** represent AIS sensory injury levels. Colored dermatomes correspond to a grade of 0 or 1 during the AIS sensory examination. AIS sensory grades correspond to 0 for absent sensory function, 1 for altered (hyper or hyposensitivity) function, and 2 for normal sensation. **Boxes** represent the primary spinal level responsible for innervating muscle groups tested during the AIS motor examination: C5 Elbow Flexors, C6 Wrist Extensors, C7 Elbow Extensors, C8 Finger Flexors, T1 Small finger abductors, L2 Hip flexors, L3 Knee extensors, L4 Ankle dorsiflexors, L5 Long toe extensors, and S1 Ankle plantar flexors. For each tested spinal level, the examiner assigns a motor grade from 0 (total paralysis) to 5 (normal function) to each muscle group based on the participant's ability to voluntarily move the muscle against resistance. A score of 3 or better is used to determine the motor level of a spinal cord injury.

## Experiment 1: Functional NeuroPhysiological Assessment (FNPA)

This study employed a neurophysiological approach to evaluate the neural transmission of spinal pathways responsible for voluntary motor control in children with SCI. Voluntary motor activity in humans is primarily attributed to CST mediation; however, there is strong evidence suggesting the involvement of the RST and brainstem-spinal pathways (Atkinson, 2016; Baker & Perez, 2017; Brownstone & Chopek, 2018). The neurophysiological integrity of these descending systems was assessed by a modified FNPA (Li et al., 2012) protocol.

The standard FNPA protocol has been utilized in multiple adult SCI studies (Atkinson, 2016; Dimitrijevic et al., 1992; Li et al., 2012; Sherwood et al., 1996) as a standardized and objective assessment of multi-segmental spinal motor output during specific movement attempts. To facilitate pediatric assessment, the standardized FNPA protocol was modified, as reported by Atkinson et al., 2019. Briefly, the number of tasks, muscles examined, and protocol presentation rate were reduced, and the wording of the instructions for each task was adjusted to ensure full comprehension and engagement from the subjects.

### *Hypothesis*

We hypothesized that most children with SCI would demonstrate impaired neural transmission of voluntary motor commands from the brain to muscles below their level of injury. Nonetheless, based on our previous work, some children with SCI may exhibit EMG activity below the lesion, not typically detected during clinical assessments.

## *Methods*

### *Data Acquisition*

While lying supine, participants were asked to attempt to perform a series of volitional movements as we recorded surface EMG activity. An experienced examiner explained and illustrated the nature of the movements to be completed by the participant. The start and end of each attempt were signaled by a verbal cue from the examiner and digitally marked for analysis manually by a trained technician. Each movement was attempted a minimum of three times, with each effort lasting a minimum of three seconds.

The volitional movements included left and right unilateral: elbow flexion, elbow extension, knee extension, ankle dorsiflexion, and ankle plantarflexion. We also examined bilateral shoulder elevation, hip adduction, and sitting up from supine. Surface EMG was recorded bilaterally from the upper trapezius (UT), biceps brachii (BB), triceps brachii (TB), rectus abdominis (RA), adductor group (ADD), rectus femoris (RF), tibialis anterior (TA), and medial gastrocnemius (MG) muscles. The corresponding volitional tasks and innervation for these muscles are presented in Figure 3.2.

Muscle activity was recorded using wireless surface EMG electrodes (PicoEMG, Cometa, Millan, Italy) with a fixed distance of 2.5 cm between the contacts. Electrodes were placed on the skin via self-adhesive pre-gelled silver-silver chloride disposable surface electrodes (H124SG-Covidien Kendall, Medtronic, Minneapolis, MN, USA). The EMG signal from each electrode was amplified 1,000 times and hardware band-passed filtered between 10 to 500 Hz

(Wave Wireless EMG receivers, Cometa, Milan, Italy) before being digitally sampled at 2,000 Hz using a 24-channel hard-wired analog to digital board and a custom-written software acquisition program (Labview, National Instruments, Austin, TX, USA).

Prior to the start of each movement attempt, study participants were encouraged to relax. This relaxation period was confirmed and monitored in real-time by continuous visualization of all EMG channels during acquisition. EMG activity during the volitional attempt to move was annotated with start and stop markers for each attempt of the movement maneuver. Extraneous EMG activity outside of the designated protocol was noted and excluded from further analysis.

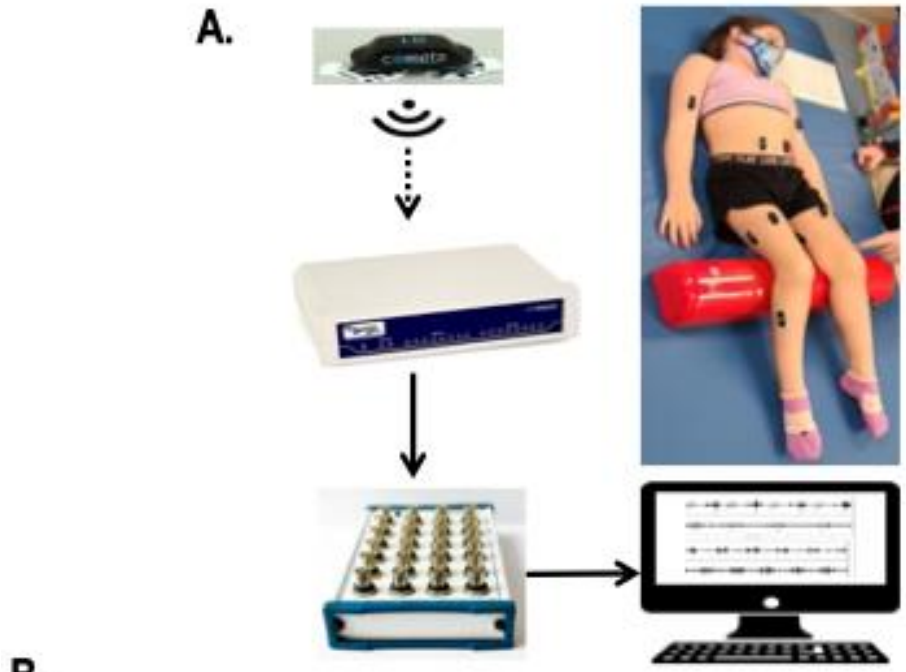


B.

| *Spinal Roots* | *Muscle* | *Task* |
|---|---|---|
| CN XI | Upper Trapezius (UT) | *Shoulder elevation* |
| C5 - C7 | Biceps Brachii (BB) | *Elbow flexion* |
| C7 - C8 | Triceps Brachii (TB) | *Elbow extension* |
| T7 - T11 | Rectus Abdominus (RA) | *Sit up* |
| L2 - L4 | Adductor Magnus (ADD) | *Bilateral hip adduction* |
| L2 - L4 | Rectus Femoris (RF) | *Knee extension* |
| L4 - S1 | Tibialis Anterior (TA) | *Ankle dorsiflexion* |
| S1 - S2 | Gastrocnemius (MG) | *Ankle plantarflexion* |

**Figure 3.2: Pediatric functional neurophysiologic assessment (FNPA) summary.**

**Panel A:** Example of the experimental setup, data acquisition, and electrode placement for the FNPA experiment. **Panel B:** Muscles from which EMG is recorded during the assessment and their respective spinal root innervation. The right-hand column lists the movements used to assess intentional activation for the applicable muscles. Written informed consent was obtained from the child's parent for the use of this image.

*Data Analysis*

The EMG signal of the primary effector muscle of each volitional task was examined during the baseline and the event time intervals. Events were defined as the interval between the examiner's cues to start and end the movement attempt. The baseline was defined as 200 milliseconds immediately before the start cue. After filtering (finite impulse response (FIR) bandpass 55 - 500 Hz), rectifying, and smoothing the raw EMG signal for each event, the mean amplitude and standard deviation values were calculated for the baseline and event intervals. For each event, primary muscle activation was defined as a rectified amplitude deflection higher than three standard deviations above the mean baseline activity. Root mean square (RMS) values for successful activations were calculated from the EMG signal of the primary mover muscle for each maneuver (see Figure 3.3). RMS values were then aggregated based on the innervation origin of each muscle for statistical comparisons. Finally, the response probability of the individual muscle was calculated by counting the total occurrence of muscle responses, dividing this number by the total number of valid trials, and multiplying this value by 100. Multiple muscles response probability was computed as the average of the response probabilities of the grouped muscles (Kofler et al., 2001a, 2001b). Results were collected into a "tidy" formatted (Wickham, 2014) tabular file for further analysis.

The Python Pandas (McKinney, 2010; Pandas, 2020) library was used for data management, while data visualization was implemented via the Matplotlib (Hunter, 2007), Seaborn (Waskom, 2021), and Statannotations (Charlier et al.,

2022) libraries. All statistical analysis was performed with the stats module of the SciPy library (Virtanen et al., 2020). Statistical comparisons of individual muscles between groups were not conducted, given that there was a single member of the TD group. We compared the RMS values for muscles grouped based on innervation between SCI and TD participants using nonparametric statistics (Mann–Whitney U) with Benjamini-Hochberg correction for multiple comparisons. Nonparametric methods were required due to violations of the normality assumption required for parametric methods and the unbalanced number of observations in each group.

*Results*

Our sole TD participant was able to produce muscle activation of the primary agonist muscles during all intentional movement tasks assessed. Participant P38 (7 year-old neurological intact female) was able to recruit 100% of the assessed muscles: UT muscles (mean RMS = 119.9 ± 41.8) during shoulder elevation, BB (RMS = 165.7 ± 58.5) during flexion of the elbows, TB (RMS = 254.9 ± 39.9) during extension of the elbows, RA (RMS = 115.2 ± 27.4) during sit-ups, ADD (RMS = 60.2 ± 4.3) during bilateral hip adductions, RF (RMS = 50.3 ± 22.4) during extension of the knee, TA (RMS = 33.9 ± 1.8) during dorsiflexion, and MG (RMS = 27.7 ± 13.9) during plantarflexion. See Figure 3.4.

The SCI group produced activations of 100% of the UT ($n_{subjects}$=9, 18/18 muscles, RMS = 101.8 ± 76.1), BB ($n_{subjects}$=9, 18/18 muscles, RMS = 115.7 ± 84.9), and TB ($n_{subjects}$=9, 18/18 muscles, RMS = 81.1 ± 57.2) muscles. While only

a few children with SCI were able to produce activations of the RA ($n_{subjects}$ =6, 12/18 muscles, RMS = 31.8 ± 35.2), ADD ($n_{subjects}$ = 1, 2/18 muscles, RMS = 5.6 ± 1.4), RF ($n_{subjects}$ = 2, 3/18 muscles, RMS = 15.2 ± 9.1), TA ($n_{subjects}$ = 1, 1/18 muscles, RMS = 8.2), and of the MG ($n_{subjects}$ = 1, 1/18 muscles, RMS = 6.8) during their corresponding movement attempts as illustrated in Figure 3.4.

While all nine SCI participants were able to generate muscle activation of the upper extremities (Figure 3.5), only two SCI participants were able to produce EMG activity in some leg muscles. Participant P16 (10 y.o. male, AIS D, motor level L2) produced EMG activity from left and right ADD and RF muscles; while only generating EMG activity from the left TA and MG. For participant P23 (7 y.o. male, AIS B, motor level C1), EMG activity was detected from the left RF during left knee extension. The other seven (AIS complete) participants produced no detectable EMG activity in the muscles of the legs.

All children with SCI were able to produce detectable activation of the primary agonist muscles during intentional movement tasks assessed above their motor injury level as defined by their AIS assessments. While about 55% of our SCI group was able to produce EMG activity from muscles innervated by spinal roots below their motor injury level. Figure 3.5 shows P14, P15, P16, P23, and P40 ability to recruit muscles distal to their AIS motor level of injury—represented by a dashed line.

Figure 3.6 – A depicts FNPA results aggregated by the motor innervation source of the muscles examined in this experiment. In panel A, Mann–Whitney tests with Benjamini-Hochberg corrections showed that there was a statistically

significant difference in the RMS values of muscles innervated by the cervical ($P$ = .006), thoracic (P = .03), lumbar ($P$ < .0001), and sacral ($P$ = .0004) levels. There were no significant differences between cranially innervated muscles among our groups ($P$ = .52). Panel B depicts the differences in the probability of eliciting a voluntary activation from muscles aggregated by their innervation origin. Statistical analysis revealed a significant decrease in the probability of muscle activations from lumbar ($P$ < .0001) and sacral ($P$ = .003) spinal levels in the SCI group. Analysis of muscles activation patterns based on their innervation origins (rostral versus caudal to the AIS motor level of injury) reveals a statistically significant lower probability ($P$ < .0001) of eliciting a response from muscles caudal to the injury site (Figure 3.6-C).

One of our SCI participants, P34, is the fraternal twin of our TD participant. A Mann-Whitney test found significant differences in the RMS values of muscles innervated by lumbar spinal cord segments ($P$ = .003) between P34 and his typically developing sister, as shown in Supplementary Figure D-0.1 A. There was a difference in the cervical innervated muscles that did not survive the multiple comparison correction. However, given lack of variance (all non-responses) and the low number of observations, the RMS values of muscles innervated by thoracic and sacral spinal segments the statistical test did not reach significance. Nonetheless, a qualitative difference in the volitional responses between P34 and his neurological intact twin sister is clearly depicted in Supplementary Figure D-0.1 A. There were, however, substantial differences in the probability of eliciting a volitional activation of muscles innervated by thoracic, lumbar, and sacral, spinal

segments. In Supplementary Figure D-0.1 B, we see that the P34 was unable to voluntarily activate the primary mover muscles for tasks that required thoracic, lumbar, and sacral mediation.

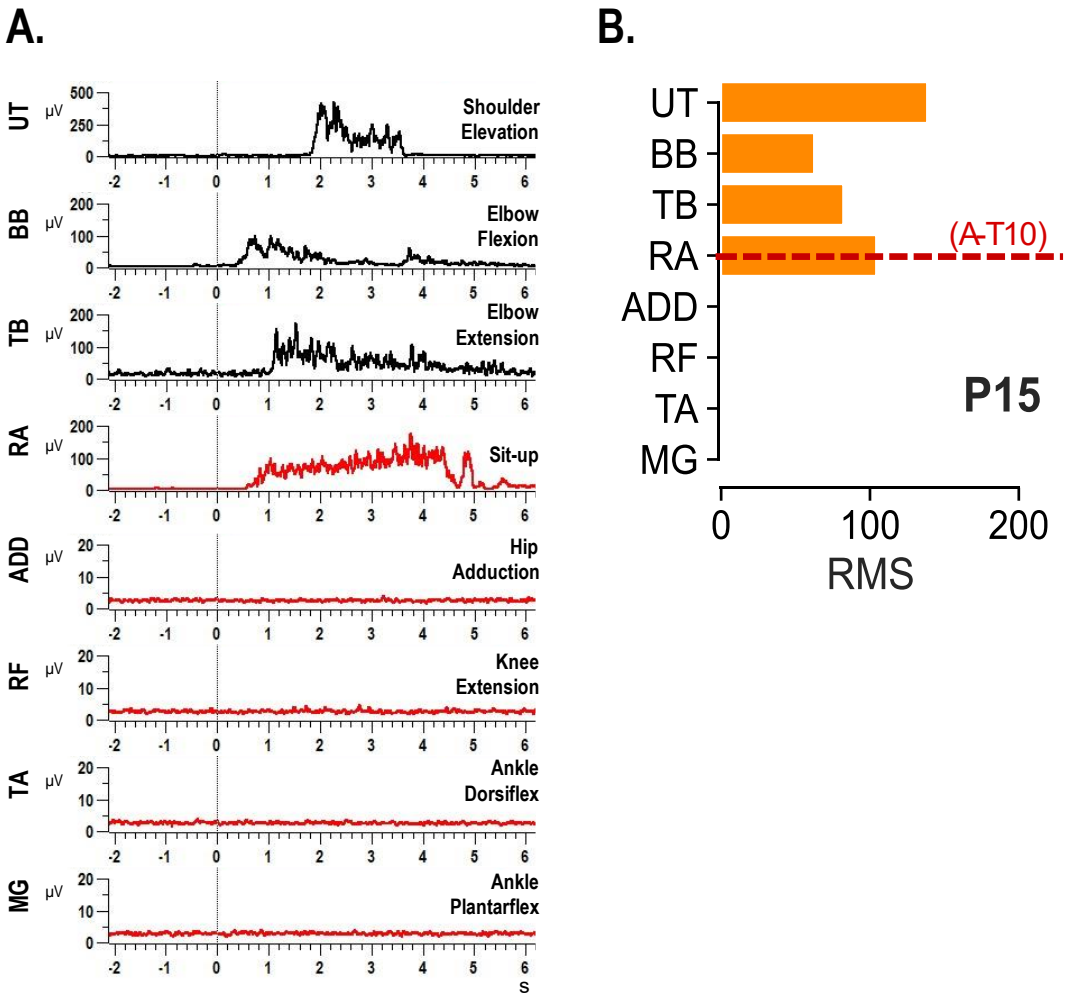


**Figure 3.3: Representative muscle recruitment pattern during FNPA.**

**Panel A:** Representative filtered, rectified, and smoothed EMG traces of a child with SCI (8 y.o. female, AIS A, motor level T10) demonstrating the muscle activation patterns observed during a single trial of each FNPA volitional task as indicated by the labels to the right of each trace. Black EMG traces represent muscles innervated by spinal roots above the motor level of injury. Muscles with innervation below the motor level of injury are represented by red traces. The vertical lines at time = 0 denote the verbal cue to attempt the corresponding motor task. Muscle activation was defined as a post-verbal-cue amplitude deflection greater than three standard deviations above the mean EMG amplitude during a 200-millisecond interval right before the verbal cue. Timebase: 1 s/division. **Panel B:** Horizontal bars represent the mean root mean square (RMS) value calculated

for muscles with detectable activation. The horizontal dashed line and the information within the parenthesis denotes the ASIA AIS grade and motor level of injury. UT, upper trapezius; BB, biceps brachii; TB, triceps brachii; RA, rectus abdominis; ADD, adductor magnus; RF, rectus femoris; TA, tibialis anterior; MG, medial gastrocnemius muscles.

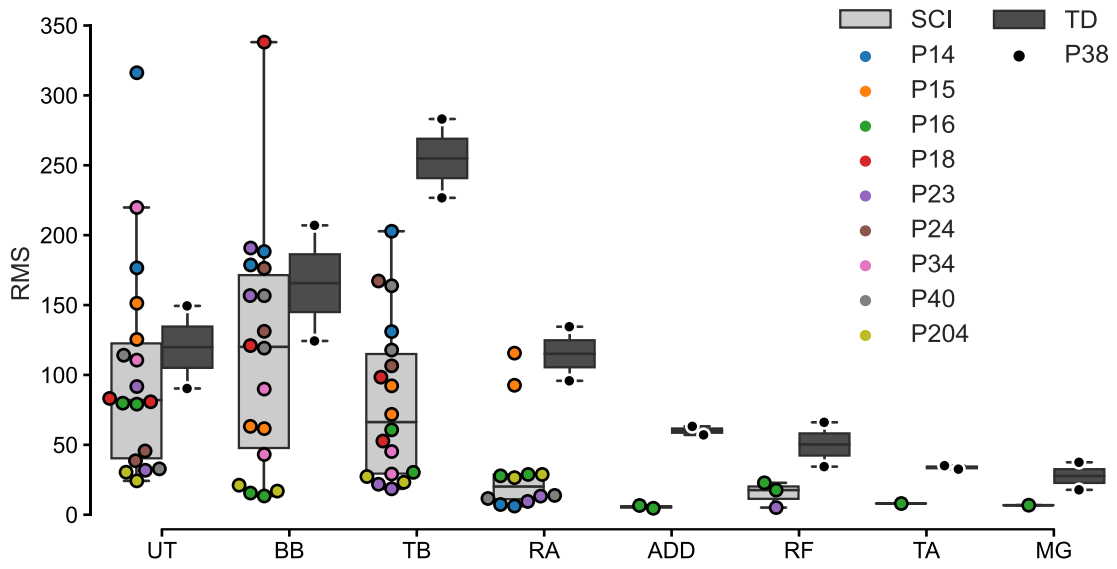


**Figure 3.4: Group FNPA results.**

Data are shown as box plots depicting root mean square (RMS) group means of the EMG activity of the primary agonist muscle during volitional tasks of the FNPA. Boxes bound the interquartile range (IQR) and are transected by a line representing the median. Whiskers extend to 1.5 times the IQR. Gray boxes indicate the SCI group (n=9) RMS values. Circles with color denote individual RMS values for the left and right muscles of each individual SCI participant. Data points of non-responses were omitted from the graph for clarity. Colors are coded to each SCI participant in all other figures within this chapter. Black boxes represent participant P38—a neurological intact 7 years-old female. Black circles denote individual RMS values for the left and right muscles of P38. UT, upper trapezius; BB, biceps brachii; TB, triceps brachii; RA, rectus abdominis; ADD, adductor magnus; RF, rectus femoris; TA, tibialis anterior; MG, medial gastrocnemius muscles.

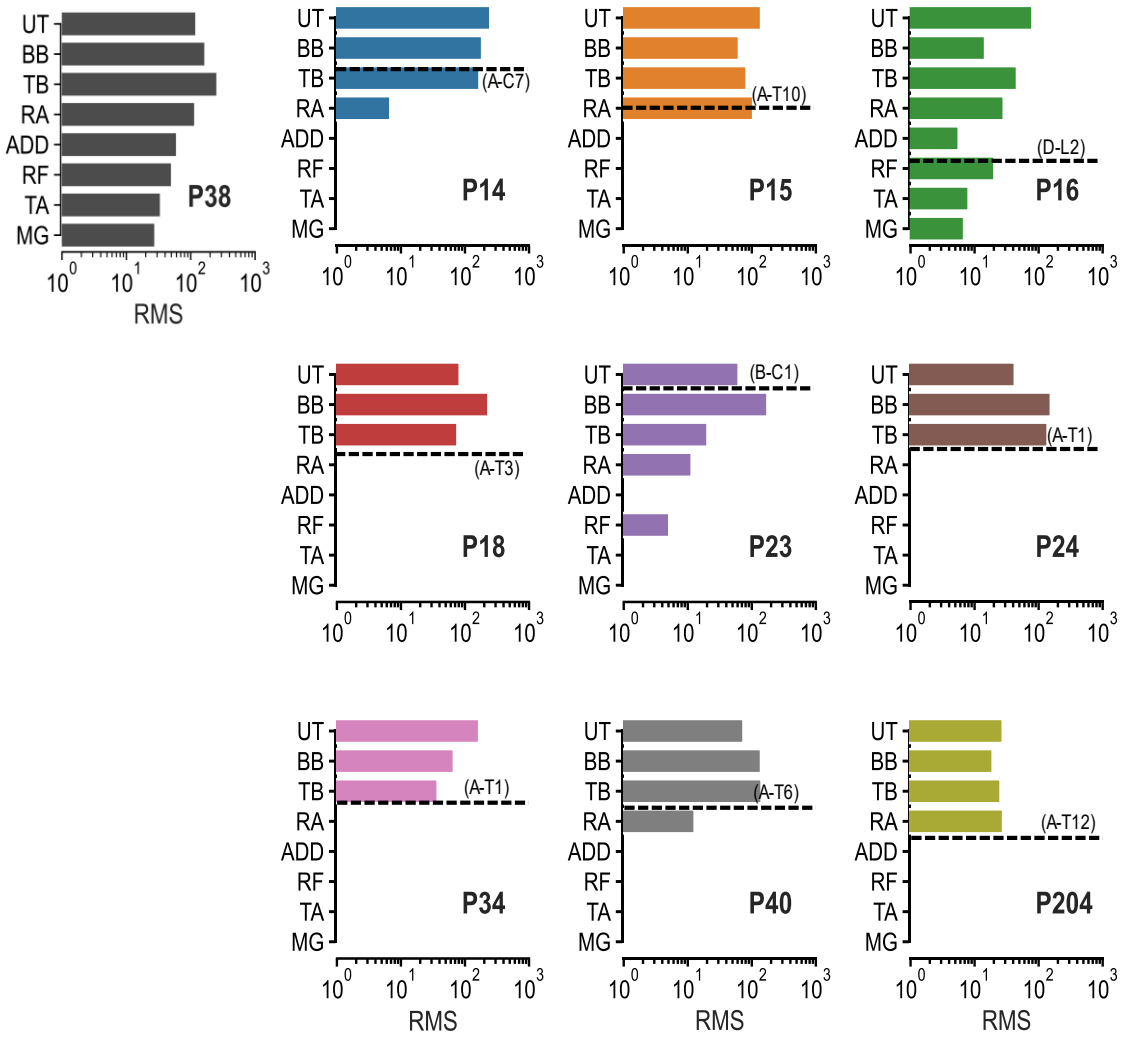


**Figure 3.5: Individual FNPA results.**

Bar graphs of each participant in this experiment depicting the average root mean square (RMS) of the EMG activity of the primary agonist muscle (in log scale) during three trials of each volitional task of the FNPA. Black bars represent a neurological intact 7 years-old female. Bars with color are coded to each SCI participant in all other figures within this chapter. Horizontal dashed lines and the information within the parentheses denote the ASIA AIS grade and motor level of injury for each participant. UT, upper trapezius; BB, biceps brachii; TB, triceps brachii; RA, rectus abdominis; ADD, adductor magnus; RF, rectus femoris; TA, tibialis anterior; MG, medial gastrocnemius muscles.

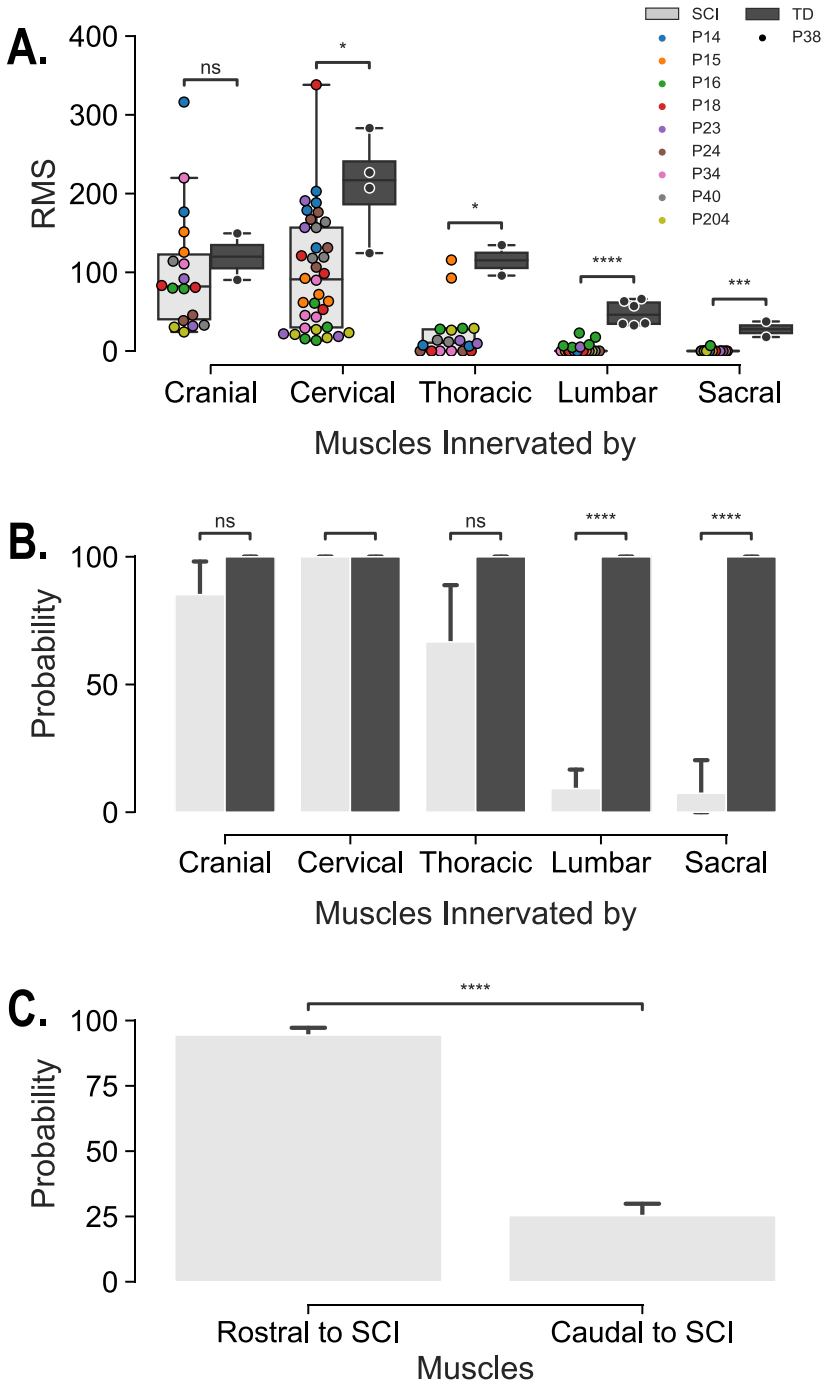


**Figure 3.6: FNPA results aggregated by muscle innervation input.**

**Panel A:** Box plot of activation patterns for muscles grouped by their innervation source (Cranial = upper trapezius; Cervical = biceps and triceps brachii; Thoracic = rectus abdominis; Lumbar = adductor magnus, rectus femoris, and tibialis anterior; and Sacral = medial gastrocnemius). Boxes

bound the interquartile range (IQR) and are transected by a line representing the median. Whiskers extend to 1.5 times the IQR. Gray boxes indicate the SCI group RMS values. Circles with color denote individual RMS values for the left and right muscles of individual SCI participants. Colors are coded to each SCI participant in all other figures within this chapter. Black boxes represent participant P38—a neurological intact 7 years-old female. Black circles denote individual RMS values for the left and right muscles of P38. **Panel B:** Bar plot comparing the probabilities of EMG activation of the primary agonist muscles aggregated by their innervation origin during volitional motor tasks between the SCI and TD group. **Panel C:** Bar plot of the probability of volitional EMG activation from muscles caudal and rostral to the AIS motor injury segment. Muscles caudal to the motor injury level are significantly less probable to generate a volitional activation. Bars represent means. The length of the error bars is the 95% confidence interval for the mean. Data were analyzed using Mann–Whitney U tests for nonparametric data with Benjamini-Hochberg corrections for multiple comparisons. (* $P < .05$; ** $P < .01$; *** $P < .001$; **** $P < .0001$).

*Discussion*

In this study, we used an established neurophysiology assessment to assess the neural transmission of supraspinal volitional motor signals in the spinal cord of children with SCI and one TD child. As expected, our sole TD participant was able to recruit all primary agonist muscles during intentional movements. The muscle activation patterns produced by this participant are consistent with previously published TD children's recruitment patterns (Atkinson et al., 2019). This coherence serves as an internal validation of our data acquisition and analysis procedures.

This experiment revealed a diverse range of motor abilities across nine pediatric SCI participants, as summarized in Figure 3.5. Out of nine children with SCI, five (3 AIS A, 1 AIS B, and 1 AIS D) were able to produce volitional muscle activity below their AIS motor injury level during attempts to produce isolated movements. In addition, the two participants with incomplete SCI were also able to activate at least one lower limb muscle. These findings align with previous reports that many adults (Lim et al., 2005; Sherwood et al., 1996) and children (Atkinson et al., 2019) with SCI demonstrate the ability to recruit muscles caudal to injury, regardless of injury level or severity.

Given the unbalanced number of participants in the SCI and TD groups, a direct statistical comparison of the recorded muscles was not conducted. However, as reported in Figure 3.6, nonparametric analysis of the aggregation of multiple muscles based on the origin of their innervation inputs suggest a significant

reduction in the neural transmission of supraspinal volitional motor signals to spinal segments caudal to the injury site.

Our findings support the notion that descending supraspinal inputs onto the spinal motor circuitry across the injury site persists even in children deemed as motor and sensory complete after a clinical AIS assessment. These residual supraspinal inputs may play a meaningful role in the neurorehabilitation and recovery of any volitional motor function after pediatric-onset SCI. Recently several seminal studies have demonstrated that in chronic motor complete adults with SCI, residual supraspinal inputs are capable of transmitting volitional motor signals to spinal networks after intensive activity-based locomotor training in combination with epidural electrical stimulation of the lumbosacral spinal cord (Angeli et al., 2018; Angeli et al., 2014; Harkema et al., 2011). Transcutaneous stimulation of the injured spinal cord is proving promising as an effective non-implanted (Gad et al., 2018; Gerasimenko et al., 2015; Sayenko et al., 2015) alternative to epidural stimulation to achieve functional recovery of sensorimotor function.

This non-implanted stimulation paradigm represents a promising development for neurorehabilitation of children with SCI, offering numerous potential benefits by circumventing the need for surgical implantation. The groundwork laid by this study will serve as one component of a battery of neurophysiology assessments intended to study the viability and efficacy of transcutaneous stimulation combined with activity-based locomotor training in children with SCI to enable stepping in children who are non-ambulatory due to SCI. The data collected in this experiment has already served as preliminary work

for an institutional grant awarded to our group from the Kentucky Spinal Cord and Head Injury Research Board (Neuromodulation of spinal locomotor circuitry to elicit stepping after pediatric spinal cord injury, University of Louisville IRB # 19.1281).

## Experiment 2: Acoustic Startle Reflex (ASR)

The ASR (Bakker, Boer, et al., 2009; Blumenthal et al., 2005; Brownstone & Chopek, 2018) is a defensive reflexive response to unexpected stimuli that starts in the ventral cochlear nucleus (Brownstone & Chopek, 2018; Lemon, 2008), and from there diverges. Part of the signal travels to the motoneurons in the midbrain reticular formation, and the other takes a turn caudally from the pontine RF towards the spinal cord via the reticulospinal tract (RST) (Valls-Sole et al., 2008). The rostral division to the midbrain reticular formation will drive a fast contraction of the orbicularis oculi muscles almost 99% of the time. The caudal signal drives a slower and probabilistic response that includes the contraction muscle of the neck, flexion of the trunk, and some arm and leg muscles.

We studied this startle reflex as a surrogate of the functional integrity of the RST of children with SCI. We compare the probability of these ASR responses to publicly available normative data (Bakker, Boer, et al., 2009).

### *Hypothesis*

We expected that children with SCI would exhibit a higher probability of eliciting an ASR response above the injury level and extinguished responses below the motor injury level.

### *Methods*

#### *Data Acquisition*

ASR assessments were conducted in a dark quiet room with subjects lying supine while playing a game projected on the ceiling consisting of trying to spot the differences between two almost identical pictures with the purpose of reducing the possibility of boredom and confounding movements (see Chapter 2). For similar reasons, the assessments were held to a maximum length of two hours from the participant's arrival.

After skin preparation, Electrodes for ECG measurements (Nissha Medical Technologies, NeuroPlus Ag/AgCl electrodes of 19mm$^2$ area) were placed according to a standard lead II configuration. For EMG measurements, small cloth electrodes (Nissha Medical Technologies, NeuroPlus Ag/AgCl electrodes of 19mm2 area) were placed below each eye and on the thenar eminence and connected to wired three lead pre-amplified electrodes (Motion Lab Systems MA-420) to assess EMG activity of the orbicularis oculi and abductor pollicis brevis muscles respectively. We recorded the EMG activity of the deltoid, paraspinal thoracic, rectus abdominis, rectus femoris, and tibialis anterior muscles by placing wired pre-amplified electrodes equipped with two 12 mm stainless steel sensor disks at a static inter-electrode distance of 17 mm (Motion Lab Systems MA-411n). The reference electrode was placed on the tibia. Headphones (Sennheiser electronic GmbH & Co. KG, HD 202) were placed over the ears. Figure 3.7 presents a schematic of the experimental setup.

Participants were informed about the experimental procedures with age-appropriate languages and instructed to relax, neither speak nor move, and to find differences in the pictures projected on the ceiling while keeping the answers in

their minds until they heard the beep. Playing this game served as a distraction to prevent the participant from concentrating on or anticipating the auditory stimulus and thus maintaining its startle effect. During picture viewing, an acoustic startle probe was administered at pseudo-random intervals ranging from 2.5 to 3 minutes after picture onset. The stimulus marked the end of a game and participants were encouraged to share their findings and play the rest of the game out loud until all the differences were found. The next picture prompted the start of a new period of silence and concentration. During the course of the assessment, participants were presented with at least five binaurally acoustic stimuli (1,000 Hz, 105 dB of sound pressure level, and 120 milliseconds duration) with instantaneous rise and fall times (Blumenthal et al., 2005). To prevent cardiac modulation of the ASR (Schulz et al., 2009), the acoustic stimuli were presented during the diastolic phase of the cardiac cycle.

A Power1401-3A and Spike2 system (Cambridge Electronic Design Limited, Cambridge, England) was utilized for stimulus generation and EMG signal acquisition. The analog signal from each EMG electrode will be amplified 2,000 times, hardware band-passed filtered between 40 to 1000 Hz, and digitally sampled at 5,000 Hz.

A.

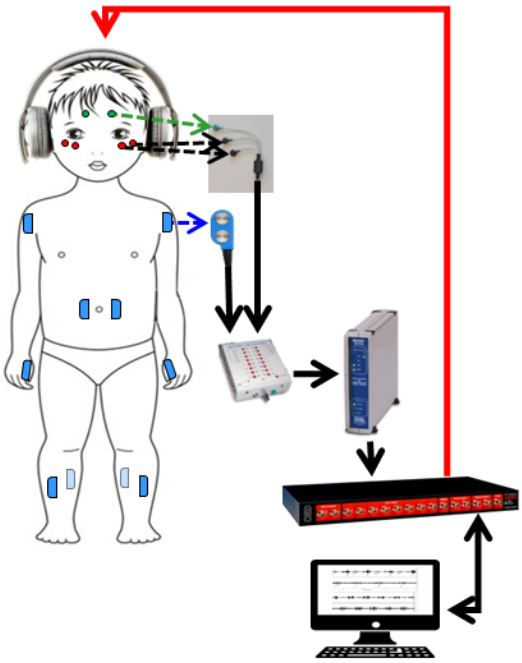

B.

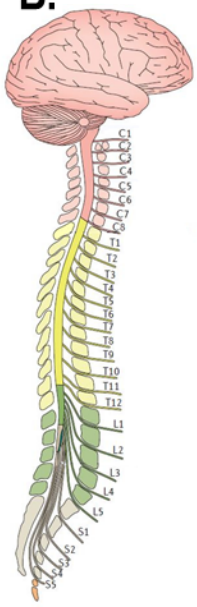

| *Spinal Roots* | *Muscle* |
|---|---|
| CN-VII | Orbicularis Oculi (OOC) |
| C5 - C6 | Deltoid (DEL) |
| C8 - T1 | Abductor Pollicis Brevis (APB) |
| C1 - T10 | Paraspinal Muscles (PS) |
| T7 - T11 | Rectus Abdominus (RA) |
| L2 - L4 | Rectus Femoris (RF) |
| L4 - S1 | Tibialis Anterior (TA) |

**Figure 3.7: Acoustic startle reflex (ASR) setup**

**Panel A:** Example of the experimental setup, data acquisition, and electrode placement for the ASR experiment. **Panel B:** Muscles from which EMG is recorded during the assessment and their respective spinal root innervation. Written informed consent was obtained from the child's parent for the use of this image.

*Data Analysis*

Offline data analysis was performed using Spike2 software (Cambridge Electronic Design Limited, v9). We digitally filtered orbicularis oculi signals with a bandpass FIR filter of 100 – 500 Hz to mitigate DC offsets and slow eye drifts (Aramideh et al., 1995). The bandpass frequency of all other muscles was 55 – 500 Hz. This distinction in bandpass filtering was implemented to isolate the orbicularis oculi EMG activity from superimposed cornea-retina potentials resulting from eye movements elicited during blinking with frequencies up to 70 Hz (Bakker, Boer, et al., 2009; Bour et al., 2000). Subsequently, the RMS amplitude for each signal was calculated with a time-period of 0.002 seconds. A response was defined as a rectified amplitude deflection higher than 3 standard deviations above the mean baseline activity for at least 30 ms within the a priori established onset window (Brown et al., 1991b; Oguro et al., 2001). For the orbicularis oculi muscle, we included responses with onset latencies between 20 and 100 ms in the analysis. For the other muscles, onset latencies were between 20 and 200 ms. EMG activity related to artifacts (e.g., cardiac signals, loose electrodes, and incidental blinks) was marked and excluded from further analysis.

The response probability of the individual muscle was calculated by counting the total occurrence of muscle responses, dividing this number by the total number of valid trials, and multiplying this value by 100 (see

Figure 3.8). Multiple muscles ASR response probability was computed as the average of the response probabilities of the grouped muscles (Kofler et al.,

2001a, 2001b). Probabilities were collected into a “tidy” format (Wickham, 2014) tabular file for further analysis.

The Python Pandas (McKinney, 2010; Pandas, 2020) library was used for data management while data visualization was implemented via the Matplotlib (Hunter, 2007), Seaborn (Waskom, 2021), and Statannotations (Charlier et al., 2022) libraries. All statistical analysis was performed with the stats module of the SciPy library (Virtanen et al., 2020). Statistical comparisons of individual muscles between groups were not conducted given that there was a single member of the TD group. We compared the RMS values of muscles grouped based on innervation between SCI and TD participants using nonparametric statistics (Mann-Whitney *U*) with Benjamini-Hochberg correction for multiple comparisons. Nonparametric methods were required due to violations of the normality assumption required for parametric methods and the unbalanced number of observations in each group.

*Results*

ASR assessment of a 7-year-old typically developing female child resulted in EMG responses probabilities of 100% for the orbicularis oculi (OOC), 20% for the deltoid (DEL), 10% for the abductor pollicis brevis (APB), 20% for the thoracic paraspinal group (PS), 30% for the rectus abdominis (RA), 10% for the rectus femoris (RF), and 10% for the tibialis anterior (TA) muscles. By contrast, after auditory stimulation of our nine children with SCI, the probabilities of eliciting an EMG response were OOC: = 96.9%, DEL = 58.6%, APB = 61.6%, PS = 67.6%, And RA = 25.2%. No responses were detected from lower extremities muscles (RF

and TA) in these nine children. These results are presented in tabular format in Table 3-2 and depicted in Figure 3.9. Of note, 7 out of the 9 children with SCI presented ASR responses across their level of injury (Figure 3.10) as determined by the American Spinal Injury Association impairment scale (AIS) motor neurological level (Figure 3.1 and Appendix C. ASIA Reports).

Figure 3.11 shows ASR results aggregated by the motor innervation source of the muscles examined in this experiment. The probabilities of eliciting a startle response from the OOC are identical for the participant in the SCI group and the one TD participant. No responses were recorded from muscles with lumbar innervation in the SCI group and there were no statistically significant differences found in the thoracically innervated muscles between the groups. The central tendency of the cervical muscles was significantly different between the groups before the correction for multiple comparisons. A visual inspection of the distribution of these results, however, reveals that a subgroup of the SCI participants presents with elevated probabilities of responding to the auditory stimulus from muscles innervated by cervical and thoracic spinal segments.

A qualitative inspection of these responses revealed two distinct patterns in the ASR responses among the nine SCI children. 66% of the participants exhibit high ASR response probabilities of arms and trunk muscles, as illustrated in Figure 3.12. While participants P14 (10 years old male, AIS A, Motor Level C7), P40 (9 years old male, AIS A, Motor Level T6), and P204 (8 years old male, AIS A, Motor Level T11) presented with a low probability of ASR responses from arms and trunk

muscles similar to the response pattern of our one TD subject. Figure 3.13-A illustrates these two distinct patterns.

Finally, a graphical summary of the motor tract transmission of each SCI participant, as assessed by experiments 1 and 2, is presented in Figure 3.14.

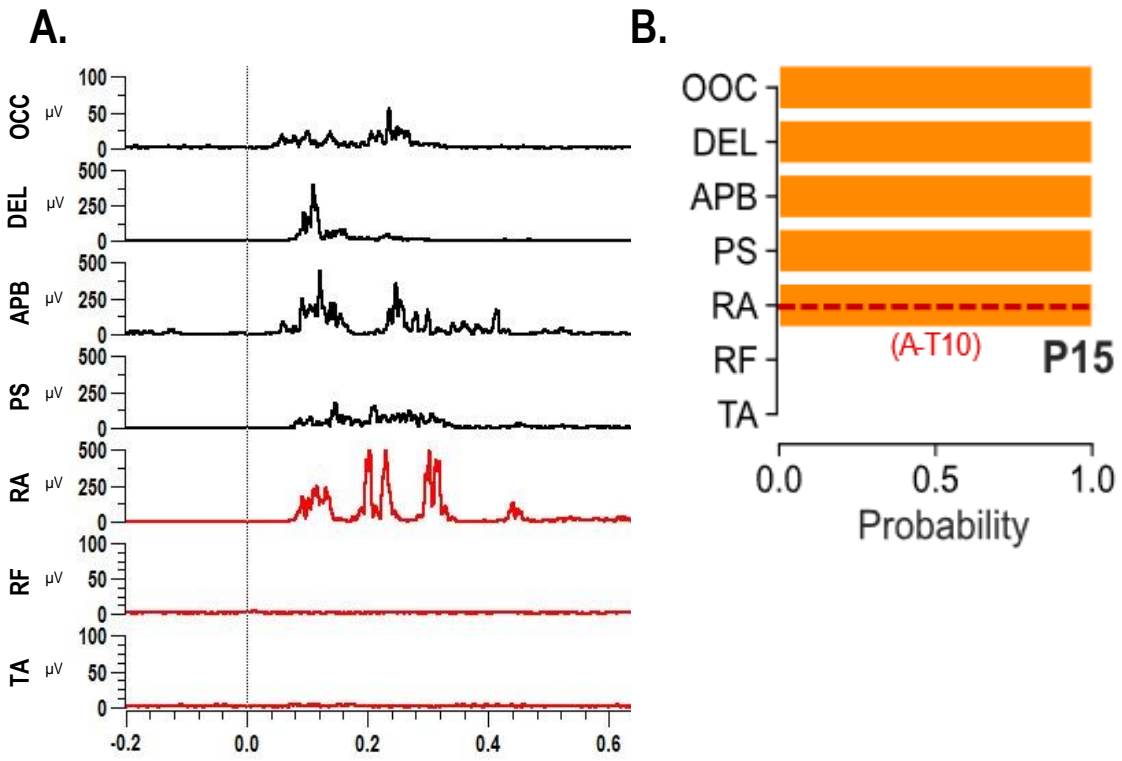


**Figure 3.8: Representative muscle recruitment pattern during ASR**

**Panel A:** Representative EMG recordings from a child with SCI (8 y.o. female, AIS A, motor level T10) demonstrating the muscle activation patterns observed during a single trial of the ASR protocol. Black EMG traces represent muscles innervated by spinal roots above the motor level of injury. Muscles with innervation below the motor level of injury are represented by red traces. The vertical lines at time = 0 denote the acoustic stimulation. ASR response was defined as a post-acoustic-stim amplitude deflection greater than three standard deviations above the mean EMG amplitude during a 200-millisecond interval right before the tone. **Panel B:** The root mean square (RMS) value was calculated for muscles with detectable activation. The horizontal red dashed line and the information within the parenthesis denotes the ASIA AIS grade and motor level of injury for this participant. OOC, orbicularis oculi; DEL, deltoid; APB, abductor pollicis brevis; PS, paraspinal; RA, rectus abdominis; RF, rectus femoris; TA, tibialis anterior.

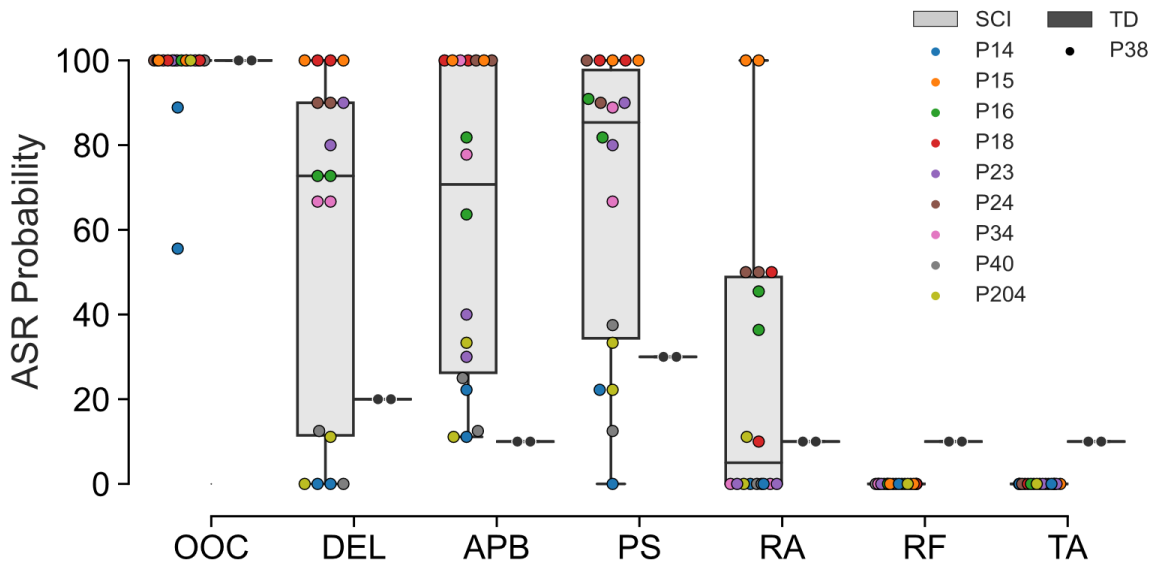


**Figure 3.9: Aggregate ASR results**

Box plots depicting group ASR probabilities of seven simultaneously monitored muscles. Boxes bound the interquartile range (IQR) and are transected by a line representing the median. Whiskers extend to 1.5 times the IQR. Gray boxes indicate the SCI group (n=9) probabilities values. Circles with color denote individual participant ASR probabilities. Colors are coded to each SCI participant in all other figures within this chapter. Black boxes represent participant P38—a neurological intact 7 years-old female. Black circles denote individual ASR probability values for P38. OOC, orbicularis oculi; DEL, deltoid; APB, abductor pollicis brevis; PS, paraspinal; RA, rectus abdominis; RF, rectus femoris; TA, tibialis anterior.

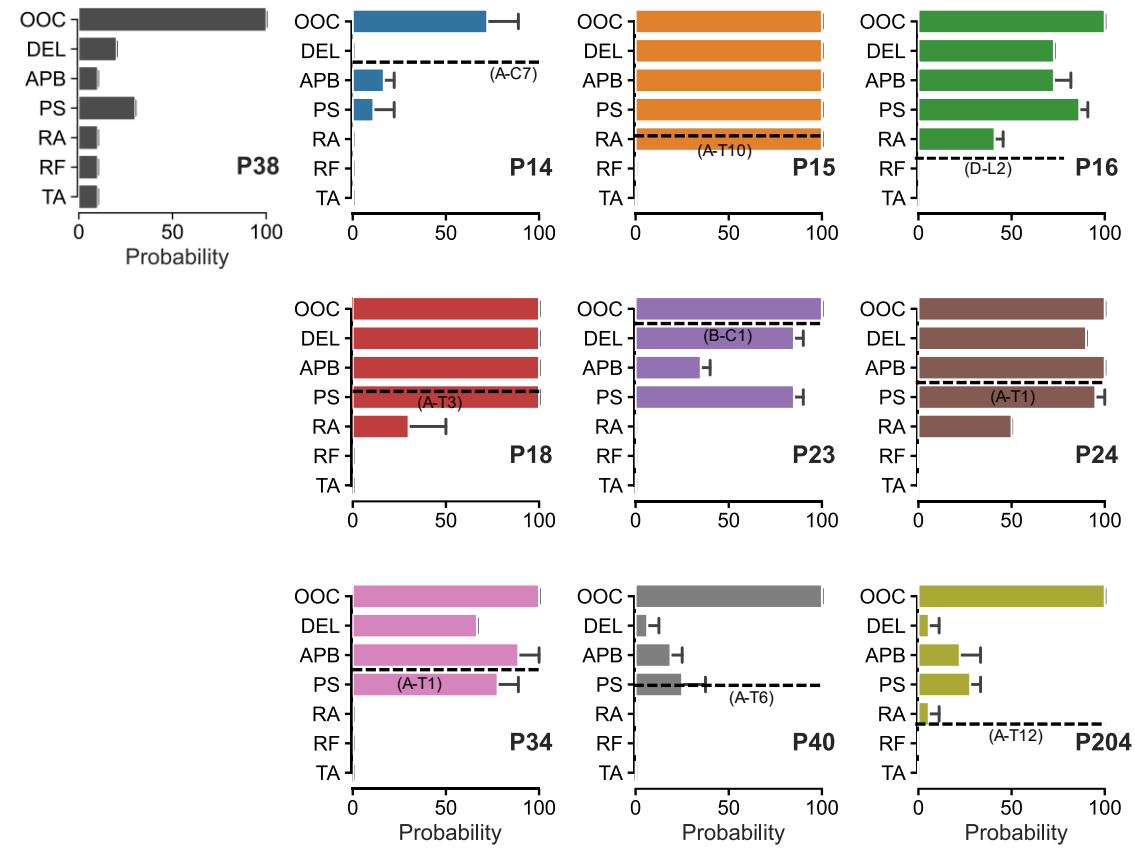


**Figure 3.10: Individual ASR results**

Bar plots of each participant in this experiment depicting their average ASR probability of a response. Black bars represent a neurological intact 7 years-old female. Bars with color are coded to each SCI participant in all other figures within this chapter. Horizontal dashed lines and the information within the parentheses denote the ASIA AIS grade and motor level of injury for each participant. OOC, orbicularis oculi; DEL, deltoid; APB, abductor pollicis brevis; PS, paraspinal; RA, rectus abdominis; RF, rectus femoris; TA, tibialis anterior.

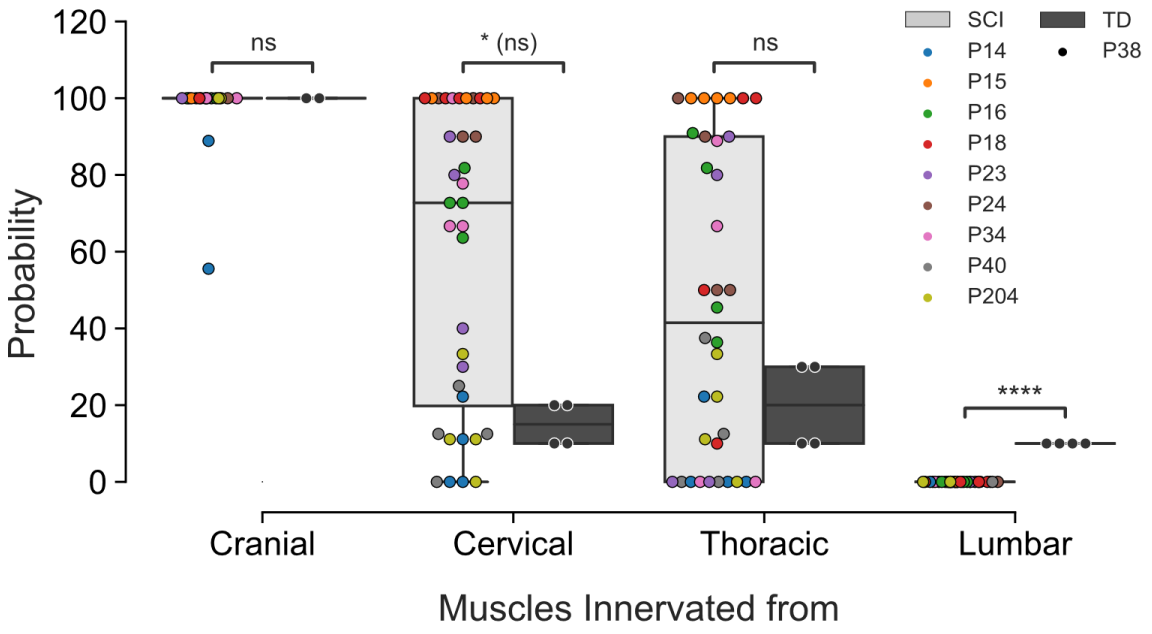


**Figure 3.11: ASR results aggregated by muscle innervation input**

Box plot of the probability of eliciting an ASR response in muscles grouped by their innervation source (cranial = orbicularis oculi; cervical = deltoid and abductor pollicis brevis; thoracic = paraspinal and rectus abdominis; and Lumbar = rectus femoris and tibialis anterior). Gray boxes indicate the SCI group probabilities. Colored circles denote individual probabilities for left and right muscles of each individual SCI participant. Colors are coded to each SCI participant in all other figures within this chapter. Black boxes represent participant P38—a neurological intact 7 years-old female. Black circles denote individual probabilities for the left and right muscles of P38. Boxes bound the interquartile range (IQR) and are transected by a line representing the median. Whiskers extend to 1.5 times the IQR. Data were analyzed using Mann–Whitney U test for nonparametric data with Benjamini-Hochberg corrections for multiple comparisons. (* P < .05; ** P < .01; *** P < .001; **** P < .0001).

| *Spinal Roots* | *Muscle* | *SCI Response Probability (mean and SD)* | *Normative Data Bakker 2009 (mean and SD)* | *7 y.o. TD Female* |
|---|---|---|---|---|
| CN VII | OOC | 96.9% (8.7) | 78.2% (40.0) | 100% |
| C5-C6 | DEL | 58.5% (39.9) | 2.8% (16.5) | 20% |
| C8-T1 | APB | 61.6% (35.6) | 3.4% (18.1) | 10% |
| C1-T10 | PS | 67.6% (33.7) | nr | 20% |
| T7-T11 | RA | 25.2% (32.3) | nr | 30% |
| L2-L4 | RF | 0% | 2.8% (16.4) | 10% |
| L4-S1 | TA | 0% | nr | 10% |

**Table 3-2: ASR probabilities**

Auditory startle reflex response probability of individual muscles in children with SCI and controls. Abbreviations: OOC, orbicularis oculi; DEL, deltoid; APB, abductor pollicis brevis; PS, paraspinal; RA, rectus abdominis; RF, rectus femoris; TA, tibialis anterior. Results from muscles not reported by Bakker et al. 2009 are identified as nr.

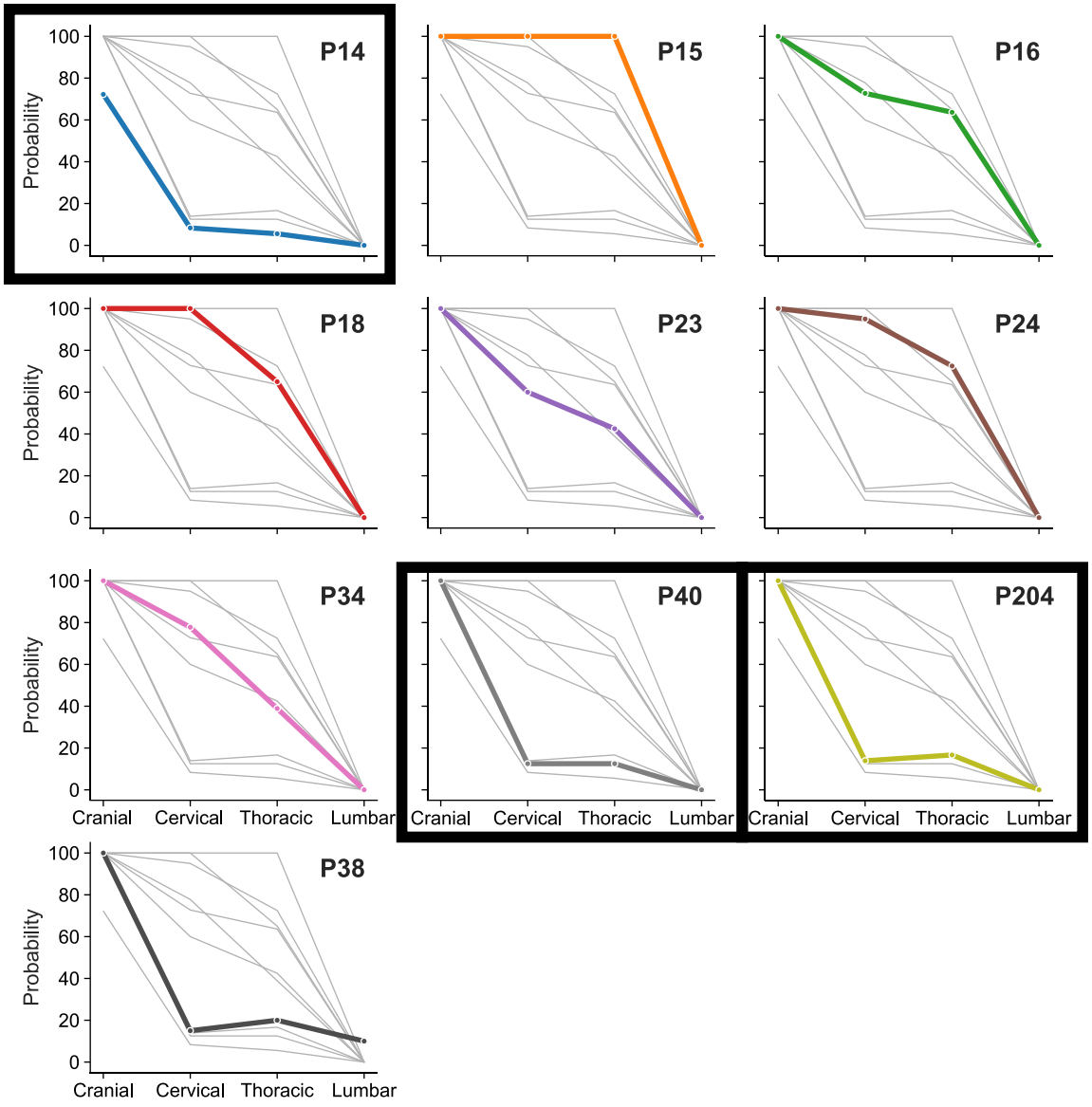


**Figure 3.12: Individual ASR recruitment patterns**

Probability of a response in children with SCI (color-coded traces) following startle auditory stimuli aggregated by spinal levels. Participants P14, P40, and P204 (black frames) do not exhibit the exaggerated ASR commonly associated with SCI. Their recruitment pattern closely resembles the response pattern from the TD participant—P38.

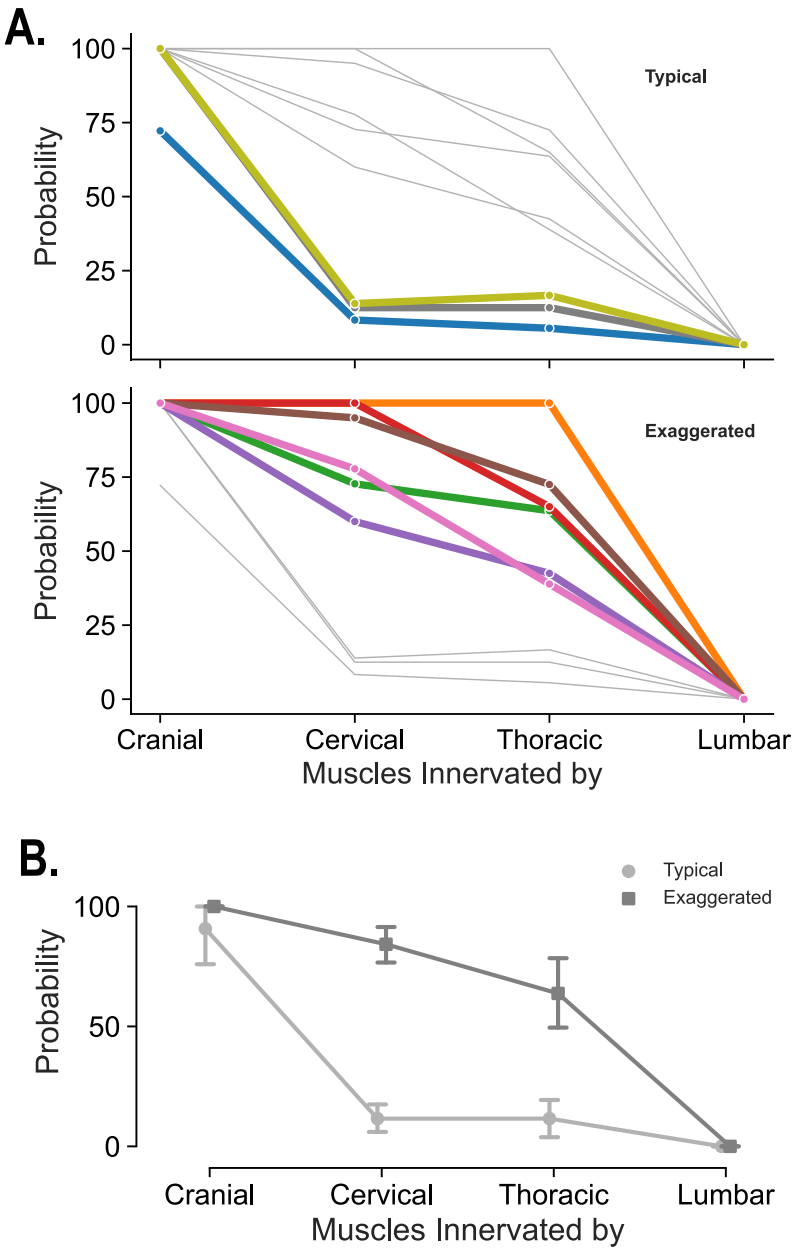


**Figure 3.13: Two distinct ASR probability patterns in Children with SCI**

**Panel A:** Probability of a response in children with SCI (color-coded traces) following startle auditory stimuli group by likeness of the response pattern. The top row of panel A depicts the ASR response patterns from three SCI participants that closely resemble the typically ASR response pattern of neurological intact children. The bottom row shows the exaggerated ASR responses of six SCI participants. **Panel B:** Aggregation of typical and exaggerated patterns of ASR responses.

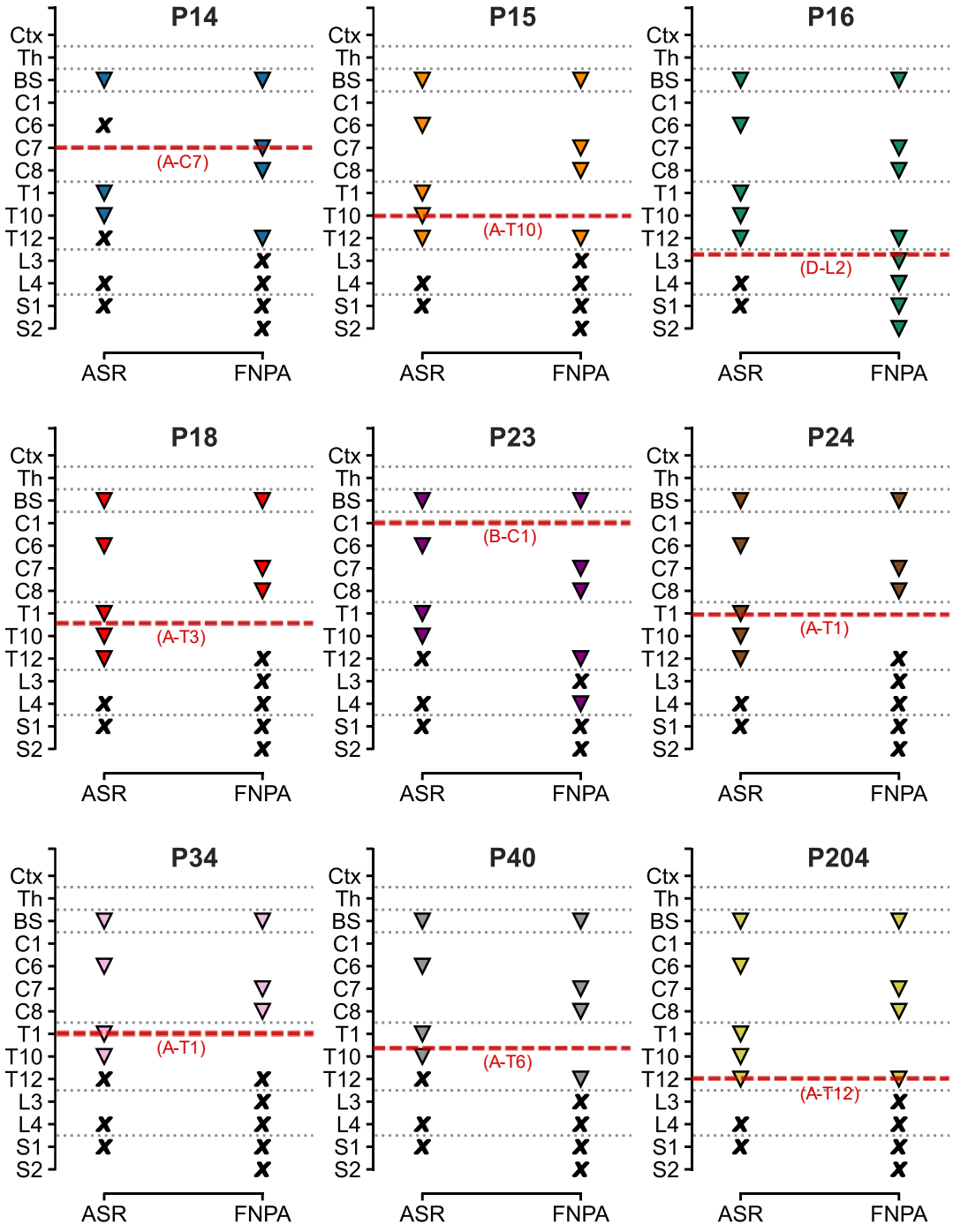


**Figure 3.14: Summary of motor pathways neural transmission.**

Graphical summary of the neural transmission of spinal motor pathways of each SCI participant as examined by the FNPA and ASR protocols. Participant-coded colored upside-down triangles represent at least one successful descending neural transmission to skeletal muscles from the

corresponding central nervous system neuraxis level (Ctx, cortical; Th, thalamus, BS, brainstem; C, cervical levels; T, thoracic levels; L, lumbar levels; S, sacral levels). Colored Xs represent no detectable motor neural outflow. Horizontal dashed lines and the information within the parentheses denote the ASIA AIS grade and motor level of injury for each participant.

*Discussion*

ASR is a generalized defense reaction that can be consistently elicited by a loud unexpected auditory stimulus. The pattern of muscle recruitment points to the brainstem as the origin of the typical startle reaction (Brown et al., 1991a). The central structure of the reflex is generally acknowledged to be the caudal pontine reticular nucleus (Davis et al., 1982; Koch, 1999; Koch et al., 1993). The afferent signal from an auditory stimulus reaches the brainstem via cranial nerve VIII and the ventral division of the lateral lemniscus. From here, the efferent signal of an ASR response reaches the effector via spinal interneurons, cranial and spinal motoneurons, and medullary reticular tracts that innervate the facial and lower cranial nerves. ASRs have been successfully used to investigate the physiology of the human reticulospinal system in health and disease.

In neurologically intact humans, the probability of ASR responses normally decreases with the increasing distance of the examined muscle from the brainstem (Kumru et al., 2008). These findings were replicated by Bakker, Boer, et al. (2009) in TD children. Typically, the muscle responding fastest and most frequently is the OOC, followed by the muscles of the upper and lower limbs. The recruitment pattern of ASR responses of our 1 TD child replicated the same results.

In this experiment, the probability of a response from the OOC was similarly high for our 9 SCI subjects. This high probability response from the OOC is consistent with previously reported normative pediatric data (Bakker, Boer, et al., 2009). However, comparison to published normative pediatric probabilities (Bakker, Boer, et al., 2009) and to our single TD participant reveals much higher

probability ASR responses in the mean ASR probabilities of our SCI group of muscles innervated by cervical and thoracic spinal levels. These higher probabilities are congruent with previously published reports that defined them as exaggerated responses in the adult SCI literature (Baker & Perez, 2017; Kumru, Kofler, et al., 2009; Kumru et al., 2008; Kumru et al., 2010). These exaggerated recruitment patterns suggest an organizational disruption of supra-injury motoneurons after SCI. These hypothetical changes may lead to disinhibition and abnormal reorganization at the level of the brain stem and spinal cord.

A novel observation of this study, however, is the emergence of two distinct response patterns in our subjects. A third of our participants lacked the typical exaggerated responses that follow SCI (Abanoz et al., 2018; Kumru, Kofler, et al., 2009; Kumru et al., 2008). This subgroup of participants presents with patterns approximating the responses of our TD subject and previously reported normative data. This differential response of the reticulospinal tract to an auditory startle stimulus after SCI has clinical implications for the use of the ASR as a potential biomarker for recovery after SCI, as the exaggerated startle reflex may result from plastic changes at the brainstem level (Kumru et al., 2008). Moreover, recent evidence (Baker & Perez, 2017; Howland et al., 2023; Sangari & Perez, 2020) suggests that the RST plays an important role in recovery after spinal cord injury, particularly in the recovery of gross motor functions. This might be in part due to the tract's capacity for regeneration and formation of new connections after injury (Filli et al., 2014; May et al., 2017; Vavrek et al., 2007). However, further

examination by better-powered future studies is necessary to determine the potential of ASR analysis as a biomarker for recovery after SCI.

Finally, 77.8% of our participants with SCI presented ASR responses below their clinically established level of motor neurological impairment. Remarkably, these 7 children with SCI were all clinically classified with motor complete injuries (AIS A and B). These findings align with a growing body of evidence that shows that many clinically complete spinal cord injuries (SCI) are, in reality, discomplete injuries. Sherwood and Dimitrijevic coined the term discomplete (Dimitrijevic, 1988; Dimitrijevic et al., 1983; Sherwood et al., 1992) to describe a lesion that presents as complete during clinical examination (AIS) but neurophysiological assessments (Atkinson et al., 2019; McKay et al., 2004) can reveal evidence of residual supraspinal influence on the spinal cord below the lesion. This means that while there may be a severe loss of motor and sensory function, some residual neural connectivity still exists below the level of injury. This distinction is crucial as it offers the potential for functional recovery through targeted rehabilitation strategies and treatments.

Multiple post-mortem anatomical studies (Bunge et al., 1993; Kakulas, 1999; Kakulas & Kaelan, 2015) have demonstrated the persistence of viable axons across the injury site in over 50% of the individuals with spinal cord injuries clinically classified as motor and sensory complete. Nonetheless, in this study, no ASR responses of muscles innervated by lumbosacral levels were detectable in any of our SCI participants. At face value, this observation may suggest a lack of motor neural input to lumbosacral centers from supraspinal structures. This

interpretation, however, needs some caveats. Most notably, recent reports have revealed that even in chronic motor complete adults with SCI, residual supraspinal inputs are capable of transmitting motor signals to spinal networks after intensive activity-based locomotor training in combination with epidural electrical stimulation of the lumbosacral spinal cord (Angeli et al., 2018; Angeli et al., 2014; Harkema et al., 2011). Perhaps the epidural stimulation plays a role in raising the baseline excitability levels of lumbosacral networks rendering them more receptive to response to supraspinal signals diminished by SCI.

The CST and RST are two of the most prominent descending pathways with convergent projections onto spinal networks (Lemon, 2008). In 2012, Zaaimi et al. showed that the RST connections to motoneurons innervating upper limb muscles of primates are strengthened after a corticospinal lesion. Others have shown that regardless of their injury status, both CST (Bareyre et al., 2004; Fouad et al., 2001) and RST (Filli et al., 2014; May et al., 2017) axons have the ability to sprout new connections with target neurons of other undamaged tracts. Crucially, findings from a recent study (Howland et al., 2023) of six children with SCI revealed that the three children who achieved reciprocal walking post-therapy demonstrated retained inputs from the RST to circuitry below the level of injury, as indicated by their ASR assessments. Remarkably, these individuals achieved this functional recovery without any indication of CST integrity, as determined by the absence of TMS-evoked responses. Therefore, knowing the post injury status of and monitoring changes in residual neural transmission of these pathways may hold substantial importance in guiding decisions about choice and the evaluation of the

efficacy of neurorehabilitation therapies after SCI. Our results examining the residual neural transition patterns of these two descending spinal tracts in children with SCI have laid the foundation for future work investigating potential mechanisms for change in stepping capacity using a neurophysiological approach to evaluate the effects of activity-based locomotor training in synergy with transcutaneous stimulation of the lumbosacral spinal cord.

## Experiment 3: Short-latency Somatosensory Evoked Potentials (SSEP)

SSEPs obtained after peripheral nerve stimulation offer a non-invasive means of measuring the functional integrity of the dorsal column medial lemniscus sensory pathway. We used this established standard clinical test (American Clinical Neurophysiology, 2006; Fagan et al., 1987; Singh, 2018) to evaluate the residual electrophysiological integrity within the dorsal column–medial lemniscus pathway of children with SCI.

### *Hypothesis*

Children with SCI would show altered cortical evoked potentials elicited from peripheral nerves below the injury level when compared to the evoked potentials elicited from peripheral nerves above their sensory injury level.

### *Methods*

#### *Data Acquisition*

The evaluation was conducted in a dark, quiet room with subjects lying supine while SSEPs were elicited via electrical stimulation of a peripheral nerve and recorded with monopolar silver/silver-chloride electrodes over standardized (American Clinical Neurophysiology, 2006; Gilmore, 1992; Mauguiere et al., 1999) points along the sensory pathway of the same peripheral nerve. We stimulated the median (mn-SSEP) and posterior tibial nerves (pt-SSEP) with a 200 microseconds stimulus generated with a Nicolet EDX system (Natus Neuro, Middleton, WI) at a

4.7 Hz rate and current amplitude slightly greater than the motor threshold of muscles innervated by the nerve under investigation.

Based on head circumference, each participant was fitted with an appropriately sized modular EEG cap with four electrodes (EASYCAP GmbH, Germany) placed over the left and right somatosensory cortex (**CPc** or **CPi**, ipsilateral or contralateral with respect to the stimulated limb and corresponding to the CP3 and CP4 (Gilmore, 1992; Kabdebon et al., 2014) position of the international 10–20 system (Klem et al., 1999; Nuwer et al., 1998), respectively), the somatosensory cortex for the legs (**CPz**), and the midsagittal plane of the forehead (**Fpz**). The EEG cap was mounted and adjusted according to standard anatomical landmarks (American Clinical Neurophysiology, 2006; Klem et al., 1999; Nuwer et al., 1998). The nasion and inion served as reference points for anterior-posterior positioning; while left-right symmetry was established by the left and right preauricular points. Each electrode was then carefully filled with electrode gel (Abralyt HiCl, EASYCAP GmbH, Germany) with a blunt-tip syringe.

In addition, nine monopolar electrodes were attached to the participants' skin over the spinous process of the fifth vertebra (**C5S**), the left and right Erb's point (**EPi** or **EPc**, ipsilateral or contralateral with respect to the stimulated limb), the spinous process of the twelfth thoracic vertebra (**T12S**), the left and right distal popliteal fossae (**Pfdi**, 2 cm above popliteal creases), the left and right proximal popliteal fossae (**Pfpi**, 5 cm above the popliteal creases), and a mid-thoracic (**MidT**) landmark like the sternum. Finally, a ground electrode soaked in saline solution (Natus Neuro, Middleton, WI) was positioned on the stimulated limb

halfway between the stimulation site and its nearest recording electrodes to diminish stimulus artifacts (McLean et al., 1996). The impedance of all recording, stimulating, and ground electrodes was below 32 KOhm.

The latencies of the SSEP responses were recorded by the Nicolet EDX system as bipolarly derived channels as recommended by the American Clinical Neurophysiology Society (ACNS) 2006 Guidelines on Short-Latency Somatosensory Evoked Potentials (American Clinical Neurophysiology, 2006). By convention, all peaks were labeled based on their polarity and expected normative latencies in adults. Table 3-3: Median nerve SSEP recording montage. and Table 3-4: Posterior tibial SSEP recording montage. describe the recording montage and obligate response potentials associated with mn-SSEP and pt-SSEP in TD children (Boor, Goebel, Doepp, et al., 1998; Boor, Goebel, & Taylor, 1998; Boor et al., 2008; Gilmore, 1992).

*Data Analysis*

The analog input from each recording electrode pair was amplified, band-passed filtered between 30 and 3000 Hz, digitally sampled at 48,000 Hz, and synchronized with the stimuli signal by the Nicolet EDX system. Trials affected by movement, stimulus, and ECG artifacts were automatically rejected by the digital Viking software operating the Nicolet EDX. Five hundred artifact-free responses were averaged and analyzed for each recording channel. mn-SSEP and pt-SSEP components (American Clinical Neurophysiology, 2006; Mauguiere et al., 1999) (summarized in tables # and #) for each channel were identified, and their peak

latencies and interpeak intervals were measured. Results were collected into a "tidy" formatted (Wickham, 2014) tabular file for further analysis.

The Python Pandas (McKinney, 2010; Pandas, 2020) library was used for data management, while data visualization was implemented via the Matplotlib (Hunter, 2007), Seaborn (Waskom, 2021), and Statannotations (Charlier et al., 2022) libraries. All statistical analysis was performed with the stats module of the SciPy library (Virtanen et al., 2020).

| | ***Active Electrode*** | ***Reference Electrode*** | ***Obligate Component*** |
|---|---|---|---|
| *Channel 1* | CPc | CPi | N20 |
| *Channel 2* | CPi | EPc | P14 |
| *Channel 3* | C5S | EPc | N13 |
| *Channel 4* | EPi | EPc | N9 (EP) |

**Table 3-3: Median nerve SSEP recording montage.**

| | ***Active Electrode*** | ***Reference Electrode*** | ***Obligate Component*** |
|---|---|---|---|
| *Channel 1* | CPi | Fpz | P39 |
| *Channel 2* | CPz | Fpz | P39 |
| *Channel 3* | Fpz | C5S | P30 |
| *Channel 4* | T12S | MidT | N22 (LP) |
| *Channel 5* | Pfpi | Pfpi | N8 |

**Table 3-4: Posterior tibial SSEP recording montage.**

*Results*

In this experiment we evaluated the neural transition of the DCML system by eliciting cortical evoked potentials via the electrical stimulation of a peripheral nerve in the forearm (median nerve) and the leg (posterior tibial nerve). Evaluation of a 7 y.o. typically developing female revealed cortical evoked potentials after median (N20) and posterior tibial (P39) electrical stimulation within normal range (see Figure 3.15-A and Figure 3.16-A).

Figure 3.15-B presents representative mn-SSEPs traces from participant P15, an 8-year-old girl who sustained a T9 spinal cord injury at the age of 3. When medial nerve stimulation was applied (as shown in Figure 3.17), all nine subjects exhibited the N9 response, which was recorded from the ipsilateral Erb's point and originated from the brachial plexus. Additionally, all children demonstrated the N13 potential, which resulted from the dorsal root entry zone and was recorded from the spinous process of the fifth cervical vertebra.

The potential arising from synaptic activity at the nucleus cuneatus and the brainstem lemniscal pathway, P13, was recorded in 8 out of the 9 children. Similarly, the cortical potential N20 was observed in 8 out of the 9 children.

Interpeak latencies reflecting plexus-cord conduction time (N9-N13) were calculated by subtracting the N13 and N9 latencies. This corresponds to conduction through the proximal plexus, roots up to the dorsal horn of the cervical cord. Subject P23, a 7-year-old male that acquired an AIS B-C1 SCI at age 2, presented with considerably longer N9-N13 Interpeak latency (7.9 ± 0.8 ms). Additionally, this same participant did not present with any cephalic EPs (P13 and

N20). Therefore, the central conduction time (calculated by the peak-to-peak N13-N20 interval) was calculated and reported for the same 8 subjects. These results are presented in tabular form as Table 3-5.

Figure 3.16-B shows representative pt-SSEPs traces from participant P15. Posterior tibial nerve stimulation evoked the peripheral potential recorded at the popliteal fossae (N8) and the lumbar cord potential (N22) from 7 of 9 SCI subjects. Notably, no cephalic potentials (P30 and P37) were detected in any of our SCI participants. The means and standard deviations of the latency and interpeak latency of all major components of the pt-SSEPs are presented in Table 3-6 with normative mean latencies obtained from the literature in parentheses.

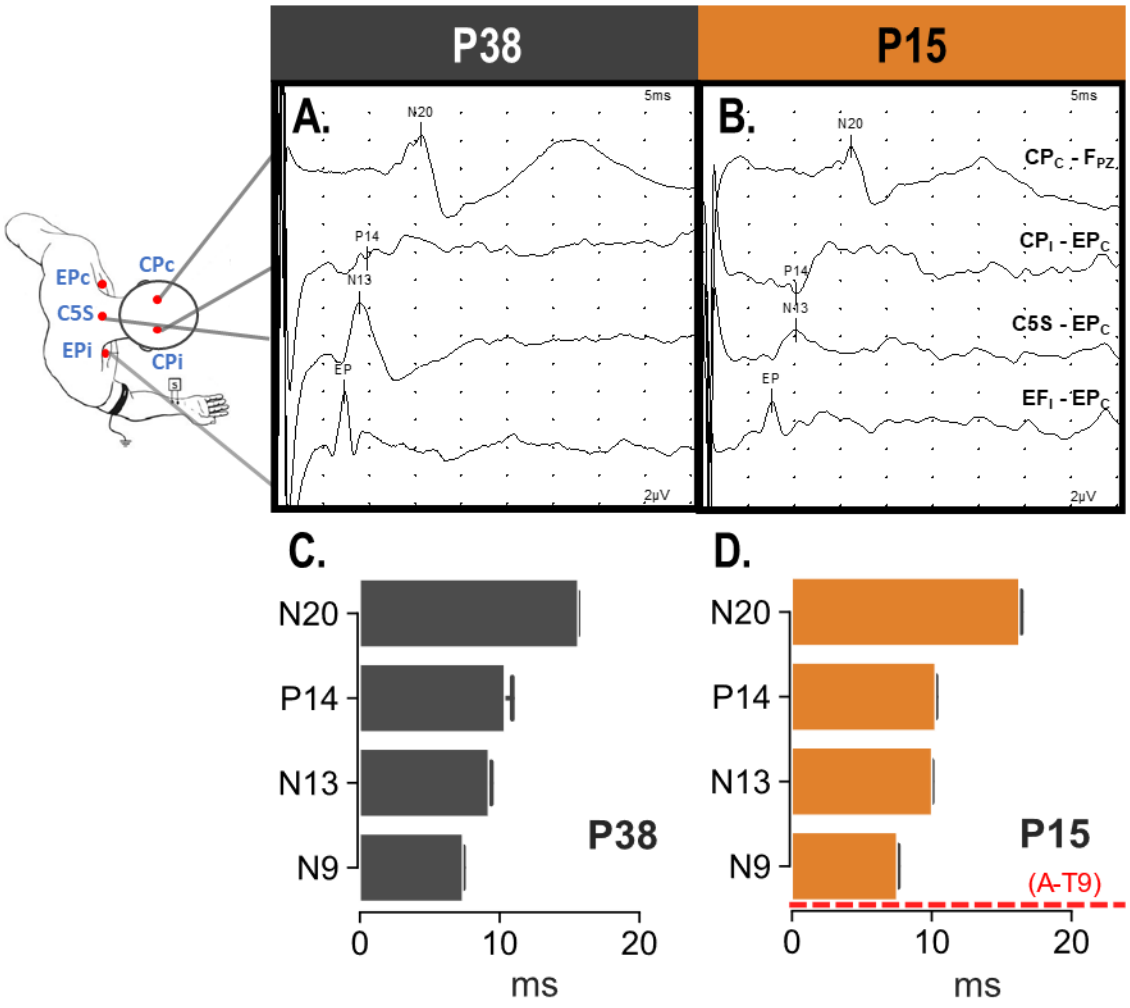


**Figure 3.15. Median nerve somatosensory evoked potentials (mn-SSEP)**

Assessments of a typically developing child (P38: 7-year-old female, **Panel A**) and a child living with spinal cord injury (P15: 8-year-old female; AIS A-T9, **Panel B**) revealed normal evoked responses. Somatosensory evoked potentials (SSEP) were elicited via electrical stimulation of the median nerve (200 microseconds, 4.7 Hz, and a current amplitude slightly greater than the motor threshold). The resulting potentials were recorded with monopolar silver/silver-chloride electrodes placed over the ipsilateral lateral somatosensory cortex (CPi), contralateral lateral somatosensory cortex (CPc), the midsagittal plane of the forehead (Fpz), the spinous process of the fifth vertebra (C5S), ipsilateral Erb's point (EPi), and the contralateral (EPc). Channel 4 (EPi – EPc) shows the peripheral EP/N9 volley of the brachial plexus traveling through Erb's point. Channel 3 (C5S – EPc) detected N13, attributed to the cervical dorsal horn synaptic activity. Channel 2 (CPi – EPc)

recorded P14, a potential attributed to activation of the cuneate nucleus. Channel 1 (CPc – Fpz) detected the cortical near-field potential, N20, generated by the somatosensory cortex. Timebase: 5 ms/division; Sensitivity 2 uV/division**.** The bar graphs represent the mean latencies for the median nerve SSEPs indicated in the ordinate for P38 **(Panel C)** and P15 **(Panel D)**. The horizontal dashed line and the information within the parenthesis denotes the ASIA AIS grade and motor level of injury.

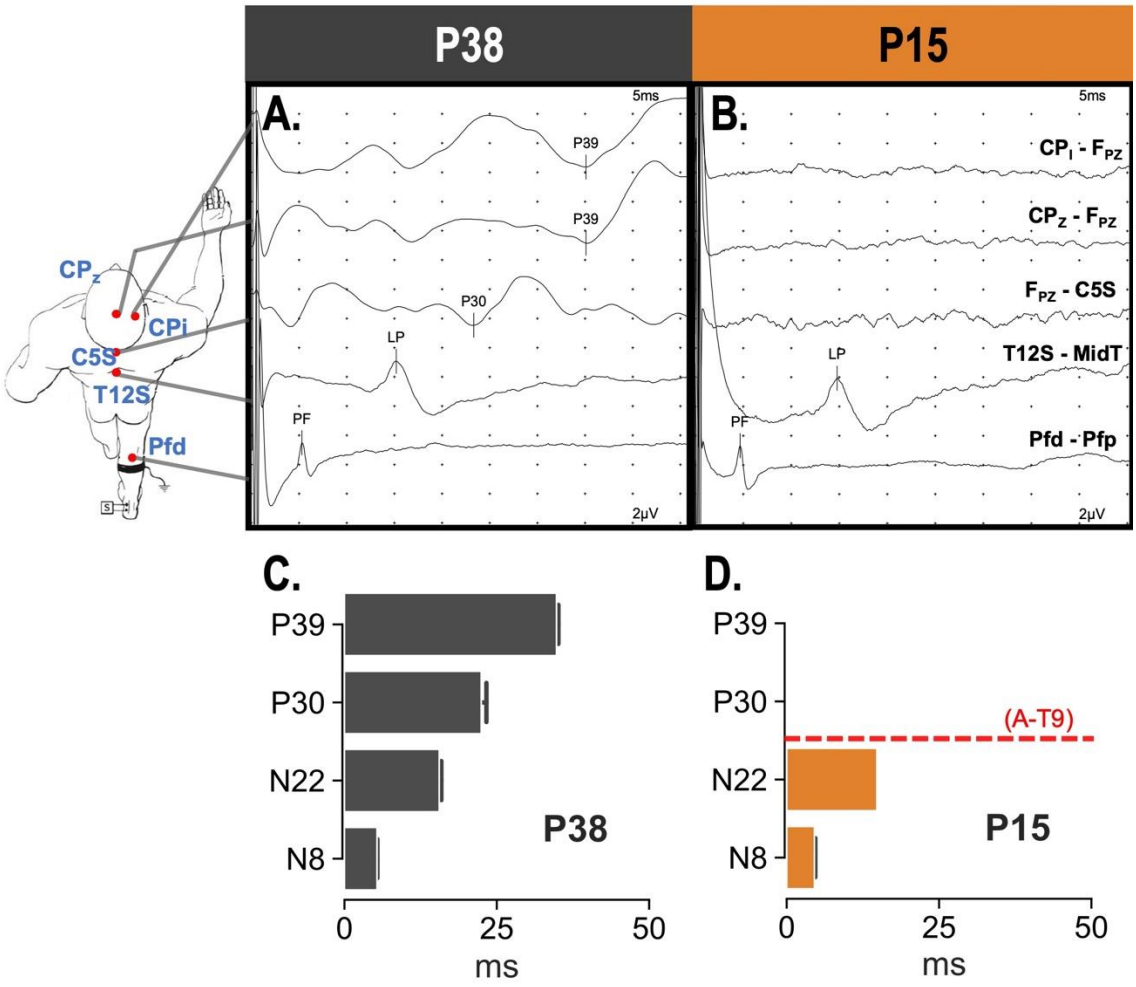


**Figure 3.16: Posterior tibial nerve somatosensory evoked potentials (pt-SSEP)**

Somatosensory evoked potentials (SSEP) were elicited via electrical stimulation of the posterior tibial nerve (200 microseconds, 4.7 Hz, and a current amplitude slightly greater than the motor threshold). The resulting potentials were recorded with monopolar silver/silver-chloride electrodes placed over the ipsilateral lateral somatosensory cortex (CPi), the mesial somatosensory cortex (CPz), the midsagittal plane of the forehead (Fpz), the spinous process of the fifth vertebra (C5S), the spinous process of the twelfth thoracic vertebra (T12S), a mid-thoracic (MidT) bony landmark like the sternum, and the ipsilateral distal (Pfd) and proximal (Pfp) popliteal fossae. **Panel A:** Evoked responses of participant P38—a 7-year-old typically developing female with all obligate responses present. Channel 1 (CPi – Fpz) and channel 2 (CPz – Fpz) detected the cortical near-field potentials, P39, generated by the somatosensory cortex. Channel 3 (Fpz – C5S) detected

P30, a potential attributed to synaptic activity of the gracile nucleus. Channel 4 (T12S – MidT) recorded the LP/N22 potential from the lumbar plexus. Channel 5 (Pfd – Pdp) shows the peripheral PF/N8 volley of the tibial nerve traveling through the popliteal fossa. **Panel B:** Assessment of participant P15—an 8-year-old female with a sensory AIS A-T9 spinal cord injury. Only potentials produced by generators below the injury (LP/N22 = lumbar plexus and PF/N8 = tibial nerve) were detected in channels 4 and 5, respectively. Cortical evoked potentials generated by the somatosensory cortex (P39) were not present in channels 1 and 2. N30 was absent from channel 3. Timebase: 5 ms/division; Sensitivity 2 uV/division. The bar graphs represent the mean latencies for the posterior median nerve SSEPs indicated in the ordinate for P38 **(Panel C)** and P15 **(Panel D)**. The horizontal dashed line and the information within the parenthesis denotes the ASIA AIS grade and motor level of injury.

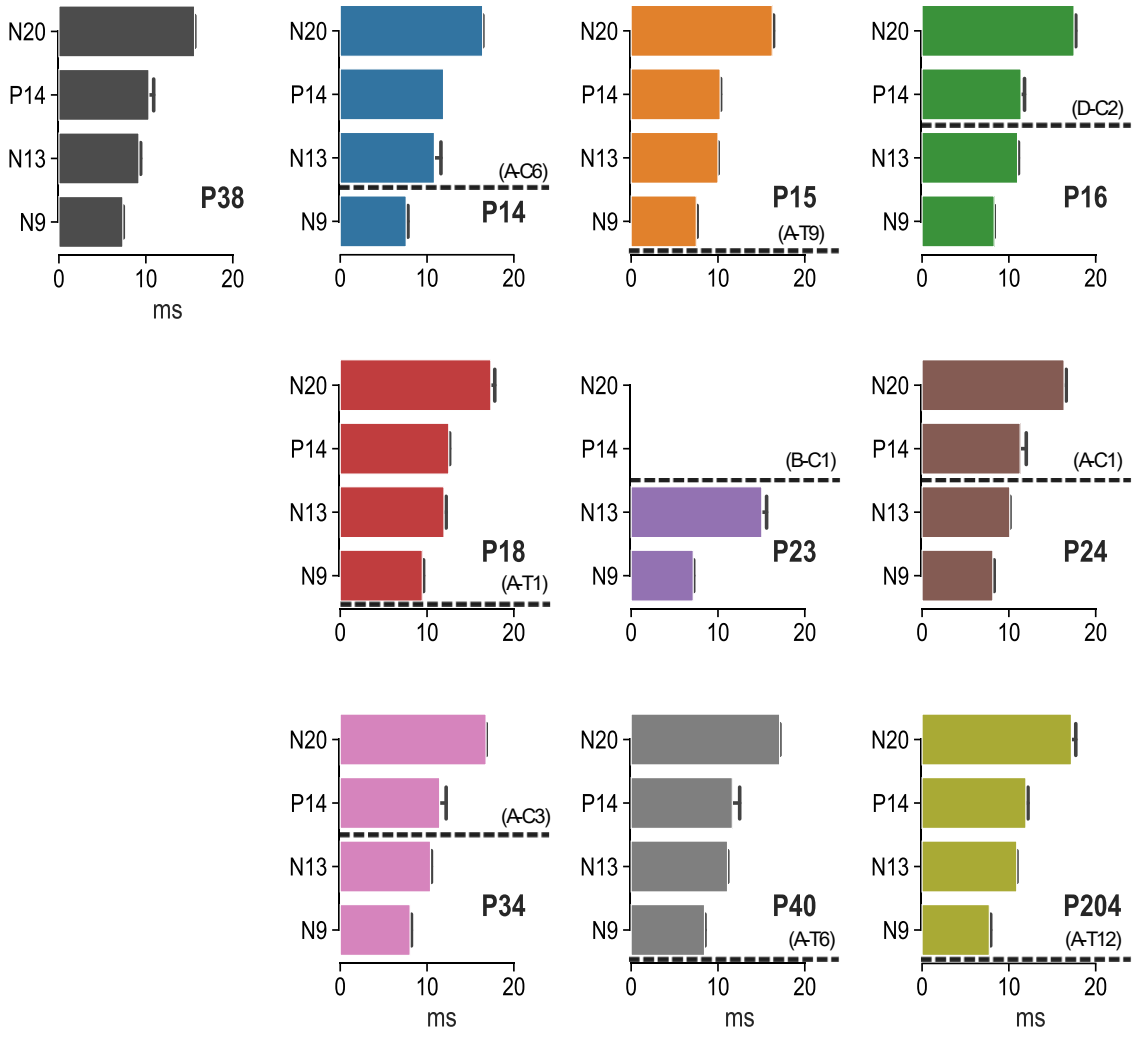


**Figure 3.17: Individual results of mn-SSEP**

The graph displays the results of median nerve SSEP experiment, with multiple panels representing the results for individual participants. The y-axis of each panel represents the expected EP, while the x-axis represents latency in milliseconds.

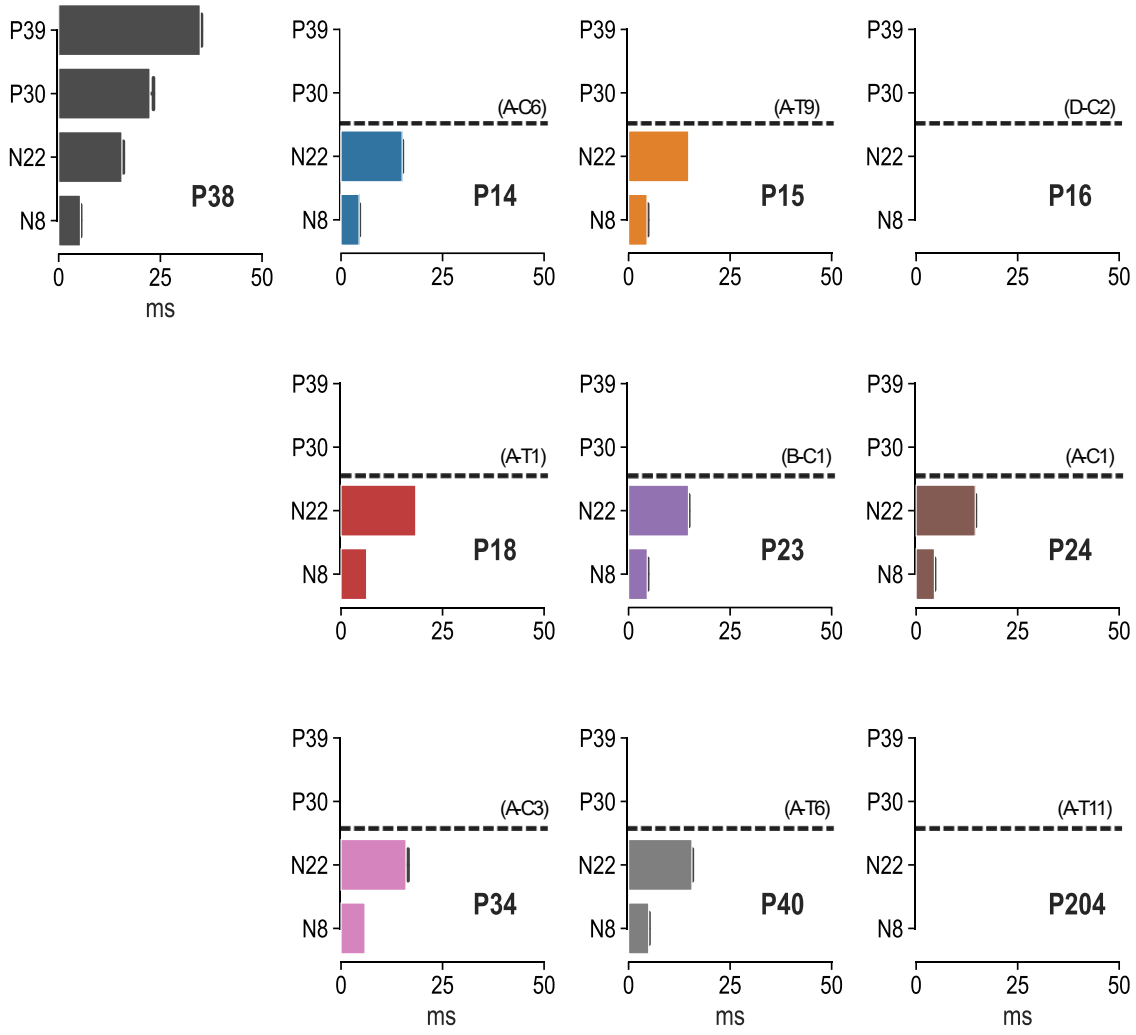


**Figure 3.18: Individual results of pt-SSEP**

The graph displays the results of posterior tibial nerve SSEP experiment, with multiple panels representing the results for individual participants. The y-axis of each panel represents the expected EP, while the x-axis represents latency in milliseconds.

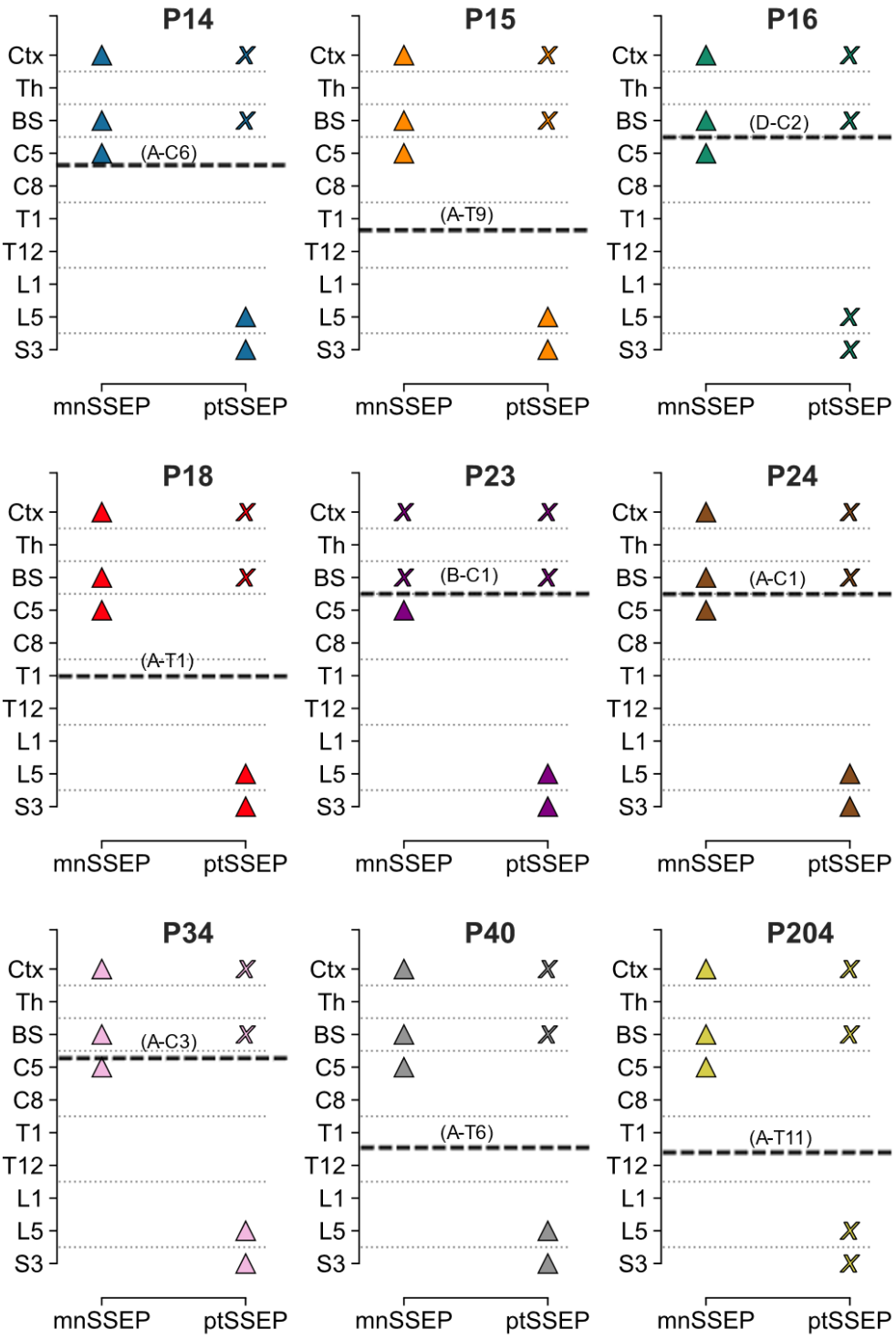


**Figure 3.19: Summary of DCML neural transmission**

Graphical summary of the neural transmission of the DCML spinal pathway of each SCI participant as examined by the SSEP protocols. Participant-coded colored triangles represent at least one

successful neural transmission to the corresponding central neuraxis level (Ctx, cortical; Th, thalamus, BS, brainstem; C, cervical levels; T, thoracic levels; L, lumbar levels; S, sacral levels) from the peripheral stimulation of the median nerve (mn-SSEP) and the posterior tibial nerve (pt-SSEP). Colored Xs represent no detectable neural transmission. Horizontal dashed lines and the information within the parentheses denote the ASIA AIS grade and sensory level of injury for each participant.

| *Participant* | *Age (years)* | *N9* | *N13* | *P13* | *N20* |
|---|---|---|---|---|---|
| *Peak Latencies (ms)* | | | | | |
| *P14* | 10.6 | 7.6 ± 0.3 (8.8) | 10.9 ± 1.1 (11.4) | 11.9 ± - (13.0) | 16.4 ± 0.0 (17.4) |
| *P15* | 8.6 | 7.5 ± 0.1 (7.7) | 10.0 ± 0.0 (10.2) | 10.3 ± 0.1 (11.6) | 16.3 ± 0.2 (16.0) |
| *P16* | 10.2 | 8.3 ± 0.0 (8.8) | 11.0 ± 0.1 (11.4) | 11.4 ± 0.6 (13.0) | 17.5 ± 0.3 (17.4) |
| *P18* | 12.9 | 9.5 ± 0.2 (8.8) | 12.0 ± 0.4 (11.4) | 12.5 ± 0.1 (13.0) | 17.4 ± 0.6 (17.4) |
| *P23* | 7.2 | 7.2 ± 0.1 (7.7) | 15.1 ± 0.8 (10.2) | nr | nr |
| *P24* | 5.8 | 8.2 ± 0.2 (7.1) | 10.1 ± 0.0 (9.4) | 11.3 ± 1.0 (11.0) | 16.4 ± 0.4 (15.7) |
| *P34* | 6.3 | 8.1 ± 0.2 (7.1) | 10.4 ± 0.1 (9.4) | 11.5 ± 1.1 (11.0) | 16.8 ± 0.0 (15.7) |
| *P40* | 9.1 | 8.5 ± 0.1 (7.7) | 11.1 ± 0.0 (10.2) | 11.7 ± 1.2 (11.6) | 17.1 ± 0.0 (16.0) |
| *P204* | 8.5 | 7.8 ± 0.2 (7.7) | 10.9 ± 0.0 (10.2) | 12.0 ± 0.4 (11.6) | 17.2 ± 0.7 (16.0) |

| | | N9-N13 | N13-N20 |
|---|---|---|---|
| *Interpeak Latencies (ms)* | | | |
| *P14* | 10.6 | 3.3 ± 0.8 (2.7) | 5.6 ± 1.1 (6.0) |
| *P15* | 8.6 | 2.5 ± 0.1 (2.5) | 6.3 ± 0.2 (5.8) |
| *P16* | 10.2 | 2.7 ± 0.1 (2.7) | 6.5 ± 0.4 (6.0) |
| *P18* | 12.9 | 2.5 ± 0.1 (2.7) | 5.4 ± 1.0 (6.0) |
| *P23* | 7.2 | 7.9 ± 0.8 (2.5) | nr |
| *P24* | 5.8 | 2.0 ± 0.2 (2.3) | 6.3 ± 0.4 (6.3) |
| *P34* | 6.3 | 2.4 ± 0.1 (2.3) | 6.4 ± 0.1 (6.3) |
| *P40* | 9.1 | 2.7 ± 0.1 (2.5) | 6.0 ± 0.0 (5.8) |
| *P204* | 8.5 | 3.2 ± 0.2 (2.5) | 6.3 ± 0.7 (5.8) |

**Table 3-5: Peak and interpeak latencies of median nerve SSEP**

The peak latencies in milliseconds for the N9, N13, P13, and N20 components of the median nerve SSEP are provided. Standard deviation (SD) depicted as "-", represent a unilateral potential recorded for the participant. Interpeak latencies between the N9 and N13 components and between the N13 and N20 components of the SSEP are also included. Absent potentials are indicated by "nr". Normative latencies for the respective age group in parentheses as reported by Boor et al. 1998.

| *Participant* | *Age (years)* | *N8* | *N22* | *P30* | *P37* |
|---|---|---|---|---|---|
| *Peak Latencies* | | | | | |
| *P14* | 10.6 | 4.5 ± 0.1 (7.5) | 15.1 ± 0.1 (19.1) | nr | nr |
| *P15* | 8.6 | 4.6 ± 0.2 (6.2) | 14.8 ± (16.1) | nr | nr |
| *P16* | 10.2 | nr | nr | nr | nr |
| *P18* | 12.9 | 6.3 ± - (7.5) | 18.4 ± - (19.1) | nr | nr |
| *P23* | 7.2 | 4.6 ± 0.1 (6.2) | 14.8 ± 0.1 (16.1) | nr | nr |
| *P24* | 5.8 | 4.5 ± 0.0 (5.4) | 14.6 ± 0.1 (13.9) | nr | nr |
| *P34* | 6.3 | 5.9 ± - (5.4) | 16.0 ± 0.7 (13.9) | nr | nr |
| *P40* | 9.1 | 5.0 ± 0.1 (6.2) | 15.6 ± 0.1 (16.1) | nr | nr |
| *P204* | 8.5 | nr | nr | nr | nr |
| | | N8-N22 | | | |
| *Interpeak Latencies* | | | | | |
| *P14* | 10.6 | 10.6 ± 0.0 (7.5) | | | |
| *P15* | 8.6 | 10.4 ± - (6.2) | | | |
| *P16* | 10.2 | nr | | | |
| *P18* | 12.9 | 12.1 ± - (7.5) | | | |
| *P23* | 7.2 | 10.2 ± 0.2 (6.2) | | | |
| *P24* | 5.8 | 10.1 ± 0.1 (5.4) | | | |
| *P34* | 6.3 | 9.6 ± - (5.4) | | | |
| *P40* | 9.1 | 10.7 ± 0.1 (6.2) | | | |
| *P204* | 8.5 | | | | |

**Table 3-6: Peak and interpeak latencies of posterior tibial nerve SSEP**

The peak latencies in milliseconds for the N8, N22, P30, and P37 components of the tibial nerve SSEP are provided. Standard deviation (SD) cell with the "-" symbol, represent a unilateral potential recorded for the participant. Interpeak latencies between the N8 and N22 components of the SSEP are also included. Absent potentials are indicated by "nr". Normative latencies for the respective age group in parentheses as reported by Boor et al. 2008.

*Discussion*

In this study we examined the residual neural transmission of the DCML system with electrical stimulation of a peripheral nerve with simultaneous monitoring of cortical responses.

The normative response for the median nerve stimulation (Boor, Goebel, & Taylor, 1998) of a 7 y.o. include a peripheral N9 volley of the brachial plexus traveling through Erb's point at about 7.7 ± 0.4 milliseconds (ms) after the stimulus. N13 a response attributed to the cervical dorsal horn synaptic activity is present at about 10.2 ± 0.5 ms. Activation of the cuneate nucleus at 10.3 ± 0.6 ms post stimulation is known as the P14 potential. Finally, at about 16 ± 0.6 ms a cortical near-field potential, N20, generated by the somatosensory cortex can be detected. In agreement with this literature, evaluation of our typically developing participant resulted in normative potentials and interpeak latencies.

Median nerve SSEP assessments of our SCI participant showed mean latency values in close agreement with published age-matched normative data (Boor, Goebel, & Taylor, 1998; Mauguiere et al., 1999). In addition, N9-N13 interpeak latencies were obtained in all nine subjects and 8/9 subjects and were consistent with previously reported normative data (Boor, Goebel, & Taylor, 1998; Mauguiere et al., 1999). As previously noted however, no cortical and subcortical potentials were detected after median nerve stimulation of participant P23. Noteworthy in this respect is the fact this participant is the only subject with a transverse myelitis diagnosis in our SCI group. P23 was graded as an AIS B-C1

and presented with the lowest AIS sensory scores during clinical evaluation (see Table 3-1).

Also noteworthy is the fact that three SCI participants presented with neural transmission across their AIS sensory injury level during mn-SSEP assessment. Participants P14, P16, and P24 (see Figure 3.19) presented with potentials widely considered to originate from generators caudal and rostral to his injury site. Participant P14 and P24 have are considered clinically complete (AIS A) with cervical injuries. Taken together with our previous experiments above, these results provide further evidence that many clinically complete SCI are in fact discomplete injuries.

Posterior tibial nerve stimulation of a typically developing 7 y.o. child (Boor et al., 2008) include The N8 peripheral volley of the tibial nerve traveling through the popliteal fossa at 6.0 ± 0.6 ms post stimulation. the N22 potential from the lumbar plexus dorsal horns at 16.1 ± 0.5 ms. This is followed by the synaptic activity at the nucleus gracilis (P30) 22.8 ± 0.8 ms after the stimulus onset. Finally, the cortical near-field potentials, P39, generated by the somatosensory cortex can be detected about 32.7 ± 2.2 ms after the stimulus. Our 7 y.o. TD participant presented with potentials and interpeak latencies in agreement with these normative values.

In contrast, posterior tibial nerve stimulation of SCI participants resulted in the total absence of supraspinal responses (P39 and P30) in all subjects (Table #) suggesting a total lack of central neuronal transmission through the DCML. It bears repeating, however, that This interpretation should be considered with a heathy

dose of caution. As discussed above, multiple recent studies have established that even when not detected by neurophysiology assessments some level of translesional neuronal connections must remain after SCI in adults (Angeli et al., 2018; Angeli et al., 2014; Harkema et al., 2011). In addition, the peripheral nerve conduction times between peripheral nerve in the popliteal fossa (N8) and the dorsal roots of the lumbar plexus (N22) were considerably slower than previously published normative data from age-matched typically developing children (Boor, Goebel, Doepp, et al., 1998; Boor, Goebel, & Taylor, 1998; Mauguiere et al., 1999). These results suggest a potential degradation of the peripheral nerve after SCI during childhood.

## Discussion

The spinal neural transmission of cortical commands for volitional motor control and afferent somatosensory information has been studied extensively in animal (Fink & Cafferty, 2016) and humans (Blumenthal, 2015) in health. Similarly, there are many reports of the impact of a SCI in the neural transition of the CST (Atkinson et al., 2019; Li et al., 2012) , RST (Nardone & Trinka, 2015), and DCML (Curt & Dietz, 1996; Spiess et al., 2008) tracts in adults. To our knowledge, however, ours is the first study to contemporaneously characterize the residual neural transmission of these three tracts in children.

The results of the studies summarized above indicate that all our SCI subjects presented with a diverse range of motor abilities not captured by the gold standard of clinical assessments after SCI—the American Spinal Injury Association Impairment Scale (AIS). For instance, 6 out of 7 children graded as having complete motor and sensory injuries (AIS A) were able to generate at least one motor or sensory response to our assessments across the AIS injury level.

Functional neurophysiological assessment (FNPA) of volitional movements demonstrated that, although diminished and not always functional, about half of our participants (P14, P15, P16, P23, P40) retained the ability to generate volitional EMG activity of muscles caudal to the AIS motor level of injury. These EMG activations were often below the levels needed to produce a movement of the muscle. Nonetheless, the existence of these volitional neural connection across the injury remains an exciting topic of exploration for future studies to leverage the potential of spinal stimulation in children.

Similarly, in our acoustic startle reflex (ASR) experiment we detected reflexive EMG activity below the AIS injury level in seven SCI participant (P14, P15, P18, P23, P24, P34, and P40). It is worth noting that some overlap exists between these lists with four participants preserving the ability elicit volitional and reflexive EMG activation across their injury level.

The somatosensory evoked potential (SSEPs) study demonstrated that all but one (P23, 7 y.o. male, AIS B-C1) of our SCI subjects were able to produce normal SSEPs following electrical stimulation of the median nerve. These included three participants for whom this represented a neural transmission across their injury site (P14, P16, P24).

*Limitations*

Neurophysiological assessment of EMG activation patterns during volitional movement attempts and reflexive responses can provide objective evidence of residual integrity of descending spinal tracts and may serve as a gauge for motor recovery after injury. In this study we described the activation patterns of muscles innervated by spinal roots along the rostral-caudal axis of the spinal cord of children with SCI. However, interpretation of these results is restricted by several experimental limitations, including the small sample size of the SCI cohort and a lack of a robust control group.

The small sample size of children with SCI represents a major limitation of this study. We recruited all geographical accessible children that met the inclusion criteria for this study within the SCI from the Human Locomotion Research Center's Potential Volunteer Database (University of Louisville IRB #06.0647).

Recruitment of TD children was hindered by the COVID-19 global pandemic during the data acquisition phase of this study (see Chapter 2). Our sample size, however, allows us to make some qualitative conclusions regarding the neural integrity of the volitional motor pathways for each of our participants. Generalization of these results will necessitate further investigation with larger sample sizes.

Another limitation in the study of recruitment patterns along the rostral-caudal axis of the spinal cord resides in the physical availability of enough EMG channels to cover enough key spinal segments to produce meaningful results. Despite this limitation, we were able to examine more spinal root segments than the ones covered by the ASIA AIS assessment.

While the study of EMG recruitment patterns serves as a direct assessment of lower motor neurons signals, it remains unclear which spinal motor pathways mediate these supraspinal signals. Further, the outcome measure of this assessment depends on the understanding, compliance, and effort of the participants. Other investigators have opted for the implementation of and direct measurement of CST integrity with a transcranial magnetic stimulation (TMS) of the primary motor cortex to elicit and record motor evoked potentials (MEPs) on distal muscles. This technique was considered during the planning and design phase of this study. We ultimately decided against TMS in favor of the FNPA as the experience of TMS might present as an undue stressor for a pediatric population. TMS experiments are loud and produced discomfort to the participants. The FNPA has been validated as an effective measurement of residual supraspinal influence on spinal motor circuits that may be present after SCI in children.

Finally, these studies only examined a limited number of spinal pathways given the scope of this work. However, studies have shown that pathways like the propriospinal (Bamford & Mushahwar, 2011) and vestibulospinal (Sayenko et al., 2018) tracts may hold significant potential to mediate functional recovery after SCI.

*Future directions*

These three studies have laid the foundations for future work to employ the protocols detailed here to examine the effect of neural stimulation paradigms such as transcutaneous stimulation of the spinal cord, on the neural transmission of these pathways and potential identification of responders/non-responders. Some of that work is currently being implemented with the award of a Kentucky Spinal Cord and Head Injury Research Board (IRB # 19.1281) grant based on large portions of this dissertation.

A potential future reincarnation of this work could adapt other electrophysiological assessments to a pediatric SCI population to study different spinal pathways. Contact heat evoked potentials (CHEPs) is a validated clinical assessment designed to interrogate the neural transmission of nociceptive pathways (Haefeli et al., 2014; Lagerburg et al., 2015) that may prove to be well suited for the study of children with SCI. Other neurophysiology techniques that could have benefited this work are galvanic responses to interrogate the vestibulospinal tract (Barthelemy et al., 2015; Cobeljic et al., 2018) and sympathetic skin responses (Berger et al., 2014; Cariga et al., 2002; Kumru, Vidal, et al., 2009) studies to assess the sympathetic system.

| | | | *Injury* | | | | *Motor* | | | *Sensory* |
|---|---|---|---|---|---|---|---|---|---|---|
| ***ID*** | ***Sex*** | ***Age (years)*** | ***Mechanism*** | ***Age at Injury (years)*** | ***AIS*** | ***AIS Level*** | ***Level R/L*** | ***FNPA Caudal to Injury level*** | ***ASR Caudal to Injury level*** | ***Level R/L*** |
| P14 | M | 10.6 | Vehicle accident | 3.5 | A | C6 | C7/C7 | ✓ | ✓ | C6/C6 |
| P15 | F | 8.6 | Epidural abscess | 3.1 | A | T9 | T10/T9 | ✓ | ✓ | T10/T9 |
| P16 | M | 10.2 | Vehicle accident | 4.0 | D | C2 | T1/L2 | ✓ | | C2/C2 |
| P18 | F | 12.9 | Vehicle accident | 4.8 | A | T1 | T1/T3 | | ✓ | T1/T3 |
| P23 | M | 7.2 | Transverse myelitis | 2.3 | B | C1 | C1/C1 | ✓ | ✓ | C1/C1 |
| P24 | M | 5.8 | Spinal Hematoma | 0.9 | A | C1 | T1/T1 | | ✓ | C1/C1 |
| P34 | M | 6.3 | Spinal Tumor | 1.2 | A | C3 | C8/T1 | | ✓ | T1/C3 |
| P40 | M | 9.1 | Vehicle accident | 4.7 | A | T6 | T6/T6 | ✓ | ✓ | T6/T6 |
| P204 | M | 8.5 | Vehicle accident | 6.7 | A | T11 | T12/T11 | | | T12/T11 |

**Table 3-7: Summary of all three electrophysiology experiments**

# CHAPTER 4: EFFECTS OF SCI ON THE PEDIATRIC BRAIN

## Introduction

In recent years, the overwhelming consensus of the evidence presented in the adult literature reveals extensive remodeling of cortical and subcortical structures of the adult brain after SCI. In humans, neuroimaging studies have reported structural and functional connectivity changes following both complete and incomplete injuries (Freund et al., 2013; Guleria et al., 2008; Hawasli et al., 2018; Jurkiewicz et al., 2006; Lotze et al., 1999; Nardone et al., 2018; Pan et al., 2017; Solstrand Dahlberg et al., 2018; Wrigley et al., 2009). These alterations are often observed from three major neuroimaging modalities:

- Structural imaging: T1-weighted (T1w) scans are employed to determine metrics such as gray matter volume, density, and thickness.
- Diffusion-weighted imaging (DWI): DWI is used to examine the microarchitecture of white matter tracts by measuring the apparent rate and direction of water diffusion within axons. Metrics like fractional anisotropy (FA) help quantify white matter integrity.

- Functional magnetic resonance imaging (fMRI): This imaging technique detects changes in regional blood-oxygen-level dependent (BOLD) response as an indirect indicator of neural activity. In traditional fMRI studies, this hemodynamic response can be correlated with the timing of specific mental tasks. More recently, low-frequency fluctuations in the BOLD signal between regions of interest (ROI) during rest have been used to measure functional connectivity (FC) between those regions.

Multiple human neuroimaging studies of adults with SCI have reported reductions in the volume and thickness of the precentral (M1) and postcentral (S1) gyri (Chen et al., 2017; Freund et al., 2013; Freund et al., 2011; Hou et al., 2014; Jurkiewicz et al., 2006). In addition, several studies have shown that SCI contributes to alterations in the strength of the functional connectivity among nodes of the resting-state network associated with sensorimotor (SMN) functions (Hawasli et al., 2018; Oni-Orisan et al., 2016; Pan et al., 2017). Similarly, recent studies have reported decreased FA values in the corticospinal tract in the brain as well as the cervical regions of the spinal cord of patients with SCI compared to controls (Freund, Wheeler-Kingshott, et al., 2012; Sun et al., 2017; Yozbatiran et al., 2017). Nonetheless, there are no reports of studies analyzing a single SCI cohort with all three modalities (structural, functional connectivity, and diffusion-weighted imaging), and there is a void of studies examining the pediatric brain after SCI. Here, we studied the effect of pediatric-onset SCI on the morphometry of the brain (Experiment 4), the fractional anisotropy of the corticospinal tract

(Experiment 5), and the functional connectivity of the sensorimotor cortical and subcortical structures (Experiment 6).

## Ethics Statement

The experiments presented in this chapter were reviewed and approved by the University of Louisville Institutional Review Board (University of Louisville IRB #19.1281 and # 06.0647), adhering to all federal and local regulations regarding the ethical involvement of human volunteers in research projects. Parents or legal guardians of each participant provided written informed consent, and participants aged seven and older gave written informed assent (University of Louisville IRB: 19.1281). To facilitate the children's comprehension of the study's procedures, we developed an age-appropriate comicbook that explained the experiment's purpose and protocols. This comicbook was presented during the consent/assent meeting and consistently referenced throughout the course of the study to ensure that the children maintained a clear and relatable grasp of the study's objectives.

## Participants

We recruited nine subjects with pediatric-onset spinal cord injury (SCI) from the Human Locomotion Research Center’s Potential Volunteer Database (University of Louisville IRB #06.0647). After medical screening, eligible candidates were informed of the study's purpose, and the parents of those who met the inclusion criteria met with the investigators for an informed consent meeting. Our final SCI cohort for the neuroimaging assessments consisted of 6

males and 2 females, with a mean age of 9.2 ± 2.0 years, following the exclusion of a 5-year-old male participant due to excessive motion artifacts. Additionally, we enrolled one typically developing (TD) child from the immediate community (sibling of a participant with SCI). To establish normative data, we accessed the publicly available data from the Child Mind Institute Healthy Brain Network (HBN) Biobank (Alexander et al., 2017), which contains phenotypical and multimodal brain imaging data from over 2,000 children and adolescents who consented to distribute their anonymized data. Our HBN search was designed to identify age- and gender-matched children with no recorded diagnoses and artifact-free neuroimaging scans. We obtained neuroimaging data from seventeen typically developing children from the HBN biobank and one TD female locally, all of whom had no neurological conditions. Together, the TD cohort included 13 males and 5 females with a group mean age of 8.2 ± 2.1 years old.

*Eligibility*

Children who fulfilled the following inclusion criteria were recruited to participate in this study:

- Children with SCI:
    - 4 and 12 years of age.
    - Acquired non-progressive SCI after they began walking, crawling, or cruising, as reported by their parent(s).
    - At least 1-year post-injury at the time of enrollment.

    - In stable medical condition without neurodevelopmental, cardiovascular, pulmonary, endocrine, or other major medical illness.
    - Discharged from inpatient rehabilitation.
    - Unable to stand, walk, or initiate steps.
- Neuroimaging normative data from HBN:
    - 4 and 12 years of age.
    - No recorded diagnoses.
    - Artifact-free MRI scans.
- Local typically developing children:
    - 4 to 12 years old.
    - No history of SCI.
    - In stable medical condition.

We excluded participants who met any of the following exclusion criteria:

- All Participants:
    - Painful musculoskeletal dysfunction, unhealed fracture, or pressure sore.
    - Progressive neurological disease/condition.
    - Total ventilator-dependence.
    - Contraindications to MRI (e.g., metallic implants, implanted medical devices, metallic foreign bodies).

- Use of Botox, baclofen, or any other antispasmodic medication that affects the neuromuscular system's ability to respond within the past 3 months.

Basic demographic information was collected for all participants. For children with SCI, we recorded any history of previous rehabilitation interventions and details related to the injury level, severity, etiology, onset age, and chronicity as per the NINDS-CDE guidelines for children with SCI (Mulcahey et al., 2017). Children with SCI over the age of six (Chafetz et al., 2009; Mulcahey et al., 2011), were clinically examined and scored on the International Standards for Neurological Classification of SCI (ISNCSCI) American Spinal Injury Association (ASIA) Impairment Scale (AIS) evaluation (Kirshblum et al., 2011) by experienced pediatric physical therapist.

## Experiment 4: Gray Matter Morphometry of the Pediatric Brain after SCI

This experiment aimed to examine changes in gray matter volume and cortical thickness in children with SCI compared to typically developing controls (TD). Cortical thickness changes have been widely studied in individuals with SCI using neuroimaging techniques such as magnetic resonance imaging (MRI). Several studies have reported significant reductions in cortical thickness in several regions of the brain in individuals with SCI compared to healthy controls. These regions include the primary sensorimotor cortex, primary somatosensory cortex, premotor cortex, supplementary motor area, and several regions of the parietal and temporal lobes. However, all these studies have been performed on adult populations and more research is needed to understand the effects of SCI on the developing brain. The present study aimed to fill this gap in the literature by examining gray matter changes in the brains of children with SCI by analyzing high-resolution T1-weighted scans and comparing the results to those of TD.

### *Hypothesis*

When compared to normative data from the HBN, children with SCI will exhibit reduced gray matter (GM) morphometry of cortical and subcortical sensorimotor structures. Specifically, cortical regions of interest in S1 and M1 representing the lower limbs would show decreased cortical thickness and that basal ganglia and thalamic nuclei involved in sensorimotor function would have lower volumes in children with SCI.

## *Methods*

### *Data Acquisition*

Structural images obtained at the University of Louisville were acquired via a T1w magnetization-prepared rapid gradient-echo sequence (MPRAGE) in 224 sagittal slices. Imaging parameters were as follows: echo time (TE) = 3.15 ms, repetition time (TR) = 2500 ms, flip angle = 8.0°, field of view (FoV) = 256 mm, and voxel size = 0.8 × 0.8 × 0.8 mm. whereas, T1w images from HBN consisted of in 224 sagittal slices with TE = 3.15 ms, TR = 2500 ms, flip angle = 8.0°, and voxel size = 0.8 × 0.8 × 0.8 mm.

### *Quality Control*

All T1w images were visually inspected for artifacts and programmatically assessed for quality control using MRIQC (Esteban et al., 2017) to extract empirical measures related to head movement and blurring artifacts. The coefficient of joint variation (cjv) of GM and WM was proposed as an objective measure of aliasing and inhomogeneity artifacts related to head-motion (Ganzetti et al., 2016). Lower cjv values represent less motion. Similarly, the entropy focus criterion (efc) for artifacts uses the Shannon entropy of voxel intensities as an indication of ghosting and blurring induced by head-motion (Atkinson et al., 1997). Lower efc values are better. One participant (P24, 5.8 years, AIS A-C1) was excluded further analysis based on cjv, efc, and visual inspection of motion-induced artifacts.

### *Preprocessing*

T1w images were preprocessed and analyzed using a stable version (v.7.2.0) of Freesurfer software (Fischl, 2012; Fischl & Dale, 2000) (link: http://surfer.nmr.mgh.harvard.edu). The automatic `recon-all` command with the `-all, -3T,` and `-parallel` options was used for preprocessing at a smoothing size of 10-mm full-width half-maximum kernels. The cortical thickness was calculated in the surface-based pipeline, which consists of several stages, including motion correction, registration to the Montreal Neurological Institute atlas, correction of intensity inhomogeneity, skull stripping, classification of voxels into white matter and non-white matter, tessellation of gray-white matter boundaries, automatic topographic correction, surface reconstruction, and finally thickness estimated by the distance between the white surface (between gray and white matter) and pial surface—defined as the boundary between gray matter and cerebrospinal fluid (Dale et al., 1999; Fischl et al., 1999). Cortical parcellation was done using the Desikan–Killiany atlas provided in the Freesurfer suite, which labeled 34 cortical regions in each cerebral hemisphere (Desikan et al., 2006; Destrieux et al., 2010).

A detailed visual inspection of the `recon-all` output was conducted manually and errors in the pial and white matter surfaces reconstruction were corrected following the guidelines for manual edits of pediatric surface-based analysis as provided by the freesurfer team (LCN, 2019). After corrections of the pial and white matter surfaces were completed, the corrected data sets were reprocessed using the `recon-all -all` command to ensure accurate cortical thickness measurements.

Next, cortical labels for the precentral (M1) and postcentral (S1) gyri were systematically dived into 5 subregions perpendicular to their long using the `mris_divide_parcellation` freesurfer binary. The resulting subregions were labeled from medial to lateral as: leg, torso, arms, face, and tongue. These new subregional labels were then resampled to the surface of each participant using the `mri_label2label` and `mris_label2annot` binaries.

Each participant's cortical thickness expressed in millimeters (mm) was then extracted from both left and right paracentral gyri (representing motor and sensory function of the foot) and from the newly created S1 and M1 subregions representing the legs and face via `mris_anatomical_stats` and aggregated into a tabular file for group analysis with the `lh.aparc.stats` and `rh.aparc.stats` commands.

The thickness of the foot and leg cortical ROIs were then normalized to the thickness of a cortical area somatotopically mapping a body part well above the level of the injury and therefore not expected to change—the face. We divided the thickness of each lower limb ROI by the thickness of the M1 and S1 subregions representing the face and scaled them to 100.

For subcortical volume analysis, the volume-based freesurfer stream was utilized to automatically segment and label the caudate (Ca), putamen (Pu), and pallidum (Pa). Volumetric measures expressed in millimeters cubed ($mm^3$) were extracted from these ROIs via the `asegstats2table` command. In addition, volume measurements for the thalamus as a whole (Th) were obtained via the `segmentThalamicNuclei.sh` bash script bundled with freesurfer. To account

for the biodiversity of individuals' head sizes, subcortical ROIs volumes were divided by the estimated total intracranial volume (eTIV) and scaled by 1000.

*Data Analysis*

Normalized cortical thickness and subcortical volume measurements were then exported into a "tidy" formatted (Wickham, 2014) tabular file for further analysis. The Python Pandas (McKinney, 2010; Pandas, 2020) library was used for data management, while data visualization was implemented via the Matplotlib (Hunter, 2007), Seaborn (Waskom, 2021), Nilearn (Abraham et al., 2014), and Statannotations (Charlier et al., 2022) libraries. All statistical analysis was performed with the stats module of the SciPy library (Virtanen et al., 2020).

Statistical comparisons of continuous variables between groups were studied using nonparametric statistics (Mann–Whitney U) with Benjamini-Hochberg correction for multiple comparisons. Nonparametric methods were required due to violations of the normality assumption required for parametric methods and the unbalanced number of observations in each group. The relationships between changes in brain morphometry (cortical thickness and subcortical volume) and electrophysiological outcomes of volitional (Chapter 3: Experiment 1) and reflexive (Chapter 3: Experiment 2) motor control was examined via linear regressions (continuous variables) and logistic regressions (categorical variables).

Considering that 17 neuroimaging datasets in our typically developing control group came from a publicity available open data repository, we did not have the opportunity to examine their electrophysiology. Nonetheless, it was reasonable

to assume that these 17 neurological intact children from the HBN would have demonstrated normal outcomes in the FNPA experiment, which evaluates each child's ability to generate voluntary movements upon request. As previously reported in the literature and based on our extensive experience with this assessment in typically developing children, they consistently perform the requested maneuvers. To account for this, we generated synthetic data grounded in the literature. For the FNPA, we assumed that these HBN children would have exhibited a 100% probability of response for each muscle during the experiment, as previously reported by our group (Atkinson et al., 2019). All instances in which these synthetic data were used are clearly denoted as such.

*Results*

When compared to normative data, children with SCI exhibited reduced gray matter (GM) morphometry of cortical and subcortical sensorimotor structures. Specifically, the primary motor cortex (M1) representing the legs and the paracentral cortex representing the foot showed decreased cortical thickness. Additionally, the thalamus had lower volumes in children with SCI.

*Subject Characteristics*

The study included a total of 8 children with spinal cord injury (SCI) and 18 typically developing controls (TD). The age range of the children with SCI was 6.3 - 12.8 years, while the age range of the TD group was 5.4 - 13.3 years. There were no significant differences in age ($P$ = .283), BMI ($P$ =.184), or gender ($P$ = .883) between the two groups. Furthermore, the results of our neuroimaging quality

control analysis indicated no statistically significant differences in motion artifact ($P$ = .356) or ghosting artifact ($P$ = .807) between the SCI and TD groups.

*Cortical Gray Matter Thickness*

A comparison of cortical thickness between the SCI and TD groups revealed a significant reduction in thickness in several regions of the sensorimotor cortex in the SCI group compared to the TD group. The statistical analysis was corrected for multiple comparisons, and a threshold of $P$ < .05 was used to determine significance. Specifically, the gray matter morphometry of the sensorimotor-representing regions of the right (left paracentral gyrus, $P$ = .005) and left (right paracentral gyrus, $P$ = .011) foot were found to be significantly reduced in children with SCI compared to neurological intact children. On average, for children with SCI, these areas were 91% as thick as the area of their brains representing the face. In contrast, the paracentral gyri of participants without a spinal cord injury were on average 96% as thick as the region of their precentral gyrus representing the face. There was also reduction in the thickness of the cortical ROI in charge of sensory (medial right postcentral gyrus, $P$ = .001) and motor (medial right precentral gyrus, $P$ < .001) function of the left leg of children with SCI. Figure 4.1 reports the results of aggregating left and right ROIs. Mann-Whitney-Wilcoxon two-sided tests with Benjamini-Hochberg correction revealed that there was a statistically significant difference between the medial precentral gyri in children with SCI compared to TD children ($P$ = .007). Similarly, a significant difference was observed between the paracentral gyri in children with SCI compared to TD children ($P$ < .001). However, the marginal difference between

these groups in the medial postcentral gyri did not reach statistically significance groups ($P$ = .061).

In addition to these changes, we also found a significant correlation between changes in cortical thickness in all three regions of interest and the overall probability of a volitional muscle activation during the FNPA experiment. Specifically, we found that cortical thickness changes in the paracentral gyri were significantly correlated (Pearson's r =.588, $P$ < .001) to the overall muscle activation probability in the FNPA experiment, where the synthetic data for TD subjects from HBN was used. Furthermore, we found that FNPA muscle activation was also directly correlated with changes in the cortical thickness of the medial precentral (r = .375, $P$ = .006) and medial postcentral gyri (r =.305, $P$ = .028). The results of a logistic regression analyses suggest a relationship between cortical thickness and the presence of volitional EMG activity in the legs among the three cortical ROIs. Specifically, FNPA responses in the legs is associated with higher normalized cortical thickness in the paracentral gyri (β = .356, LLR p-value < .001). The medial postcentral gyri (β =.098, LLR p-value = .054) and precentral gyri (β = .113, LLR p-value = .054) exhibited marginal relationships between the predictor and outcome variables, suggesting a positive relationship with FNPA responses in the leg but not statistically significant at the .05 level. See Figure 4.2.

Additional analysis was conducted to examine the correlation between the overall probability of a response during the auditory somatosensory reflex (ASR) experiment and the normalized cortical thickness in the same three regions of interest. The results revealed that there was no significant correlation between the

probability of eliciting an ASR response from any of the muscles monitored and cortical thickness (paracentral, *P* = .114; medial precentral, *P* = .145; and medial postcentral, *P* =.811). Further, based on the results of a logistic regression analyses, it appears that there were no significant relationships between normalized cortical thickness and the patterns of ASR responses described in Chapter 3 for none of the cortical ROIs. In the paracentral, medial postcentral, and medial precentral gyri, the coefficients for normalized thickness were non-significant with p-values of .08, .369, and .227, respectively. See Figure 4.3.

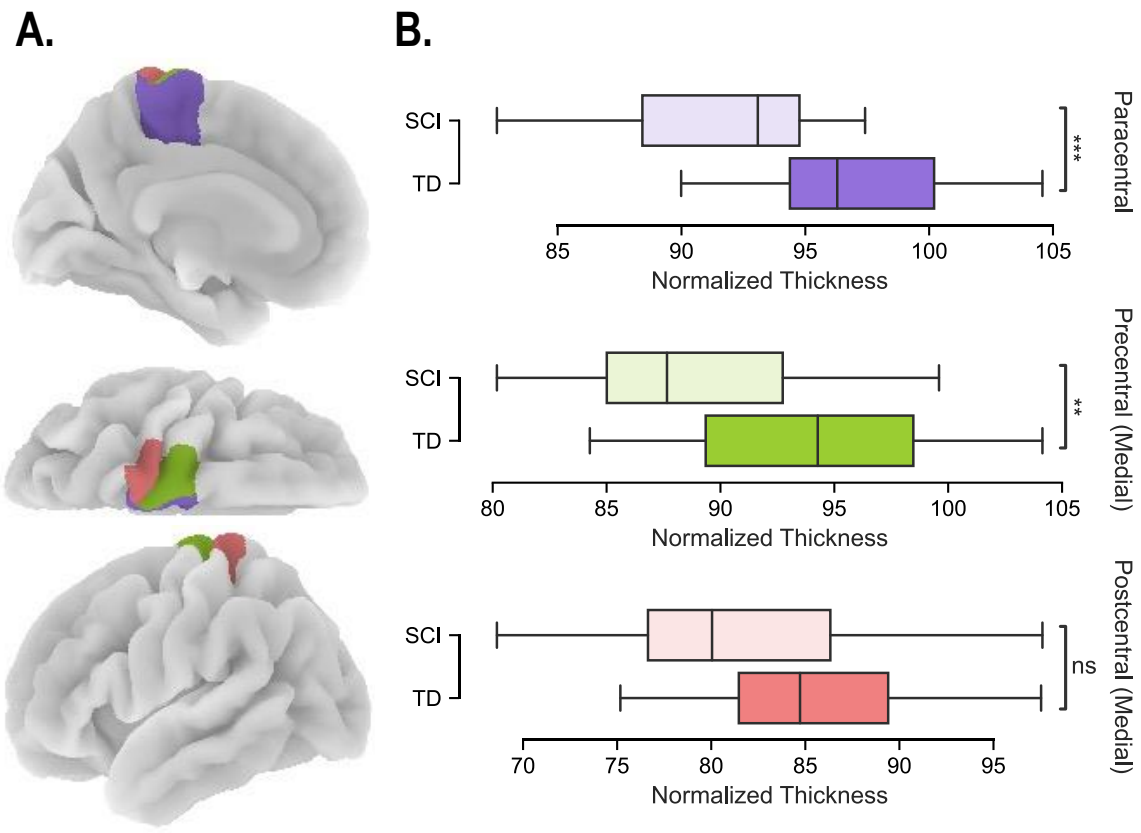


**Figure 4.1: Cortical thickness differences among SCI and TD children**

**Panel A** displays medial, dorsal, and lateral views of the brain, highlighting the examined ROIs: the paracentral gyrus responsible for sensorimotor function of the lower leg and foot in purple; the medial precentral gyrus responsible for motor function of the thigh in green; and the medial postcentral gyrus shaded in coral, which maps the sensory input from the thigh. **Panel B** shows a series of horizontal box graphs that represent the differences in cortical thickness among the three regions of interest between typically developing children (TD) and children with spinal cord injuries (SCI). Each box graph displays the median, upper and lower quartiles, and the range of the cortical thickness values for each region of interest. The statistical significance of the differences is shown by the asterisks next to the boxes (* P < .05; ** P < .01; *** P < .001).

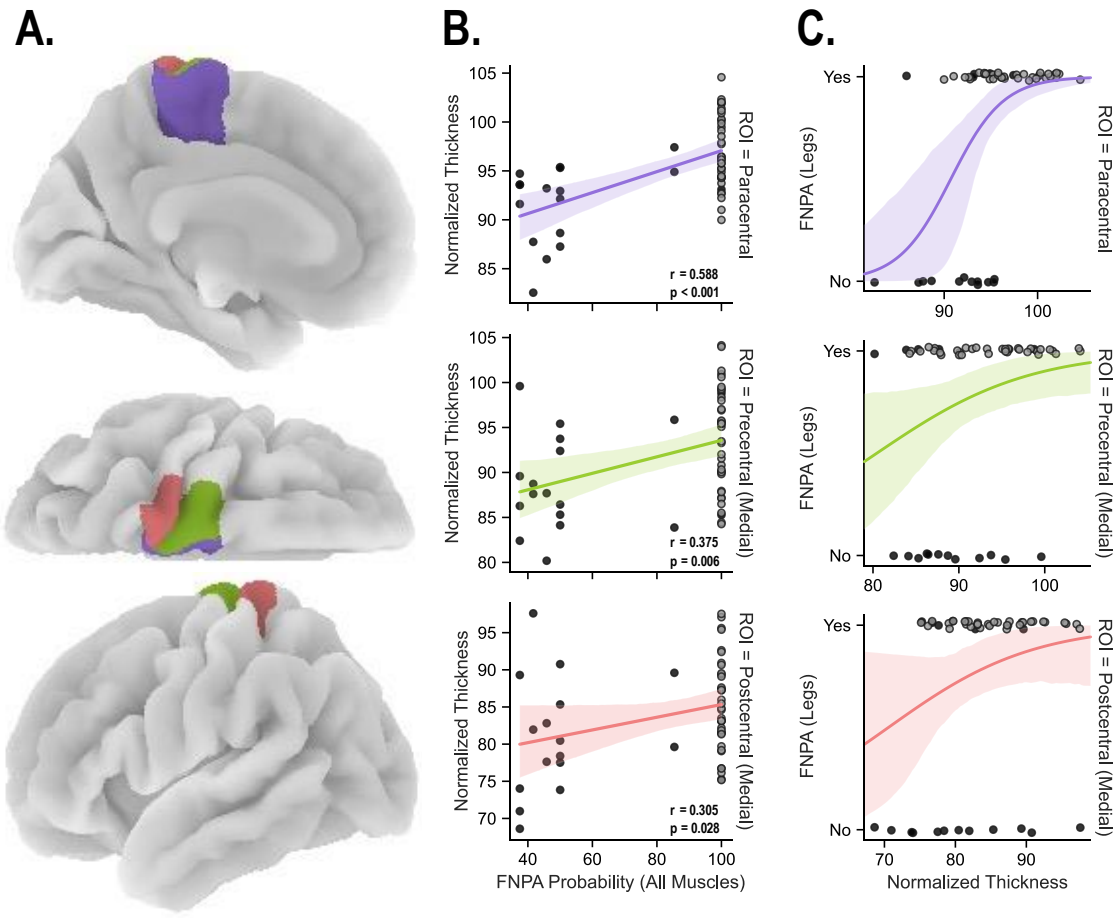


**Figure 4.2: Correlations between cortical thickness and volitional motor output**

**Panel A** displays medial, dorsal, and lateral views of the brain, highlighting the examined ROIs: the paracentral gyrus responsible for sensorimotor function of the lower leg and foot in purple; the medial precentral gyrus responsible for motor function of the thigh in green; and the medial postcentral gyrus shaded in coral, which maps the sensory input from the thigh. **Panel B** reveals the correlation between the normalized cortical thickness (y-axis) and the probability of a functional neurophysiological assessment (FNPA) response for all muscles tested (x-axis). The correlation coefficients (r) and p-values are presented in each sub-plot. The shaded region represents the confidence interval (CI) of the correlation. **Panel C** presents logistic regression analyses of the normalized cortical thickness (x-axis) to a categorical variable representing the presence or absence of a response in the legs during the FNPA experiment (y-axis). Gray data points represent synthetic data used for FNPA measurements for the HBN datasets.

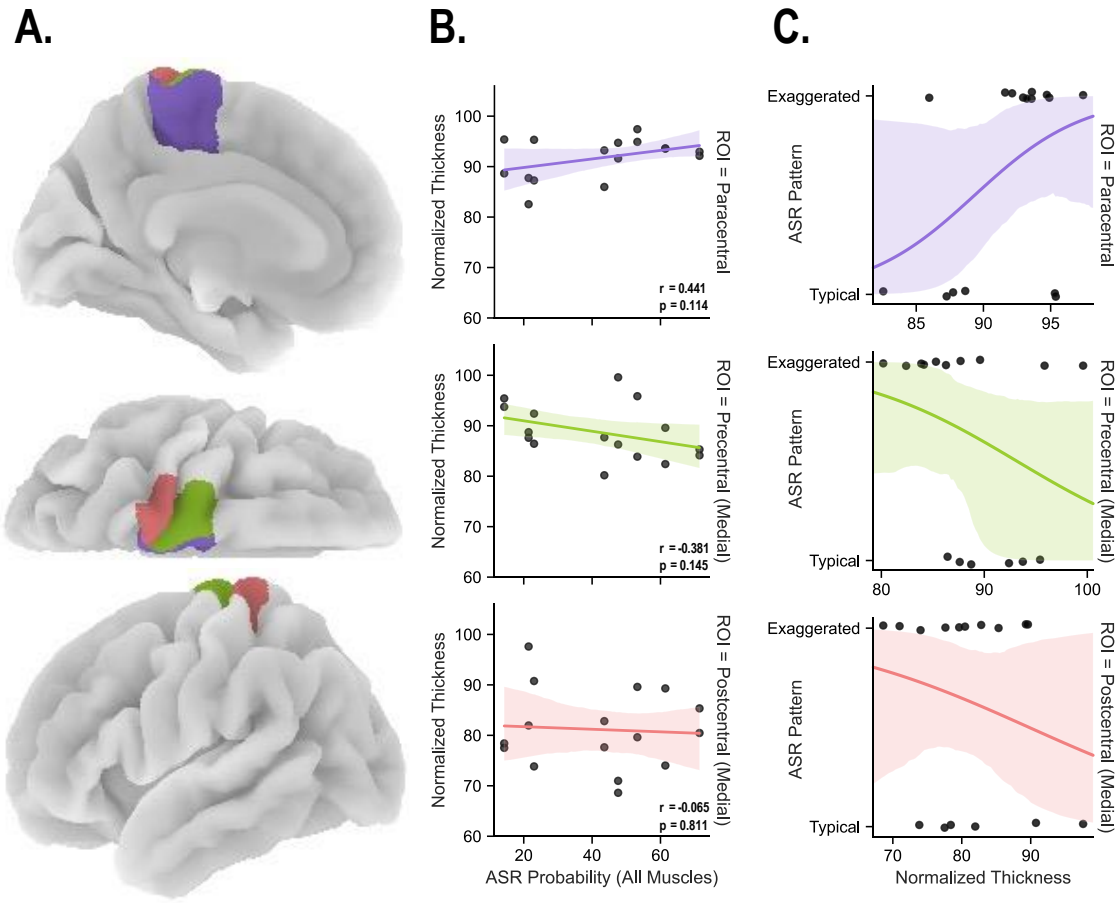


**Figure 4.3: Correlations between cortical thickness and acoustic startle reflex**

**Panel A** displays medial, dorsal, and lateral views of the brain, highlighting the examined ROIs: the paracentral gyrus responsible for sensorimotor function of the lower leg and foot in purple; the medial precentral gyrus responsible for motor function of the thigh in green; and the medial postcentral gyrus shaded in coral, which maps the sensory input from the thigh. **Panel B** reveals the correlation between the normalized cortical thickness (y-axis) and the probability of an acoustic startle reflex (ASR) response for all muscles tested (x-axis). The correlation coefficients (r) and p-values are presented in each sub-plot. The shaded region represents the confidence interval (CI) of the correlation. **Panel C** presents logistic regression analyses of the normalized cortical thickness (x-axis) to a categorical variable representing the pattern of ASR response (y-axis).

*Subcortical Volume*

The normalized volume of subcortical structures involved in sensorimotor function were compared between the SCI and TD groups. The results showed a statistically significant difference between thalamus of the SCI and TD groups (*P* = .016). A marginally significant difference was found in the putamen between the two groups (*P* = .042) that did not survive the multiple comparisons correction. Conversely, there was no significant difference in the volume of the caudate (*P* = .532) and the pallidum (*P* = .271) between the SCI and TD groups. See Figure 4.4.

Correlation analysis of the overall probability of volitionally eliciting EMG during the FNPA experiment and normalized volume of subcortical ROIs was conducted among the children with SCI and the healthy controls (synthetic data used for HBN controls as). The strength of the correlation varied across the ROIs, with the highest correlation observed in the thalamus (r = .463, *P* = .001). A moderate correlation was observed in the putamen ROI (r = .313, *P* = .024), and marginal to no correlations were observed in the caudate (r = .142, *P* = .315) and pallidum (r = .245, *P* = .08). In addition, for each subcortical ROI, a logistic regression was performed to examine the relationship between normalized volume and volitional motor output from the legs during the FNPA experiment. The results showed a significant positive relationship between normalized volume and a categorical variable (Yes/No) related to voluntary leg EMG activation during the FNPA in the pallidum (β = 9.219, *P* = .026), putamen (β = 3.19, LLR p-value = .01), and thalamus (β = 4.978, LLR p-value < .001). In the caudate, no significant relationship was found (β = 1.197, LLR p-value = .44). See Figure 4.5.

We then, investigated the correlation between the probability of ASR in any muscle and the normalized volume of our four subcortical ROIs. Figure 4.6 shows a positive correlation was found between the two variables in all ROIs, with significant Pearson correlation coefficients and p-values. Specifically, for the caudate ($r = .563$, $P = .023$), pallidum ($r = .799$, $P = .001$), putamen ($r = .633$, $P = .009$), and thalamus ($r = .612$, $P = .012$) of SCI children with higher probability of an ASR response have a higher normalized volume. Building upon these findings, we explored the relationship between the children with SCI that presented with an exaggerated versus a typical ASR recruitment pattern and the normalized volume of the four subcortical ROIs. The results indicate that there was a significant correlation was observed in the pallidum ($\beta = 69.253$, LLR p-value $< .001$), putamen ($\beta = 19.809$, LLR p-value $= .001$), and thalamus ($\beta = 4.242$, LLR p-value $= .016$) regions. In addition, there was a marginally significant positive relationship between the normalized volume of the caudate ($\beta = 4.731$, LLR p-value $= .072$) and the reflexive recruitment pattern during the ASR assessment.

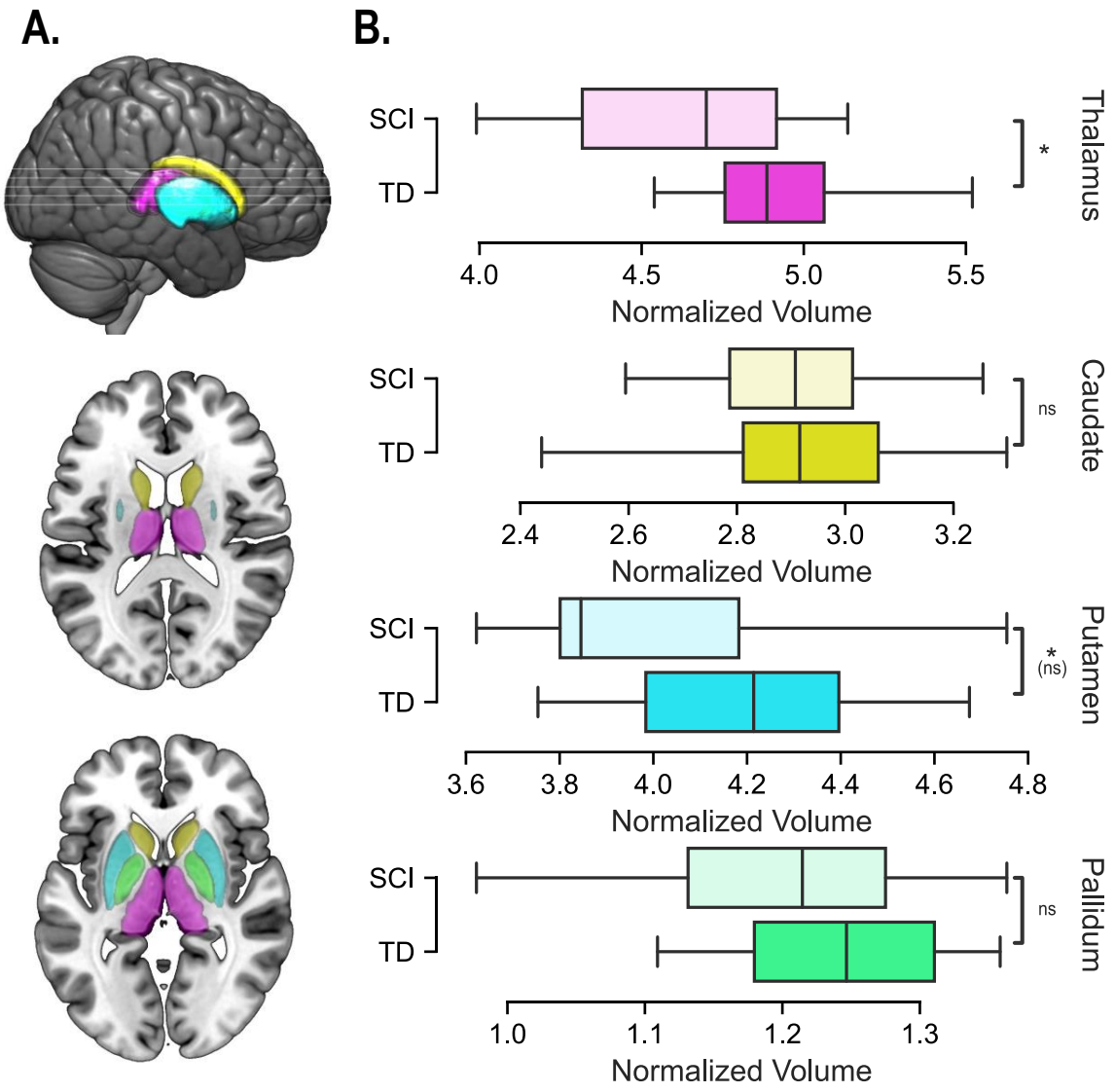


**Figure 4.4: Subcortical volume differences among SCI and TD children**

**Panel A** displays a three-dimensional rendering and two axial sections of brain, highlighting the examined ROIs: the thalamus in pink; the caudate in yellow; the putamen in blue; and the pallidum in green. **Panel B** shows a series of horizontal box graphs that represent the differences in normalized volume among the four regions of interest between typically developing children (TD) and children with spinal cord injuries (SCI). Each box graph displays the median, upper and lower quartiles, and the range of the normalized volume for each region of interest. The statistical significance of the differences is shown by the asterisks next to the boxes (* P < .05; ** P < .01; *** P < .001).

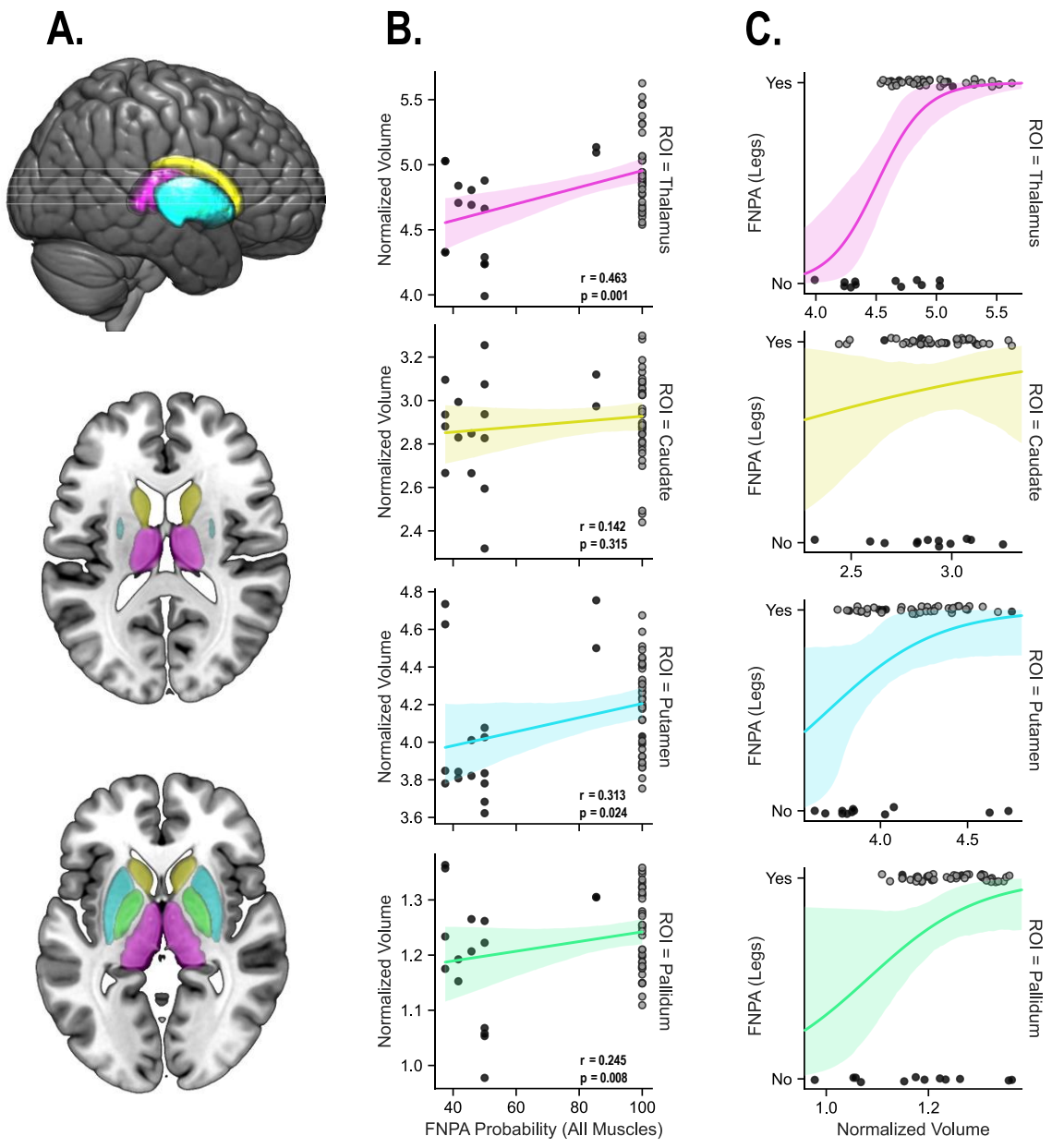


**Figure 4.5: Correlations between subcortical volume and volitional motor output**

**Panel A** displays a three-dimensional rendering and two axial sections of brain, highlighting the examined ROIs: the thalamus in pink; the caudate in yellow; the putamen in blue; and the pallidum in green. **Panel B** reveals the correlation between the normalized ROI volume (y-axis) and the probability of a functional neurophysiological assessment (FNPA) response for all muscles tested (x-axis). The correlation coefficients (r) and p-values are presented in each sub-plot. The shaded

region represents the confidence interval (CI) of the correlation. **Panel C** presents logistic regression analyses of the normalized ROI volume (x-axis) to a categorical variable representing the presence or absence of a response in the legs during the FNPA experiment (y-axis). Gray data points represent synthetic data used for FNPA measurements in HBN datasets.

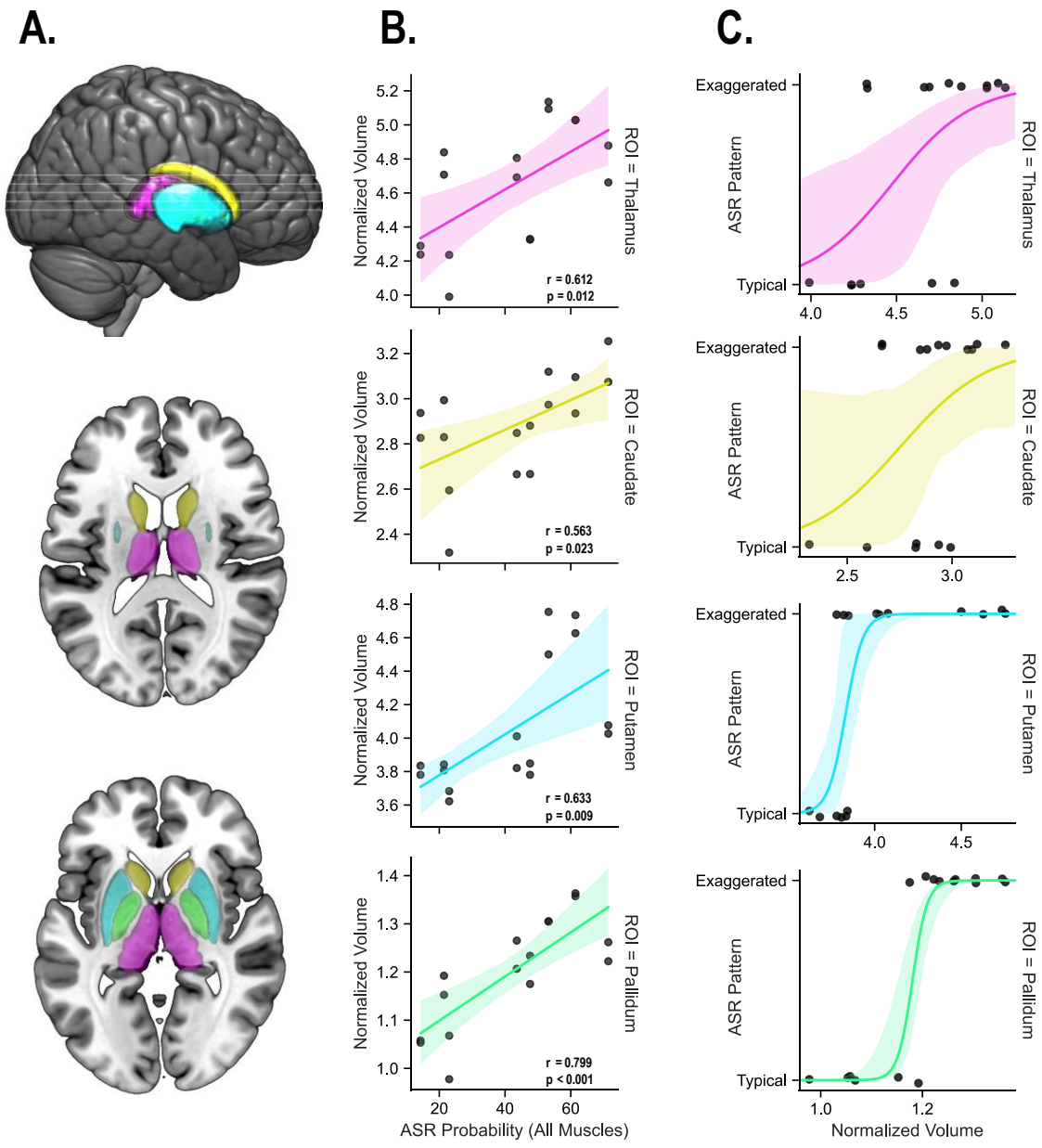


**Figure 4.6: Correlations between subcortical volume and acoustic startle reflex**

**Panel A** displays a three-dimensional rendering and two axial sections of brain, highlighting the examined ROIs: the thalamus in pink; the caudate in yellow; the putamen in blue; and the pallidum in green. **Panel B** reveals the correlation between the normalized ROI volume (y-axis) and the probability of an acoustic startle reflex (ASR) response for all muscles tested (x-axis). The correlation coefficients (r) and p-values are presented in each sub-plot. The shaded region represents the confidence interval (CI) of the correlation. **Panel C** presents logistic regression

analyses of the normalized ROI volume (x-axis) to a categorical variable representing the pattern of ASR response (y-axis).

*Discussion*

This experiment aimed to investigate differences in cortical and subcortical brain regions involved in sensorimotor function between children with spinal cord injury (SCI) and typically developing controls (TD). Our findings suggest significant differences in both cortical and subcortical regions between the two groups. Further, we found novel correlations between these changes and electrophysiological measurements of residual translesional neural transmission in motor spinal pathways, providing insight into potential neural mechanisms mediating supraspinal reorganization in children with SCI.

We analyzed 8 children with SCI and 18 typically developing controls (TD) and found no significant differences in age, BMI, or gender distribution between the two groups, indicating that the groups were well-matched. Thus, any differences observed in the study can be attributed to the injury status of the participants rather than demographic factors. We also used a respected neuroimaging quality control analysis to evaluate motion and ghosting artifacts and found no significant differences between the SCI and TD groups.

In terms of cortical thickness, we found significant reductions in thickness in several regions of the sensorimotor cortex in the SCI group compared to the TD group. Specifically, gray matter morphometry of the sensorimotor-representing regions of the right and left foot, as well as the cortical ROI in charge of sensory and motor function of the left leg, were significantly reduced in children with SCI compared to neurological intact children.

A novel aspect of this work is the simultaneous exploration of cortical morphometry changes and their relationship to electrophysiological measurements of spinal tracts integrity. We found that changes in cortical thickness in all three regions of interest were significantly correlated with the overall probability of volitional muscle activation during the FNPA experiment, with the strongest correlation observed in the paracentral gyri. The overall provability of volitional EMG activity during the FNPA was also directly correlated with changes in the cortical thickness of the medial precentral and medial postcentral gyri. When we conducted a logistic regression to analyze whether having any voluntary EMG activations in the lower extremities was related to the cortical thickness of sensorimotor regions, we found the strongest correlation with the paracentral gyri. When we conducted a logistic regression to analyze whether having any voluntary EMG activations in the lower extremities had an effect on the cortical thickness of sensorimotor regions, we found the strongest correlation with the paracentral gyri. In other words, cortical thinning of the region representing the foot and lower leg described after SCI is not as drastic for children who preserve the voluntary ability to recruit lower motor neurons dedicated to activating muscles of the leg. The literature widely attributes this ability to a joint effort between the CST and non-pyramidal tracts, such as the RST.

When we probed the relationship between the probability of eliciting an ASR response mediated by the RST and cortical thickness after SCI, we did not find a significant correlation in any of the regions of interest. Furthermore, our logistic regression analyses did not reveal any significant relationships between

normalized cortical thickness and SCI-associated exaggerated patterns of ASR responses. These results are consistent with the underlining neural mechanisms driving ASR responses as they are reported to act at the level of the brain stem without cortical targets directly.

Our examination of subcortical volume changes after pediatric onset SCI presented similar results. We found a statistically significant difference in the volume of the thalamus between the SCI and TD groups, as well as a marginally significant difference in the putamen. These changes were again significantly correlated with the overall probability of eliciting a volitional response from any muscles during the FNPA experiment and with the ability to drive EMG activation of the legs. However, we found a previously unreported relationship between the overall probability of evoking an acoustic startle reflex (ASR) response and the normalized volume of all four subcortical regions. Our results indicate a strong positive correlation between the probability of eliciting ASR responses and preserved subcortical volume. Of greater clinical relevance, our findings show a significant correlation between subcortical morphometry and children with SCI who exhibit an exaggerated ASR recruitment pattern. In a recent study of six children with SCI (Howland et al., 2023), a relationship was found between preserved reticulospinal inputs to circuitry below the level of injury, assessed by ASR responses, and the ability of three subjects to achieve walking after activity-based locomotor training (ABLT). Of note, those who achieved walking after ABLT presented with no indication of corticospinal integrity, as demonstrated by the lack of TMS-evoked responses. These findings, and others (Baker & Perez, 2017;

Sangari & Perez, 2020), suggest that supraspinal drive mediated by the RST might play a key role in promoting functional gains in the motor control of spinal networks. Our results, however, indicate that both volitional and reflexive descending translesional transmission are involved in preserving subcortical volume and that only the relative residual integrity of voluntary descending neural drive is associated with preserving gray matter thickness in the somatosensory cortex.

In summary, these findings present a novel understanding of the neural mechanisms involved in supraspinal sensorimotor reorganization in children with spinal cord injury (SCI) and their association with the residual neural transmission of motor pathways. However, caution should be exercised when interpreting our results, as our study had a relatively small sample size, and the cohorts were scanned at different MRI sites. Nevertheless, our well-matched groups and rigorous quality control analysis support the validity of our study and suggest that observed differences can be attributed to the effects of spinal cord injury during childhood. Future studies with larger sample sizes and multi-site scanning protocols are needed to confirm our findings and advance our understanding of the neuroplasticity underlying sensorimotor reorganization in children with SCI.

## Experiment 5: Microstructural Integrity of the CST after Pediatric SCI

The aim of this study was to investigate the impact of spinal cord injury (SCI) on the microstructural integrity of the corticospinal tract (CST) in children using neuroimaging techniques. Specifically, we used diffusion-weighted imaging (DWI) to assess the CST integrity in children with SCI and compared it to a group of typically developing controls (TD). Specifically, we used diffusion-weighted imaging (DWI) to assess the CST integrity in children with SCI and compared it to a group of typically developing controls (TD). DWI is a widely used neuroimaging technique that provides a way to assess the microstructural integrity of white matter in the brain. Essentially, DWI is used to measure the diffusion of water molecules in tissue. The water within and around bundles of white matter is restricted from moving in every direction due to the hydrophobic myelin sheets that surround the axons. This restriction of isotropic water diffusion is measured as fractional anisotropy (FA). High FA values indicate that water within axons is not free to move with equal probability in every direction and correlates with the microstructural integrity of myelin. Conversely, low FA values indicate a lack of the restriction provided by myelin and thus low integrity of white matter bundles.

Several studies have used DWI to investigate the impact of SCI on the integrity of white matter in the adult brain. These studies have reported significant reductions in the FA of white matter tracts, such as the CST, in individuals with SCI compared to healthy controls. This reduction in FA suggests that the microstructural integrity and, therefore, the effectiveness of the CST is often affected by the injury, leading to motor deficits. Overall, DWI studies have offered

significant contributions to our knowledge of the impact of SCI on white matter integrity and have aided in understanding the relationship.

*Hypothesis*

Children with SCI would show reduced microstructural integrity of the CST compared to TD controls, as measured by FA values derived from diffusion-weighted imaging. It was expected that a significant difference in CST FA values would be observed between the SCI and control groups, with lower FA values in the SCI group indicating lower functional integrity of the CST.

*Participants*

For this experiment, our SCI cohort consisted of the same six males and two females (mean age = 9.2 ± 2.0 years old) analyzed in the previous experiment. However, due to a lack of diffusion-weighted imaging (DWI) datasets of sufficient quality, our HBN (Alexander et al., 2017) TD participants were reduced to eight typically developing children. The TD cohort for this experiment included six males and three females with a group mean age of 9.4 ± 2.2 years old. There were no statistically significant differences observed between the two groups in terms of age (P = .795), BMI (P = .907), sex (P = .706), and the occurrence of MRI artifacts such as motion (P = .969) and ghosting (P = .406).

*Methods*

*Data Acquisition*

Locally obtained DWI scans were acquired in 64 diffusion directions with b-values of 0 s/mm$^2$, 1000 s/mm$^2$, and 2000 s/mm$^2$. Data were acquired parallel to AC–PC line with 1.8 mm isotropic voxels, FoV = 187 mm, TR = 3200ms, and with a multiband acceleration factor of 3. During structural and DWI acquisition, children were allowed to watch any movie or video of their choosing. For the HBN DWI scans, the data were acquired in 64 directions with b-values equal to 0 s/mm$^2$, 1000 s/mm$^2$, and 2000 s/mm$^2$ with 1.8 mm isotropic voxels, TR = 3320ms, and using a multiband acceleration factor of 3.

*Preprocessing*

The diffusion-weighted data were preprocessed using QSIPrep, version 0.16.0RC3 (Cieslak et al., 2021), which employs Nipype 1.8.1 (Esteban, 2022; Gorgolewski et al., 2011) to standardize and ensure reproducibility in the preprocessing pipeline for diffusion MRI. QSIPrep is a containerized application that integrates multiple software tools to perform various preprocessing steps.

First, T1-weighted images were corrected for intensity non-uniformity (INU) using `N4BiasFieldCorrection` from ANTs, version 2.3.1 (Tustison et al., 2010). The resulting T1w-reference image was used throughout the QSIPrep pipeline and was skull-stripped using `antsBrainExtraction.sh` (ANTs 2.3.1). Next, it was spatially normalized to the ICBM 152 Nonlinear Asymmetrical template, version 2009c (Fonov et al., 2009), through nonlinear registration with `antsRegistration` (ANTs 2.3.1). To segment the brain tissue into cerebrospinal fluid (CSF), white matter (WM), and gray matter (GM), FAST from FSL, version 6.0.5.1 (Zhang et al., 2001) was used on the brain-extracted T1w images.

DWI data preprocessing consisted of denoising applied using a principal component analysis (PCA) algorithm based on the Marcenko-Pastur distribution (MP-PCA) implemented in MRtrix3's `dwidenoise` (Veraart et al., 2016) with a 5-voxel window , followed by B1 field inhomogeneity correction using `dwibiascorrect` from MRtrix3 with the N4 algorithm (Tustison et al., 2010). After bias correction, the mean intensity was adjusted so that the mean intensity of the b=0 images matched across each DWI scanning sequence. Head motion correction was performed using the b=0 images, and an unbiased b=0 template was constructed over three iterations of affine registrations. The SHORELine method (Cieslak et al., 2021) was used to estimate head motion in b>0 images, and a deformation field was estimated to correct for susceptibility distortions based on fmriprep's fieldmapless (Treiber et al., 2016) approach. The deformation field was generated by coregistering the b=0 reference to the same-subject's intensity-inverted T1w-reference (Huntenburg, 2014; Wang et al., 2017). Finally, the b=0 image was co-registered to the T1-weighted image via the `antsRegistration` binary from ANTs, and the DWI time-series were resampled to AC-PC to generate a preprocessed DWI dataset with 2mm isotropic voxels ready for the reconstruction of white matter fiber tracts.

*Data Analysis*

We conducted a tractography analysis of the corticospinal tract using DSI Studio (version 22.04). Tractography computes streamlines into bundles representing the major WM tracts and extracts tract profiles of diffusion properties along those bundles. We compared the CST of children with SCI and TD children

to assess microstructural changes of the axons reflected by changes of FA along the reconstructed tract.

The CST for all participants was reconstructed using a multishell diffusion scheme with b-values of 1000 and 2000 s/mm², and 64 diffusion sampling directions for each non-zero b-value. The in-plane resolution was set to 2 mm, and the slice thickness was 2 mm. To assess the accuracy of the b-table orientation, we compared fiber orientations with those of a population-averaged template (Yeh et al., 2018). The diffusion data were reconstructed in the MNI space using q-space diffeomorphic reconstruction (Yeh & Tseng, 2011) to obtain the spin distribution function (Yeh et al., 2010), with a diffusion sampling length ratio of 1.25.

For each participant, FA measurements were sampled along the newly reconstructed corticospinal tract from caudal to rostral. These caudal-rostral FA profiles of the CST were then exported into “tidy” (Wickham, 2014) tabular output files for subsequent analysis. The CST FA profiles for each participant were reduced to a 20-point series using a piecewise aggregate approximation method (Keogh et al., 2001). Finally, the resulting series were compared between the SCI and TD groups using nonparametric statistics with Benjamini-Hochberg correction for multiple comparisons. The relationships between changes in FA and electrophysiological outcomes of volitional (Chapter 3: Experiment 1) and reflexive (Chapter 3: Experiment 2) motor control was examined via linear regressions and logistic regressions. The Python Pandas (McKinney, 2010; Pandas, 2020) library was used for data management, while data visualization was implemented via the Matplotlib (Hunter, 2007), Seaborn (Waskom, 2021), Nilearn (Abraham et al.,

2014), and Statannotations (Charlier et al., 2022) libraries. All statistical analysis was performed with the stats module of the SciPy library (Virtanen et al., 2020).

*Results*

We conducted a study to compare the fractional anisotropy (FA) along the reconstructed corticospinal tracts (CST) between 8 children with spinal cord injury (SCI) and 9 typically developing (TD) children. The FA profiles were measured at 20 sections along the tract, from caudal to rostral, which were then averaged to obtain a 20-point series for each participant. Our analysis revealed significant differences in the CST FA between the two groups, with lower median FA values observed for the SCI group in both the left and right CSTs (Figure 4.7-D). These differences were highly significant ($P < .001$) according to Mann-Whitney-Wilcoxon tests and were observed across almost every point of the CSTs (Figure 4.7).

Given the observed differences in CST FA between SCI and TD children, we sought to explore the potential associations of these changes to motor function. One relevant measure of motor function is the ability to recruit muscles volitionally, which is in part mediated by descending drive of the CST. To investigate the relationship between FA changes in the CST and volitional muscle recruitment, we analyzed the correlation between mean FA (a summary measure of each CST) and the probability of volitional muscle recruitment during an FNPA experiment. Our analysis revealed a strong positive correlation between mean FA and overall FNPA probability of a volitional muscle activation ($r = .854$, $P < .001$), suggesting that CST FA is a strong predictor of motor function in children with and without SCI. See Figure 4.8-A.

To further inspect the relationship between CST FA and volitional muscle recruitment during FNPA experiments, we conducted a logistic regression analysis to determine whether the mean FA of the CST predicts the presence of voluntary legs muscle recruitment responses during the FNPA experiment. We fitted a logistic regression model to the data and obtained a coefficient of 31.390 and log-likelihood ratio (LLR) p-value of < .001. These results suggest that the mean FA of the CST is a strong predictor of the presence of a FNPA response in the legs. See Figure 4.8-B.

While we observed a significant relationship between the CST FA and volitional motor output as assessed by the FNPA, we also explored the association of CST microstructural integrity and the overall probability of obtaining reflexive muscle responses in the ASR experiment. We revealed a weak positive correlation that was not statistically significant (r = .103, *P* = .705). Finally, a logistic regression analysis was performed to investigate the association between the mean FA of the CST and the pattern of ASR responses. Specifically, the analysis aimed to determine whether the FA values could predict whether the ASR response was exaggerated or typical in with SCI. However, the analysis did not find any significant results (*P* = .8236). See Figure 4.9.

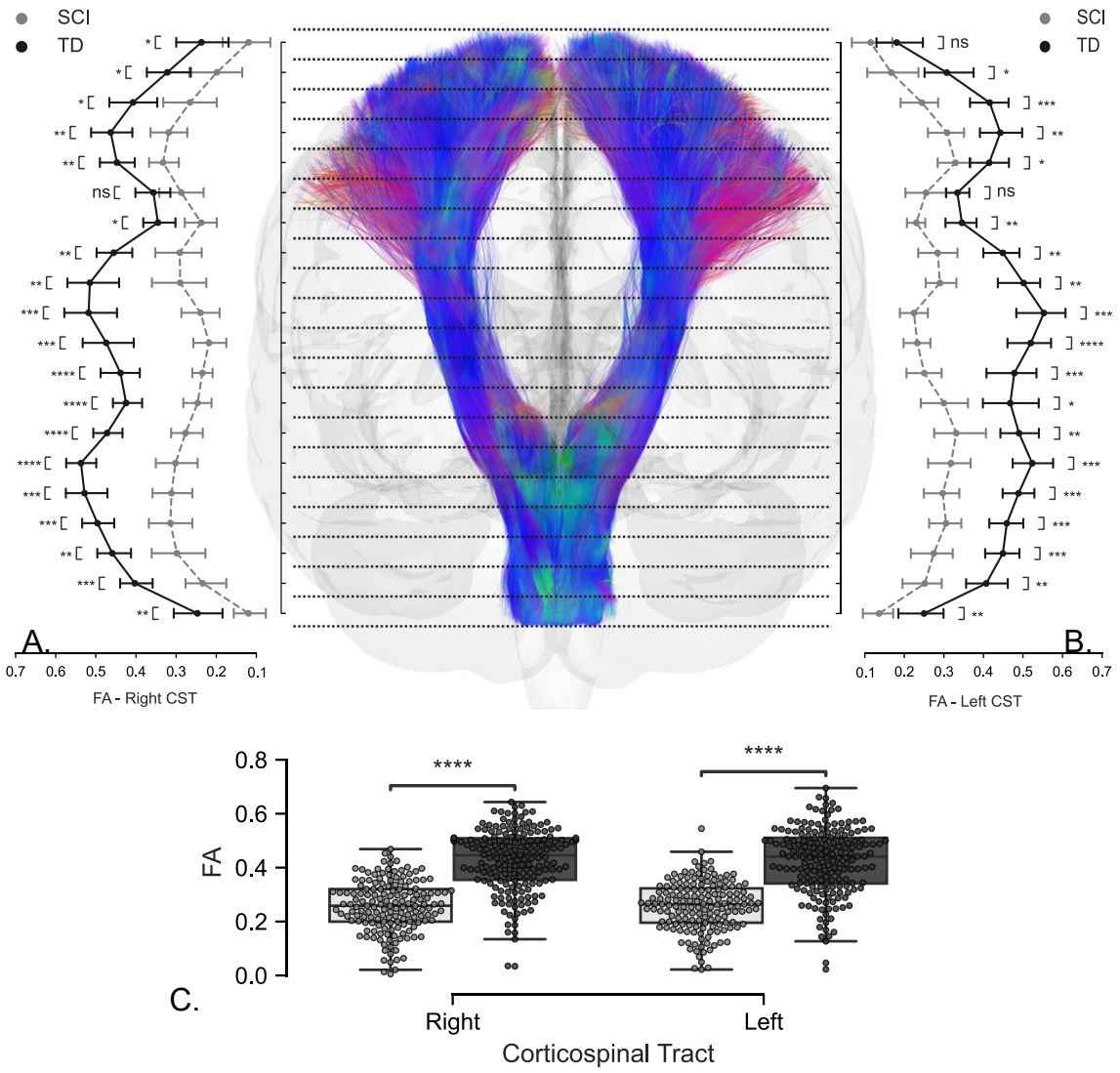


**Figure 4.7: Fractional Anisotropy (FA) profiles along the CST**

Differences in FA between children with spinal cord injury (SCI, n = 8) and typically developing (TD, n = 9) children along the reconstructed right **(Panel A)** and left **(Panel B)** corticospinal tracts (CST). FA measurements were sampled at 20 points along the CST. Significant differences in FA between groups were observed at almost every point along the tract, with lower FA values in the SCI group compared to the TD group. The SCI group is represented by the dashed line, while the TD group is represented by the solid line. Analysis of FA values for the entire tract **(Panel C)** show significant differences among the groups. Data were analyzed using Mann–Whitney U tests for nonparametric data with Benjamini-Hochberg corrections for multiple comparisons. Error bars represent the

standard error of the mean, and asterisks denote significant differences between groups. (* P < .05; ** P < .01; *** P < .001; **** P < .0001).

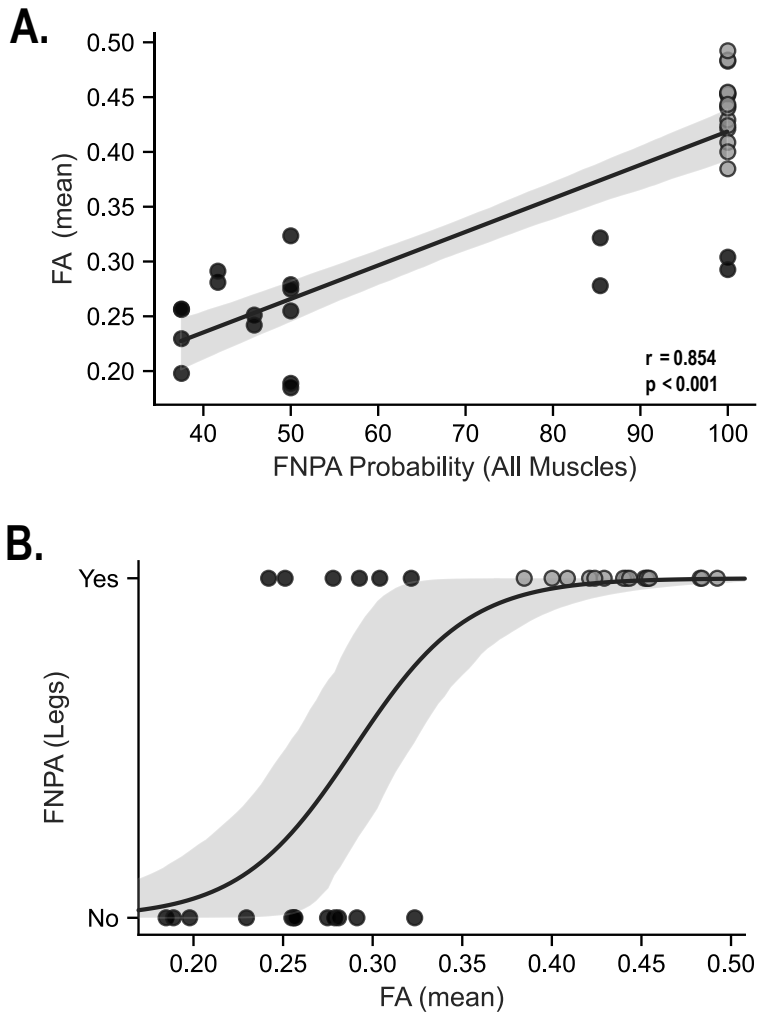


**Figure 4.8: Correlations between CST FA and volitional motor output**

**Panel A** reveals the correlation between the mean fractional anisotropy (FA) of the corticospinal tract (CST) (y-axis) and the overall probability of a functional neurophysiological assessment (FNPA) response for all muscles tested in experiment 1 (x-axis). The correlation coefficients (r) and p-values are presented in the sub-plot. The shaded region represents the confidence interval (CI) of the correlation. **Panel B** presents logistic regression analyses of the mean FA of the CST (x-axis) to a categorical variable representing the presence or absence of a response in the legs during the FNPA experiment (y-axis). Gray data points represent synthetic data used for FNPA measurements of the HBN datasets.

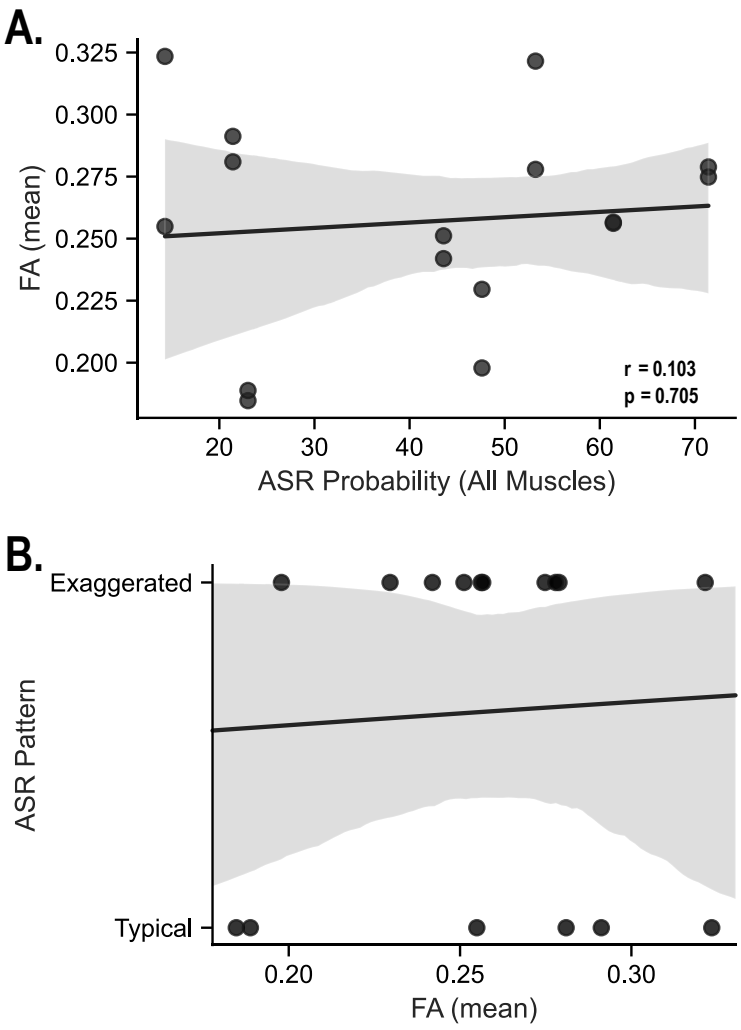


**Figure 4.9: Correlations between CST FA and acoustic startle reflex**

**Panel A** reveals the correlation between the mean fractional anisotropy (FA) of the corticospinal tract (CST) (y-axis) and the probability of an acoustic startle reflex (ASR) response for all muscles tested in experiment 2 (x-axis). The correlation coefficients (r) and p-values are presented in each sub-plot. The shaded region represents the confidence interval (CI) of the correlation. **Panel B** presents logistic regression analyses of the mean FA of the CST (x-axis) to a categorical variable representing the pattern of ASR response (y-axis).

*Discussion*

This experiment was designed to investigate the impact of SCI on the microstructural integrity of the CST in children. In order to achieve this aim, we analyzed the CST of the same 8 children with SCI from experiment 4 above. However, due to the requirement for artifact-free anatomical (t1W) and DWI datasets, our typically developing controls (TD) group was pruned down to 9 subjects. Despite the reduced number of TD controls, the two groups remained comparable in terms of age, BMI, and gender distribution.

Our study found a significant reduction in FA values of the CST in children with SCI compared to age- and sex-matched TD controls, supporting our hypothesis. These differences were highly significant and present across almost every point of the CSTs, indicating a significant impact of SCI on the microstructural integrity of the CST. These findings are consistent with previous studies that reported a decrease in FA values of white matter tracts, including the CST, in adults with SCI. (Guleria et al., 2008; Wrigley et al., 2009).

We also found a strong positive correlation between the mean FA of the CST and the probability of volitional muscle recruitment during an FNPA experiment. This indicates that CST FA is a strong predictor of motor function in both SCI and TD children. Our logistic regression analysis further supports this finding, as we found that the mean FA of the CST is a strong predictor of the presence of an FNPA response in the legs. These results suggest that a reduction in CST FA may be a key factor contributing to motor deficits in children with SCI. This is in line with our understanding of the function of the CST as a major mediator

of voluntary motor drive. In our case, both FA measurements of the CST by DWI and the FNPA protocol are indeed probing the same system from different locations and prospecting. FA is an indirect measurement of the microanatomy of white matter bundles caudally carrying the signals involved in the recruitment of spinal motor pools across the injury site required to produce an FNPA response. It makes sense then that both of these outcome measures are so well correlated with one another.

Conversely, we did not find a significant association between CST microstructural integrity and the overall probability of obtaining reflexive muscle responses in the ASR experiment mediated by a descending spinal pathway altogether. Additionally, our logistic regression analysis did not find any significant association between the mean FA of the CST and the pattern of ASR responses. These findings suggest that the relationship between CST microstructural integrity and reflexive motor output may be more indirect, if existent at all, than that between CST integrity and volitional motor output.

One limitation of this particular experiment is the small sample size, particularly the limited number of TD controls available for comparison. Larger studies with a more extensive control group may provide a more comprehensive understanding of the relationship between CST integrity and motor function in children with SCI and extend our preliminary findings into more generalizable concepts.

## Experiment 6: Functional Connectivity in the Pediatric Brain after SCI

Functional connectivity (FC) is an increasingly utilized tool for the study of supraspinal changes associated with SCI in adults. FC refers to the temporal correlation of neural activity between different brain regions. Studies using functional magnetic resonance imaging (fMRI) have reported reductions in functional connectivity in several regions of the brain in individuals with SCI compared to healthy controls (Hawasli et al., 2018; Min, Park, et al., 2015; Oni-Orisan et al., 2016; Pan et al., 2017; Zhu et al., 2015), including the primary sensorimotor cortex, primary somatosensory cortex, premotor cortex, supplementary motor area, and some subcortical regions such as the basal ganglia. These reductions have been associated with motor and sensory deficits. However, most studies have been conducted on adult populations, and less is known about the effects of SCI on the developing brain. The present study aimed to investigate the impact of SCI on functional connectivity in the brains of children using neuroimaging and to compare it to a group of typically developing controls (TD). Resting-state fMRI was used to identify brain networks that are spontaneously active in the absence of a specific task, such as the sensorimotor network (SMN).

### *Hypothesis*

Children with spinal cord injury (SCI) were expected to show reduced functional connectivity (FC) in the sensorimotor network (SMN) compared to normative data from the HBN. Additionally, the study hypothesized decreased FC

among subcortical structures involved in sensorimotor processing, such as the basal ganglia nuclei and the thalamus, in children with SCI.

## *Methods*

### *Data Acquisition*

Functional blood oxygenation level-dependent (BOLD) images were collected at the University of Louisville using gradient-echo T2*-weighted echoplanar imaging (TE = 30 ms; TR = 1003 ms; flip angle = 31°; FoV = 224 mm; voxel size = 3.3 mm3) with 45 interleaved slices oriented parallel to the anterior commissure – posterior commissure (AC-PC) line. During this 10-minute run, a clip with audio from the movie Despicable Me was shown to all participants. HBN BOLD datasets (TE = 30 ms; TR = 800 ms; flip angle = 30°; and isometric voxel size = 2.4 $mm^3$) were also obtained during the showing of a 10-minute clip from the movie Despicable Me.

### *Quality Control*

All BOLD images were visually inspected for artifacts and programmatically assessed for quality control using MRIQC (Esteban et al., 2017) to extract empirical measures of head movement and blurring artifacts as described in the previous experiment.

*Preprocessing*

FC analysis was performed by using the CONN functional connectivity toolbox (v.22e) (Whitfield-Gabrieli & Nieto-Castanon, 2012; Whitfield-Gabrieli & Nieto-Castanon, 2017) using the default preprocessing pipeline as follows: slice timing correction (interleaved), realignment (subject-motion threshold: 2 mm), and co-registration. The co-registered images were segmented into the GM, WM, and CSF using standard SPM tissue probability maps. These images were then smoothed with an 8 mm FWHM Gaussian kernel. Unwanted noises of blood-oxygenation-level-dependent (BOLD) signals such as motion, physiologic, and other artifacts were reduced using an anatomical component-based noise correction method (aCompCor), which extracts principal components from white matter and cerebrospinal fluid time series. The six head motion parameters from the ART toolbox were also included as confound regressors to reduce spurious spatial correlations due to physiological noise. Band-pass filtering was performed with a frequency window of 0.08~0.09 Hz. All preprocessed data were visually checked for quality control.

*Data Analysis*

We performed a data-driven exploratory group-level independent component analysis (ICA) using the CONN toolbox (Whitfield-Gabrieli & Nieto-Castanon, 2012) to identify the canonical nodes of the sensorimotor network of the brain. This involved applying the fast-ICA algorithm to dynamic volumes concatenated across subjects to identify independent spatial components, which

were then back-projected to individual subjects to generate maps of regression coefficients representing FC between the IC network and every voxel in the brain (Calhoun et al., 2001). We identified 40 independent components (ICs), with three components classified as nodes of the sensorimotor network and labeled lateral, medial, and superior SMN (Figure 4.10). To examine FC differences within the network, we conducted an ROI-to-ROI analysis of the ICA-identified SMN nodes using the CONN toolbox. We then performed a hypothesis-driven analysis of a priori determined subcortical ROI, including the thalamus, caudate, putamen, and pallidum, based on previous studies that indicated functional connectivity abnormalities in adult patients with SCI.

The relationship between the examined regions of interest (ROIs) was modeled using the general linear model (GLM) implemented in the CONN toolbox. This approach allowed us to perform multiple regression analyses to explore the association between the sensorimotor network (SMN) nodes and subcortical regions while accounting for confounding variables such as age and handedness preference. The GLM was used to estimate the beta coefficients representing the strength of functional connectivity between regions. Contrast images were generated by calculating the difference between beta coefficients for each comparison of interest, which were used for group-level statistical analysis. Type I error was controlled using cluster-level FDR-corrected p-value. The significance threshold was adjusted to p-FDR < .005.

In addition, we conducted ad hoc analyses to examine the association between changes in functional connectivity and electrophysiological outcomes of

volitional (Chapter 3: Experiment 1) and reflexive (Chapter 3: Experiment 2) motor control. Linear regressions and logistic regressions were performed using the Python Pandas library for data management, while data visualization was implemented via the CONN toolbox, Matplotlib, Seaborn, Nilearn, and Statannotations libraries.

*Results*

Group-ICA analysis of the same 26 children (SCI = 8 and TD = 18) who underwent our structural analysis in experiment 4 resulted in 40 components, of which 3 were identified as nodes of the sensorimotor network (SMN) through the default CONN atlas, including the lateral SMN (r = .452), medial SMN (r = .214), and superior SMN (r = .451). The activation patters of these 3 components were then binarized into five ROI masks shown in Figure 4.10.

A subsequent ROI-to-ROI analysis of the FC between these 5 cortical ROIs revealed a significant decrease in functional connectivity between the superior SMN ROI and the left ($T(22) = -2.90$, p-unc = .004, p-FDR = .032) and right ($T(22) = -2.71$, p-unc = .006, p-FDR = .032) lateral SMN ROIs. The left and right medial SMN ROIs did not show any significant differences in functional connectivity with the superior SMN ROI. See Figure 4.11.

We examined the relationship between FC of these affected cortical ROI pairs (superior SMN / left lateral SMN and superior SMN / right lateral SMN) and the overall probability of eliciting volitional FNPA responses, which is thought to be at least partly mediated by the CST. We exported the FC values for the ROI pair of superior SMN to left lateral SMN and superior SMN to right lateral SMN for each

subject into a pandas dataframe. The FC values of these two ROI pairs were combined in long form as 'Cortical FC'. Figure 4.11 showed a positive correlation between the overall FNPA probability and FC values between the superior SMN and lateral SMN ($r = .44$, $p < .05$). These results suggest that higher levels of FC between the superior SMN and lateral SMN regions may be indicative of stronger CST-mediated motor function, as evidenced by the overall probability of eliciting volitional FNPA responses. We also explore the association of FC connectivity between the superior SMN and lateral SMN regions and the ability to elicit any volitional motor responses from the leg muscles during the FNPA. A logistic regression analysis was performed using the FC values of the two ROI pairs as a predictor of leg FNPA probability. The results of the logistic regression showed a significant positive association between FC and the presence of a leg FNPA response ($\beta = 4.083$, LLR p-value $< .028$). These results suggest that higher FC between the superior SMN and lateral SMN regions may be associated with an increased ability to elicit volitional motor responses from the leg muscles during the FNPA.

Next, we aimed to investigate the functional connectivity (FC) among subcortical somatosensory structures in children with spinal cord injury (SCI) and their association with electrophysiological outcomes related to the efferent drive of the reticulospinal tract (RST). See Figure 4.12.

Our analysis of FC among. It revealed a significantly lower FC in children with SCI compared to TD control among bilateral connections between the left and right caudate, left and right putamen, and left and right pallidum. The specific characteristics of these connections are presented in tabular form below. Compared to normative publicly available neuroimaging data sets, the basal ganglia nuclei of children with SCI are less functionally connected (synchronous activation and rest fluctuations) among themselves. A correlation analysis of these ROI-to-ROI pairs affected by pediatric SCI and the overall probability of eliciting a volitional response during an FNPA experiment showed a significant positive correlation between the FC of subcortical ROI pairs that were significantly reduced in children with SCI ($r = .399$, $p < .001$). In addition, a logistic regression analysis demonstrated a significant association between the FC of the affected ROI pairs and the presence of leg responses during the FNPA ($\beta = 4.962$, LLR p-value = .001). Unlike the cortical correlation analysis, where no significant association between the motor output of the RST and the FC were detected, the connectivity strength of subcortical ROI pairs affected by pediatric SCI is highly associated with the efferent outflow of the RST. We observed a significant positive correlation between the subcortical FC values and the overall probability of eliciting a muscle

| | | Statistic | p-unc | p-FDR |
|---|---|---|---|---|
| **Cluster 1/10** | | **F(1,22) = 8.68** | **0.007** | **0.042** |
| R. Putamen | R. Caudate | T(22) = -3.17 | 0.004 | 0.031 |
| R. Putamen | L. Caudate | T(22) = -2.34 | 0.028 | 0.100 |
| L. Putamen | R. Caudate | T(22) = -2.59 | 0.017 | 0.116 |
| **Cluster 2/10** | | **F(2,21) = 6.06** | **0.008** | **0.042** |
| R. Pallidum | R. Caudate | T(22) = -4.15 | 0.000 | 0.003 |
| L. Pallidum | L. Caudate | T(22) = -2.14 | 0.044 | 0.246 |

**Table 4-1: Subcortical ROI-to-ROI FC results**

response after an auditory startle stimulus (r = .591, p < .001). Finally, our logistic regression analysis also revealed a significant association between the subcortical FC and electrophysiological outcomes related to the RST, specifically the recruitment pattern during the ASR assessment. Where exaggerated response ASR patterns of children with SCI are associated with less pronounced reduction of FC among subcortical nuclei (β = 7.128, LLR p-value = .007).

The cortical and subcortical regions exhibiting significantly altered FC in the SCI group were then included in an ad hoc ROI-to-ROI analysis. This analysis identified several cortical and subcortical regions that demonstrated significantly reduced functional connectivity in children with SCI compared to TD controls, as indicated by the low FC values and the following statistical values: right caudate (p-unc = .003, p-FDR = .019), right pallidum (p-unc = .004, p-FDR = .019), right putamen (p-unc = .024, p-FDR = .054), the superior SMN (p-unc = .024, p-FDR = .054), and left caudate (p-unc = .054, p-FDR = .075). Moreover, significant differences were observed in the connectivity patterns of these regions with other ROIs, as indicated by Figure 4.13.

Finally, the post hoc correlation between the normalized thickness of the paracentral gyri (shown to be decreased after SCI, Chapter 3 – Experiment 1) and the functional connectivity values of the superior SMN (greatly overlapping the location the paracentral gyri, Figure 4.10) to the lateral SMN nodes were analyzed. The results (Supplementary Figure D-0.3: Normalized Thickness of Paracentral Gyri correlates to SMN FC) showed a significant positive correlation between the two variables, with a correlation coefficient of r = 0.4 (*P* = .003). These findings

suggest that the thickness of the paracentral gyri is associated with its own functional connectivity to the lateral SMN. This relationship may be indicative of a crucial role played by the paracentral gyri in the connectivity between different regions of the motor network. These results provide valuable insights into the relationship between structural and functional changes in the motor network and can aid in our understanding of the neural mechanisms underlying motor function.

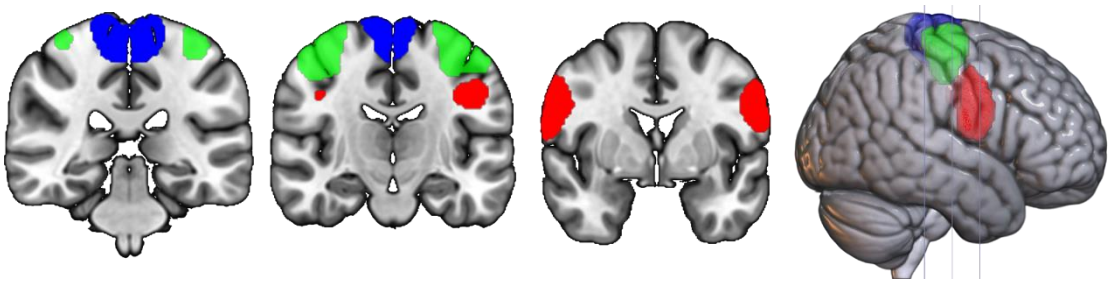

| Color | ICA Component | Correlation to canonical SMN node (r) | ROI Abbreviation | ROI Name | Side | *MNI coordiantes* | | |
|---|---|---|---|---|---|---|---|---|
| | | | | | | *X* | *Y* | *z* |
| Red | 28 | 0.452 | Lat_SMN | Lateral Node | Right | 56 | -5 | 29 |
| | | | | | Left | -53 | -7 | 30 |
| Green | 36 | 0.214 | Mid_SMN | Median Node | Right | 39 | -20 | 59 |
| | | | | | Left | -38 | -21 | 59 |
| Blue | 37 | 0.451 | Sup_SMN | Superior Node | Both | 1 | -27 | 68 |

**Figure 4.10: Sensorimotor network (SMN) regions of interest (ROIs)**

A three-dimensional rendering of an MNI standard space brain is shown along with three representative coronal slices. Overlaid on the brain are regions of interest (ROIs) that were identified based on ICA components using the CONN toolbox. These ROIs were validated as nodes of the SMN by correlating them with the CONN toolbox default atlas for resting-state connectivity and based on prior research indicating their involvement in motor function and sensorimotor processing. The table below the brain slices provides information on the names, abbreviations, and MNI coordinates of the ROIs.

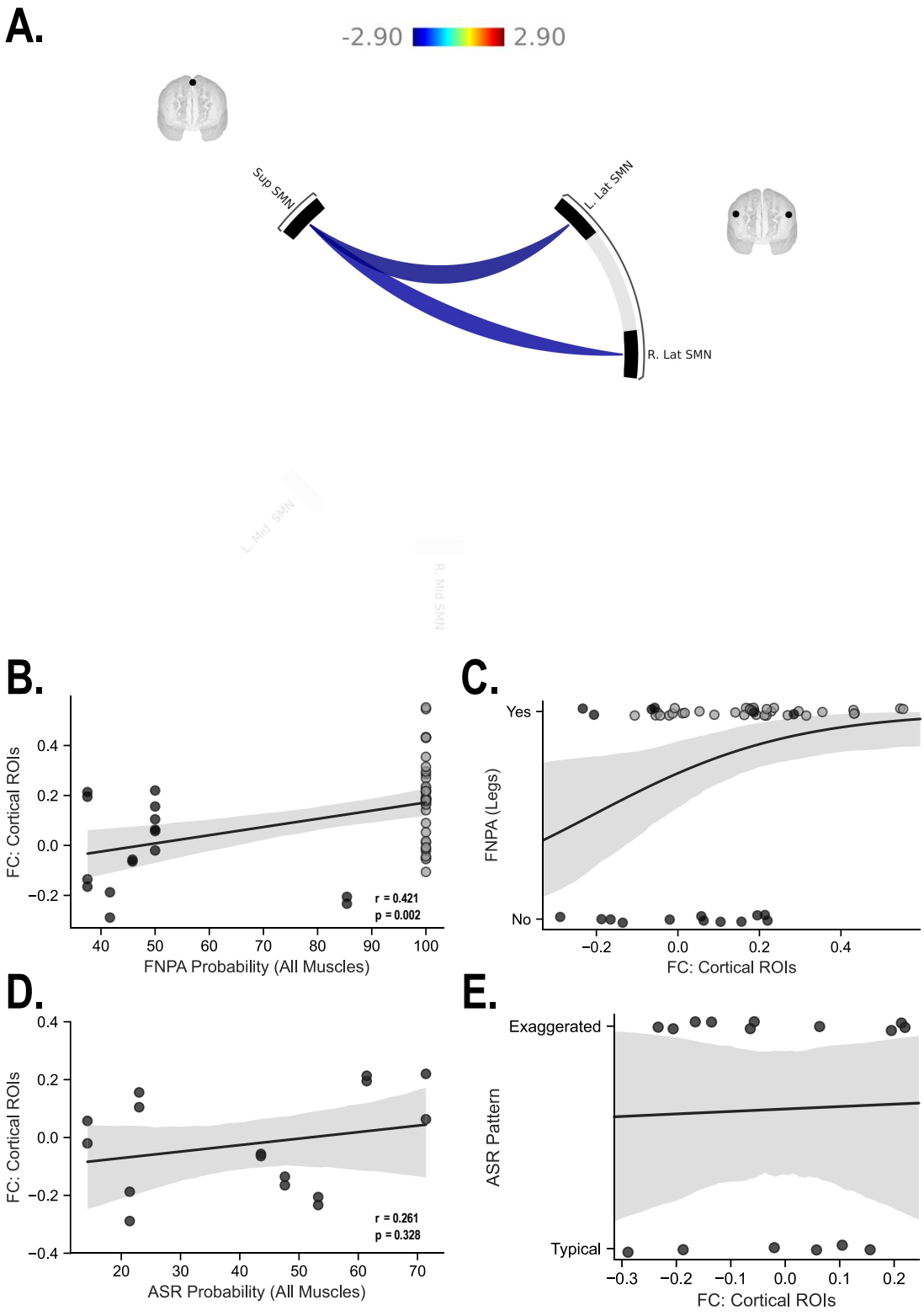
A.
-2.90
2.90
Sup SMN
L. Lat SMN
R. Lat SMN
B.
FC: Cortical ROIs
FNPA Probability (All Muscles)
r = 0.421
p = 0.002
C.
FNPA (Legs)
Yes
No
FC: Cortical ROIs
D.
FC: Cortical ROIs
ASR Probability (All Muscles)
r = 0.261
p = 0.328
E.
ASR Pattern
Exaggerated
Typical
FC: Cortical ROIs

**Figure 4.11: Functional Connectivity (FC) changes in the SMN nodes and their association to motor output.**

**Panel A** shows a connectogram illustrating the results of an ROI-to-ROI analysis of functional connectivity (FC) among the five regions of interest (ROIs) within the sensorimotor network (SMN) in children with SCI. The analysis shows decreasing FC between the superior SMN and both lateral SMN. The color of each line connecting the ROIs represents the direction and strength of the FC between them, with redder lines indicating stronger positive connectivity and bluer lines indicating weaker connectivity. **Panel B** shows the correlation analysis of the FC between the ROI pairs altered by SCI to the overall probability of eliciting a volitional response during an FNPA, revealing a significant positive correlation. The Pearson correlation coefficient and p-value are displayed. A logistic regression between FC of the affected ROI pairs and the presence of leg responses during the FNPA shows a significant association between these variables, as shown in **panel C**. **Panels D and E** show the lack of association between the cortical FC values and electrophysiological outcomes related to the efferent drive of the RST, specifically the overall probability of eliciting a muscle response after a startle stimuli and the recruitment pattern during the ASR assessment. Gray data points represent synthetic data used for FNPA measurements for the HBN datasets.

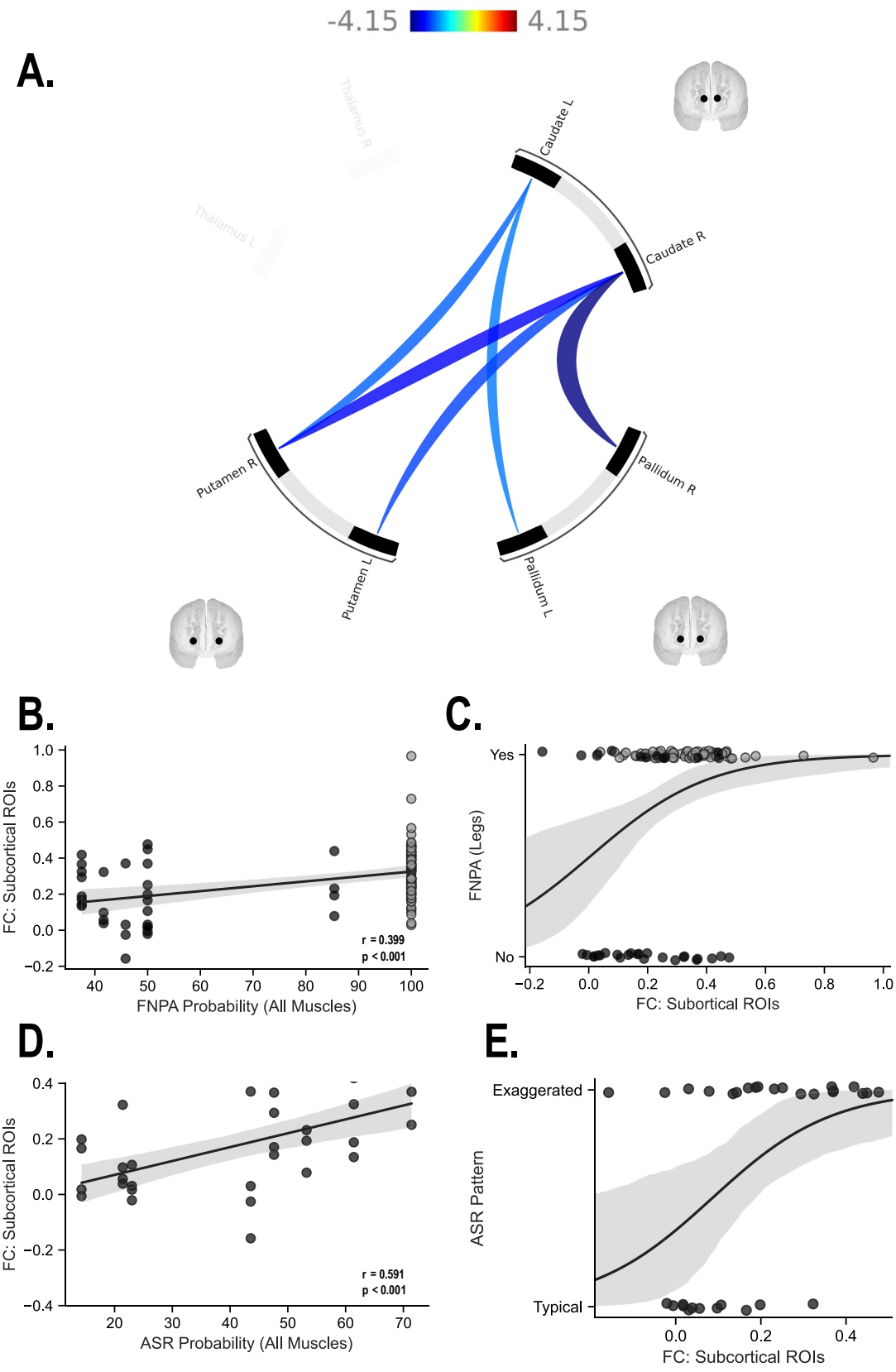
-4.15
4.15
A.
Thalamus R
Thalamus L
Caudate L
Caudate R
Putamen R
Putamen L
Pallidum R
Pallidum L
B.
FC: Subcortical ROIs
FNPA Probability (All Muscles)
r = 0.399
p < 0.001
C.
FNPA (Legs)
Yes
No
FC: Subortical ROIs
D.
FC: Subcortical ROIs
ASR Probability (All Muscles)
r = 0.591
p < 0.001
E.
ASR Pattern
Exaggerated
Typical
FC: Subcortical ROIs

**Figure 4.12: Subcortical nuclei FC changes and their association to motor output.**

**Panel A** shows a connectogram illustrating the results of an ROI-to-ROI analysis of functional connectivity (FC) among the thalamus, caudate, putamen, and pallidum in children with SCI, showing decreasing FC between the caudate, putamen, and pallidum. The color of each line connecting the ROIs represents the direction and strength of the FC between them, with redder lines indicating stronger positive connectivity and bluer lines indicating weaker connectivity. **Panel B** shows the correlation analysis of the FC between the ROI pairs altered by SCI to the overall probability of eliciting a volitional response during an FNPA, revealing a significant positive correlation. The Pearson correlation coefficient and p-value are displayed. A logistic regression between FC of the affected ROI pairs and the presence of leg responses during the FNPA shows a significant association between these variables, as shown in **panel C**. Unlike the cortical FC analysis, here, **panels D and E** show significant associations between the subcortical FC values and electrophysiological outcomes related to the efferent drive of the RST, specifically the overall probability of eliciting a muscle response after a startle stimulus and the recruitment pattern during the ASR assessment. Gray data points represent synthetic data used for FNPA measurements for the HBN datasets.

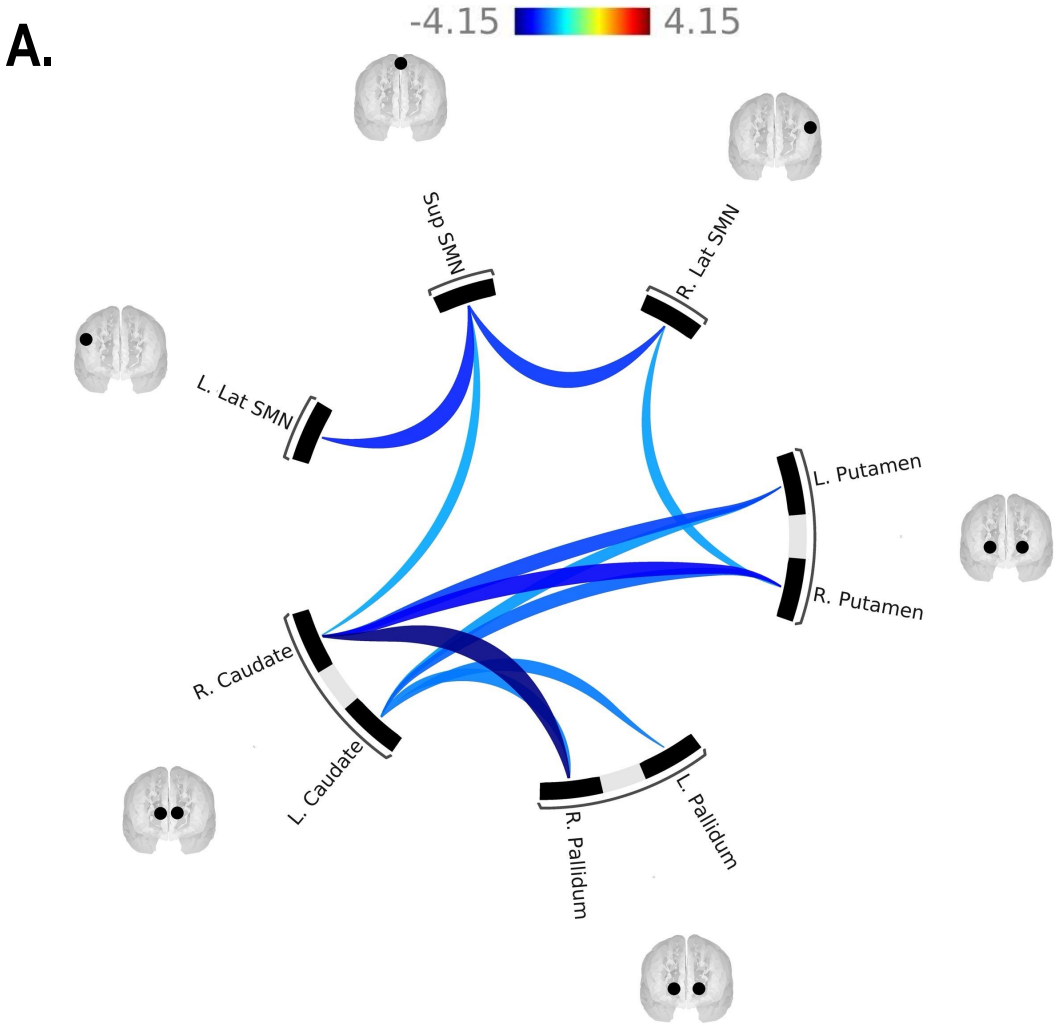
A.
-4.15
4.15
Sup SMN
R. Lat SMN
L. Lat SMN
L. Putamen
R. Putamen
R. Caudate
L. Caudate
L. Pallidum
R. Pallidum
B.
Sup SMN
R. Lat SMN
Caudate R
Putamen R
Caudate L
Putamen L
Pallidum L
Pallidum R
L. Lat SMN

**Figure 4.13: Altered Functional Connectivity in Cortical and Subcortical ROIs**

**Panel A** shows a connectogram displaying significant differences in the functional connectivity (FC) among regions of interest (ROIs) between children with spinal cord injury (SCI) and typically developing (TD) controls. Each node in the connectogram represents an ROI. Color and opacity of the lines connecting the nodes represents the strength of the connections, with darker lines indicating stronger connections. The color of the lines represents the direction of the connections, with red indicating that the ROIs are more synchronized in their pattern of activation over time in the SCI group than in the TD group (SCI > TD). Blue connections between ROIs indicate that those ROIs are more unsynchronized in the SCI group than in the TD group. The connections that reach statistical significance ($p < .05$, FDR-corrected) are shown in the connectogram. **Panel B** shows a lateral, inferior, and anterior view of transparent pial surfaces, each containing the significant ROIs identified in our study. These results were obtained by analyzing the data using a contrast of SCI > TD, while controlling for the effects of age and handedness using these variables as covariates. Together, these panels provide a visual representation of the significant connections between ROIs identified in our study and highlight the regions that are most affected by SCI. The connectogram in panel A provides an overview of the significant connections between all the ROIs, while the transparent pial surfaces in panel B provide a more detailed anatomical view of the connections involving each significant ROI.

*Discussion*

Our results in this experiment shed some light on the changes in functional connectivity that occur following pediatric spinal cord injury (SCI). Our findings reveal significant alterations in both cortical and subcortical functional connectivity in children with SCI, highlighting the potential for functional connectivity measures to serve as valuable tools for understanding the pathophysiology of pediatric SCI and their potential as a tool for monitoring the progression of recovery or the effectiveness of therapeutic interventions.

Of particular interest, our study identified significant correlations between changes in both cortical and subcortical functional connectivity measurements and the electrophysiological integrity of spinal tracts that mediate volitional movement, as assessed via the FNPA. These results are in line with the established understanding of the fundamental role of the CST in maintaining functional brain networks that support voluntary motor control. Furthermore, our findings suggest that the strength of the functional connectivity between the superior SMN and lateral SMN regions may be indicative of stronger CST-mediated motor function.

While the association between the RST and altered subcortical functional connectivity was somewhat surprising, our results suggest that the efferent activity patterns of the RST have detectable effects on the anatomy and functional connectivity of subcortical nuclei via neuroimaging techniques. The RST has been increasingly recognized as playing a prominent role in functional recovery of motor control after SCI, and our findings suggest that functional connectivity measures

may be valuable tools for assessing the efferent outflow of the RST and its association with subcortical functional connectivity changes.

Overall, the findings of this study offer crucial understanding regarding the pathophysiology of pediatric SCI and the underlying mechanisms responsible for motor deficits. Our results suggest that functional connectivity measures may have significant potential as tools for predicting motor outcomes and assessing the efficacy of therapeutic interventions in children with SCI. Further studies are necessary to confirm the present findings and to explore the potential applications of functional connectivity measures in the assessment of motor outcomes in children with SCI.

Taken together, the findings across all three neuroimaging studies in this chapter provide a clear pattern of supraspinal remodeling associated with pediatric spinal cord injuries. This pioneering approach, which incorporates structural and functional imaging techniques with electrophysiological assessment of the spinal cord, offers a novel insight into the correlations between supraspinal gray matter morphometry, microstructural integrity of white matter, and functional connectivity outcomes and their impact on the translesional motor capacity of individuals with SCI. To the best of our knowledge, this is the first report to investigate these relationships using a multimodal neuroimaging and electrophysiological approach in children with SCI. The results suggest that SCI has a significant impact on cortical and subcortical structures with sensorimotor functions, revealing potential long-term effects on supraspinal structures and networks that could be contributing to sensorimotor deficits in affected individuals and potentially affecting the typical

maturation of downstream systems (e.g., muscular, skeletal, respiratory). The findings from this chapter underscore the value of a multimodal approach to neuroimaging in the study of pediatric SCI, offering a deeper understanding of the underlying pathophysiology. As future research builds upon these findings, there is potential to discover new biomarkers or therapeutic targets that can enhance the recovery and rehabilitation process for children with SCI.

# CHAPTER 5: CONCLUSIONS AND FUTURE WORK

This chapter summarizes the work presented in this dissertation and discusses its implications in understanding the supraspinal changes that follow a spinal cord injury during childhood and how they relate to the neurophysiological integrity of the spinal cord. It also highlights the significance of the findings obtained throughout this dissertation while acknowledging the limitations in implementing such findings in future research.

Pediatric spinal cord injury (SCI) is a rare but serious condition that may have a significant impact on the developing brain. The injury can disrupt the normal growth and maturation of neural pathways and supraspinal structures. Nonetheless, the literature on the effects of pediatric-onset SCI on the brain is currently lacking. Understanding the patterns of supraspinal reorganization and its relation to the severity of the spinal pathways disruption secondary to pediatric SCI is essential for gaining a deeper understanding of the neural mechanisms of recovery and for the development of effective treatments. The objective of this project was to investigate the neural changes that follow pediatric SCI utilizing electrophysiology and neuroimaging methods, with the aim of determining the relationship between residual electrophysiological identification of spinal transmission and supraspinal reorganization. To accomplish this, we used well-established electrophysiological assessments to examine the residual neural

transmission of the corticospinal, reticulospinal, and dorsal column medial lemniscus tracts of nine children who sustained spinal cord injuries after the acquisition of crawling, standing, or walking abilities and one typically developing child. Furthermore, we evaluated supraspinal changes in eight of these children by utilizing a multimodal neuroimaging approach that compared their cortical thickness, white matter integrity, and functional connectivity to publicly available age- and gender-matched normative datasets.

In Chapter 3, we evaluated the residual neural transmission of three spinal pathways in children with SCI using established non-invasive electrophysiological assessments. Researchers have suggested that residual connections between the supraspinal and spinal networks may persist even in individuals clinically diagnosed with complete spinal injuries (Kakulas & Kaelan, 2015; Sherwood et al., 1992). Nonetheless, efforts have been limited to identify the pathways mediating such connections with nearly all of these exclusively concentrating on the adult corticospinal tract (Calancie et al., 1999; Curt et al., 1998; McKay et al., 2005) and ascending interlimb reflexes (Calancie, 1991; Calancie et al., 1996). To our knowledge this project is the first to simultaneously characterize the residual neural transmission of three spinal tracts in children with SCI.

Experiment 1 examined the neural transmission of spinal pathways that control voluntary movement in children with SCI. The corticospinal tract (CST) is broadly believed to be primarily responsible for voluntary motor activity in humans; however, recent research has provided strong evidence for the involvement of the reticulospinal tract (RST) and brainstem-spinal pathways in this process (Atkinson,

2016; Baker & Perez, 2017; Brownstone & Chopek, 2018). We examined the volitional transmission of these pathways with a modified version of the standard FNPA (Li et al., 2012) protocol, which has been used in previous studies of adults with SCI. The modified protocol (Atkinson et al., 2019) made it easier for children to understand and participate in the study by reducing the number of tasks, muscles examined and the pace of the protocol. As expected, the one typically developing child in our study was able to recruit all primary agonist muscles during intentional movements, while the children with SCI had a diverse range of motor abilities. Out of nine children with SCI, five were able to produce volitional muscle activity below their injury level, and two participants with incomplete SCI were able to activate at least one lower limb muscle. A nonparametric analysis of multiple muscle groups based on their innervation origin suggests a significant reduction in the neural transmission of supraspinal volitional motor signals to spinal segments caudal to the injury site. These findings support the idea that descending supraspinal inputs onto the spinal motor circuitry persist even in children deemed as motor and sensory complete after a clinical assessment (Dimitrijevic, 1988; Dimitrijevic et al., 1983; Sherwood et al., 1992).

Experiment 2 employed the acoustic startle reflex (ASR) as a measure of the functional integrity of the RST in children with SCI. The ASR is a defensive reflexive response to unexpected stimuli that starts in the ventral cochlear nucleus and travels through the midbrain reticular formation and the RST to the spinal cord. ASRs have been used to investigate the physiology of the human reticulospinal system in health and disease. In neurological intact humans, the probability of ASR

responses normally decreases with the increasing distance of the examined muscle from the brainstem. Our results revealed that the probability of a response from the orbicularis oculi (OOC) muscle was similarly high for the SCI subjects as it was for the typically developing (TD) child. However, in the SCI group, the mean ASR probabilities of muscles innervated by cervical and thoracic spinal levels were much higher, suggesting an organizational disruption of supra-injury motoneurons after SCI. Additionally, we found that while a third of the SCI subjects lacked the typical exaggerated responses that follow SCI (Bakker, Boer, et al., 2009) and presented with patterns approximating the responses of the TD subject, the majority of the SCI participants presented with exaggerated recruitment patterns previously reported in the adult SCI literature. Additionally, we found that 77.8% of the SCI participants presented ASR responses below their injury level as determined by the American Spinal Injury Association impairment scale, which is consistent with the concept of discomplete injuries previously reported by multiple authors (Dimitrijevic, 1988; Dimitrijevic et al., 1983; Sherwood et al., 1992).

In experiment 3, somatosensory evoked potentials (SSEPs) were used to evaluate the residual electrophysiological integrity within the dorsal column-medial lemniscus pathway of children with SCI. The evaluation was conducted in a dark, quiet room with subjects lying supine while SSEPs were elicited via electrical stimulation of the median and posterior tibial nerves and recorded with monopolar silver/silver-chloride electrodes over standardized points along the sensory pathway of the same peripheral nerves. The study found that children with SCI showed a different response pattern of cortical evoked potentials elicited from

peripheral nerves below the injury level when compared to the evoked potentials elicited from peripheral nerves above their sensory injury level. We conducted median nerve SSEP assessments on 9 SCI children and 1 TD child. Of these, 8 of the SCI participants and the TD participant showed mean latency values that were in close agreement with the published age-matched normative data (Boor, Goebel, Doepp, et al., 1998; Boor, Goebel, & Taylor, 1998; Mauguiere et al., 1999). One SCI participant (AIS-B C1), however, exhibited no cortical and subcortical potentials following medial nerve stimulation. It is worth noting that out of the eight SCI participants who showed normal median nerve SSEP responses, three (AIS-D C2, AIS-A C1, and AIS-A C3) had lesions above the spinal entry of the median nerve (C6-T1). This observation echoes the suggestion that some spinal pathways may retain the capacity for subclinical neural transmission across the injury site. The results from the posterior tibial nerve stimulation were less surprising, as all SCI participants displayed a complete absence of supraspinal responses.

Taken together the results of Chapter 3 highlighted that subjects with SCI subjects presented with a diverse range of sensorimotor abilities not captured by the gold standard of clinical assessments after SCI, the American Spinal Injury Association Impairment Scale (AIS). For instance, six out of seven children graded as having complete motor and sensory injuries (AIS A) were able to generate at least one motor or sensory response to the assessments used in the study across the AIS injury level. Functional neurophysiological assessment of volitional movements revealed that, although diminished and not always functional, approximately half of the study participants retained the ability to generate

volitional electromyography (EMG) activity of muscles caudal to the AIS motor level of injury. These EMG activations were often below the levels needed to produce a movement of the muscle. Nonetheless, the existence of these volitional neural connections across the injury remains an exciting area of exploration for future studies to leverage the potential of spinal stimulation in children. Similarly, in the ASR experiment, reflexive EMG activity below the AIS injury level was detected in 66% of the SCI participants. It is worth noting that some overlap exists between these lists, with three participants demonstrating residual neural transmission of both volitional and reflexive pathways. Lastly, the SSEPs study revealed that all but one of the SCI subjects were able to produce normal SSEPs following electrical stimulation of the median nerve, including three participants for whom this represented a neural transmission across their injury site. In conclusion, this study provided valuable insight into the residual neural transmission in pediatric SCI subjects, highlighting the diverse range of motor abilities present in this population and the potential for future studies to leverage this information to evaluate rehabilitation outcomes and improve therapies.

Chapter 4, examines the multiple ways in which the pediatric brain is affected by SCI. Neuroimaging studies have been utilized for decades to explore the underlying changes in brain structure and function following adult SCI. However, no studies have been dedicated to investigating the developing brain of children with SCI until now. In this chapter, we presented for the first-time results from three experiments aimed at understanding the supraspinal reorganization after pediatric-onset SCI and their underlying relationship to the neural mediation

of motor output. To that end we analyzed neuroimaging data from 8 children with SCI and 18 TD controls

In Experiment 4, the goal was to examine the effect of SCI on the gray matter morphometry of the pediatric brain. High-resolution T1-weighted scans were used to analyze changes in the brains of children with SCI. The thickness of the foot and leg cortical regions of interest (ROIs) were normalized to the thickness of a cortical area representing the face. Volumetric measures of subcortical structures, including the caudate, putamen, pallidum, and thalamus, were obtained and analyzed. The study found that children with SCI have reduced gray matter in cortical and subcortical sensorimotor structures compared to typically developing controls. Specifically, the primary motor cortex and paracentral cortex representing the foot showed decreased cortical thickness in children with SCI. The study also found significant correlations between changes in cortical thickness and the overall probability of volitional muscle activation during the FNPA experiment. Additionally, there were correlations between the probability of ASR responses and normalized subcortical volumes. The results suggest that SCI has significant effects on sensorimotor brain structures and their functioning in children.

Experiment 5 aimed to compare the microstructural changes of the axons along the CST between children with SCI and TD children and investigate the relationship between these changes and motor function. DWI scans were acquired, preprocessed, the CST reconstructed with fractional anisotropy (FA, an indirect measurement of the integrity of axonal myelin) measurements along the tract, from caudal to rostral. The results showed significantly lower median FA

values in the SCI group in both the left and right CSTs compared to the TD group. The analysis also revealed a strong positive correlation between mean CST FA and the probability of volitional muscle recruitment during an FNPA experiment, suggesting that CST FA may be a good predictor of motor function capacity in children with and without SCI. However, there was no significant association between CST microstructural integrity and the overall probability of obtaining reflexive muscle responses in the ASR experiment.

Experiment 6 aimed to investigate functional connectivity (FC) in children with spinal cord injury (SCI) and its association with electrophysiological outcomes related to motor function. The study included 26 children (8 with SCI and 18 typically developing controls) who underwent functional magnetic resonance imaging (fMRI) while watching a movie clip. Data were preprocessed using the CONN functional connectivity toolbox, and group-level independent component analysis (ICA) was performed to identify the sensorimotor network (SMN) nodes. ROI-to-ROI analysis was conducted to examine FC differences within the network, and a hypothesis-driven analysis was performed on subcortical regions. The results revealed a significant decrease in FC between the superior and lateral nodes of the sensorimotor network and a positive correlation between FC of affected cortical ROI pairs and the probability of eliciting volitional muscle responses. In addition, the study found a significant positive correlation between the subcortical FC values and the overall probability of eliciting a muscle response after an auditory startle stimulus. Finally, a logistic regression analysis revealed a significant association between the subcortical FC and electrophysiological

outcomes related to the reticulospinal tract, specifically the characteristic exaggerated response to ASR that follows SCI was associated with higher FC of subcortical regions.

Chapter 4 not only offers a new understanding of the patterns of supraspinal organization in the pediatric brain after SCI but also explores the association of these supraspinal changes with electrophysiological measures of spinal neural transmission across the injury. Our findings reveal significant correlations between the electrophysiological integrity of the CST and higher morphometric and FC measures. for every neuroimaging experiment, higher probabilities of a volitional muscle response were associated with better neuroimaging metrics. This finding is consistent with our current understanding of the neuroanatomy of the CST, indicating its critical role in the maintenance of functional brain networks that support voluntary motor control. Furthermore, the synchronous activation of these networks appears to play a role in maintaining the morphometry characteristics of their nodes as demonstrated in by positive correlation between the cortical thickness of a node of the SMN to their functional connectivity to other SMN nodes (Supplementary Figure D-0.3: Normalized Thickness of Paracentral Gyri correlates to SMN FC). This finding may have important implications for our understanding of the relationship between brain structure and function in the context of motor control.

In contrast to the consistent associations between the probability of volitional muscle activation (mediated at least in part by the CST) and both structural and functional connectivity changes in the cortex and basal ganglia, we

found that the RST activity, as assessed by the ASR, was only associated with subcortical morphometry and functional connectivity measurements. This finding is somewhat surprising given the known role of the RST in both voluntary and reflexive motor control. However, given that the widely reported (Abanoz et al., 2018; Kumru, Kofler, et al., 2009; Kumru et al., 2008) exaggerated responses to an sudden acoustic stimuli associated with SCI are thought to be the result of supraspinal plasticity of the RST (Kumru et al., 2008) and the fact that these same exaggerated responses were found to be associated with better subcortical morphometric (Figure 4.6) and FC (Figure 4.12) values in our SCI cohort, it is reasonable to ponder the role this tract might have as a potential biomarker to assess recovery or track the effectiveness of various interventions aimed at altering the excitability of spinal networks.

Taken together, the significant alterations in both cortical and subcortical functional connectivity observed in this study offer a deeper understanding of the pathophysiology of pediatric SCI and the underlying mechanisms of motor deficits. Our findings suggest that functional connectivity measures could be valuable for predicting motor outcomes in pediatric SCI. Nonetheless, additional studies are necessary to further confirm the present findings and to explore the potential applications of neuroimaging measures in the assessment of motor outcomes in children with SCI.

## Limitations

While this study offers a novel understanding on the relationship between SCI-induced supraspinal changes and the residual transmission capacity of the pediatric spinal cord, it is crucial to recognize and consider certain limitations.

The neurophysiological assessments in Chapter 3 aimed to understand the residual integrity of descending spinal tracts. However, the interpretation of those results is limited due to a small sample size and lack of a robust control group, stemming from restrictions associated with the COVID-19 global pandemic during the recruitment and data acquisition phases of this study. While our results provide some insightful conclusions about the neural integrity of specific spinal pathways in our participants, generalizing these results requires further investigation with larger sample sizes. Moreover, we only examined two motor and one sensory spinal pathway, excluding potential contributions from other tracts like the propriospinal and vestibulospinal tracts. The correlations we describe between the activity levels of the CST and RST and the extent of supraspinal reorganization following pediatric SCI might only represent part of the picture, with the synergistic activity of other tracts potentially providing a more comprehensive understanding.

The neuroimaging assessments in Chapter 4 aimed to Investigate the impact of SCI on the structural and functional connectivity of the pediatric brain and establish relationships between these changes and the residual integrity of spinal pathways. These results are also limited by a relatively small sample size of 26 subjects. While the results of this study are statistically significant, a larger sample size would help confirm and extend the findings, increasing the

generalizability of the results. We attempted to mitigate this issue by carefully matching the control group to the demographic characteristics (age, BMI, gender, handedness) of our SCI group and by implementing a rigorous MRI quality control procedure that includes participant training to help them feel comfortable in the MRI environment, become knowledgeable about the procedure, and take ownership of the success of the artifact-free acquisitions.

Another limitation in interpreting these results is that they correspond to a cross-sectional examination of a highly dynamic system like the developing pediatric central nervous system. This limitation makes it difficult to draw inferences about the relationships between electrophysiology and neuroimaging as they may evolve over time as the subjects age.

## Future directions

Spinal cord injury (SCI) in children significantly impacts their sensorimotor abilities and alters the morphology and functional connectivity of their brains. Currently, limited research exists on the neural mechanisms underlying these changes in pediatric SCI patients. As such, future research should focus on gaining a better understanding of these mechanisms while identifying biomarkers that could help predict clinical outcomes, track recovery progression, and evaluate the efficacy of novel SCI treatments.

Future better-powered neuroimaging studies can provide more generalizable insights into brain function and structure in children with SCI, helping researchers understand the impact of the injury on development. By understanding

the brain changes that occur after SCI in children, more effective therapies can be developed to address their specific needs. This knowledge can inform the development of targeted interventions that promote neuroplasticity and improve outcomes for children with SCI.

For children and adults, multimodal MRI techniques of the brain and spinal cord offer promising avenues to track microstructural and functional changes after SCI, which can help predict clinical outcomes. This could represent a more objective and comprehensive approach to the diagnosis and classification of SCI. Neuroimaging biomarkers have shown promise as indicators of injury severity and predictors of outcomes, which could serve as surrogate endpoints for efficient future trials targeting acute and chronic SCI. By utilizing these imaging biomarkers and developing personalized patient care strategies, clinical trials could become more efficient, ultimately leading to better outcomes for SCI patients.

The work presented in this dissertation lays the foundation for future research of neuroimaging measurements that correlate with the levels of residual neuronal transmission of the spinal cord. Replication and extension of these results could lead to the identification of reliable biomarkers to assess injury severity, determine residual capacity, and predict outcomes after SCI. Additionally, the methods and techniques developed in this dissertation are currently being used to investigate the spinal and supraspinal mechanisms underlying the recovery of motor function following a combined intervention of activity-based locomotor training and transcutaneous lumbosacral spinal stimulation through a Kentucky Spinal Cord and Head Injury Research Board grant (IRB # 19.1281).

While our work provided initial evidence that the residual capacity for neural transmission of specific motor tracts is directly correlated to the reorganization of the brain after SCI, there are still several outstanding questions regarding the involvement of other spinal tracts. It would be worthwhile for future research to examine other spinal pathways and their relationship to supraspinal reorganization. Thus, providing a more complete understanding of the mechanisms underlying supraspinal reorganization after SCI.

In closing, a multifaceted approach to SCI research is essential for making progress in our understanding and treatment of spinal cord injuries. Investigating the neural mechanisms underlying SCI-related disabilities, identifying predictive biomarkers, evaluating treatment efficacy, and exploring the potential of neuroplasticity and neural repair are all critical components of this comprehensive strategy. This approach will not only expand our knowledge of the condition but also aid in the optimization of individualized treatments, ultimately enhancing long-term outcomes and quality of life for those affected by spinal cord injuries. Special emphasis should be placed on pediatric populations, as early interventions can have a significant impact on their development and prognosis.

.

# REFERENCES


Abanoz, Y., Abanoz, Y., Gunduz, A., Uludag, M., Ornek, N. I., Uzun, N., Unalan, H., & Kiziltan, M. (2018). Pattern of startle reflex to somatosensory stimuli changes after spinal cord injury. *J Spinal Cord Med*, *41*(1), 36-41. https://doi.org/10.1080/10790268.2016.1211580

Abraham, A., Pedregosa, F., Eickenberg, M., Gervais, P., Mueller, A., Kossaifi, J., Gramfort, A., Thirion, B., & Varoquaux, G. (2014). Machine learning for neuroimaging with scikit-learn [Methods]. *Front Neuroinform*, *8*(14), 14. https://doi.org/10.3389/fninf.2014.00014

Ahuja, C. S., Wilson, J. R., Nori, S., Kotter, M. R. N., Druschel, C., Curt, A., & Fehlings, M. G. (2017). Traumatic spinal cord injury. *Nat Rev Dis Primers*, *3*, 17018. https://doi.org/10.1038/nrdp.2017.18

Al-Chalabi, M., Reddy, V., & Alsalman, I. (2022). Neuroanatomy, Posterior Column (Dorsal Column). In *StatPearls*. StatPearls Publishing. https://www.ncbi.nlm.nih.gov/pubmed/29939665

Alexander, L. M., Escalera, J., Ai, L., Andreotti, C., Febre, K., Mangone, A., Vega-Potler, N., Langer, N., Alexander, A., Kovacs, M., Litke, S., O'Hagan, B., Andersen, J., Bronstein, B., Bui, A., Bushey, M., Butler, H., Castagna, V., Camacho, N., . . . Milham, M. P. (2017). An open resource for transdiagnostic research in pediatric mental health and learning disorders. *Sci Data*, *4*, 170181. https://doi.org/10.1038/sdata.2017.181

Allen, C. H., Kluger, B. M., & Buard, I. (2017). Safety of Transcranial Magnetic Stimulation in Children: A Systematic Review of the Literature. *Pediatr Neurol*, *68*, 3-17. https://doi.org/10.1016/j.pediatrneurol.2016.12.009

American Clinical Neurophysiology, S. (2006). Guideline 9D: Guidelines on short-latency somatosensory evoked potentials. *J Clin Neurophysiol*, *23*(2), 168-179. https://doi.org/10.1097/00004691-200604000-00013

Angeli, C. A., Boakye, M., Morton, R. A., Vogt, J., Benton, K., Chen, Y., Ferreira, C. K., & Harkema, S. J. (2018). Recovery of Over-Ground Walking after Chronic Motor Complete Spinal Cord Injury. *N Engl J Med*, *379*(13), 1244-1250. https://doi.org/10.1056/NEJMoa1803588

Angeli, C. A., Edgerton, V. R., Gerasimenko, Y. P., & Harkema, S. J. (2014). Altering spinal cord excitability enables voluntary movements after chronic complete paralysis in humans. *Brain*, *137*(Pt 5), 1394-1409. https://doi.org/10.1093/brain/awu038

Aramideh, M., Eekhof, J. L., Bour, L. J., Koelman, J. H., Speelman, J. D., & Ongerboer de Visser, B. W. (1995). Electromyography and recovery of the blink reflex in involuntary eyelid closure: a comparative study. *J Neurol Neurosurg Psychiatry*, *58*(6), 692-698. https://doi.org/10.1136/jnnp.58.6.692

Atkinson, D., Hill, D. L., Stoyle, P. N., Summers, P. E., & Keevil, S. F. (1997). Automatic correction of motion artifacts in magnetic resonance images using an entropy focus

criterion. *IEEE Trans Med Imaging*, *16*(6), 903-910. https://doi.org/10.1109/42.650886

Atkinson, D. A. (2016). *Identification of residual descending pathways after human spinal cord injury* [Doctoral Dissertation, University of Louisville]. Louisville, KY. https://doi.org/10.18297/etd/2591

Atkinson, D. A., Mendez, L., Goodrich, N., Aslan, S. C., Ugiliweneza, B., & Behrman, A. L. (2019). Muscle Activation Patterns During Movement Attempts in Children With Acquired Spinal Cord Injury: Neurophysiological Assessment of Residual Motor Function Below the Level of Lesion. *Front Neurol*, *10*, 1295. https://doi.org/10.3389/fneur.2019.01295

Azouz, H. G., Khalil, M., Ghani, H. M. A. E., & Hamed, H. M. (2019). Somatosensory evoked potentials in children with autism [article-journal]. *Alexandria Journal of Medicine*, *50*(2), 99-105. https://doi.org/10.1016/j.ajme.2013.07.002

Baker, S. N. (2011). The primate reticulospinal tract, hand function and functional recovery. *J Physiol*, *589*(Pt 23), 5603-5612. https://doi.org/10.1113/jphysiol.2011.215160

Baker, S. N., & Perez, M. A. (2017). Reticulospinal Contributions to Gross Hand Function after Human Spinal Cord Injury. *J Neurosci*, *37*(40), 9778-9784. https://doi.org/10.1523/JNEUROSCI.3368-16.2017

Bakker, M. J., Boer, F., van der Meer, J. N., Koelman, J. H., Boeree, T., Bour, L., & Tijssen, M. A. (2009). Quantification of the auditory startle reflex in children. *Clin Neurophysiol*, *120*(2), 424-430. https://doi.org/10.1016/j.clinph.2008.11.014

Bakker, M. J., Tijssen, M. A., van der Meer, J. N., Koelman, J. H., & Boer, F. (2009). Increased whole-body auditory startle reflex and autonomic reactivity in children with anxiety disorders. *J Psychiatry Neurosci*, *34*(4), 314-322. https://www.ncbi.nlm.nih.gov/pubmed/19568483

Bamford, J. A., & Mushahwar, V. K. (2011). Intraspinal microstimulation for the recovery of function following spinal cord injury [article-journal]. *Prog Brain Res*, *194*, 227-239. https://doi.org/10.1016/B978-0-444-53815-4.00004-2

Bareyre, F. M., Kerschensteiner, M., Raineteau, O., Mettenleiter, T. C., Weinmann, O., & Schwab, M. E. (2004). The injured spinal cord spontaneously forms a new intraspinal circuit in adult rats. *Nat Neurosci*, *7*(3), 269-277. https://doi.org/10.1038/nn1195

Barthelemy, D., Willerslev-Olsen, M., Lundell, H., Biering-Sorensen, F., & Nielsen, J. B. (2015). Assessment of transmission in specific descending pathways in relation to gait and balance following spinal cord injury [article-journal]. *Prog Brain Res*, *218*, 79-101. https://doi.org/10.1016/bs.pbr.2014.12.012

Berger, M. J., Hubli, M., & Krassioukov, A. V. (2014). Sympathetic skin responses and autonomic dysfunction in spinal cord injury. *J Neurotrauma*, *31*(18), 1531-1539. https://doi.org/10.1089/neu.2014.3373

Biswal, B., Yetkin, F. Z., Haughton, V. M., & Hyde, J. S. (1995). Functional connectivity in the motor cortex of resting human brain using echo-planar MRI [article-journal]. *Magn Reson Med*, *34*(4), 537-541. https://doi.org/10.1002/mrm.1910340409

Bjerkefors, A., Squair, J. W., Chua, R., Lam, T., Chen, Z., & Carpenter, M. G. (2015). Assessment of abdominal muscle function in individuals with motor-complete spinal cord injury above T6 in response to transcranial magnetic stimulation. *J Rehabil Med*, *47*(2), 138-146. https://doi.org/10.2340/16501977-1901

Blumenthal, T. D. (2015). Startle Reflex and Health. In *International Encyclopedia of the Social & Behavioral Sciences* (pp. 331-337). Elsevier. https://doi.org/10.1016/b978-0-08-097086-8.14151-0

Blumenthal, T. D., Cuthbert, B. N., Filion, D. L., Hackley, S., Lipp, O. V., & van Boxtel, A. (2005). Committee report: Guidelines for human startle eyeblink electromyographic studies. *Psychophysiology*, *42*(1), 1-15. https://doi.org/10.1111/j.1469-8986.2005.00271.x

Boakye, M., Harkema, S., Ellaway, P. H., & Skelly, A. C. (2012). Quantitative testing in spinal cord injury: overview of reliability and predictive validity. *J Neurosurg Spine*, *17*(1 Suppl), 141-150. https://doi.org/10.3171/2012.5.AOSPINE1296

Bockowski, L., Smigielska Kuzia, J., Sobaniec, W., & Sendrowski, K. (2010). Somatosensory evoked potentials in children with migraine with aura and without aura. *Przegl Lek*, *67*(9), 688-691. https://www.ncbi.nlm.nih.gov/pubmed/21384789

Boezaart, A. P., Smith, C. R., Chembrovich, S., Zasimovich, Y., Server, A., Morgan, G., Theron, A., Booysen, K., & Reina, M. A. (2021). Visceral versus somatic pain: an educational review of anatomy and clinical implications. *Reg Anesth Pain Med*, *46*(7), 629-636. https://doi.org/10.1136/rapm-2020-102084

Boor, R., Goebel, B., Doepp, M., & Taylor, M. J. (1998). Somatosensory evoked potentials after posterior tibial nerve stimulation--normative data in children. *Eur J Paediatr Neurol*, *2*(3), 145-152. https://doi.org/10.1016/s1090-3798(98)80030-5

Boor, R., Goebel, B., & Taylor, M. J. (1998). Subcortical somatosensory evoked potentials after median nerve stimulation in children. *Eur J Paediatr Neurol*, *2*(3), 137-143. https://doi.org/10.1016/s1090-3798(98)80029-9

Boor, R., Li, L., Goebel, B., & Reitter, B. (2008). Subcortical somatosensory evoked potentials after posterior tibial nerve stimulation in children. *Brain Dev*, *30*(8), 493-498. https://doi.org/10.1016/j.braindev.2007.06.010

Bour, L. J., Aramideh, M., & de Visser, B. W. (2000). Neurophysiological aspects of eye and eyelid movements during blinking in humans. *J Neurophysiol*, *83*(1), 166-176. https://doi.org/10.1152/jn.2000.83.1.166

Brown, P., Rothwell, J. C., Thompson, P. D., Britton, T. C., Day, B. L., & Marsden, C. D. (1991a). NEW OBSERVATIONS ON THE NORMAL AUDITORY STARTLE REFLEX IN MAN. *Brain*, *114*(4), 1891-1902. https://doi.org/10.1093/brain/114.4.1891

Brown, P., Rothwell, J. C., Thompson, P. D., Britton, T. C., Day, B. L., & Marsden, C. D. (1991b). New observations on the normal auditory startle reflex in man. *Brain*, *114 ( Pt 4)*, 1891-1902. https://doi.org/10.1093/brain/114.4.1891

Brownstone, R. M., & Chopek, J. W. (2018). Reticulospinal Systems for Tuning Motor Commands. *Front Neural Circuits*, *12*, 30. https://doi.org/10.3389/fncir.2018.00030

Bunge, R. P., Puckett, W. R., Becerra, J. L., Marcillo, A., & Quencer, R. M. (1993). Observations on the pathology of human spinal cord injury. A review and classification of 22 new cases with details from a case of chronic cord compression with extensive focal demyelination. *Adv Neurol*, *59*, 75-89. https://www.ncbi.nlm.nih.gov/pubmed/8420126

Calancie, B. (1991). Interlimb reflexes following cervical spinal cord injury in man. *Exp Brain Res*, *85*(2), 458-469. https://doi.org/10.1007/bf00229423

Calancie, B., Alexeeva, N., Broton, J. G., Suys, S., Hall, A., & Klose, K. J. (1999). Distribution and latency of muscle responses to transcranial magnetic stimulation of motor cortex after spinal cord injury in humans. *J Neurotrauma*, *16*(1), 49-67. https://doi.org/10.1089/neu.1999.16.49

Calancie, B., Lutton, S., & Broton, J. G. (1996). Central nervous system plasticity after spinal cord injury in man: interlimb reflexes and the influence of cutaneous stimulation. *Electroencephalogr Clin Neurophysiol*, *101*(4), 304-315. https://doi.org/10.1016/0924-980x(96)95194-2

Calhoun, C. L., Schottler, J., & Vogel, L. C. (2013). Recommendations for mobility in children with spinal cord injury. *Top Spinal Cord Inj Rehabil*, *19*(2), 142-151. https://doi.org/10.1310/sci1902-142

Calhoun, V. D., Adali, T., Pearlson, G. D., & Pekar, J. J. (2001). A method for making group inferences from functional MRI data using independent component analysis. *Hum Brain Mapp*, *14*(3), 140-151. https://doi.org/10.1002/hbm.1048

Cariga, P., Catley, M., Mathias, C. J., Savic, G., Frankel, H. L., & Ellaway, P. H. (2002). Organisation of the sympathetic skin response in spinal cord injury. *J Neurol Neurosurg Psychiatry*, *72*(3), 356-360. https://doi.org/10.1136/jnnp.72.3.356

Catani, M. (2017). A little man of some importance. *Brain*, *140*(11), 3055-3061. https://doi.org/10.1093/brain/awx270

Chabot, R., York, D. H., Watts, C., & Waugh, W. A. (1985). Somatosensory evoked potentials evaluated in normal subjects and spinal cord-injured patients. *J Neurosurg*, *63*(4), 544-551. https://doi.org/10.3171/jns.1985.63.4.0544

Chafetz, R. S., Gaughan, J. P., Vogel, L. C., Betz, R., & Mulcahey, M. J. (2009). The international standards for neurological classification of spinal cord injury: intra-rater agreement of total motor and sensory scores in the pediatric population. *J Spinal Cord Med*, *32*(2), 157-161. https://doi.org/10.1080/10790268.2009.11760767

Chams, N., Chams, S., Badran, R., Shams, A., Araji, A., Raad, M., Mukhopadhyay, S., Stroberg, E., Duval, E. J., Barton, L. M., & Hajj Hussein, I. (2020). COVID-19: A Multidisciplinary Review. *Front Public Health*, *8*, 383. https://doi.org/10.3389/fpubh.2020.00383

Charlier, F., Weber, M., Izak, D., Harkin, E., Magnus, M., Lalli, J., Fresnais, L., Chan, M., Markov, N., Amsalem, O., Proost, S., Krasoulis, A., getzze, & Repplinger, S. (2022). *Statannotations*. In (Version v0.5) Zenodo. https://doi.org/10.5281/zenodo.7213391

Chen, Q., Zheng, W., Chen, X., Wan, L., Qin, W., Qi, Z., Chen, N., & Li, K. (2017). Brain Gray Matter Atrophy after Spinal Cord Injury: A Voxel-Based Morphometry Study. *Front Hum Neurosci*, *11*, 211. https://doi.org/10.3389/fnhum.2017.00211

Cheng, A. V., & Tadi, P. (2022). Neuroanatomy, White Rami Communicans. In *StatPearls*. StatPearls Publishing

Copyright © 2022, StatPearls Publishing LLC. https://www.ncbi.nlm.nih.gov/pubmed/31751100

Cho, T. A. (2015). Spinal cord functional anatomy. *Continuum (Minneap Minn)*, *21*(1 Spinal Cord Disorders), 13-35. https://doi.org/10.1212/01.CON.0000461082.25876.4a

Cieslak, M., Cook, P. A., He, X., Yeh, F. C., Dhollander, T., Adebimpe, A., Aguirre, G. K., Bassett, D. S., Betzel, R. F., Bourque, J., Cabral, L. M., Davatzikos, C., Detre, J. A., Earl, E., Elliott, M. A., Fadnavis, S., Fair, D. A., Foran, W., Fotiadis, P., . . . Satterthwaite, T. D. (2021). QSIPrep: an integrative platform for preprocessing and reconstructing diffusion MRI data. *Nat Methods*, *18*(7), 775-778. https://doi.org/10.1038/s41592-021-01185-5

Cobeljic, R. D., Ribaric-Jankes, K., Aleksic, A., Popovic-Maneski, L. Z., Schwirtlich, L. B., & Popovic, D. B. (2018). Does galvanic vestibular stimulation decrease spasticity in clinically complete spinal cord injury? *Int J Rehabil Res*, *41*(3), 251-257. https://doi.org/10.1097/MRR.0000000000000297

Curt, A., & Dietz, V. (1996). Traumatic cervical spinal cord injury: relation between somatosensory evoked potentials, neurological deficit, and hand function. *Arch Phys Med Rehabil*, *77*(1), 48-53. https://doi.org/10.1016/s0003-9993(96)90219-1

Curt, A., & Dietz, V. (1999). Electrophysiological recordings in patients with spinal cord injury: significance for predicting outcome. *Spinal Cord*, *37*(3), 157-165. https://doi.org/10.1038/sj.sc.3100809

Curt, A., & Ellaway, P. H. (2012). Clinical neurophysiology in the prognosis and monitoring of traumatic spinal cord injury. *Handb Clin Neurol*, *109*, 63-75. https://doi.org/10.1016/B978-0-444-52137-8.00004-8

Curt, A., Keck, M. E., & Dietz, V. (1998). Functional outcome following spinal cord injury: significance of motor-evoked potentials and ASIA scores. *Arch Phys Med Rehabil*, *79*(1), 81-86. https://doi.org/10.1016/s0003-9993(98)90213-1

Dale, A. M., Fischl, B., & Sereno, M. I. (1999). Cortical surface-based analysis. I. Segmentation and surface reconstruction. *NeuroImage*, *9*(2), 179-194. https://doi.org/10.1006/nimg.1998.0395

Davis, M., Gendelman, D. S., Tischler, M. D., & Gendelman, P. M. (1982). A primary acoustic startle circuit: lesion and stimulation studies. *J Neurosci*, *2*(6), 791-805. https://doi.org/10.1523/JNEUROSCI.02-06-00791.1982

de Haan, P., & Kalkman, C. J. (2001). Spinal cord monitoring: somatosensory- and motor-evoked potentials. *Anesthesiol Clin North Am*, *19*(4), 923-945. https://doi.org/10.1016/s0889-8537(01)80017-1

Delcour, M., Russier, M., Castets, F., Turle-Lorenzo, N., Canu, M. H., Cayetanot, F., Barbe, M. F., & Coq, J. O. (2018). Early movement restriction leads to maladaptive plasticity in the sensorimotor cortex and to movement disorders. *Sci Rep*, *8*(1), 16328. https://doi.org/10.1038/s41598-018-34312-y

Desikan, R. S., Segonne, F., Fischl, B., Quinn, B. T., Dickerson, B. C., Blacker, D., Buckner, R. L., Dale, A. M., Maguire, R. P., Hyman, B. T., Albert, M. S., & Killiany, R. J. (2006). An automated labeling system for subdividing the human cerebral cortex on MRI scans into gyral based regions of interest. *NeuroImage*, *31*(3), 968-980. https://doi.org/10.1016/j.neuroimage.2006.01.021

Desmurget, M., & Sirigu, A. (2015). Revealing humans' sensorimotor functions with electrical cortical stimulation. *Philos Trans R Soc Lond B Biol Sci*, *370*(1677), 20140207. https://doi.org/10.1098/rstb.2014.0207

Destrieux, C., Fischl, B., Dale, A., & Halgren, E. (2010). Automatic parcellation of human cortical gyri and sulci using standard anatomical nomenclature. *NeuroImage*, *53*(1), 1-15. https://doi.org/10.1016/j.neuroimage.2010.06.010

Dimitrijevic, M. R. (1988). Residual motor functions in spinal cord injury. *Adv Neurol*, *47*, 138-155. https://www.ncbi.nlm.nih.gov/pubmed/3278516

Dimitrijevic, M. R., Dimitrijevic, M. M., Sherwood, A. M., & Faganel, J. (1980). Neurophysiological evaluation of chronic spinal cord stimulation in patients with upper motor neuron disorders. *Int Rehabil Med*, *2*(2), 82-85. https://doi.org/10.3109/09638288009163962

Dimitrijevic, M. R., Faganel, J., Lehmkuhl, D., & Sherwood, A. (1983). Motor control in man after partial or complete spinal cord injury [article-journal]. *Adv Neurol*, *39*, 915-926. https://www.ncbi.nlm.nih.gov/pubmed/6660129

Dimitrijevic, M. R., Hsu, C. Y., & McKay, W. B. (1992). Neurophysiological assessment of spinal cord and head injury [article-journal]. *J Neurotrauma*, *9 Suppl 1*, S293-300. https://www.ncbi.nlm.nih.gov/pubmed/1588619

Dum, R. P., & Strick, P. L. (1991). The origin of corticospinal projections from the premotor areas in the frontal lobe. *J Neurosci*, *11*(3), 667-689. https://doi.org/10.1523/jneurosci.11-03-00667.1991

Dum, R. P., & Strick, P. L. (2002). Motor areas in the frontal lobe of the primate. *Physiol Behav*, *77*(4-5), 677-682. https://doi.org/10.1016/s0031-9384(02)00929-0

Durston, S., Nederveen, H., van Dijk, S., van Belle, J., de Zeeuw, P., Langen, M., & van Dijk, A. (2009). Magnetic resonance simulation is effective in reducing anxiety related to magnetic resonance scanning in children. *J Am Acad Child Adolesc Psychiatry*, *48*(2), 206-207. https://doi.org/10.1097/CHI.0b013e3181930673

Eluvathingal, T. J., Chugani, H. T., Behen, M. E., Juhasz, C., Muzik, O., Maqbool, M., Chugani, D. C., & Makki, M. (2006). Abnormal brain connectivity in children after early severe socioemotional deprivation: a diffusion tensor imaging study. *Pediatrics*, *117*(6), 2093-2100. https://doi.org/10.1542/peds.2005-1727

Esteban, O., Birman, D., Schaer, M., Koyejo, O. O., Poldrack, R. A., & Gorgolewski, K. J. (2017). MRIQC: Advancing the automatic prediction of image quality in MRI from unseen sites. *PLoS One*, *12*(9), e0184661. https://doi.org/10.1371/journal.pone.0184661

Esteban, O. M., Christopher J.; Burns, Christopher; Goncalves, Mathias; Jarecka, Dorota; Ziegler, Erik; Berleant, Shoshana; Ellis, David Gage; Pinsard, Basile; Madison, Cindee; Waskom, Michael; Notter, Michael Philipp; Clark, Daniel. (2022). Nipype. In *Zenodo*.

Fagan, E. R., Taylor, M. J., & Logan, W. J. (1987). Somatosensory evoked potentials: Part II. A review of the clinical applications in pediatric neurology. *Pediatr Neurol*, *3*(5), 249-255. https://doi.org/10.1016/0887-8994(87)90063-4

Filli, L., Engmann, A. K., Zorner, B., Weinmann, O., Moraitis, T., Gullo, M., Kasper, H., Schneider, R., & Schwab, M. E. (2014). Bridging the gap: a reticulo-propriospinal detour bypassing an incomplete spinal cord injury. *J Neurosci*, *34*(40), 13399-13410. https://doi.org/10.1523/JNEUROSCI.0701-14.2014

Fink, K. L., & Cafferty, W. B. (2016). Reorganization of Intact Descending Motor Circuits to Replace Lost Connections After Injury. *Neurotherapeutics*, *13*(2), 370-381. https://doi.org/10.1007/s13311-016-0422-x

Fischl, B. (2012). FreeSurfer [article-journal]. *NeuroImage*, *62*(2), 774-781. https://doi.org/10.1016/j.neuroimage.2012.01.021

Fischl, B., & Dale, A. M. (2000). Measuring the thickness of the human cerebral cortex from magnetic resonance images. *Proc Natl Acad Sci U S A*, *97*(20), 11050-11055. https://doi.org/10.1073/pnas.200033797

Fischl, B., Sereno, M. I., & Dale, A. M. (1999). Cortical surface-based analysis. II: Inflation, flattening, and a surface-based coordinate system. *NeuroImage*, *9*(2), 195-207. https://doi.org/10.1006/nimg.1998.0396

Fonov, V. S., Evans, A. C., McKinstry, R. C., Almli, C. R., & Collins, D. L. (2009). Unbiased nonlinear average age-appropriate brain templates from birth to adulthood. *NeuroImage*, *47*, S102. https://doi.org/10.1016/s1053-8119(09)70884-5

Fouad, K., Pedersen, V., Schwab, M. E., & Brosamle, C. (2001). Cervical sprouting of corticospinal fibers after thoracic spinal cord injury accompanies shifts in evoked motor responses. *Curr Biol*, *11*(22), 1766-1770. https://doi.org/10.1016/s0960-9822(01)00535-8

Freund, P., Schneider, T., Nagy, Z., Hutton, C., Weiskopf, N., Friston, K., Wheeler-Kingshott, C. A., & Thompson, A. J. (2012). Degeneration of the injured cervical cord is associated with remote changes in corticospinal tract integrity and upper limb impairment [article-journal]. *PLoS One*, *7*(12), e51729. https://doi.org/10.1371/journal.pone.0051729

Freund, P., Seif, M., Weiskopf, N., Friston, K., Fehlings, M. G., Thompson, A. J., & Curt, A. (2019). MRI in traumatic spinal cord injury: from clinical assessment to neuroimaging biomarkers. *Lancet Neurol*, *18*(12), 1123-1135. https://doi.org/10.1016/S1474-4422(19)30138-3

Freund, P., Weiskopf, N., Ashburner, J., Wolf, K., Sutter, R., Altmann, D. R., Friston, K., Thompson, A., & Curt, A. (2013). MRI investigation of the sensorimotor cortex and the corticospinal tract after acute spinal cord injury: a prospective longitudinal study [article-journal]. *Lancet Neurol*, *12*(9), 873-881. https://doi.org/10.1016/S1474-4422(13)70146-7

Freund, P., Weiskopf, N., Ward, N. S., Hutton, C., Gall, A., Ciccarelli, O., Craggs, M., Friston, K., & Thompson, A. J. (2011). Disability, atrophy and cortical reorganization following spinal cord injury [article-journal]. *Brain*, *134*(Pt 6), 1610-1622. https://doi.org/10.1093/brain/awr093

Freund, P., Wheeler-Kingshott, C. A., Nagy, Z., Gorgoraptis, N., Weiskopf, N., Friston, K., Thompson, A. J., & Hutton, C. (2012). Axonal integrity predicts cortical reorganisation following cervical injury [article-journal]. *J Neurol Neurosurg Psychiatry*, *83*(6), 629-637. https://doi.org/10.1136/jnnp-2011-301875

Gad, P., Lee, S., Terrafranca, N., Zhong, H., Turner, A., Gerasimenko, Y., & Edgerton, V. R. (2018). Non-Invasive Activation of Cervical Spinal Networks after Severe Paralysis. *J Neurotrauma*, *35*(18), 2145-2158. https://doi.org/10.1089/neu.2017.5461

Ganzetti, M., Wenderoth, N., & Mantini, D. (2016). Intensity Inhomogeneity Correction of Structural MR Images: A Data-Driven Approach to Define Input Algorithm Parameters [Original Research]. *Front Neuroinform*, *10*, 10. https://doi.org/10.3389/fninf.2016.00010

Gerasimenko, Y. P., Lu, D. C., Modaber, M., Zdunowski, S., Gad, P., Sayenko, D. G., Morikawa, E., Haakana, P., Ferguson, A. R., Roy, R. R., & Edgerton, V. R. (2015). Noninvasive Reactivation of Motor Descending Control after Paralysis [article-journal]. *J Neurotrauma*, *32*(24), 1968-1980. https://doi.org/10.1089/neu.2015.4008

Gilmore, R. (1992). Somatosensory evoked potential testing in infants and children. *J Clin Neurophysiol*, *9*(3), 324-341. https://doi.org/10.1097/00004691-199207010-00002

Gorgolewski, K., Burns, C. D., Madison, C., Clark, D., Halchenko, Y. O., Waskom, M. L., & Ghosh, S. S. (2011). Nipype: a flexible, lightweight and extensible neuroimaging data processing framework in python [article-journal]. *Front Neuroinform*, *5*, 13. https://doi.org/10.3389/fninf.2011.00013

Govindan, R. M., Behen, M. E., Helder, E., Makki, M. I., & Chugani, H. T. (2010). Altered water diffusivity in cortical association tracts in children with early deprivation identified with Tract-Based Spatial Statistics (TBSS). *Cereb Cortex*, *20*(3), 561-569. https://doi.org/10.1093/cercor/bhp122

Grabher, P., Callaghan, M. F., Ashburner, J., Weiskopf, N., Thompson, A. J., Curt, A., & Freund, P. (2015). Tracking sensory system atrophy and outcome prediction in spinal cord injury [article-journal]. *Ann Neurol*, *78*(5), 751-761. https://doi.org/10.1002/ana.24508

Gregg, B. A., & Scott, M. (2015). Comparison of Acoustic Startle Response in School-age Children who Stutter and their Fluent Peers. *Procedia - Social and Behavioral Sciences*, *193*, 115-122. https://doi.org/10.1016/j.sbspro.2015.03.250

Guleria, S., Gupta, R. K., Saksena, S., Chandra, A., Srivastava, R. N., Husain, M., Rathore, R., & Narayana, P. A. (2008). Retrograde Wallerian degeneration of cranial corticospinal tracts in cervical spinal cord injury patients using diffusion tensor imaging. *J Neurosci Res*, *86*(10), 2271-2280. https://doi.org/10.1002/jnr.21664

Guo, W., Chambers, A. R., Darrow, K. N., Hancock, K. E., Shinn-Cunningham, B. G., & Polley, D. B. (2012). Robustness of Cortical Topography across Fields, Laminae,

Anesthetic States, and Neurophysiological Signal Types. *The Journal of Neuroscience*, *32*(27), 9159. https://doi.org/10.1523/JNEUROSCI.0065-12.2012

Haefeli, J., Kramer, J. L., Blum, J., & Curt, A. (2014). Assessment of Spinothalamic Tract Function Beyond Pinprick in Spinal Cord Lesions: A Contact Heat Evoked Potential Study. *Neurorehabil Neural Repair*, *28*(5), 494-503. https://doi.org/10.1177/1545968313517755

Haines, D. E. (2004a). Chapter 4. Internal Morphology of the Brain in Slices and MRI. In D. E. Haines (Ed.), *Neuroanatomy: An Atlas of Structures, Sections, and Systems* (6th ed.). Lippincott Williams & Wilkins.

Haines, D. E. (2004b). Chapter 5. Internal Morphology of the Spinal Cord and Brain in Stained Sections. In D. E. Haines (Ed.), *Neuroanatomy: An Atlas of Structures, Sections, and Systems* (6th ed.). Lippincott Williams & Wilkins.

Haines, D. E. (2004c). Chapter 7. Synopsis of Functional Components, Tracts, Pathways, and Systems. In D. E. Haines (Ed.), *Neuroanatomy: An Atlas of Structures, Sections, and Systems* (6th ed.). Lippincott Williams & Wilkins.

Harkema, S., Gerasimenko, Y., Hodes, J., Burdick, J., Angeli, C., Chen, Y., Ferreira, C., Willhite, A., Rejc, E., Grossman, R. G., & Edgerton, V. R. (2011). Effect of epidural stimulation of the lumbosacral spinal cord on voluntary movement, standing, and assisted stepping after motor complete paraplegia: a case study. *Lancet*, *377*(9781), 1938-1947. https://doi.org/10.1016/S0140-6736(11)60547-3

Harkema, S. J., Legg Ditterline, B., Wang, S., Aslan, S., Angeli, C. A., Ovechkin, A., & Hirsch, G. A. (2018). Epidural Spinal Cord Stimulation Training and Sustained Recovery of Cardiovascular Function in Individuals With Chronic Cervical Spinal Cord Injury. *JAMA Neurol*, *75*(12), 1569-1571. https://doi.org/10.1001/jamaneurol.2018.2617

Hawasli, A. H., Rutlin, J., Roland, J. L., Murphy, R. K. J., Song, S. K., Leuthardt, E. C., Shimony, J. S., & Ray, W. Z. (2018). Spinal Cord Injury Disrupts Resting-State Networks in the Human Brain. *J Neurotrauma*, *35*(6), 864-873. https://doi.org/10.1089/neu.2017.5212

Hermens, H. J., Freriks, B., Disselhorst-Klug, C., & Rau, G. (2000). Development of recommendations for SEMG sensors and sensor placement procedures. *J Electromyogr Kinesiol*, *10*(5), 361-374. https://doi.org/10.1016/s1050-6411(00)00027-4

Hou, J., Xiang, Z., Yan, R., Zhao, M., Wu, Y., Zhong, J., Guo, L., Li, H., Wang, J., Wu, J., Sun, T., & Liu, H. (2016). Motor recovery at 6 months after admission is related to structural and functional reorganization of the spine and brain in patients with spinal cord injury [article-journal]. *Hum Brain Mapp*, *37*(6), 2195-2209. https://doi.org/10.1002/hbm.23163

Hou, J. M., Yan, R. B., Xiang, Z. M., Zhang, H., Liu, J., Wu, Y. T., Zhao, M., Pan, Q. Y., Song, L. H., Zhang, W., Li, H. T., Liu, H. L., & Sun, T. S. (2014). Brain sensorimotor system atrophy during the early stage of spinal cord injury in humans [article-journal]. *Neuroscience*, *266*, 208-215. https://doi.org/10.1016/j.neuroscience.2014.02.013

Howland, D. R., Trimble, S. A., & Behrman, A. L. (2014). Neurological Recovery and Restorative Rehabilitation. In L. C. Vogel, K. Zebracki, R. R. Betz, & M. Mulcahey (Eds.), *Spinal Cord Injury in the Child and Young Adult* (pp. 399-410). Mac Keith Press.

Howland, D. R., Trimble, S. A., Fox, E. J., Tester, N. J., Spiess, M. R., Senesac, C. R., Kleim, J. A., Spierre, L. Z., Rose, D. K., Johns, J. S., Ugiliweneza, B., Reier, P. J., & Behrman, A. L. (2023). Recovery of walking in nonambulatory children with

chronic spinal cord injuries: Case series. *J Neurosci Res*. https://doi.org/10.1002/jnr.25162

Huang, R. S., & Sereno, M. I. (2018). Multisensory and sensorimotor maps. *Handb Clin Neurol*, *151*, 141-161. https://doi.org/10.1016/B978-0-444-63622-5.00007-3

Hubscher, C. H., Herrity, A. N., Williams, C. S., Montgomery, L. R., Willhite, A. M., Angeli, C. A., & Harkema, S. J. (2018). Improvements in bladder, bowel and sexual outcomes following task-specific locomotor training in human spinal cord injury. *PLoS One*, *13*(1), e0190998. https://doi.org/10.1371/journal.pone.0190998

Huntenburg, J. M. (2014). *Evaluating nonlinear coregistration of BOLD EPI and T1w images* Freie Universität]. http://hdl.handle.net/11858/00-001M-0000-002B-1CB5-A

Hunter, J. D. (2007). Matplotlib: A 2D Graphics Environment. *Computing in Science & Engineering*, *9*(3), 90-95. https://doi.org/10.1109/mcse.2007.55

Johnson, V., Hart, R., & Colwell, J. (2014). *Steps for Engaging Young Children in Research. Volume 1: The Guide*. https://bernardvanleer.org/publications-reports/steps-engaging-young-children-research-volume-1-guide/

Jurkiewicz, M. T., Crawley, A. P., Verrier, M. C., Fehlings, M. G., & Mikulis, D. J. (2006). Somatosensory cortical atrophy after spinal cord injury: a voxel-based morphometry study. *Neurology*, *66*(5), 762-764. https://doi.org/10.1212/01.wnl.0000201276.28141.40

Kabdebon, C., Leroy, F., Simmonet, H., Perrot, M., Dubois, J., & Dehaene-Lambertz, G. (2014). Anatomical correlations of the international 10-20 sensor placement system in infants. *NeuroImage*, *99*, 342-356. https://doi.org/10.1016/j.neuroimage.2014.05.046

Kakulas, B. A. (1999). The applied neuropathology of human spinal cord injury. *Spinal Cord*, *37*(2), 79-88. https://doi.org/10.1038/sj.sc.3100807

Kakulas, B. A., & Kaelan, C. (2015). The neuropathological foundations for the restorative neurology of spinal cord injury. *Clin Neurol Neurosurg*, *129 Suppl 1*, S1-7. https://doi.org/10.1016/j.clineuro.2015.01.012

Kelly, M. (2019). *Celebrate National Comicbook day! (Yes, There's a Reason We Spell it as One Word)*. https://therealstanlee.com/comics/celebrate-national-comicbook-day-yes-theres-a-reason-we-spell-it-as-one-word/

Keogh, E., Chakrabarti, K., Pazzani, M., & Mehrotra, S. (2001). *Locally adaptive dimensionality reduction for indexing large time series databases* Proceedings of the 2001 ACM SIGMOD international conference on Management of data - SIGMOD '01, Santa Barbara, California, USA. https://doi-org.echo.louisville.edu/10.1145/375663.375680

Kirshblum, S. C., Waring, W., Biering-Sorensen, F., Burns, S. P., Johansen, M., Schmidt-Read, M., Donovan, W., Graves, D., Jha, A., Jones, L., Mulcahey, M. J., & Krassioukov, A. (2011). Reference for the 2011 revision of the International Standards for Neurological Classification of Spinal Cord Injury. *J Spinal Cord Med*, *34*(6), 547-554. https://doi.org/10.1179/107902611X13186000420242

Kiziltan, M. E., Gunduz, A., Apaydin, H., Ertan, S., & Kiziltan, G. (2015). Auditory startle reflex and startle reflex to somatosensory inputs in generalized dystonia. *Clin Neurophysiol*, *126*(9), 1740-1745. https://doi.org/10.1016/j.clinph.2014.11.004

Klem, G. H., Luders, H. O., Jasper, H. H., & Elger, C. (1999). The ten-twenty electrode system of the International Federation. The International Federation of Clinical Neurophysiology. *Electroencephalogr Clin Neurophysiol Suppl*, *52*, 3-6. https://www.ncbi.nlm.nih.gov/pubmed/10590970

Klorman, R., Cicchetti, D., Thatcher, J. E., & Ison, J. R. (2003). Acoustic startle in maltreated children. *J Abnorm Child Psychol*, *31*(4), 359-370. https://doi.org/10.1023/a:1023835417070

Koch, M. (1999). The neurobiology of startle. *Prog Neurobiol*, *59*(2), 107-128. https://doi.org/10.1016/s0301-0082(98)00098-7

Koch, M., Kungel, M., & Herbert, H. (1993). Cholinergic neurons in the pedunculopontine tegmental nucleus are involved in the mediation of prepulse inhibition of the acoustic startle response in the rat. *Exp Brain Res*, *97*(1), 71-82. https://doi.org/10.1007/bf00228818

Kofler, M., Muller, J., Reggiani, L., & Valls-Sole, J. (2001a). Influence of age on auditory startle responses in humans. *Neurosci Lett*, *307*(2), 65-68. https://doi.org/10.1016/s0304-3940(01)01908-5

Kofler, M., Muller, J., Reggiani, L., & Valls-Sole, J. (2001b). Influence of gender on auditory startle responses. *Brain Res*, *921*(1-2), 206-210. https://doi.org/10.1016/s0006-8993(01)03120-1

Kumru, H., Kofler, M., Valls-Sole, J., Portell, E., & Vidal, J. (2009). Brainstem reflexes are enhanced following severe spinal cord injury and reduced by continuous intrathecal baclofen. *Neurorehabil Neural Repair*, *23*(9), 921-927. https://doi.org/10.1177/1545968309335979

Kumru, H., Vidal, J., Kofler, M., Benito, J., Garcia, A., & Valls-Sole, J. (2008). Exaggerated auditory startle responses in patients with spinal cord injury. *J Neurol*, *255*(5), 703-709. https://doi.org/10.1007/s00415-008-0780-3

Kumru, H., Vidal, J., Kofler, M., Portell, E., & Valls-Sole, J. (2010). Alterations in excitatory and inhibitory brainstem interneuronal circuits after severe spinal cord injury. *J Neurotrauma*, *27*(4), 721-728. https://doi.org/10.1089/neu.2009.1089

Kumru, H., Vidal, J., Perez, M., Schestatsky, P., & Valls-Sole, J. (2009). Sympathetic skin responses evoked by different stimuli modalities in spinal cord injury patients. *Neurorehabil Neural Repair*, *23*(6), 553-558. https://doi.org/10.1177/1545968308328721

Lagerburg, V., Bakkers, M., Bouwhuis, A., Hoeijmakers, J. G., Smit, A. M., Van Den Berg, S. J., Hordijk-De Boer, I., Brouwer-Van Der Lee, M. D., Kranendonk, D., Reulen, J. P., Faber, C. G., & Merkies, I. S. (2015). Contact heat evoked potentials: normal values and use in small-fiber neuropathy. *Muscle Nerve*, *51*(5), 743-749. https://doi.org/10.1002/mus.24465

LCN. (2019). *Guide for Manual Edits on FreeSurfer Recon of Pediatric Datasets* [Webpage]. Athinoula A. Martinos Center for Biomedical Imaging. https://surfer.nmr.mgh.harvard.edu/fswiki/ChildBrainManualEdits

Lee, D. C., Lim, H. K., McKay, W. B., Priebe, M. M., Holmes, S. A., & Sherwood, A. M. (2004). Toward an objective interpretation of surface EMG patterns: a voluntary response index (VRI). *J Electromyogr Kinesiol*, *14*(3), 379-388. https://doi.org/10.1016/j.jelekin.2003.10.006

Lee, S. (2014, 10/03/2014). *"Comicbook" Stan Lee's Crusade*, youtube.com. https://youtu.be/eI-mKEyd25s

Leitner, D. S., Powers, A. S., & Hoffman, H. S. (1980). The neural substrate of the startle response. *Physiol Behav*, *25*(2), 291-297. https://doi.org/10.1016/0031-9384(80)90219-x

Lemon, R. (1988). The output map of the primate motor cortex. *Trends Neurosci*, *11*(11), 501-506. https://doi.org/10.1016/0166-2236(88)90012-4

Lemon, R. N. (2008). Descending pathways in motor control. *Annu Rev Neurosci*, *31*, 195-218. https://doi.org/10.1146/annurev.neuro.31.060407.125547

Li, C., Houlden, D. A., & Rowed, D. W. (1990). Somatosensory evoked potentials and neurological grades as predictors of outcome in acute spinal cord injury. *J Neurosurg*, *72*(4), 600-609. https://doi.org/10.3171/jns.1990.72.4.0600

Li, K., Atkinson, D., Boakye, M., Tolfo, C. Z., Aslan, S., Green, M., McKay, B., Ovechkin, A., & Harkema, S. J. (2012). Quantitative and sensitive assessment of neurophysiological status after human spinal cord injury [article-journal]. *J Neurosurg Spine*, *17*(1 Suppl), 77-86. https://doi.org/10.3171/2012.6.AOSPINE12117

Lim, H. K., Lee, D. C., McKay, W. B., Priebe, M. M., Holmes, S. A., & Sherwood, A. M. (2005). Neurophysiological assessment of lower-limb voluntary control in incomplete spinal cord injury. *Spinal Cord*, *43*(5), 283-290. https://doi.org/10.1038/sj.sc.3101679

Lotze, M., Laubis-Herrmann, U., Topka, H., Erb, M., & Grodd, W. (1999). Reorganization in the primary motor cortex after spinal cord injury - A functional Magnetic Resonance (fMRI) study [article-journal]. *Restorative neurology and neuroscience*, *14*(2-3), 183-187. http://www.ncbi.nlm.nih.gov/pubmed/12671262

Ludewig, K., Ludewig, S., Seitz, A., Obrist, M., Geyer, M. A., & Vollenweider, F. X. (2003). The acoustic startle reflex and its modulation: effects of age and gender in humans. *Biol Psychol*, *63*(3), 311-323. https://doi.org/10.1016/s0301-0511(03)00074-7

Mancall, E. L. (2011a). Chapter 1: Overview of the Organization of the Nervous System. In D. G. Brock & E. L. Mancall (Eds.), *Gray's Clinical Neuroanatomy: The Anatomic Basis for Clinical Neuroscience* (1st Edition ed.).

Mancall, E. L. (2011b). Chapter 8: Spinal Cord and Nerve Roots. In D. G. Brock & E. L. Mancall (Eds.), *Gray's Clinical Neuroanatomy: The Anatomic Basis for Clinical Neuroscience* (1st Edition ed.).

Martin, J. H. (2005). The corticospinal system: from development to motor control [article-journal]. *Neuroscientist*, *11*(2), 161-173. https://doi.org/10.1177/1073858404270843

Mauguiere, F., Allison, T., Babiloni, C., Buchner, H., Eisen, A. A., Goodin, D. S., Jones, S. J., Kakigi, R., Matsuoka, S., Nuwer, M. R., Rossini, P. M., & Shibasaki, H. (1999). Somatosensory evoked potentials. In G. Deuschl & A. Eisen (Eds.), *Recommendations for the practice of clinical neurophysiology: guidelines of the International Federation of Clinical Neurophysiology* (2000/01/05 ed., Vol. 52, pp. 79 - 90). Elsevier Science B.V.

May, Z., Fenrich, K. K., Dahlby, J., Batty, N. J., Torres-Espin, A., & Fouad, K. (2017). Following Spinal Cord Injury Transected Reticulospinal Tract Axons Develop New Collateral Inputs to Spinal Interneurons in Parallel with Locomotor Recovery. *Neural Plast*, *2017*, 1932875. https://doi.org/10.1155/2017/1932875

McKay, W. B., Lee, D. C., Lim, H. K., Holmes, S. A., & Sherwood, A. M. (2005). Neurophysiological examination of the corticospinal system and voluntary motor control in motor-incomplete human spinal cord injury. *Exp Brain Res*, *163*(3), 379-387. https://doi.org/10.1007/s00221-004-2190-9

McKay, W. B., Lim, H. K., Priebe, M. M., Stokic, D. S., & Sherwood, A. M. (2004). Clinical neurophysiological assessment of residual motor control in post-spinal cord injury paralysis. *Neurorehabil Neural Repair*, *18*(3), 144-153. https://doi.org/10.1177/0888439004267674

McKinney, W. (2010). *Data Structures for Statistical Computing in Python*. https://doi.org/10.25080/Majora-92bf1922-00a

McLean, L., Scott, R. N., & Parker, P. A. (1996). Stimulus artifact reduction in evoked potential measurements. *Arch Phys Med Rehabil*, *77*(12), 1286-1292. https://doi.org/10.1016/s0003-9993(96)90194-x

Mehta, M. A., Golembo, N. I., Nosarti, C., Colvert, E., Mota, A., Williams, S. C., Rutter, M., & Sonuga-Barke, E. J. (2009). Amygdala, hippocampal and corpus callosum size following severe early institutional deprivation: the English and Romanian Adoptees study pilot. *J Child Psychol Psychiatry*, *50*(8), 943-951. https://doi.org/10.1111/j.1469-7610.2009.02084.x

Min, Y. S., Chang, Y., Park, J. W., Lee, J. M., Cha, J., Yang, J. J., Kim, C. H., Hwang, J. M., Yoo, J. N., & Jung, T. D. (2015). Change of Brain Functional Connectivity in Patients With Spinal Cord Injury: Graph Theory Based Approach [article-journal]. *Ann Rehabil Med*, *39*(3), 374-383. https://doi.org/10.5535/arm.2015.39.3.374

Min, Y. S., Park, J. W., Jin, S. U., Jang, K. E., Nam, H. U., Lee, Y. S., Jung, T. D., & Chang, Y. (2015). Alteration of Resting-State Brain Sensorimotor Connectivity following Spinal Cord Injury: A Resting-State Functional Magnetic Resonance Imaging Study. *J Neurotrauma*, *32*(18), 1422-1427. https://doi.org/10.1089/neu.2014.3661

Mulcahey, M. J., Gaughan, J. P., Chafetz, R. S., Vogel, L. C., Samdani, A. F., & Betz, R. R. (2011). Interrater reliability of the international standards for neurological classification of spinal cord injury in youths with chronic spinal cord injury. *Arch Phys Med Rehabil*, *92*(8), 1264-1269. https://doi.org/10.1016/j.apmr.2011.03.003

Mulcahey, M. J., Vogel, L. C., Sheikh, M., Arango-Lasprilla, J. C., Augutis, M., Garner, E., Hagen, E. M., Jakeman, L. B., Kelly, E., Martin, R., Odenkirchen, J., Scheel-Sailer, A., Schottler, J., Taylor, H., Thielen, C. C., & Zebracki, K. (2017). Recommendations for the National Institute for Neurologic Disorders and Stroke spinal cord injury common data elements for children and youth with SCI [article-journal]. *Spinal Cord*, *55*(4), 331-340. https://doi.org/10.1038/sc.2016.139

Nardone, R., Holler, Y., Sebastianelli, L., Versace, V., Saltuari, L., Brigo, F., Lochner, P., & Trinka, E. (2018). Cortical morphometric changes after spinal cord injury. *Brain Res Bull*, *137*, 107-119. https://doi.org/10.1016/j.brainresbull.2017.11.013

Nardone, R., & Trinka, E. (2015). Reorganization of spinal neural circuitry and functional recovery after spinal cord injury [Perspective]. *Neural Regen Res*, *10*(2), 201-202. https://doi.org/10.4103/1673-5374.152368

Nathan, P. W., Smith, M., & Deacon, P. (1996). Vestibulospinal, reticulospinal and descending propriospinal nerve fibres in man. *Brain*, *119 ( Pt 6)*, 1809-1833. https://doi.org/10.1093/brain/119.6.1809

Nuwer, M. R., Comi, G., Emerson, R., Fuglsang-Frederiksen, A., Guerit, J. M., Hinrichs, H., Ikeda, A., Luccas, F. J., & Rappelsburger, P. (1998). IFCN standards for digital recording of clinical EEG. International Federation of Clinical Neurophysiology. *Electroencephalogr Clin Neurophysiol*, *106*(3), 259-261. https://doi.org/10.1016/s0013-4694(97)00106-5

Oguro, K., Aiba, H., & Hojo, H. (2001). Different responses to auditory and somaesthetic stimulation in patients with an excessive startle: a report of pediatric experience. *Clin Neurophysiol*, *112*(7), 1266-1272. https://doi.org/10.1016/s1388-2457(01)00568-5

Oni-Orisan, A., Kaushal, M., Li, W., Leschke, J., Ward, B. D., Vedantam, A., Kalinosky, B., Budde, M. D., Schmit, B. D., Li, S. J., Muqeet, V., & Kurpad, S. N. (2016). Alterations in Cortical Sensorimotor Connectivity following Complete Cervical Spinal Cord Injury: A Prospective Resting-State fMRI Study [article-journal]. *PLoS One*, *11*(3), e0150351. https://doi.org/10.1371/journal.pone.0150351

Pan, Y., Dou, W. B., Wang, Y. H., Luo, H. W., Ge, Y. X., Yan, S. Y., Xu, Q., Tu, Y. Y., Xiao, Y. Q., Wu, Q., Zheng, Z. Z., & Zhao, H. L. (2017). Non-concomitant cortical structural and functional alterations in sensorimotor areas following incomplete spinal cord injury. *Neural Regen Res*, *12*(12), 2059-2066. https://doi.org/10.4103/1673-5374.221165

Pandas. (2020). *Pandas*. In (Version 1.5.1) Zenodo. https://doi.org/10.5281/zenodo.3509134

Parent, S., Dimar, J., Dekutoski, M., & Roy-Beaudry, M. (2010). Unique features of pediatric spinal cord injury [article-journal]. *Spine (Phila Pa 1976)*, *35*(21 Suppl), S202-208. https://doi.org/10.1097/BRS.0b013e3181f35acb

Patestas, M. A. G., L.P. (2016). Ascending sensory Pathways. In *A Textbook of Neuroanatomy* (2nd ed.). Wiley-Blackwell.

Penfield, W., & Boldrey, E. (1937). Somatic Motor and Sensory Representation in the Cerebral Cortex of Man as Studied by Electrical Stimulation. *Brain*, *60*(4), 389-443. https://doi.org/10.1093/brain/60.4.389

Penfield, W., & Rasmussen, T. (1950). *The cerebral cortex of man; a clinical study of localization of function*. Macmillan.

Petersen, J. A., Wilm, B. J., von Meyenburg, J., Schubert, M., Seifert, B., Najafi, Y., Dietz, V., & Kollias, S. (2012). Chronic cervical spinal cord injury: DTI correlates with clinical and electrophysiological measures. *J Neurotrauma*, *29*(8), 1556-1566. https://doi.org/10.1089/neu.2011.2027

Powell, A., & Davidson, L. (2015). Pediatric spinal cord injury: a review by organ system. *Phys Med Rehabil Clin N Am*, *26*(1), 109-132. https://doi.org/10.1016/j.pmr.2014.09.002

Pressdee, D., May, L., Eastman, E., & Grier, D. (1997). The use of play therapy in the preparation of children undergoing MR imaging. *Clin Radiol*, *52*(12), 945-947. https://doi.org/10.1016/s0009-9260(97)80229-2

Purves, D., Augustine, G. J., Fitzpatrick, D., Katz, L. C., LaMantia, A.-S., McNamara, J. O., & Williams, S. M. (2001a). Chapter 1. The Organization of the Nervous System. In D. Purves, G. J. Augustine, D. Fitzpatrick, L. C. Katz, A.-S. LaMantia, J. O. McNamara, & S. M. Williams (Eds.), *Neuroscience. 2nd edition*. Sinauer Associates 2001.

Purves, D., Augustine, G. J., Fitzpatrick, D., Katz, L. C., LaMantia, A.-S., McNamara, J. O., & Williams, S. M. (2001b). Chapter 9. The Somatic Sensory System. In D. Purves, G. J. Augustine, D. Fitzpatrick, L. C. Katz, A.-S. LaMantia, J. O. McNamara, & S. M. Williams (Eds.), *Neuroscience. 2nd edition*. Sinauer Associates 2001.

Raschle, N., Zuk, J., Ortiz-Mantilla, S., Sliva, D. D., Franceschi, A., Grant, P. E., Benasich, A. A., & Gaab, N. (2012). Pediatric neuroimaging in early childhood and infancy: challenges and practical guidelines [article-journal]. *Ann N Y Acad Sci*, *1252*, 43-50. https://doi.org/10.1111/j.1749-6632.2012.06457.x

Rosenberg, D. R., Sweeney, J. A., Gillen, J. S., Kim, J., Varanelli, M. J., O'Hearn, K. M., Erb, P. A., Davis, D., & Thulborn, K. R. (1997). Magnetic resonance imaging of children without sedation: preparation with simulation. *J Am Acad Child Adolesc Psychiatry*, *36*(6), 853-859. https://doi.org/10.1097/00004583-199706000-00024

Roux, F. E., Djidjeli, I., & Durand, J. B. (2018). Functional architecture of the somatosensory homunculus detected by electrostimulation. *J Physiol*, *596*(5), 941-956. https://doi.org/10.1113/JP275243

Roux, F. E., Niare, M., Charni, S., Giussani, C., & Durand, J. B. (2020). Functional architecture of the motor homunculus detected by electrostimulation. *J Physiol*, *598*(23), 5487-5504. https://doi.org/10.1113/JP280156

Rutter, M., Beckett, C., Castle, J., Colvert, E., Kreppner, J., Mehta, M., Stevens, S., & Sonuga-Barke, E. (2007). Effects of profound early institutional deprivation: An overview of findings from a UK longitudinal study of Romanian adoptees. *European Journal of Developmental Psychology*, *4*(3), 332-350. https://doi.org/10.1080/17405620701401846

Saksena, S., Mohamed, F. B., Middleton, D. M., Krisa, L., Alizadeh, M., Shahrampour, S., Conklin, C. J., Flanders, A., Finsterbusch, J., Mulcahey, M. J., & Faro, S. H. (2019). Diffusion Tensor Imaging Assessment of Regional White Matter Changes in the Cervical and Thoracic Spinal Cord in Pediatric Subjects. *J Neurotrauma*, *36*(6), 853-861. https://doi.org/10.1089/neu.2018.5826

Sangari, S., & Perez, M. A. (2020). Distinct Corticospinal and Reticulospinal Contributions to Voluntary Control of Elbow Flexor and Extensor Muscles in Humans with Tetraplegia. *J Neurosci*, *40*(46), 8831-8841. https://doi.org/10.1523/JNEUROSCI.1107-20.2020

Sanvictores, T., & Tadi, P. (2022). Neuroanatomy, Autonomic Nervous System Visceral Afferent Fibers and Pain. In *StatPearls*. https://www.ncbi.nlm.nih.gov/pubmed/32809678

Sayenko, D. G., Atkinson, D. A., Floyd, T. C., Gorodnichev, R. M., Moshonkina, T. R., Harkema, S. J., Edgerton, V. R., & Gerasimenko, Y. P. (2015). Effects of paired transcutaneous electrical stimulation delivered at single and dual sites over lumbosacral spinal cord [article-journal]. *Neurosci Lett*, *609*, 229-234. https://doi.org/10.1016/j.neulet.2015.10.005

Sayenko, D. G., Atkinson, D. A., Mink, A. M., Gurley, K. M., Edgerton, V. R., Harkema, S. J., & Gerasimenko, Y. P. (2018). Vestibulospinal and Corticospinal Modulation of Lumbosacral Network Excitability in Human Subjects. *Front Physiol*, *9*, 1746. https://doi.org/10.3389/fphys.2018.01746

Schottler, J., Vogel, L. C., & Sturm, P. (2012). Spinal cord injuries in young children: a review of children injured at 5 years of age and younger [article-journal]. *Dev Med Child Neurol*, *54*(12), 1138-1143. https://doi.org/10.1111/j.1469-8749.2012.04411.x

Schulz, A., Lass-Hennemann, J., Nees, F., Blumenthal, T. D., Berger, W., & Schachinger, H. (2009). Cardiac modulation of startle eye blink. *Psychophysiology*, *46*(2), 234-240. https://doi.org/10.1111/j.1469-8986.2008.00768.x

Seif, M., Curt, A., Thompson, A. J., Grabher, P., Weiskopf, N., & Freund, P. (2018). Quantitative MRI of rostral spinal cord and brain regions is predictive of functional recovery in acute spinal cord injury. *Neuroimage Clin*, *20*, 556-563. https://doi.org/10.1016/j.nicl.2018.08.026

Sheridan, M. A., Fox, N. A., Zeanah, C. H., McLaughlin, K. A., & Nelson, C. A., 3rd. (2012). Variation in neural development as a result of exposure to institutionalization early in childhood [article-journal]. *Proc Natl Acad Sci U S A*, *109*(32), 12927-12932. https://doi.org/10.1073/pnas.1200041109

Sherwood, A. M., Dimitrijevic, M. R., & McKay, W. B. (1992). Evidence of subclinical brain influence in clinically complete spinal cord injury: discomplete SCI [article-journal]. *J Neurol Sci*, *110*(1-2), 90-98. https://doi.org/10.1016/0022-510x(92)90014-c

Sherwood, A. M., McKay, W. B., & Dimitrijevic, M. R. (1996). Motor control after spinal cord injury: assessment using surface EMG. *Muscle Nerve*, *19*(8), 966-979.

https://doi.org/10.1002/(SICI)1097-4598(199608)19:8<966::AID-MUS5>3.0.CO;2-6
Singh, G. (2018). Somatosensory evoked potential monitoring. *Journal of Neuroanaesthesiology and Critical Care*, *03*(04), S97-S104. https://doi.org/10.4103/2348-0548.174745
Singh, G., Behrman, A. L., Aslan, S. C., Trimble, S., & Ovechkin, A. V. (2018). Respiratory functional and motor control deficits in children with spinal cord injury. *Respir Physiol Neurobiol*, *247*, 174-180. https://doi.org/10.1016/j.resp.2017.10.006
Solstrand Dahlberg, L., Becerra, L., Borsook, D., & Linnman, C. (2018). Brain changes after spinal cord injury, a quantitative meta-analysis and review. *Neurosci Biobehav Rev*, *90*, 272-293. https://doi.org/10.1016/j.neubiorev.2018.04.018
Spiess, M., Schubert, M., Kliesch, U., group, E.-S. S., & Halder, P. (2008). Evolution of tibial SSEP after traumatic spinal cord injury: baseline for clinical trials. *Clin Neurophysiol*, *119*(5), 1051-1061. https://doi.org/10.1016/j.clinph.2008.01.021
Standring, S. (2021a). Brainstem. In S. Standring (Ed.), *Gray's Anatomy: The Anatomical Basis of Clinical Practice* (Forty-second edition ed., pp. 442-464). Elsevier.
Standring, S. (2021b). Overview of the nervous system. In S. Standring (Ed.), *Gray's Anatomy: The Anatomical Basis of Clinical Practice* (Forty-second edition ed., pp. 386-397). Elsevier.
Standring, S. (2021c). Spinal cord. In S. Standring (Ed.), *Gray's Anatomy: The Anatomical Basis of Clinical Practice* (Forty-second edition ed., pp. 425-441). Elsevier.
Sun, P., Murphy, R. K., Gamble, P., George, A., Song, S. K., & Ray, W. Z. (2017). Diffusion Assessment of Cortical Changes, Induced by Traumatic Spinal Cord Injury. *Brain Sci*, *7*(2). https://doi.org/10.3390/brainsci7020021
Suzuki, A., Yamaguchi, R., Kim, L., Kawahara, T., & Ishii-Takahashi, A. (2022). Effectiveness of mock scanners and preparation programs for successful magnetic resonance imaging: a systematic review and meta-analysis. *Pediatr Radiol*. https://doi.org/10.1007/s00247-022-05394-8
Treiber, J. M., White, N. S., Steed, T. C., Bartsch, H., Holland, D., Farid, N., McDonald, C. R., Carter, B. S., Dale, A. M., & Chen, C. C. (2016). Characterization and Correction of Geometric Distortions in 814 Diffusion Weighted Images. *PLoS One*, *11*(3), e0152472. https://doi.org/10.1371/journal.pone.0152472
Tustison, N. J., Avants, B. B., Cook, P. A., Zheng, Y., Egan, A., Yushkevich, P. A., & Gee, J. C. (2010). N4ITK: improved N3 bias correction. *IEEE Trans Med Imaging*, *29*(6), 1310-1320. https://doi.org/10.1109/TMI.2010.2046908
Vallotton, K., Huber, E., Sutter, R., Curt, A., Hupp, M., & Freund, P. (2019). Width and neurophysiologic properties of tissue bridges predict recovery after cervical injury. *Neurology*, *92*(24), e2793-e2802. https://doi.org/10.1212/WNL.0000000000007642
Valls-Sole, J., Kumru, H., & Kofler, M. (2008). Interaction between startle and voluntary reactions in humans. *Exp Brain Res*, *187*(4), 497-507. https://doi.org/10.1007/s00221-008-1402-0
Vavrek, R., Pearse, D. D., & Fouad, K. (2007). Neuronal populations capable of regeneration following a combined treatment in rats with spinal cord transection. *J Neurotrauma*, *24*(10), 1667-1673. https://doi.org/10.1089/neu.2007.0290
Veraart, J., Novikov, D. S., Christiaens, D., Ades-Aron, B., Sijbers, J., & Fieremans, E. (2016). Denoising of diffusion MRI using random matrix theory. *NeuroImage*, *142*, 394-406. https://doi.org/10.1016/j.neuroimage.2016.08.016
Virtanen, P., Gommers, R., Oliphant, T. E., Haberland, M., Reddy, T., Cournapeau, D., Burovski, E., Peterson, P., Weckesser, W., Bright, J., van der Walt, S. J., Brett, M.,

Wilson, J., Millman, K. J., Mayorov, N., Nelson, A. R. J., Jones, E., Kern, R., Larson, E., . . . SciPy, C. (2020). SciPy 1.0: fundamental algorithms for scientific computing in Python. *Nat Methods*, *17*(3), 261-272. https://doi.org/10.1038/s41592-019-0686-2

Vogel, L. C., Betz, R. R., & Mulcahey, M. J. (2012). Spinal cord injuries in children and adolescents. *Handb Clin Neurol*, *109*, 131-148. https://doi.org/10.1016/B978-0-444-52137-8.00008-5

Wang, S., Peterson, D. J., Gatenby, J. C., Li, W., Grabowski, T. J., & Madhyastha, T. M. (2017). Evaluation of Field Map and Nonlinear Registration Methods for Correction of Susceptibility Artifacts in Diffusion MRI [Original Research]. *Front Neuroinform*, *11*, 17. https://doi.org/10.3389/fninf.2017.00017

Waskom, M. (2021). seaborn: statistical data visualization. *Journal of Open Source Software*, *6*(60), 3021. https://doi.org/10.21105/joss.03021

Whitfield-Gabrieli, S., & Nieto-Castanon, A. (2012). Conn: a functional connectivity toolbox for correlated and anticorrelated brain networks. *Brain Connect*, *2*(3), 125-141. https://doi.org/10.1089/brain.2012.0073

Whitfield-Gabrieli, S., & Nieto-Castanon, A. (2017). CONN fMRI Functional connectivity toolbox manual v17. In M. I. o. Technology (Ed.), *Gabrieli Lab. McGovern Institute for Brain Research*.

Wickham, H. (2014). Tidy Data. *Journal of Statistical Software*, *59*(10), 1 - 23. https://doi.org/10.18637/jss.v059.i10

Wrigley, P. J., Gustin, S. M., Macey, P. M., Nash, P. G., Gandevia, S. C., Macefield, V. G., Siddall, P. J., & Henderson, L. A. (2009). Anatomical changes in human motor cortex and motor pathways following complete thoracic spinal cord injury [article-journal]. *Cereb Cortex*, *19*(1), 224-232. https://doi.org/10.1093/cercor/bhn072

Xie, J., & Boakye, M. (2008). Electrophysiological outcomes after spinal cord injury. *Neurosurg Focus*, *25*(5), E11. https://doi.org/10.3171/FOC.2008.25.11.E11

Yeh, F. C., Panesar, S., Fernandes, D., Meola, A., Yoshino, M., Fernandez-Miranda, J. C., Vettel, J. M., & Verstynen, T. (2018). Population-averaged atlas of the macroscale human structural connectome and its network topology. *NeuroImage*, *178*, 57-68. https://doi.org/10.1016/j.neuroimage.2018.05.027

Yeh, F. C., & Tseng, W. Y. (2011). NTU-90: a high angular resolution brain atlas constructed by q-space diffeomorphic reconstruction. *NeuroImage*, *58*(1), 91-99. https://doi.org/10.1016/j.neuroimage.2011.06.021

Yeh, F. C., Wedeen, V. J., & Tseng, W. Y. (2010). Generalized q-sampling imaging. *IEEE Trans Med Imaging*, *29*(9), 1626-1635. https://doi.org/10.1109/tmi.2010.2045126

Yozbatiran, N., Keser, Z., Hasan, K., Stampas, A., Korupolu, R., Kim, S., O'Malley, M. K., Fregni, F., & Francisco, G. E. (2017). White matter changes in corticospinal tract associated with improvement in arm and hand functions in incomplete cervical spinal cord injury: pilot case series. *Spinal Cord Ser Cases*, *3*, 17028. https://doi.org/10.1038/scsandc.2017.28

Zaaimi, B., Edgley, S. A., Soteropoulos, D. S., & Baker, S. N. (2012). Changes in descending motor pathway connectivity after corticospinal tract lesion in macaque monkey. *Brain*, *135*(Pt 7), 2277-2289. https://doi.org/10.1093/brain/aws115

Zhang, Y., Brady, M., & Smith, S. (2001). Segmentation of brain MR images through a hidden Markov random field model and the expectation-maximization algorithm. *IEEE Trans Med Imaging*, *20*(1), 45-57. https://doi.org/10.1109/42.906424

Zhu, L., Wu, G., Zhou, X., Li, J., Wen, Z., & Lin, F. (2015). Altered spontaneous brain activity in patients with acute spinal cord injury revealed by resting-state functional

MRI [article-journal]. *PLoS One*, *10*(3), e0118816. https://doi.org/10.1371/journal.pone.0118816

Zhu, N., Zhang, D., Wang, W., Li, X., Yang, B., Song, J., Zhao, X., Huang, B., Shi, W., Lu, R., Niu, P., Zhan, F., Ma, X., Wang, D., Xu, W., Wu, G., Gao, G. F., Tan, W., China Novel Coronavirus, I., & Research, T. (2020). A Novel Coronavirus from Patients with Pneumonia in China, 2019. *N Engl J Med*, *382*(8), 727-733. https://doi.org/10.1056/NEJMoa2001017

Ziegler, G., Grabher, P., Thompson, A., Altmann, D., Hupp, M., Ashburner, J., Friston, K., Weiskopf, N., Curt, A., & Freund, P. (2018). Progressive neurodegeneration following spinal cord injury: Implications for clinical trials. *Neurology*, *90*(14), e1257-e1266. https://doi.org/10.1212/WNL.0000000000005258

# APPENDICES

## Appendix A. List of Abbreviations

| Abbreviation | Full Term |
|---|---|
| ACNS | American Clinical Neurophysiology Society |
| ACPC | Anterior commissure - posterior commissure |
| ADD | Adductor group |
| AIS | American Spinal Injury Association Impairment Scale |
| ALS | Anterolateral system |
| APB | Abductor pollicis brevis |
| ASIA | American Spinal Injury Association |
| ASR | Acoustic startle response |
| BB | Biceps brachii |
| BG | Basal ganglia |
| BOLD | Blood-oxygen-level dependent |
| C | Cervical |
| C5S | Spinous process of the fifth vertebra |
| Ca | Caudate |
| CI | Confidence interval |
| cjv | Coefficient of joint variation |
| CNS | Central nervous system |
| COVID-19 | Coronavirus disease-2019 |
| CPc | Contralateral lateral somatosensory cortex |
| CPi | Ipsilateral lateral somatosensory cortex |
| CPz | Mesial somatosensory cortex |
| CST | Corticospinal tract |
| DCML | Dorsal column-medial lemniscus |
| DEL | Deltoid |
| DWI | Diffusion-weighted imaging |
| EEG | Electroencephalogram |
| efc | Entropy focus criterion |
| EMG | Electromyography |

| | |
|---|---|
| EPc | Contralateral Erb's point |
| EPi | Ipsilateral Erb's point |
| ERA | English and Romanian Adoptees |
| eTIV | Estimated total intracranial volume |
| F | Female |
| FA | Fractional anisotropy |
| FC | Functional connectivity |
| FD | Framewise displacement |
| FIR | Finite impulse response |
| FNPA | Functional neurophysiological assessment |
| FoV | Field of view |
| Fpz | Midsagittal plane of the forehead |
| GLM | General linear model |
| GM | Gray matter |
| GSA | General somatic afferent |
| HBN | Child Mind Institute Healthy Brain Network |
| ICA | Independent component analysis |
| INU | Intensity non-uniformity |
| IQR | Interquartile range |
| IRB | Institutional Review Board |
| ISNCSCI | International Standards for Neurological Classification of SCI |
| L | Lumbar |
| LMN | Lower motor neurons |
| M | Male |
| M1 | Primary motor cortex |
| MEP | Motor-evoked potentials |
| MG | Medial gastrocnemius |
| MidT | Mid-thoracic |
| mm | Millimeters |
| MPRAGE | Magnetization-prepared rapid gradient-echo sequence |
| MRI | Magnetic resonance imaging |
| mn-SSEP | Median nerve short-latency somatosensory evoked potentials |
| OOC | Orbicularis oculi |
| Pa | Pallidum |
| Pfd | Distal popliteal fossae |
| Pfp | Proximal popliteal fossae |
| PM | Premotor area |
| PNS | Peripheral nervous system |
| PS | Thoracic paraspinal group |
| pt-SSEP | Posterior tibial nerve short-latency somatosensory evoked potentials |

| | |
|---|---|
| Pu | Putamen |
| r | Correlation coefficients |
| RA | Rectus abdominis |
| RF | Rectus femoris |
| RMS | Root Mean Square |
| ROIs | Regions of interest |
| rs-FC | Resting-state functional connectivity |
| rs-fMRI | Resting-state functional MRI |
| RST | Reticulospinal tract |
| S | Sacral |
| S1 | Primary sensory cortex |
| SARS-CoV-2 | Severe acute respiratory syndrome coronavirus-2 |
| SCI | Spinal cord injury |
| SD | Standard deviation |
| SMA | Supplementary motor area |
| SMN | Sensorimotor resting-state network |
| SSA | Special somatic afferent |
| SSEP | Short-latency somatosensory evoked potentials |
| T | Thoracic |
| T12S | Spinous process of the twelfth thoracic vertebra |
| TA | Tibialis anterior |
| TB | Triceps brachii |
| TD | Typically developing |
| TE | Echo time |
| Th | Thalamus |
| TMS | Transcranial magnetic stimulation |
| TR | Repetition time |
| UMN | Upper motor neuron |
| UT | Upper trapezius |
| WM | White matter |

## Appendix B. Comicbook Illustration of Study

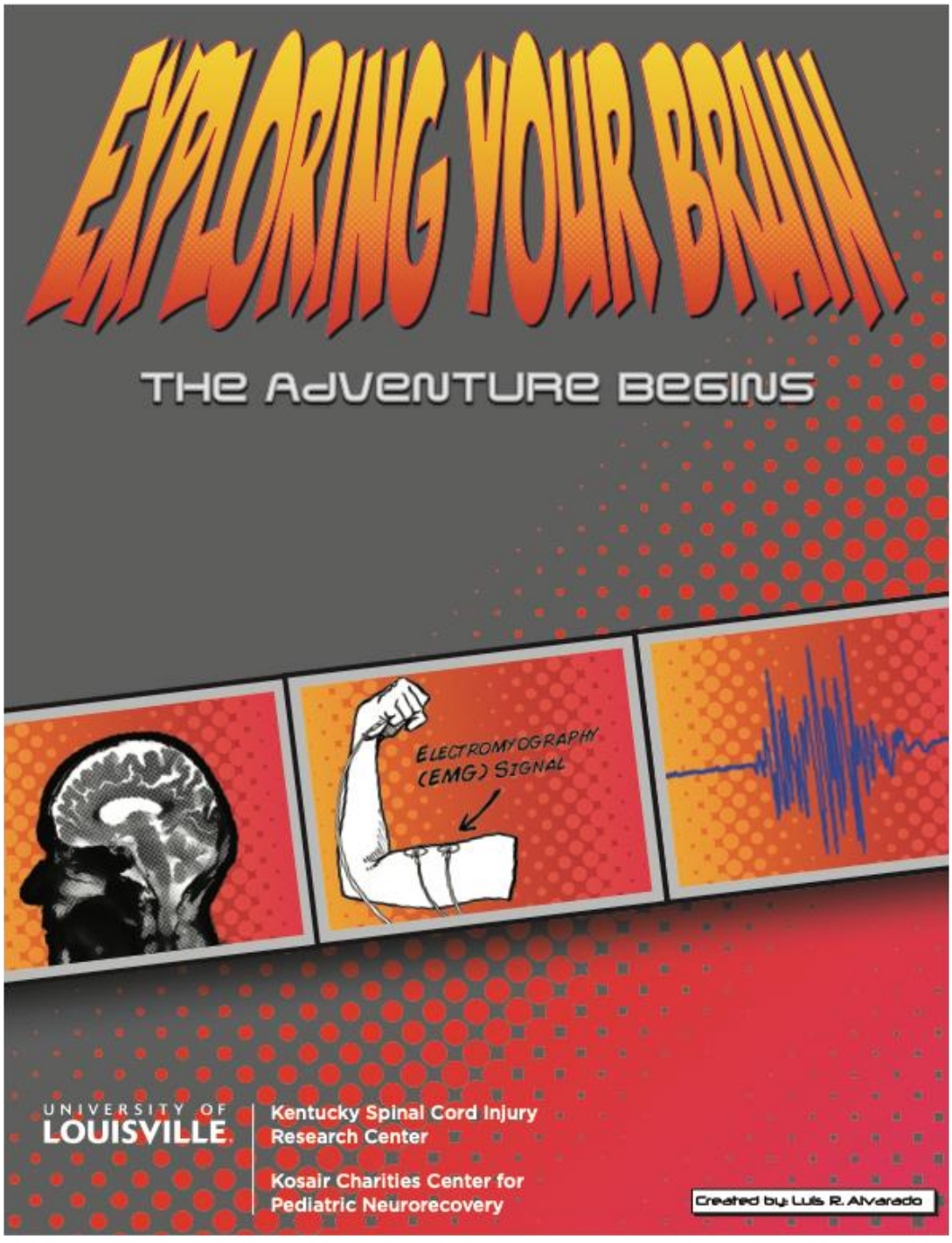


Comicbook created for the informed assent process. The book invites the child to explore the brain and explains in a child-centric manner the protocols for all the experiments in this dissertation.


WE WILL EXPLAIN
ALL THE STEPS
IN THIS QUEST
READY TO EXPLORE THE BRAIN?
YES!!
STEP 1. PRACTICE TAKING PICTURES OF THE BRAIN
STEP 2. LISTEN TO THE MUSCLES
STEP 3. LISTEN TO THE BRAIN
STEP 4. TAKE PICTURES OF THE BRAIN
STEP 5. CHECK THE BLINK REFLEX
DR. B AND MR. LUIS WILL ANSWER YOUR QUESTIONS


1. PRACTICE TAKING PICTURES OF THE BRAIN
STAYING STILL IS VERY IMPORTANT FOR GOOD PICTURES
SELFIE TIME!!!
WHAAA!? WHY IS IT SO BLURRY?
BECAUSE YOU MOVED... TRY STAYING STILL
THE MRI MACHINE TAKES PICTURES OF THE BRAIN
CLICK!!
SO....
IT IS ALSO VERY IMPORTANT
TO STAY VERY STILL DURING AN MRI
To practice how to stay very still we will play games and watch movies

# 2. LISTEN TO THE MUSCLES

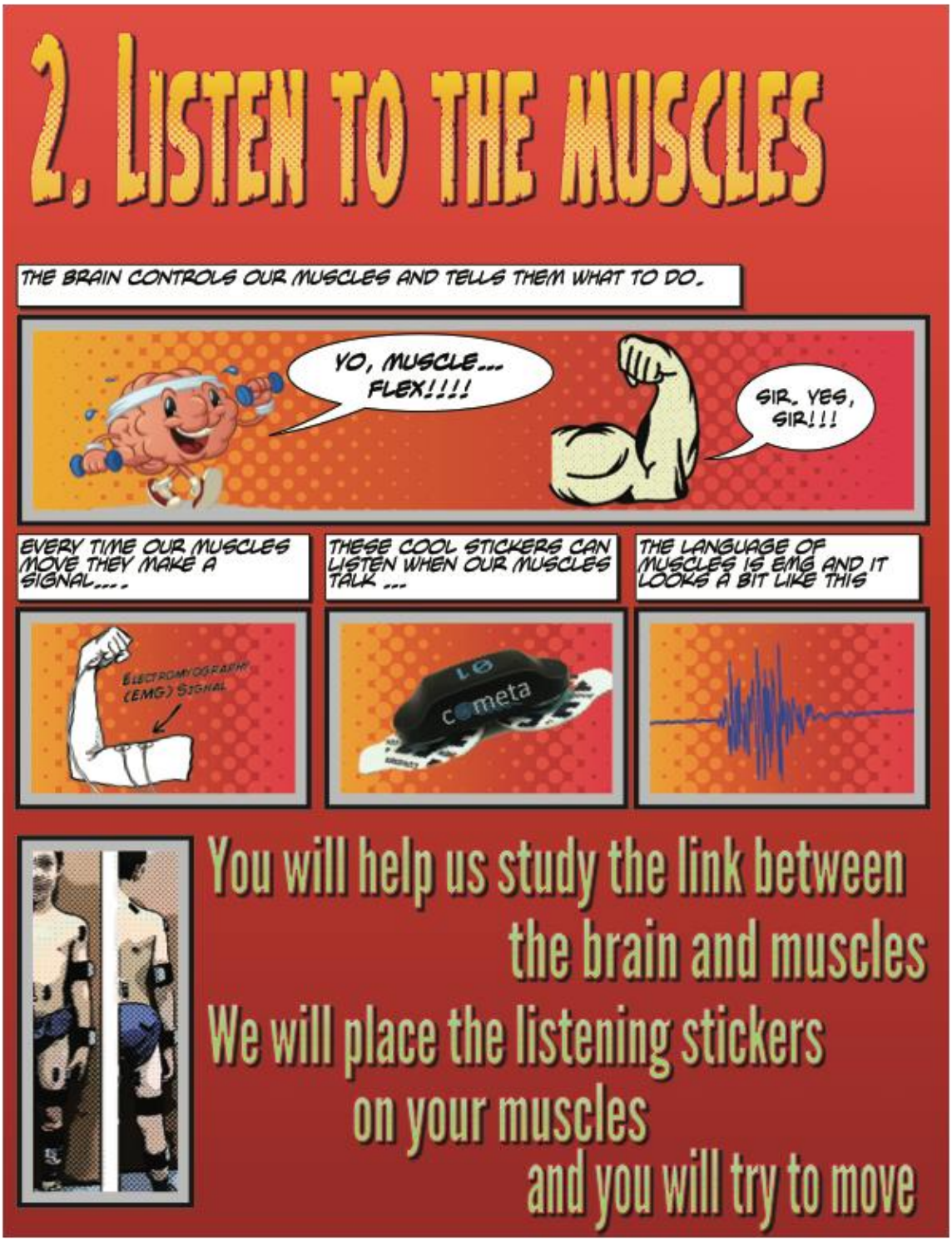


3, LISTEN TO THE BRAIN
NERVES IN OUR BODY TELL THE BRAIN WHAT IS HAPPENING AT ALL TIMES...
MR. BRAIN SOMEONE IS POKING OUR ARM!
ROGER THAT, MR. NERVE!
EVERY TIME OUR NERVES FEEL SOMETHING, THEY SEND A SIGNAL....
PST! PSSSST! MR. BRAIN
THESE SPECIAL CAPS CAN LISTEN WHEN OUR BRAINS GET MESSAGES...
THE LANGUAGE OF THE BRAIN IS EEG AND IT LOOKS A BIT LIKE THIS
You will help us study the link from muscles to the brain
We will place the listening cap on your head and tingle your nerves

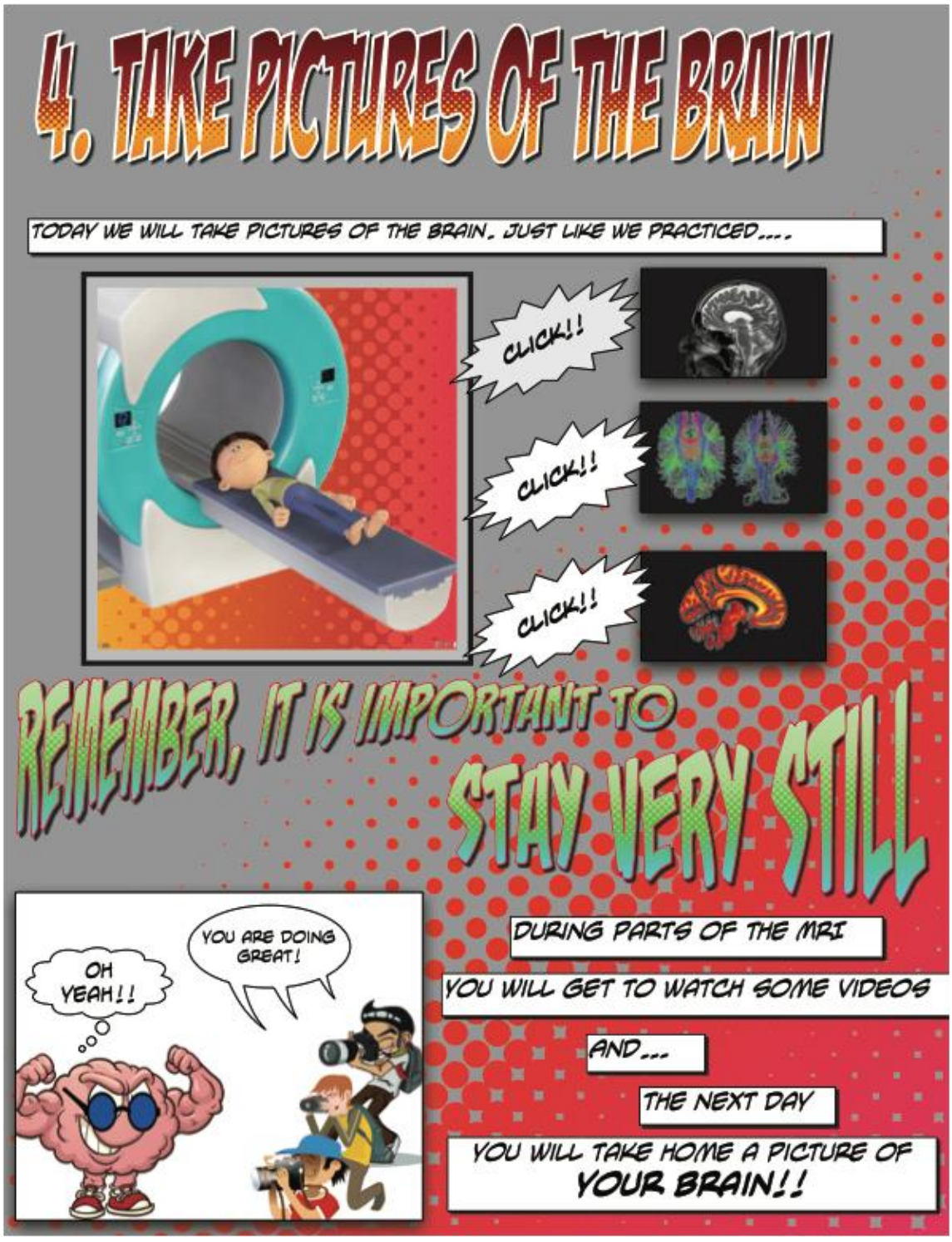
4. TAKE PICTURES OF THE BRAIN
TODAY WE WILL TAKE PICTURES OF THE BRAIN. JUST LIKE WE PRACTICED....
CLICK!!
CLICK!!
CLICK!!
REMEMBER, IT IS IMPORTANT TO
STAY VERY STILL
OH YEAH!!
YOU ARE DOING GREAT!
DURING PARTS OF THE MRI
YOU WILL GET TO WATCH SOME VIDEOS
AND...
THE NEXT DAY
YOU WILL TAKE HOME A PICTURE OF
YOUR BRAIN!!

# 5. CHECK THE BLINK REFLEX

WHEN A LOUD NOISE TAKES US BY SURPRISE, OUR BRAIN ORDERS OUR EYES TO BLINK


OUR BRAIN MAKES OUR EYES BLINK IN ORDER TO PROTECT THEM.

WE CAN LISTEN TO MUSCLES AROUND THE EYE USING EMG STICKERS.


REMEMBER, EMG IS THE MUSCLE LANGUAGE AND IT LOOKS A BIT LIKE THIS..

We will place listening stickers on your muscles

and headphones on your ears

at some point you will hear a noise.

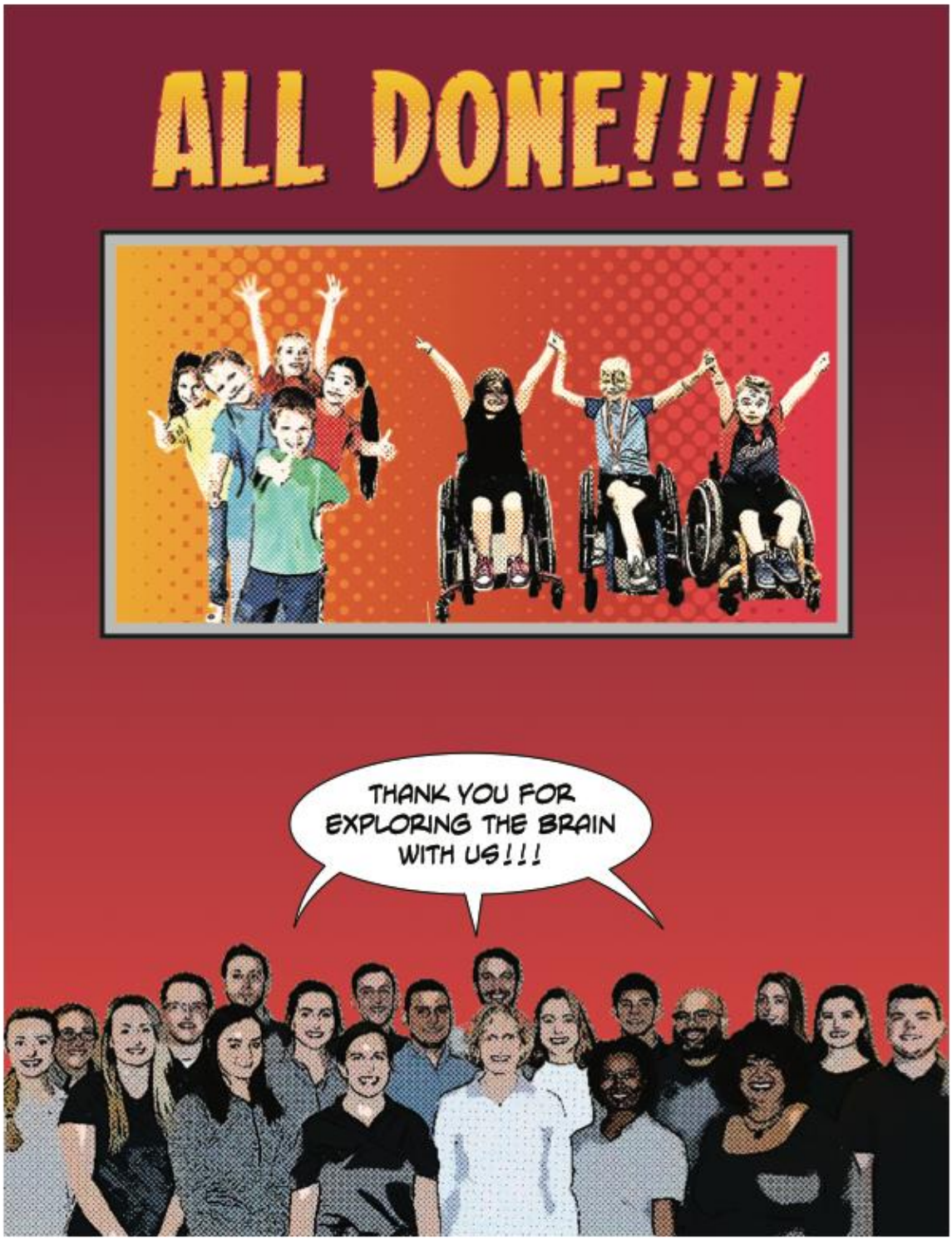
ALL DONE!!!!
THANK YOU FOR EXPLORING THE BRAIN WITH US!!!

# P14

**INTERNATIONAL STANDARDS FOR NEUROLOGICAL CLASSIFICATION OF SPINAL CORD INJURY (ISNCSCI)**

ASIA American Spinal Injury Association — ISCOS International Spinal Cord Society

## RIGHT

| | | MOTOR KEY MUSCLES | Light Touch (LTR) | Pin Prick (PPR) |
|---|---|---|---|---|
| | C2 | | 2 | 2 |
| | C3 | | 2 | 2 |
| | C4 | | 2 | 2 |
| UER (Upper Extremity Right) | C5 | Elbow flexors | 5 | 2 |
| | C6 | Wrist extensors | 5 | 2 |
| | C7 | Elbow extensors | 5 | 2 |
| | C8 | Finger flexors | 0 | 1 |
| | T1 | Finger abductors (little finger) | 1 | 1 |
| | T2 | | 1 | 1 |
| | T3 | | 0 | 0 |
| | T4 | | 0 | 0 |
| | T5 | | 0 | 0 |
| | T6 | | 0 | 0 |
| | T7 | | 0 | 0 |
| | T8 | | 0 | 0 |
| | T9 | | 0 | 0 |
| | T10 | | 0 | 0 |
| | T11 | | 0 | 0 |
| | T12 | | 0 | 0 |
| | L1 | | 0 | 0 |
| LER (Lower Extremity Right) | L2 | Hip flexors | 0 | 0 |
| | L3 | Knee extensors | 0 | 0 |
| | L4 | Ankle dorsiflexors | 0 | 0 |
| | L5 | Long toe extensors | 0 | 0 |
| | S1 | Ankle plantar flexors | 0 | 0 |
| | S2 | | 0 | 0 |
| | S3 | | 0 | 0 |
| | S4-5 | | 0 | 0 |
| | | RIGHT TOTALS (MAXIMUM) | 16 (50) | 15 (56) |

Comments (Non-key Muscle? Reason for NT? Pain? Non-SCI condition?):

(VAC) Voluntary Anal Contraction (Yes/No): N

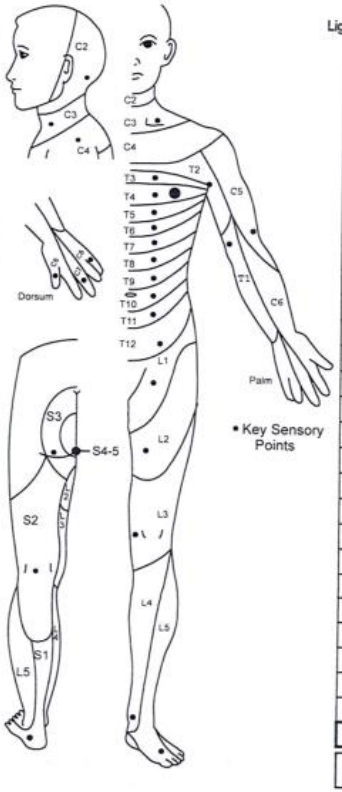


## LEFT

| | | SENSORY KEY SENSORY POINTS | Light Touch (LTL) | Pin Prick (PPL) | MOTOR KEY MUSCLES |
|---|---|---|---|---|---|
| | C2 | | 2 | 2 | |
| | C3 | | 2 | 2 | |
| | C4 | | 2 | 2 | |
| | C5 | | 2 | 2 | 5 Elbow flexors |
| | C6 | | 2 | 2 | 5 Wrist extensors |
| UEL (Upper Extremity Left) | C7 | | 2 | 2 | 5 Elbow extensors |
| | C8 | | 1 | 1 | 1 Finger flexors |
| | T1 | | 1 | 0 | 0 Finger abductors (little finger) |
| | T2 | | 0 | 1 | |
| | T3 | | 0 | 0 | |
| | T4 | | 0 | 0 | |
| | T5 | | 0 | 0 | |
| | T6 | | 0 | 0 | |
| | T7 | | 0 | 0 | |
| | T8 | | 0 | 0 | |
| | T9 | | 0 | 0 | |
| | T10 | | 0 | 0 | |
| | T11 | | 0 | 0 | |
| | T12 | | 0 | 0 | |
| | L1 | | 0 | 0 | |
| LEL (Lower Extremity Left) | L2 | | 0 | 0 | 0 Hip flexors |
| | L3 | | 0 | 0 | 0 Knee extensors |
| | L4 | | 0 | 0 | 0 Ankle dorsiflexors |
| | L5 | | 0 | 0 | 0 Long toe extensors |
| | S1 | | 0 | 0 | 0 Ankle plantar flexors |
| | S2 | | 0 | 0 | |
| | S3 | | 0 | 0 | |
| | S4-5 | | 0 | 0 | |
| | | LEFT TOTALS (MAXIMUM) | 14 (56) | 13 (56) | 16 (50) |

**MOTOR (SCORING ON REVERSE SIDE)**

0 = Total paralysis
1 = Palpable or visible contraction
2 = Active movement, gravity eliminated
3 = Active movement, against gravity
4 = Active movement, against some resistance
5 = Active movement, against full resistance
NT = Not testable
0*, 1*, 2*, 3*, 4*, NT* = Non-SCI condition present

**SENSORY (SCORING ON REVERSE SIDE)**

0 = Absent
1 = Altered
2 = Normal
NT = Not testable
0*, 1*, NT* = Non-SCI condition present

(DAP) Deep Anal Pressure (Yes/No): N

**MOTOR SUBSCORES**

UER 16 + UEL 16 = UEMS TOTAL 32 (MAX (25) (25) (50))

LER 0 + LEL 0 = LEMS TOTAL 0 (MAX (25) (25) (50))

**SENSORY SUBSCORES**

LTR 15 + LTL 14 = LT TOTAL 29 (MAX (56) (56) (112))

PPR 14 + PPL 13 = PP TOTAL 27 (MAX (56) (56) (112))

| NEUROLOGICAL LEVELS (Steps 1- 6 for classification as on reverse) | R | L |
|---|---|---|
| 1. SENSORY | C6 | C6 |
| 2. MOTOR | C7 | C7 |

3. NEUROLOGICAL LEVEL OF INJURY (NLI): C6

4. COMPLETE OR INCOMPLETE? (Incomplete = Any sensory or motor function in S4-5): C (In injuries with absent motor OR sensory function in S4-5 only)

5. ASIA IMPAIRMENT SCALE (AIS): A

6. ZONE OF PARTIAL PRESERVATION (Most caudal levels with any innervation)

| | R | L |
|---|---|---|
| SENSORY | T5 | T2 |
| MOTOR | T1 | C8 |





REV 04/19

# P15

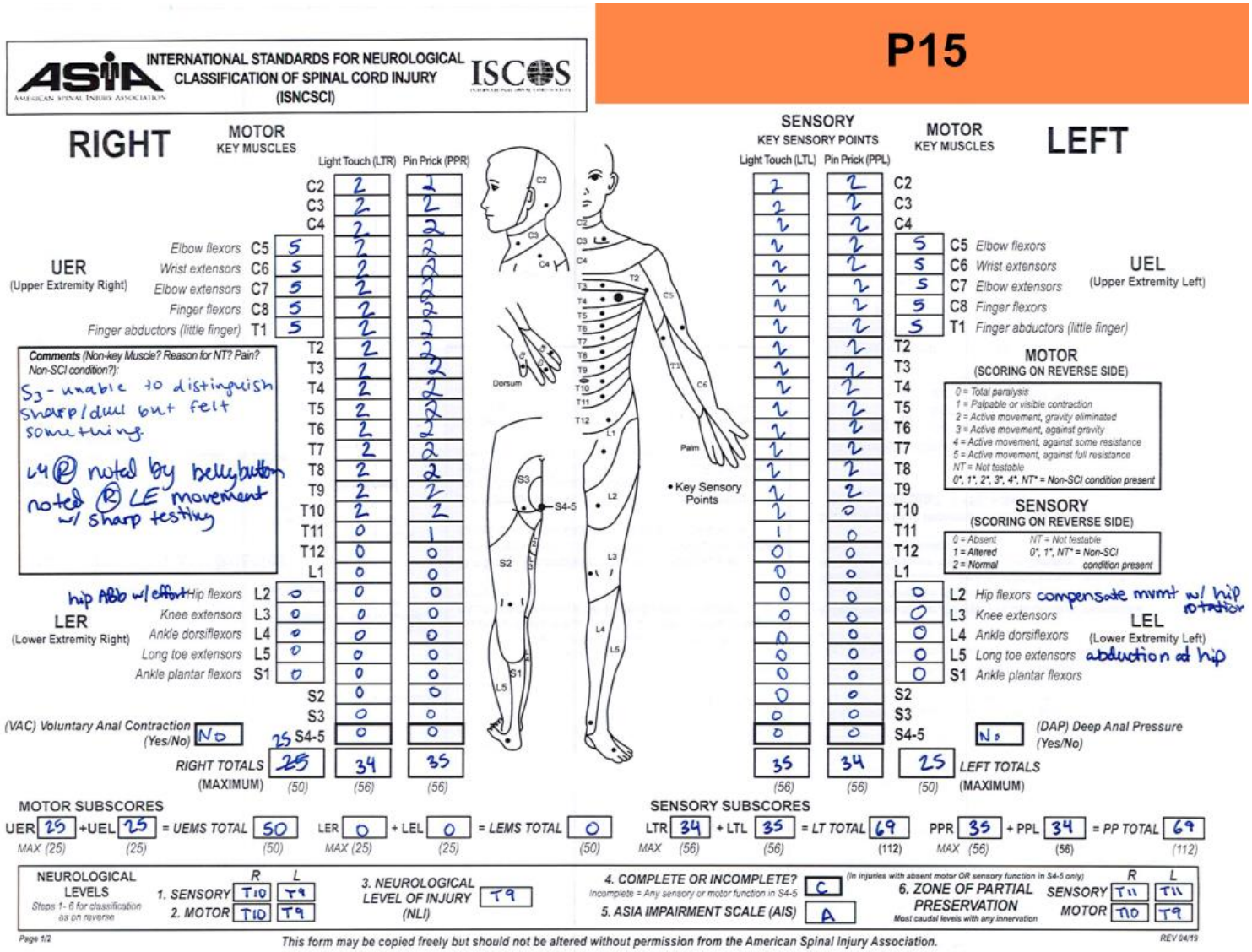

INTERNATIONAL STANDARDS FOR NEUROLOGICAL CLASSIFICATION OF SPINAL CORD INJURY (ISNCSCI)

ASIA American Spinal Injury Association — ISCOS International Spinal Cord Society

## RIGHT

| | | MOTOR KEY MUSCLES | Light Touch (LTR) | Pin Prick (PPR) |
|---|---|---|---|---|
| | C2 | | 2 | 2 |
| | C3 | | 2 | 2 |
| | C4 | | 2 | 2 |
| Elbow flexors | C5 | 5 | 2 | 2 |
| Wrist extensors | C6 | 5 | 2 | 2 |
| Elbow extensors | C7 | 5 | 2 | 2 |
| Finger flexors | C8 | 5 | 2 | 2 |
| Finger abductors (little finger) | T1 | 5 | 2 | 2 |
| | T2 | | 2 | 2 |
| | T3 | | 2 | 2 |
| | T4 | | 2 | 2 |
| | T5 | | 2 | 2 |
| | T6 | | 2 | 2 |
| | T7 | | 2 | 2 |
| | T8 | | 2 | 2 |
| | T9 | | 2 | 2 |
| | T10 | | 2 | 2 |
| | T11 | | 0 | 1 |
| | T12 | | 0 | 0 |
| | L1 | | 0 | 0 |
| hip ABD w/ effort Hip flexors | L2 | 0 | 0 | 0 |
| Knee extensors | L3 | 0 | 0 | 0 |
| Ankle dorsiflexors | L4 | 0 | 0 | 0 |
| Long toe extensors | L5 | 0 | 0 | 0 |
| Ankle plantar flexors | S1 | 0 | 0 | 0 |
| | S2 | | 0 | 0 |
| | S3 | | 0 | 0 |
| | S4-5 | | 0 | 0 |
| RIGHT TOTALS (MAXIMUM) | | 25 | 34 (56) | 35 (56) |

UER (Upper Extremity Right)

LER (Lower Extremity Right)

Comments (Non-key Muscle? Reason for NT? Pain? Non-SCI condition?):
S3 - unable to distinguish sharp/dull but felt something.
L4 ® noted by belly button
noted ® LE movement w/ sharp testing

(VAC) Voluntary Anal Contraction (Yes/No): NO

Dorsum

Palm

• Key Sensory Points

## LEFT

| | | SENSORY KEY SENSORY POINTS Light Touch (LTL) | Pin Prick (PPL) | MOTOR KEY MUSCLES |
|---|---|---|---|---|
| | C2 | 2 | 2 | |
| | C3 | 2 | 2 | |
| | C4 | 2 | 2 | |
| Elbow flexors | C5 | 2 | 2 | 5 |
| Wrist extensors | C6 | 2 | 2 | 5 |
| Elbow extensors | C7 | 2 | 2 | 5 |
| Finger flexors | C8 | 2 | 2 | 5 |
| Finger abductors (little finger) | T1 | 2 | 2 | 5 |
| | T2 | 2 | 2 | |
| | T3 | 2 | 2 | |
| | T4 | 2 | 2 | |
| | T5 | 2 | 2 | |
| | T6 | 2 | 2 | |
| | T7 | 2 | 2 | |
| | T8 | 2 | 2 | |
| | T9 | 2 | 2 | |
| | T10 | 2 | 0 | |
| | T11 | 1 | 0 | |
| | T12 | 0 | 0 | |
| | L1 | 0 | 0 | |
| Hip flexors compensate mvmt w/ hip rotation | L2 | 0 | 0 | 0 |
| Knee extensors | L3 | 0 | 0 | 0 |
| Ankle dorsiflexors | L4 | 0 | 0 | 0 |
| Long toe extensors abduction at hip | L5 | 0 | 0 | 0 |
| Ankle plantar flexors | S1 | 0 | 0 | 0 |
| | S2 | 0 | 0 | |
| | S3 | 0 | 0 | |
| | S4-5 | 0 | 0 | |
| LEFT TOTALS (MAXIMUM) | | 35 (56) | 34 (56) | 25 (50) |

UEL (Upper Extremity Left)

LEL (Lower Extremity Left)

MOTOR (SCORING ON REVERSE SIDE)

0 = Total paralysis
1 = Palpable or visible contraction
2 = Active movement, gravity eliminated
3 = Active movement, against gravity
4 = Active movement, against some resistance
5 = Active movement, against full resistance
NT = Not testable
0*, 1*, 2*, 3*, 4*, NT* = Non-SCI condition present

SENSORY (SCORING ON REVERSE SIDE)

0 = Absent
1 = Altered
2 = Normal
NT = Not testable
0*, 1*, NT* = Non-SCI condition present

(DAP) Deep Anal Pressure (Yes/No): No

**MOTOR SUBSCORES**

UER 25 (MAX 25) + UEL 25 (25) = UEMS TOTAL 50 (50)

LER 0 (MAX 25) + LEL 0 (25) = LEMS TOTAL 0 (50)

**SENSORY SUBSCORES**

LTR 34 (MAX 56) + LTL 35 (56) = LT TOTAL 69 (112)

PPR 35 (MAX 56) + PPL 34 (56) = PP TOTAL 69 (112)

| NEUROLOGICAL LEVELS (Steps 1- 6 for classification as on reverse) | R | L |
|---|---|---|
| 1. SENSORY | T10 | T9 |
| 2. MOTOR | T10 | T9 |

3. NEUROLOGICAL LEVEL OF INJURY (NLI): T9

4. COMPLETE OR INCOMPLETE? (Incomplete = Any sensory or motor function in S4-5): C

5. ASIA IMPAIRMENT SCALE (AIS): A

6. ZONE OF PARTIAL PRESERVATION (Most caudal levels with any innervation; In injuries with absent motor OR sensory function in S4-5 only)

| | R | L |
|---|---|---|
| SENSORY | T11 | T11 |
| MOTOR | T10 | T9 |

Page 1/2



REV 04/19

# P16

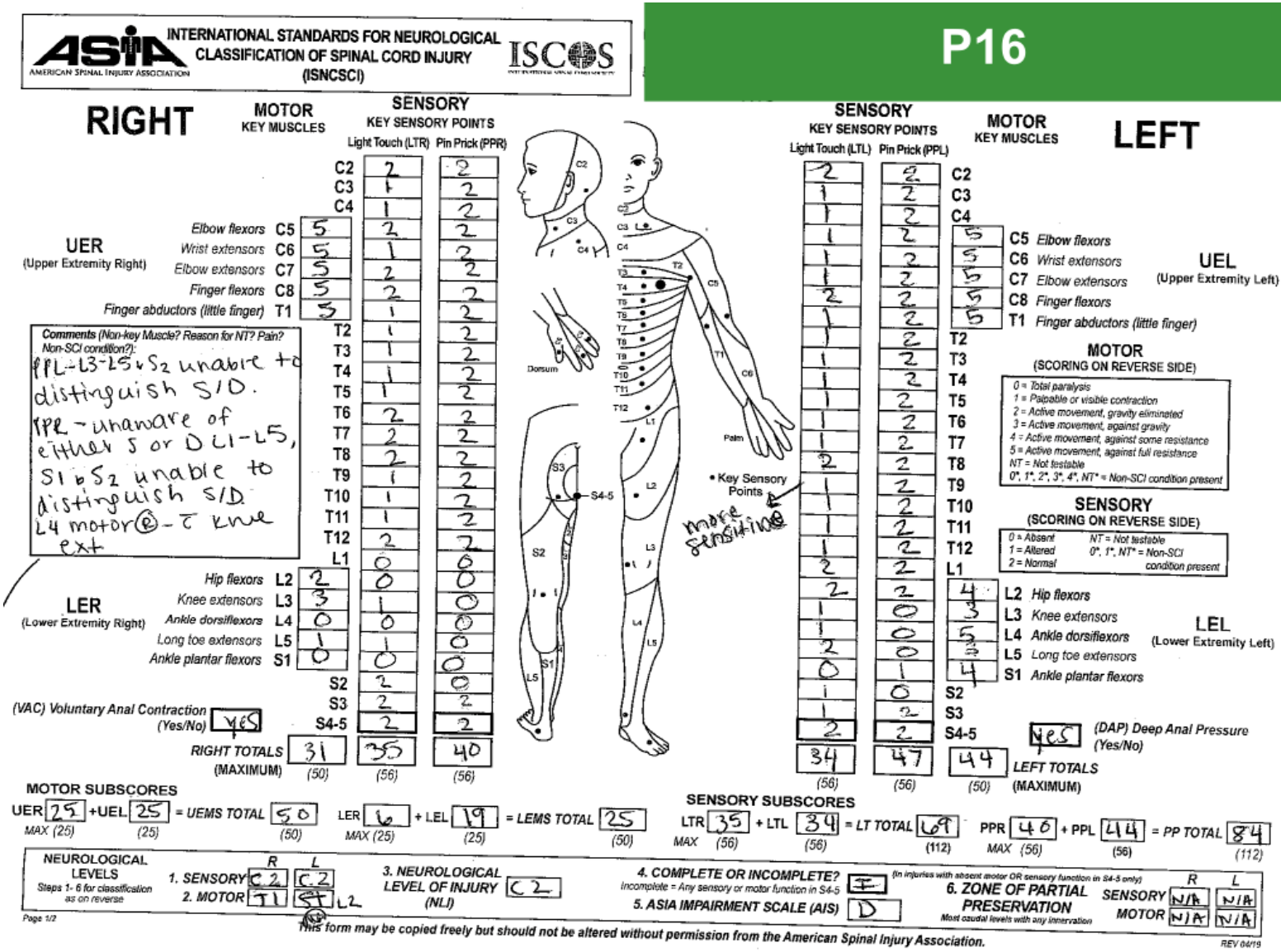

INTERNATIONAL STANDARDS FOR NEUROLOGICAL CLASSIFICATION OF SPINAL CORD INJURY (ISNCSCI)

AMERICAN SPINAL INJURY ASSOCIATION — ISCOS

## RIGHT

| | MOTOR KEY MUSCLES | | SENSORY KEY SENSORY POINTS Light Touch (LTR) | Pin Prick (PPR) |
|---|---|---|---|---|
| | | C2 | 2 | 2 |
| | | C3 | 1 | 2 |
| | | C4 | 1 | 2 |
| UER (Upper Extremity Right) | Elbow flexors | C5 | 5 | 2 |
| | Wrist extensors | C6 | 5 | 1 |
| | Elbow extensors | C7 | 5 | 2 |
| | Finger flexors | C8 | 5 | 2 |
| | Finger abductors (little finger) | T1 | 5 | 1 |
| | | T2 | 1 | 2 |
| | | T3 | 1 | 2 |
| | | T4 | 1 | 2 |
| | | T5 | 1 | 2 |
| | | T6 | 2 | 2 |
| | | T7 | 2 | 2 |
| | | T8 | 2 | 2 |
| | | T9 | 1 | 2 |
| | | T10 | 1 | 2 |
| | | T11 | 1 | 2 |
| | | T12 | 2 | 2 |
| | | L1 | 0 | 0 |
| LER (Lower Extremity Right) | Hip flexors | L2 | 2 | 0 |
| | Knee extensors | L3 | 3 | 0 |
| | Ankle dorsiflexors | L4 | 0 | 0 |
| | Long toe extensors | L5 | 1 | 0 |
| | Ankle plantar flexors | S1 | 0 | 0 |
| | | S2 | 2 | 0 |
| | | S3 | 2 | 2 |
| | | S4-5 | 2 | 2 |
| | RIGHT TOTALS (MAXIMUM) | | 35 (56) | 40 (56) |

Comments (Non-key Muscle? Reason for NT? Pain? Non-SCI condition?):
RPL-L3-L5 & S2 unable to distinguish S/D.
RPP - unaware of either S or D L1-L5, S1 & S2 unable to distinguish S/D
L4 motor ® - 2 knee ext

(VAC) Voluntary Anal Contraction (Yes/No): Yes




## LEFT

| | SENSORY KEY SENSORY POINTS Light Touch (LTL) | Pin Prick (PPL) | MOTOR KEY MUSCLES | |
|---|---|---|---|---|
| | 2 | 2 | C2 | |
| | 1 | 2 | C3 | |
| | 1 | 2 | C4 | |
| | 1 | 2 | C5 | Elbow flexors |
| | 1 | 2 | C6 | Wrist extensors |
| | 1 | 2 | C7 | Elbow extensors |
| | 2 | 2 | C8 | Finger flexors |
| | 1 | 2 | T1 | Finger abductors (little finger) |
| | 1 | 2 | T2 | |
| | 1 | 2 | T3 | |
| | 1 | 2 | T4 | |
| | 1 | 2 | T5 | |
| | 1 | 2 | T6 | |
| | 1 | 2 | T7 | |
| | 1 | 2 | T8 | |
| | 2 | 2 | T9 | |
| | 1 | 2 | T10 | |
| | 1 | 2 | T11 | |
| | 1 | 2 | T12 | |
| | 2 | 2 | L1 | |
| | 2 | 2 | L2 | Hip flexors |
| | 1 | 0 | L3 | Knee extensors |
| | 1 | 0 | L4 | Ankle dorsiflexors |
| | 2 | 0 | L5 | Long toe extensors |
| | 0 | 1 | S1 | Ankle plantar flexors |
| | 1 | 0 | S2 | |
| | 1 | 2 | S3 | |
| | 2 | 2 | S4-5 | |
| | 34 (56) | 47 (56) | LEFT TOTALS (MAXIMUM) | 44 (50) |

UEL (Upper Extremity Left)

LEL (Lower Extremity Left)

MOTOR (SCORING ON REVERSE SIDE)

0 = Total paralysis
1 = Palpable or visible contraction
2 = Active movement, gravity eliminated
3 = Active movement, against gravity
4 = Active movement, against some resistance
5 = Active movement, against full resistance
NT = Not testable
0*, 1*, 2*, 3*, 4*, NT* = Non-SCI condition present

SENSORY (SCORING ON REVERSE SIDE)

0 = Absent
1 = Altered
2 = Normal
NT = Not testable
0*, 1*, NT* = Non-SCI condition present

(DAP) Deep Anal Pressure (Yes/No): Yes

**MOTOR SUBSCORES**

UER 25 (MAX 25) + UEL 25 (25) = UEMS TOTAL 50 (50)

LER 6 (MAX 25) + LEL 19 (25) = LEMS TOTAL 25 (50)

**SENSORY SUBSCORES**

LTR 35 (MAX 56) + LTL 34 (56) = LT TOTAL 69 (112)

PPR 40 (MAX 56) + PPL 44 (56) = PP TOTAL 84 (112)

| NEUROLOGICAL LEVELS (Steps 1- 6 for classification as on reverse) | R | L |
|---|---|---|
| 1. SENSORY | C2 | C2 |
| 2. MOTOR | T1 | ST L2 |

3. NEUROLOGICAL LEVEL OF INJURY (NLI): C2

4. COMPLETE OR INCOMPLETE? (Incomplete = Any sensory or motor function in S4-5): I

5. ASIA IMPAIRMENT SCALE (AIS): D

6. ZONE OF PARTIAL PRESERVATION (Most caudal levels with any innervation) (In injuries with absent motor OR sensory function in S4-5 only)

| | R | L |
|---|---|---|
| SENSORY | N/A | N/A |
| MOTOR | N/A | N/A |

Page 1/2



REV 04/19

# P18

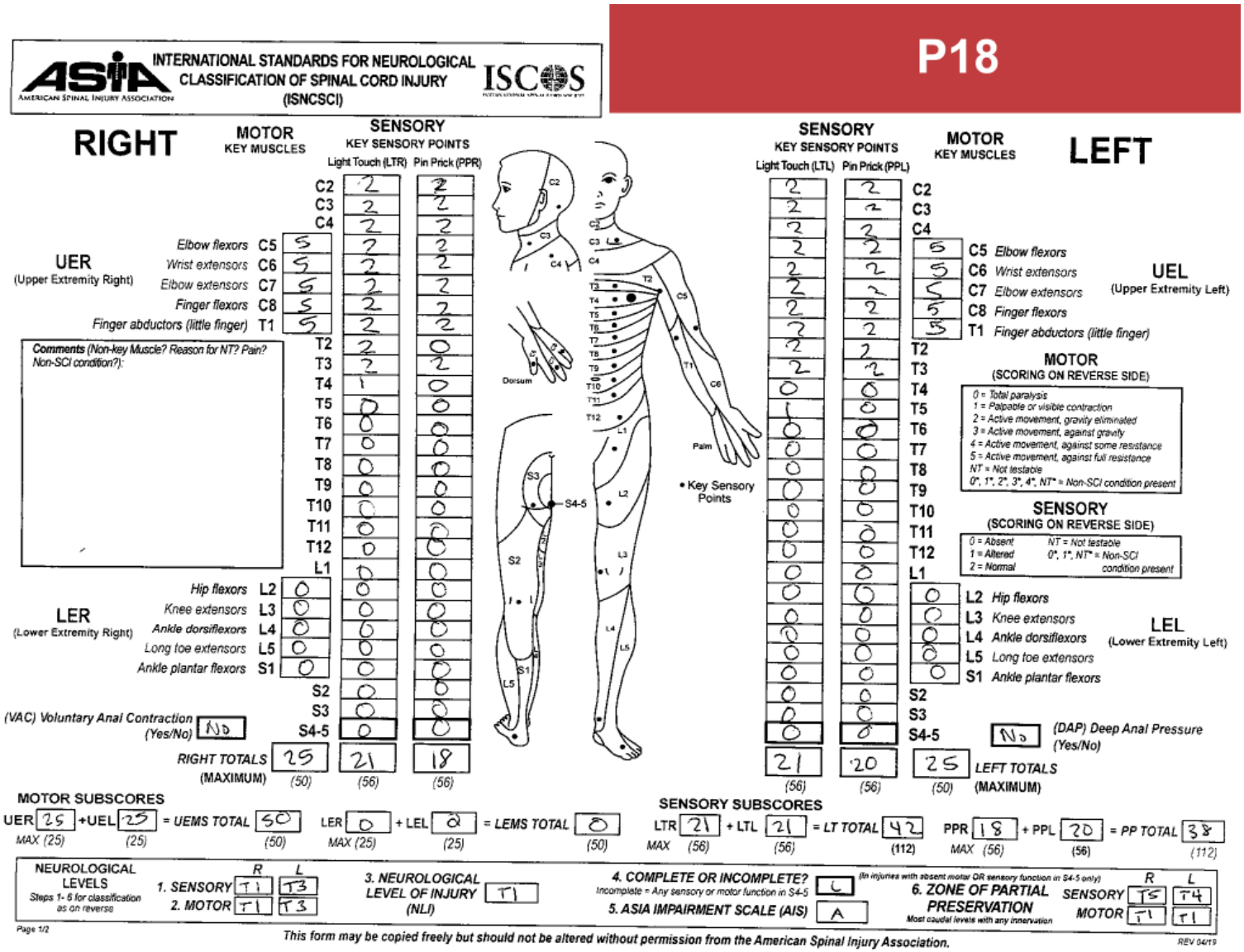

INTERNATIONAL STANDARDS FOR NEUROLOGICAL CLASSIFICATION OF SPINAL CORD INJURY (ISNCSCI)

AMERICAN SPINAL INJURY ASSOCIATION — ISCOS

## RIGHT

| | | MOTOR KEY MUSCLES | SENSORY KEY SENSORY POINTS Light Touch (LTR) | SENSORY KEY SENSORY POINTS Pin Prick (PPR) |
|---|---|---|---|---|
| | C2 | | 2 | 2 |
| | C3 | | 2 | 2 |
| | C4 | | 2 | 2 |
| Elbow flexors | C5 | 5 | 2 | 2 |
| Wrist extensors | C6 | 5 | 2 | 2 |
| Elbow extensors | C7 | 5 | 2 | 2 |
| Finger flexors | C8 | 5 | 2 | 2 |
| Finger abductors (little finger) | T1 | 5 | 2 | 2 |
| | T2 | | 2 | 0 |
| | T3 | | 2 | 0 |
| | T4 | | 1 | 0 |
| | T5 | | 0 | 0 |
| | T6 | | 0 | 0 |
| | T7 | | 0 | 0 |
| | T8 | | 0 | 0 |
| | T9 | | 0 | 0 |
| | T10 | | 0 | 0 |
| | T11 | | 0 | 0 |
| | T12 | | 0 | 0 |
| | L1 | | 0 | 0 |
| Hip flexors | L2 | 0 | 0 | 0 |
| Knee extensors | L3 | 0 | 0 | 0 |
| Ankle dorsiflexors | L4 | 0 | 0 | 0 |
| Long toe extensors | L5 | 0 | 0 | 0 |
| Ankle plantar flexors | S1 | 0 | 0 | 0 |
| | S2 | | 0 | 0 |
| | S3 | | 0 | 0 |
| | S4-5 | | 0 | 0 |
| RIGHT TOTALS (MAXIMUM) | | 25 (50) | 21 (56) | 18 (56) |

UER (Upper Extremity Right)

LER (Lower Extremity Right)

Comments (Non-key Muscle? Reason for NT? Pain? Non-SCI condition?):

(VAC) Voluntary Anal Contraction (Yes/No): No

• Key Sensory Points

## LEFT

| | | SENSORY KEY SENSORY POINTS Light Touch (LTL) | SENSORY KEY SENSORY POINTS Pin Prick (PPL) | MOTOR KEY MUSCLES | |
|---|---|---|---|---|---|
| | C2 | 2 | 2 | | |
| | C3 | 2 | 2 | | |
| | C4 | 2 | 2 | | |
| | C5 | 2 | 2 | 5 | Elbow flexors |
| | C6 | 2 | 2 | 5 | Wrist extensors |
| | C7 | 2 | 2 | 5 | Elbow extensors |
| | C8 | 2 | 2 | 5 | Finger flexors |
| | T1 | 2 | 2 | 5 | Finger abductors (little finger) |
| | T2 | 2 | 0 | | |
| | T3 | 1 | 0 | | |
| | T4 | 0 | 0 | | |
| | T5 | 0 | 0 | | |
| | T6 | 0 | 0 | | |
| | T7 | 0 | 0 | | |
| | T8 | 0 | 0 | | |
| | T9 | 0 | 0 | | |
| | T10 | 0 | 0 | | |
| | T11 | 0 | 0 | | |
| | T12 | 0 | 0 | | |
| | L1 | 0 | 0 | | |
| | L2 | 0 | 0 | 0 | Hip flexors |
| | L3 | 0 | 0 | 0 | Knee extensors |
| | L4 | 0 | 0 | 0 | Ankle dorsiflexors |
| | L5 | 0 | 0 | 0 | Long toe extensors |
| | S1 | 0 | 0 | 0 | Ankle plantar flexors |
| | S2 | 0 | 0 | | |
| | S3 | 0 | 0 | | |
| | S4-5 | 0 | 0 | | |
| LEFT TOTALS (MAXIMUM) | | 21 (56) | 20 (56) | 25 (50) | |

UEL (Upper Extremity Left)

LEL (Lower Extremity Left)

(DAP) Deep Anal Pressure (Yes/No): No

**MOTOR (SCORING ON REVERSE SIDE)**

0 = Total paralysis
1 = Palpable or visible contraction
2 = Active movement, gravity eliminated
3 = Active movement, against gravity
4 = Active movement, against some resistance
5 = Active movement, against full resistance
NT = Not testable
0*, 1*, 2*, 3*, 4*, NT* = Non-SCI condition present

**SENSORY (SCORING ON REVERSE SIDE)**

0 = Absent
1 = Altered
2 = Normal
NT = Not testable
0*, 1*, NT* = Non-SCI condition present

**MOTOR SUBSCORES**

UER 25 + UEL 25 = UEMS TOTAL 50 (MAX (25) (25) (50))

LER 0 + LEL 0 = LEMS TOTAL 0 (MAX (25) (25) (50))

**SENSORY SUBSCORES**

LTR 21 + LTL 21 = LT TOTAL 42 (MAX (56) (56) (112))

PPR 18 + PPL 20 = PP TOTAL 38 (MAX (56) (56) (112))

| | R | L |
|---|---|---|
| NEUROLOGICAL LEVELS (Steps 1- 5 for classification as on reverse) | | |
| 1. SENSORY | T1 | T3 |
| 2. MOTOR | T1 | T3 |

3. NEUROLOGICAL LEVEL OF INJURY (NLI): T1

4. COMPLETE OR INCOMPLETE? (In injuries with absent motor OR sensory function in S4-5 only): C
Incomplete = Any sensory or motor function in S4-5

5. ASIA IMPAIRMENT SCALE (AIS): A

6. ZONE OF PARTIAL PRESERVATION (Most caudal levels with any innervation)

| | R | L |
|---|---|---|
| SENSORY | T5 | T4 |
| MOTOR | T1 | T1 |

Page 1/2



REV 04/19

# P23

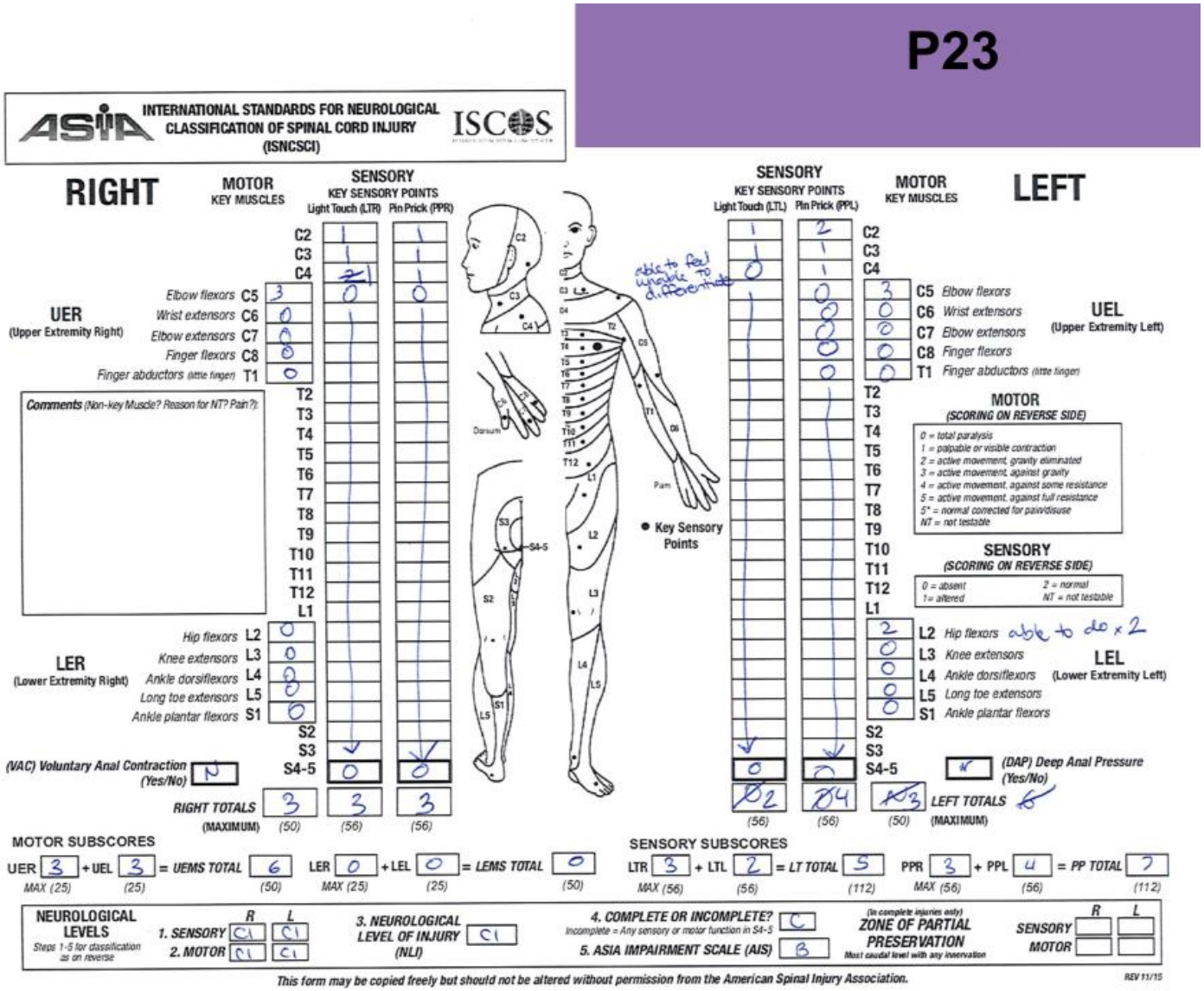

INTERNATIONAL STANDARDS FOR NEUROLOGICAL CLASSIFICATION OF SPINAL CORD INJURY (ISNCSCI)

ISCOS

## RIGHT

| | MOTOR KEY MUSCLES | SENSORY KEY SENSORY POINTS Light Touch (LTR) | Pin Prick (PPR) |
|---|---|---|---|
| C2 | | 1 | 1 |
| C3 | | 1 | 1 |
| C4 | | 2 | 1 |
| C5 | Elbow flexors 3 | 0 | 0 |
| C6 | Wrist extensors 0 | 1 | 1 |
| C7 | Elbow extensors 0 | 1 | 1 |
| C8 | Finger flexors 0 | 1 | 1 |
| T1 | Finger abductors (little finger) 0 | 1 | 1 |
| T2 | | 1 | 1 |
| T3 | | 1 | 1 |
| T4 | | 1 | 1 |
| T5 | | 1 | 1 |
| T6 | | 1 | 1 |
| T7 | | 1 | 1 |
| T8 | | 1 | 1 |
| T9 | | 1 | 1 |
| T10 | | 1 | 1 |
| T11 | | 1 | 1 |
| T12 | | 1 | 1 |
| L1 | | 1 | 1 |
| L2 | Hip flexors 0 | 1 | 1 |
| L3 | Knee extensors 0 | 1 | 1 |
| L4 | Ankle dorsiflexors 0 | 1 | 1 |
| L5 | Long toe extensors 0 | 1 | 1 |
| S1 | Ankle plantar flexors 0 | 1 | 1 |
| S2 | | 1 | 1 |
| S3 | | 1 | 1 |
| S4-5 | | 0 | 0 |
| | RIGHT TOTALS (MAXIMUM) | 3 (50) | 3 (56) | 3 (56) |

UER (Upper Extremity Right)

LER (Lower Extremity Right)

Comments (Non-key Muscle? Reason for NT? Pain?):

(VAC) Voluntary Anal Contraction (Yes/No): N

## LEFT

| | SENSORY KEY SENSORY POINTS Light Touch (LTL) | Pin Prick (PPL) | MOTOR KEY MUSCLES |
|---|---|---|---|
| C2 | 1 | 2 | |
| C3 | 1 | 1 | |
| C4 | 0 | 1 | |
| C5 | 1 | 0 | Elbow flexors 3 |
| C6 | 1 | 0 | Wrist extensors 0 |
| C7 | 1 | 0 | Elbow extensors 0 |
| C8 | 1 | 0 | Finger flexors 0 |
| T1 | 1 | 0 | Finger abductors (little finger) 0 |
| T2 | 1 | 1 | |
| T3 | 1 | 1 | |
| T4 | 1 | 1 | |
| T5 | 1 | 1 | |
| T6 | 1 | 1 | |
| T7 | 1 | 1 | |
| T8 | 1 | 1 | |
| T9 | 1 | 1 | |
| T10 | 1 | 1 | |
| T11 | 1 | 1 | |
| T12 | 1 | 1 | |
| L1 | 1 | 1 | |
| L2 | 1 | 1 | Hip flexors able to do x 2 |
| L3 | 1 | 1 | Knee extensors 0 |
| L4 | 1 | 1 | Ankle dorsiflexors 0 |
| L5 | 1 | 1 | Long toe extensors 0 |
| S1 | 1 | 1 | Ankle plantar flexors 0 |
| S2 | 1 | 1 | |
| S3 | 1 | 1 | |
| S4-5 | 0 | 0 | |
| | 02 | 04 | 03 |
| | (56) | (56) | (50) |

UEL (Upper Extremity Left)

LEL (Lower Extremity Left)

able to feel unable to differentiate

Key Sensory Points

MOTOR (SCORING ON REVERSE SIDE)

0 = total paralysis
1 = palpable or visible contraction
2 = active movement, gravity eliminated
3 = active movement, against gravity
4 = active movement, against some resistance
5 = active movement, against full resistance
5* = normal corrected for pain/disuse
NT = not testable

SENSORY (SCORING ON REVERSE SIDE)

0 = absent
1 = altered
2 = normal
NT = not testable

NT (DAP) Deep Anal Pressure (Yes/No)

LEFT TOTALS (MAXIMUM) 6

### MOTOR SUBSCORES

UER 3 (MAX 25) + UEL 3 (25) = UEMS TOTAL 6 (50)

LER 0 (MAX 25) + LEL 0 (25) = LEMS TOTAL 0 (50)

### SENSORY SUBSCORES

LTR 3 (MAX 56) + LTL 2 (56) = LT TOTAL 5 (112)

PPR 3 (MAX 56) + PPL 4 (56) = PP TOTAL 7 (112)

### NEUROLOGICAL LEVELS

Steps 1-5 for classification as on reverse

| | R | L |
|---|---|---|
| 1. SENSORY | C1 | C1 |
| 2. MOTOR | C1 | C1 |

3. NEUROLOGICAL LEVEL OF INJURY (NLI): C1

4. COMPLETE OR INCOMPLETE? C
Incomplete = Any sensory or motor function in S4-5

5. ASIA IMPAIRMENT SCALE (AIS): B

ZONE OF PARTIAL PRESERVATION (In complete injuries only)
Most caudal level with any innervation

| | R | L |
|---|---|---|
| SENSORY | | |
| MOTOR | | |



REV 11/15

# P24

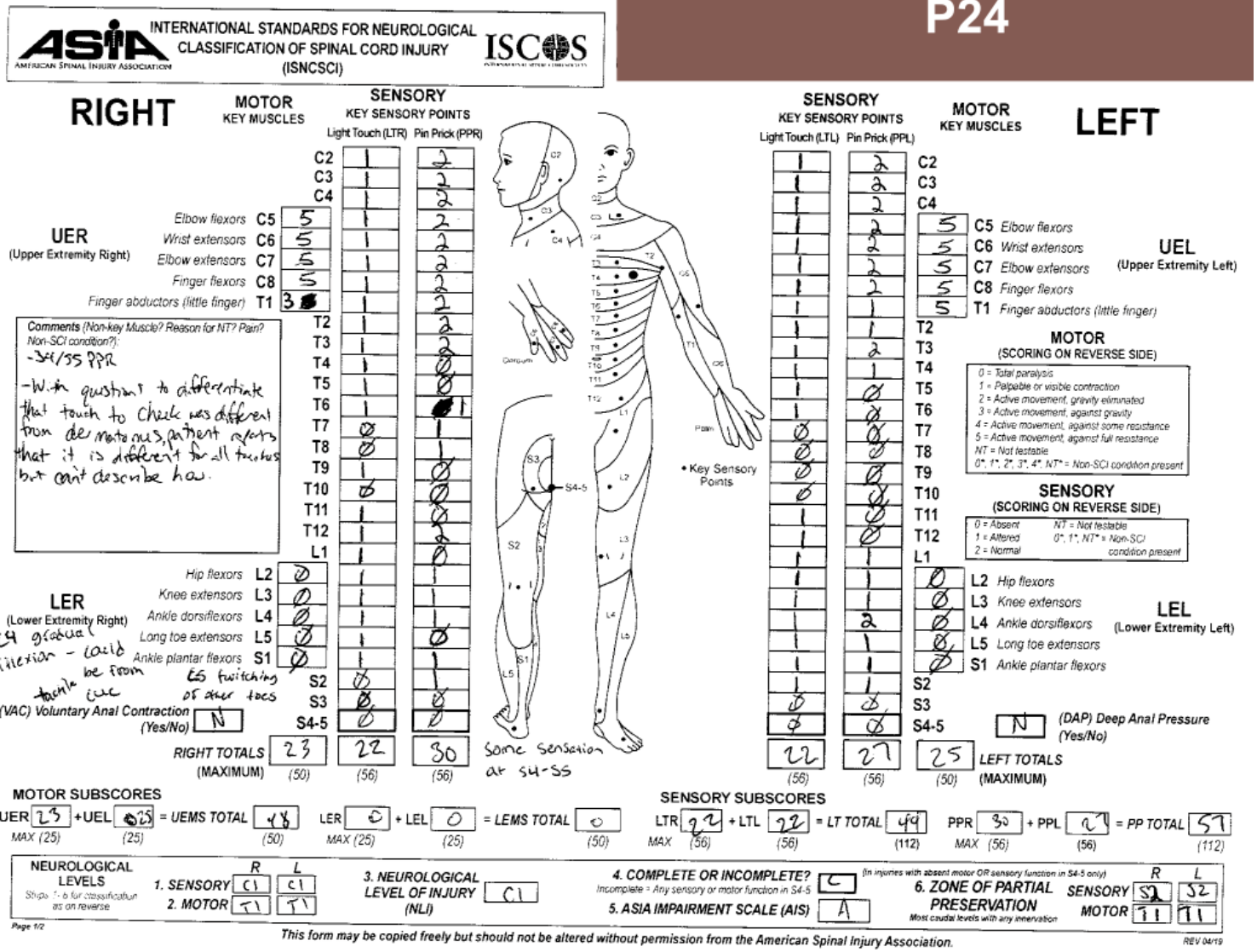

INTERNATIONAL STANDARDS FOR NEUROLOGICAL CLASSIFICATION OF SPINAL CORD INJURY (ISNCSCI)

AMERICAN SPINAL INJURY ASSOCIATION

ISCOS

## RIGHT

| | MOTOR KEY MUSCLES | | SENSORY KEY SENSORY POINTS Light Touch (LTR) | Pin Prick (PPR) |
|---|---|---|---|---|
| | | C2 | 2 | 2 |
| | | C3 | 2 | 2 |
| | | C4 | 2 | 2 |
| UER (Upper Extremity Right) | Elbow flexors | C5 | 5 | 2 |
| | Wrist extensors | C6 | 5 | 2 |
| | Elbow extensors | C7 | 5 | 2 |
| | Finger flexors | C8 | 5 | 2 |
| | Finger abductors (little finger) | T1 | 3 | 2 |
| | | T2 | 2 | 2 |
| | | T3 | 2 | 2 |
| | | T4 | 2 | 2 |
| | | T5 | 2 | 2 |
| | | T6 | 2 | 1 |
| | | T7 | 0 | 0 |
| | | T8 | 0 | 0 |
| | | T9 | 1 | 0 |
| | | T10 | 0 | 0 |
| | | T11 | 1 | 0 |
| | | T12 | 1 | 0 |
| | | L1 | 1 | 0 |
| LER (Lower Extremity Right) | Hip flexors | L2 | 0 | 1 |
| | Knee extensors | L3 | 0 | 1 |
| | Ankle dorsiflexors | L4 | 0 | 0 |
| | Long toe extensors | L5 | 0 | 1 |
| | Ankle plantar flexors | S1 | 0 | 1 |
| | | S2 | 0 | 1 |
| | | S3 | 0 | 1 |
| | | S4-5 | 0 | 0 |
| | RIGHT TOTALS (MAXIMUM) | | 23 (50) | 22 (56) | 30 (56) |

Comments (Non-key Muscle? Reason for NT? Pain? Non-SCI condition?):
-34/35 PPR
-With question to differentiate that touch to cheek was different from dermatomes, patient reports that it is different for all touches but can't describe how.

L4 grade ( dorsiflexion - could be from tactile input

ES twitching of other toes

(VAC) Voluntary Anal Contraction (Yes/No) N

Some sensation at S4-5S

• Key Sensory Points

## LEFT

| | SENSORY KEY SENSORY POINTS Light Touch (LTL) | Pin Prick (PPL) | MOTOR KEY MUSCLES | |
|---|---|---|---|---|
| | | | C2 | |
| | | | C3 | |
| | | | C4 | |
| UEL (Upper Extremity Left) | | | C5 | Elbow flexors |
| | | | C6 | Wrist extensors |
| | | | C7 | Elbow extensors |
| | | | C8 | Finger flexors |
| | | | T1 | Finger abductors (little finger) |
| | | | T2 | |
| | | | T3 | |
| | | | T4 | |
| | | | T5 | |
| | | | T6 | |
| | | | T7 | |
| | | | T8 | |
| | | | T9 | |
| | | | T10 | |
| | | | T11 | |
| | | | T12 | |
| | | | L1 | |
| LEL (Lower Extremity Left) | | | L2 | Hip flexors |
| | | | L3 | Knee extensors |
| | | | L4 | Ankle dorsiflexors |
| | | | L5 | Long toe extensors |
| | | | S1 | Ankle plantar flexors |
| | | | S2 | |
| | | | S3 | |
| | | | S4-5 | |
| | 22 (56) | 27 (56) | 25 (50) | LEFT TOTALS (MAXIMUM) |

**MOTOR (SCORING ON REVERSE SIDE)**

0 = Total paralysis
1 = Palpable or visible contraction
2 = Active movement, gravity eliminated
3 = Active movement, against gravity
4 = Active movement, against some resistance
5 = Active movement, against full resistance
NT = Not testable
0*, 1*, 2*, 3*, 4*, NT* = Non-SCI condition present

**SENSORY (SCORING ON REVERSE SIDE)**

0 = Absent, 1 = Altered, 2 = Normal, NT = Not testable, 0*, 1*, NT* = Non-SCI condition present

N (DAP) Deep Anal Pressure (Yes/No)

**MOTOR SUBSCORES**

UER 23 (MAX 25) + UEL 25 (25) = UEMS TOTAL 48 (50)

LER 0 (MAX 25) + LEL 0 (25) = LEMS TOTAL 0 (50)

**SENSORY SUBSCORES**

LTR 22 (MAX 56) + LTL 22 (56) = LT TOTAL 44 (112)

PPR 30 (MAX 56) + PPL 27 (56) = PP TOTAL 57 (112)

| | R | L |
|---|---|---|
| NEUROLOGICAL LEVELS (Strips 1 - 6 for classification as on reverse) | | |
| 1. SENSORY | C1 | C1 |
| 2. MOTOR | T1 | T1 |

3. NEUROLOGICAL LEVEL OF INJURY (NLI): C1

4. COMPLETE OR INCOMPLETE? C (In injuries with absent motor OR sensory function in S4-5 only)
Incomplete = Any sensory or motor function in S4-5

5. ASIA IMPAIRMENT SCALE (AIS): A

6. ZONE OF PARTIAL PRESERVATION (Most caudal levels with any innervation)

| | R | L |
|---|---|---|
| SENSORY | S2 | S2 |
| MOTOR | T1 | T1 |

Page 1/2



REV 04/19

# P34

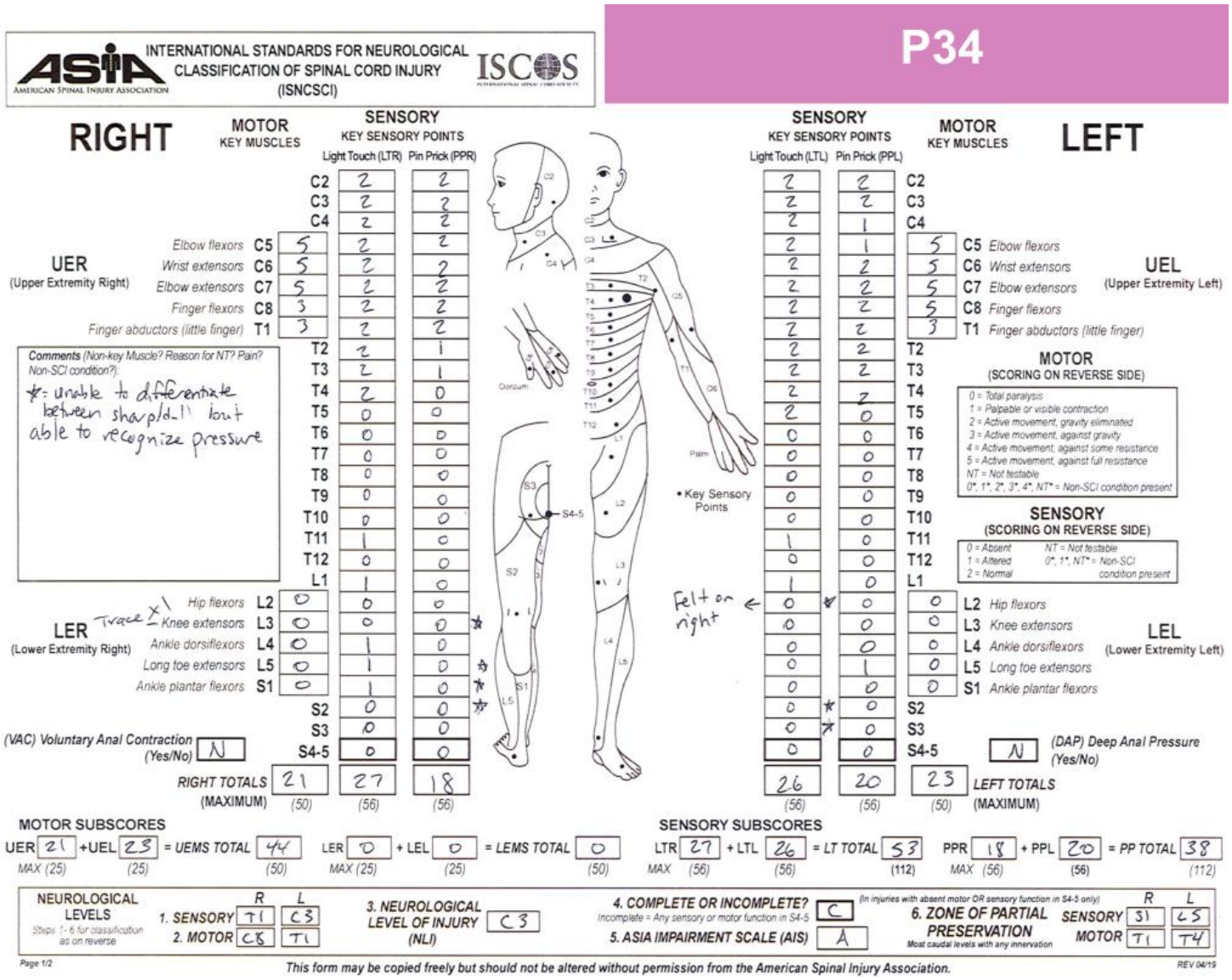

INTERNATIONAL STANDARDS FOR NEUROLOGICAL CLASSIFICATION OF SPINAL CORD INJURY (ISNCSCI)

ASIA American Spinal Injury Association — ISCOS International Spinal Cord Society

## RIGHT

| | | MOTOR KEY MUSCLES | SENSORY KEY SENSORY POINTS Light Touch (LTR) | SENSORY KEY SENSORY POINTS Pin Prick (PPR) |
|---|---|---|---|---|
| | C2 | | 2 | 2 |
| | C3 | | 2 | 2 |
| | C4 | | 2 | 2 |
| Elbow flexors | C5 | 5 | 2 | 2 |
| Wrist extensors | C6 | 5 | 2 | 2 |
| Elbow extensors | C7 | 5 | 2 | 2 |
| Finger flexors | C8 | 3 | 2 | 2 |
| Finger abductors (little finger) | T1 | 3 | 2 | 2 |
| | T2 | | 2 | 1 |
| | T3 | | 2 | 1 |
| | T4 | | 2 | 0 |
| | T5 | | 0 | 0 |
| | T6 | | 0 | 0 |
| | T7 | | 0 | 0 |
| | T8 | | 0 | 0 |
| | T9 | | 0 | 0 |
| | T10 | | 0 | 0 |
| | T11 | | 1 | 0 |
| | T12 | | 0 | 0 |
| | L1 | | 1 | 0 |
| Hip flexors | L2 | 0 | 0 | 0 |
| Knee extensors | L3 | 0 | 0 | 0 ★ |
| Ankle dorsiflexors | L4 | 0 | 1 | 0 |
| Long toe extensors | L5 | 0 | 1 | 0 ★ |
| Ankle plantar flexors | S1 | 0 | 1 | 0 ★ |
| | S2 | | 0 | 0 |
| | S3 | | 0 | 0 |
| | S4-5 | | 0 | 0 |
| RIGHT TOTALS (MAXIMUM) | | 21 (50) | 27 (56) | 18 (56) |

UER (Upper Extremity Right)

LER (Lower Extremity Right)

Comments (Non-key Muscle? Reason for NT? Pain? Non-SCI condition?):
★ = unable to differentiate between sharp/dull but able to recognize pressure

(VAC) Voluntary Anal Contraction (Yes/No): N

## LEFT

| | | SENSORY KEY SENSORY POINTS Light Touch (LTL) | SENSORY KEY SENSORY POINTS Pin Prick (PPL) | MOTOR KEY MUSCLES |
|---|---|---|---|---|
| | C2 | 2 | 2 | |
| | C3 | 2 | 2 | |
| | C4 | 2 | 1 | |
| Elbow flexors | C5 | 2 | 1 | 5 |
| Wrist extensors | C6 | 2 | 2 | 5 |
| Elbow extensors | C7 | 2 | 2 | 5 |
| Finger flexors | C8 | 2 | 2 | 5 |
| Finger abductors (little finger) | T1 | 2 | 2 | 3 |
| | T2 | 2 | 2 | |
| | T3 | 2 | 2 | |
| | T4 | 2 | 2 | |
| | T5 | 2 | 0 | |
| | T6 | 0 | 0 | |
| | T7 | 0 | 0 | |
| | T8 | 0 | 0 | |
| | T9 | 0 | 0 | |
| | T10 | 0 | 0 | |
| | T11 | 1 | 0 | |
| | T12 | 0 | 0 | |
| | L1 | 1 | 0 | |
| Hip flexors | L2 | 0 ★ | 0 | 0 |
| Knee extensors | L3 | 0 | 0 | 0 |
| Ankle dorsiflexors | L4 | 0 | 0 | 0 |
| Long toe extensors | L5 | 0 | 1 | 0 |
| Ankle plantar flexors | S1 | 0 | 0 | 0 |
| | S2 | 0 ★ | 0 | |
| | S3 | 0 ★ | 0 | |
| | S4-5 | 0 | 0 | |
| LEFT TOTALS (MAXIMUM) | | 26 (56) | 20 (56) | 23 (50) |

UEL (Upper Extremity Left)

LEL (Lower Extremity Left)

Felt on right ←

• Key Sensory Points

(DAP) Deep Anal Pressure (Yes/No): N

### MOTOR (SCORING ON REVERSE SIDE)

0 = Total paralysis
1 = Palpable or visible contraction
2 = Active movement, gravity eliminated
3 = Active movement, against gravity
4 = Active movement, against some resistance
5 = Active movement, against full resistance
NT = Not testable
0*, 1*, 2*, 3*, 4*, NT* = Non-SCI condition present

### SENSORY (SCORING ON REVERSE SIDE)

0 = Absent
1 = Altered
2 = Normal
NT = Not testable
0*, 1*, NT* = Non-SCI condition present

### MOTOR SUBSCORES

UER 21 + UEL 23 = UEMS TOTAL 44 (MAX (25) (25) (50))

LER 0 + LEL 0 = LEMS TOTAL 0 (MAX (25) (25) (50))

### SENSORY SUBSCORES

LTR 27 + LTL 26 = LT TOTAL 53 (MAX (56) (56) (112))

PPR 18 + PPL 20 = PP TOTAL 38 (MAX (56) (56) (112))

### NEUROLOGICAL LEVELS

Steps 1 - 6 for classification as on reverse

| | R | L |
|---|---|---|
| 1. SENSORY | T1 | C3 |
| 2. MOTOR | C5 | T1 |

3. NEUROLOGICAL LEVEL OF INJURY (NLI): C3

4. COMPLETE OR INCOMPLETE? C
Incomplete = Any sensory or motor function in S4-5

5. ASIA IMPAIRMENT SCALE (AIS): A

(In injuries with absent motor OR sensory function in S4-5 only)

6. ZONE OF PARTIAL PRESERVATION
Most caudal levels with any innervation

| | R | L |
|---|---|---|
| SENSORY | S1 | C5 |
| MOTOR | T1 | T4 |

Page 1/2



REV 04/19

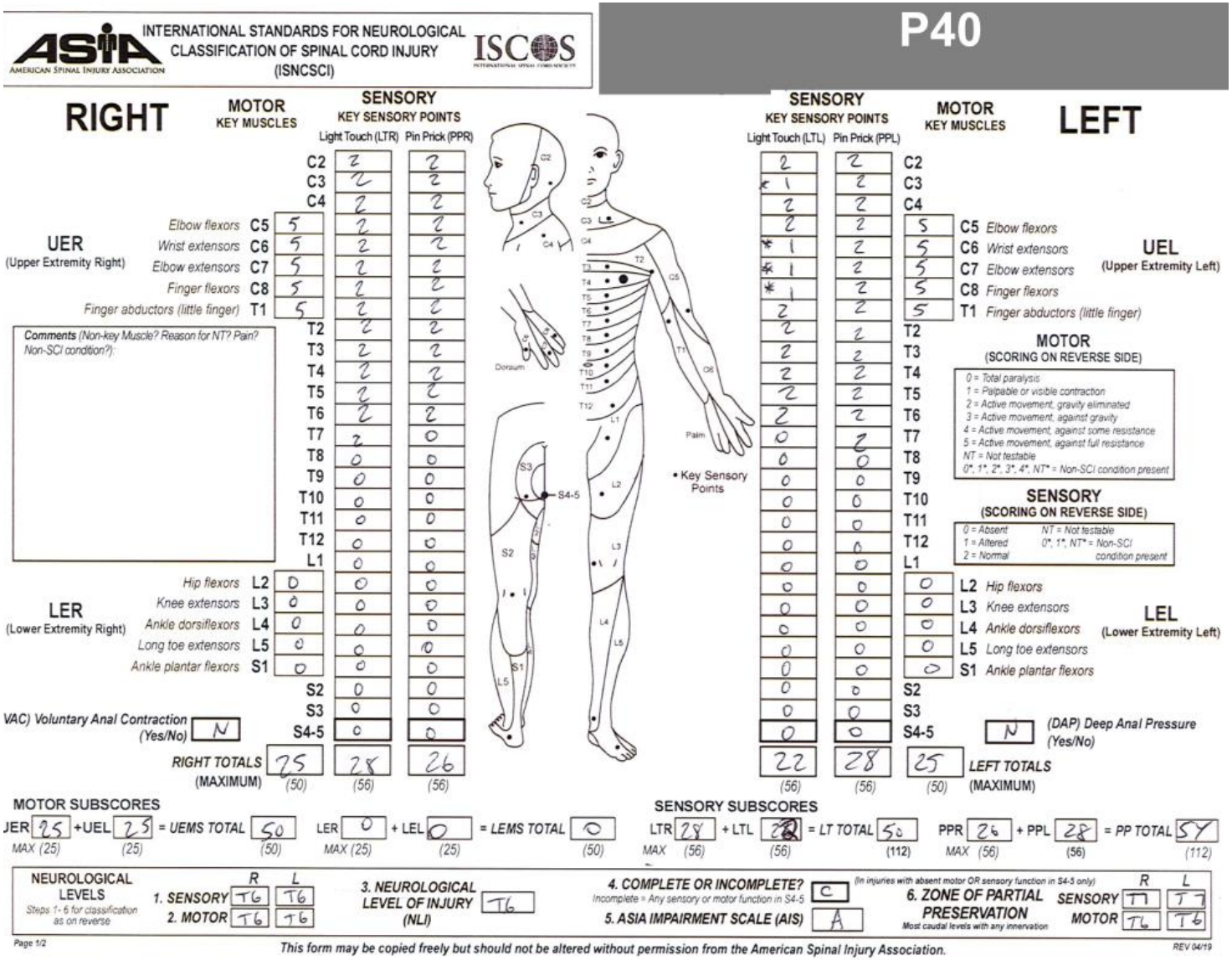

INTERNATIONAL STANDARDS FOR NEUROLOGICAL CLASSIFICATION OF SPINAL CORD INJURY (ISNCSCI)

AMERICAN SPINAL INJURY ASSOCIATION

ISCOS

## RIGHT

| | MOTOR KEY MUSCLES | | SENSORY KEY SENSORY POINTS Light Touch (LTR) | Pin Prick (PPR) |
|---|---|---|---|---|
| C2 | | | 2 | 2 |
| C3 | | | 2 | 2 |
| C4 | | | 2 | 2 |
| C5 | Elbow flexors | 5 | 2 | 2 |
| C6 | Wrist extensors | 5 | 2 | 2 |
| C7 | Elbow extensors | 5 | 2 | 2 |
| C8 | Finger flexors | 5 | 2 | 2 |
| T1 | Finger abductors (little finger) | 5 | 2 | 2 |
| T2 | | | 2 | 2 |
| T3 | | | 2 | 2 |
| T4 | | | 2 | 2 |
| T5 | | | 2 | 2 |
| T6 | | | 2 | 2 |
| T7 | | | 2 | 0 |
| T8 | | | 0 | 0 |
| T9 | | | 0 | 0 |
| T10 | | | 0 | 0 |
| T11 | | | 0 | 0 |
| T12 | | | 0 | 0 |
| L1 | | | 0 | 0 |
| L2 | Hip flexors | 0 | 0 | 0 |
| L3 | Knee extensors | 0 | 0 | 0 |
| L4 | Ankle dorsiflexors | 0 | 0 | 0 |
| L5 | Long toe extensors | 0 | 0 | 0 |
| S1 | Ankle plantar flexors | 0 | 0 | 0 |
| S2 | | | 0 | 0 |
| S3 | | | 0 | 0 |
| S4-5 | | | 0 | 0 |

UER (Upper Extremity Right)

LER (Lower Extremity Right)

Comments (Non-key Muscle? Reason for NT? Pain? Non-SCI condition?):

VAC) Voluntary Anal Contraction (Yes/No): N

RIGHT TOTALS (MAXIMUM): 25 (50) | 28 (56) | 26 (56)

• Key Sensory Points

## LEFT

| | SENSORY KEY SENSORY POINTS Light Touch (LTL) | Pin Prick (PPL) | MOTOR KEY MUSCLES | |
|---|---|---|---|---|
| C2 | 2 | 2 | | |
| C3 | 1 | 2 | | |
| C4 | 2 | 2 | | |
| C5 | 2 | 2 | 5 | Elbow flexors |
| C6 | 1 | 2 | 5 | Wrist extensors |
| C7 | 1 | 2 | 5 | Elbow extensors |
| C8 | 1 | 2 | 5 | Finger flexors |
| T1 | 2 | 2 | 5 | Finger abductors (little finger) |
| T2 | 2 | 2 | | |
| T3 | 2 | 2 | | |
| T4 | 2 | 2 | | |
| T5 | 2 | 2 | | |
| T6 | 2 | 2 | | |
| T7 | 0 | 2 | | |
| T8 | 0 | 0 | | |
| T9 | 0 | 0 | | |
| T10 | 0 | 0 | | |
| T11 | 0 | 0 | | |
| T12 | 0 | 0 | | |
| L1 | 0 | 0 | | |
| L2 | 0 | 0 | 0 | Hip flexors |
| L3 | 0 | 0 | 0 | Knee extensors |
| L4 | 0 | 0 | 0 | Ankle dorsiflexors |
| L5 | 0 | 0 | 0 | Long toe extensors |
| S1 | 0 | 0 | 0 | Ankle plantar flexors |
| S2 | 0 | 0 | | |
| S3 | 0 | 0 | | |
| S4-5 | 0 | 0 | | |

UEL (Upper Extremity Left)

LEL (Lower Extremity Left)

MOTOR (SCORING ON REVERSE SIDE)

0 = Total paralysis
1 = Palpable or visible contraction
2 = Active movement, gravity eliminated
3 = Active movement, against gravity
4 = Active movement, against some resistance
5 = Active movement, against full resistance
NT = Not testable
0*, 1*, 2*, 3*, 4*, NT* = Non-SCI condition present

SENSORY (SCORING ON REVERSE SIDE)

0 = Absent
1 = Altered
2 = Normal
NT = Not testable
0*, 1*, NT* = Non-SCI condition present

N (DAP) Deep Anal Pressure (Yes/No)

LEFT TOTALS (MAXIMUM): 22 (56) | 28 (56) | 25 (50)

### MOTOR SUBSCORES

UER 25 (MAX 25) + UEL 25 (25) = UEMS TOTAL 50 (50)

LER 0 (MAX 25) + LEL 0 (25) = LEMS TOTAL 0 (50)

### SENSORY SUBSCORES

LTR 28 (MAX 56) + LTL 28 (56) = LT TOTAL 56 (112)

PPR 28 (MAX 56) + PPL 28 (56) = PP TOTAL 56 (112)

| NEUROLOGICAL LEVELS (Steps 1 - 6 for classification as on reverse) | R | L |
|---|---|---|
| 1. SENSORY | T6 | T6 |
| 2. MOTOR | T6 | T6 |

3. NEUROLOGICAL LEVEL OF INJURY (NLI): T6

4. COMPLETE OR INCOMPLETE? (Incomplete = Any sensory or motor function in S4-5): C

5. ASIA IMPAIRMENT SCALE (AIS): A

(In injuries with absent motor OR sensory function in S4-5 only)

6. ZONE OF PARTIAL PRESERVATION (Most caudal levels with any innervation)

| | R | L |
|---|---|---|
| SENSORY | T1 | T1 |
| MOTOR | T6 | T6 |

Page 1/2



REV 04/19

# P204

**INTERNATIONAL STANDARDS FOR NEUROLOGICAL CLASSIFICATION OF SPINAL CORD INJURY (ISNCSCI)**

ASIA — American Spinal Injury Association

ISCOS — International Spinal Cord Society

## RIGHT

| | MOTOR KEY MUSCLES | | SENSORY KEY SENSORY POINTS Light Touch (LTR) | Pin Prick (PPR) |
|---|---|---|---|---|
| | | C2 | 2 | 2 |
| | | C3 | 2 | 2 |
| | | C4 | 2 | 2 |
| UER (Upper Extremity Right) | Elbow flexors | C5 | 5 | 2 |
| | Wrist extensors | C6 | 5 | 2 |
| | Elbow extensors | C7 | 5 | 2 |
| | Finger flexors | C8 | 5 | 2 |
| | Finger abductors (little finger) | T1 | 5 | 2 |
| | | T2 | 2 | 2 |
| | | T3 | 2 | 2 |
| | | T4 | 2 | 2 |
| | | T5 | 2 | 2 |
| | | T6 | 2 | 2 |
| | | T7 | 2 | 2 |
| | | T8 | 2 | 2 |
| | | T9 | 2 | 2 |
| | | T10 | 2 | 2 |
| | | T11 | 2 | 2 |
| | | T12 | 2 | 2 |
| | | L1 | 1 | 0 |
| LER (Lower Extremity Right) | Hip flexors | L2 | 1 | 0 |
| | Knee extensors | L3 | 0 | 0 |
| | Ankle dorsiflexors | L4 | 0 | 0 |
| | Long toe extensors | L5 | 0 | 0 |
| | Ankle plantar flexors | S1 | 0 | 0 |
| | | S2 | 0 | 0 |
| | | S3 | 0 | 0 |
| | | S4-5 | 0 | 0 |
| | RIGHT TOTALS (MAXIMUM) | | 26 (50) | 39 (56) | 38 (56) |

Comments (Non-key Muscle? Reason for NT? Pain? Non-SCI condition?):
L1 ppl - unable to tell difference between S & 0 accurately
- reflexive anal contraction & insertion.

(VAC) Voluntary Anal Contraction (Yes/No): NO

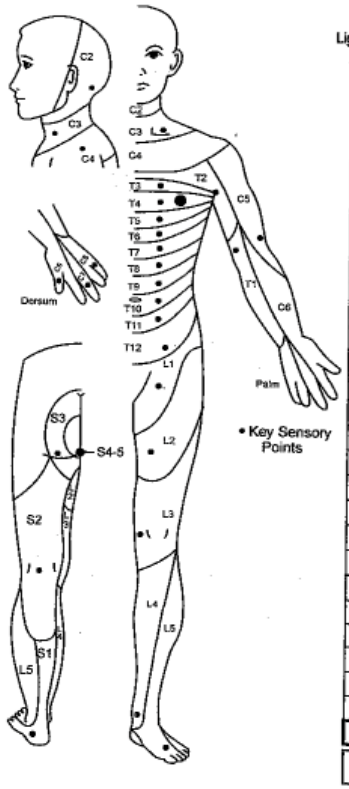


## LEFT

| | SENSORY KEY SENSORY POINTS Light Touch (LTL) | Pin Prick (PPL) | MOTOR KEY MUSCLES | |
|---|---|---|---|---|
| C2 | 2 | 2 | | |
| C3 | 2 | 2 | | |
| C4 | 2 | 2 | | |
| C5 | 2 | 2 | 5 | Elbow flexors |
| C6 | 2 | 2 | 5 | Wrist extensors |
| C7 | 2 | 2 | 5 | Elbow extensors |
| C8 | 2 | 2 | 5 | Finger flexors |
| T1 | 2 | 2 | 5 | Finger abductors (little finger) |
| T2 | 2 | 2 | | |
| T3 | 2 | 2 | | |
| T4 | 2 | 2 | | |
| T5 | 2 | 2 | | |
| T6 | 2 | 2 | | |
| T7 | 2 | 2 | | |
| T8 | 2 | 2 | | |
| T9 | 2 | 2 | | |
| T10 | 2 | 2 | | |
| T11 | 2 | 2 | | |
| T12 | 2 | 2 | | |
| L1 | 0 | 0 | | |
| L2 | 0 | 0 | 0 | Hip flexors |
| L3 | 0 | 0 | 0 | Knee extensors |
| L4 | 0 | 0 | 0 | Ankle dorsiflexors |
| L5 | 0 | 0 | 0 | Long toe extensors |
| S1 | 0 | 0 | 0 | Ankle plantar flexors |
| S2 | 0 | 0 | | |
| S3 | 0 | 0 | | |
| S4-5 | 0 | 0 | | |
| LEFT TOTALS (MAXIMUM) | 38 (56) | 37 (56) | 25 (50) | |

UEL (Upper Extremity Left)

LEL (Lower Extremity Left)

**MOTOR (SCORING ON REVERSE SIDE)**
0 = Total paralysis
1 = Palpable or visible contraction
2 = Active movement, gravity eliminated
3 = Active movement, against gravity
4 = Active movement, against some resistance
5 = Active movement, against full resistance
NT = Not testable
0*, 1*, 2*, 3*, 4*, NT* = Non-SCI condition present

**SENSORY (SCORING ON REVERSE SIDE)**
0 = Absent
1 = Altered
2 = Normal
NT = Not testable
0*, 1*, NT* = Non-SCI condition present

(DAP) Deep Anal Pressure (Yes/No): No

**MOTOR SUBSCORES**
UER 25 (MAX 25) + UEL 25 (25) = UEMS TOTAL 60 (50)
LER 1 (MAX 25) + LEL 0 (25) = LEMS TOTAL 1 (50)

**SENSORY SUBSCORES**
LTR 39 (MAX 56) + LTL 38 (56) = LT TOTAL 77 (112)
PPR 38 (MAX 56) + PPL 37 (56) = PP TOTAL 75 (112)

**NEUROLOGICAL LEVELS** (Steps 1- 6 for classification as on reverse)

| | R | L |
|---|---|---|
| 1. SENSORY | T12 | T11 |
| 2. MOTOR | T12 | T11 |

3. NEUROLOGICAL LEVEL OF INJURY (NLI): T11

4. COMPLETE OR INCOMPLETE? C
Incomplete = Any sensory or motor function in S4-5 (In injuries with absent motor OR sensory function in S4-5 only)

5. ASIA IMPAIRMENT SCALE (AIS): A

6. ZONE OF PARTIAL PRESERVATION (Most caudal levels with any innervation)

| | R | L |
|---|---|---|
| SENSORY | L1 | T12 |
| MOTOR | L2 | T1 |

Page 1/2



REV 04/19

## Appendix D. Supplementary Figures

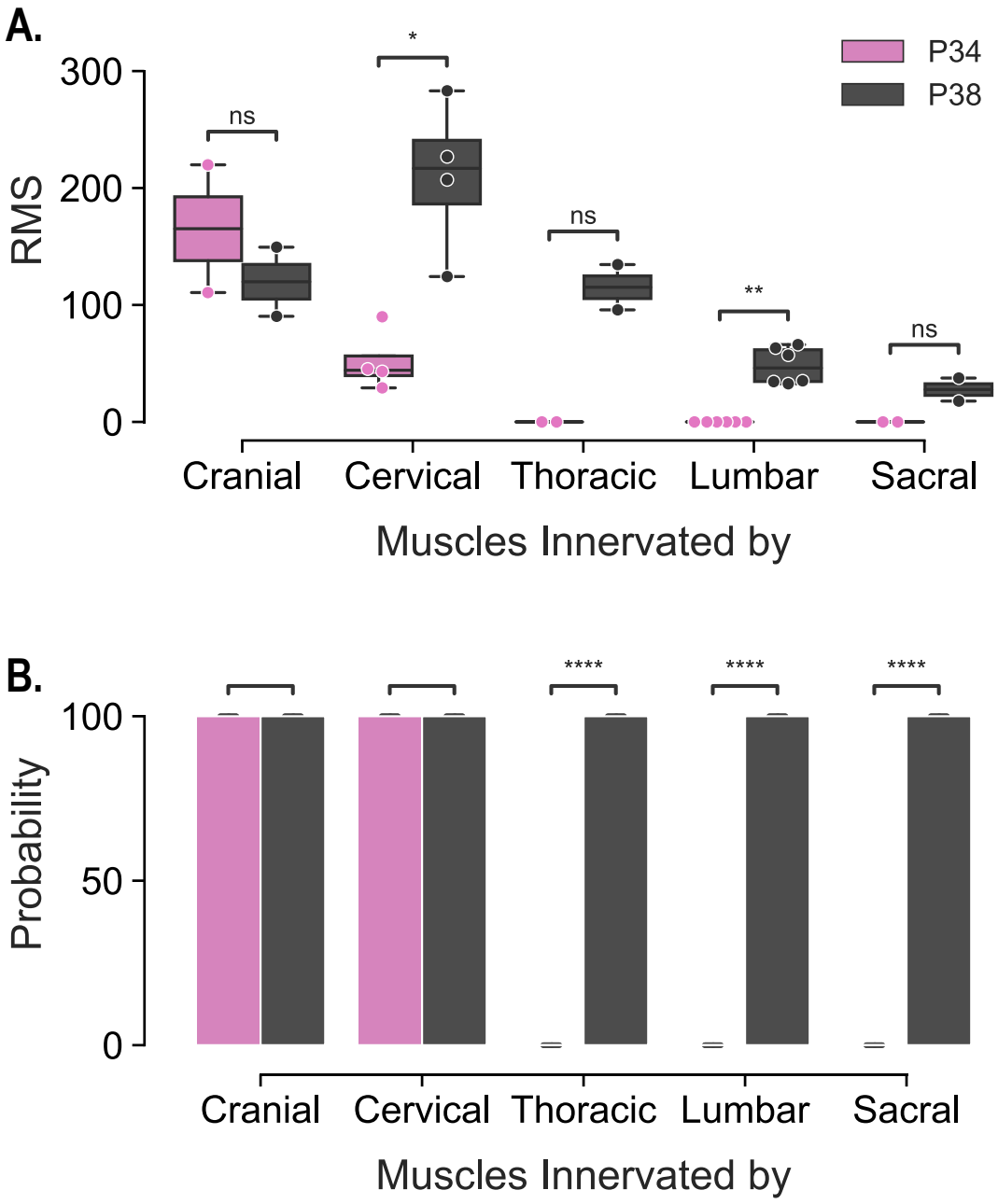


**Figure D-0.1: FNPA results of twin participants.**

**A.** Box plot comparing muscle activation patterns of two fraternal twins enrolled in this study. Muscles were grouped by their innervation source (Cranial = UT; Cervical = BB and TB; Thoracic = RA; Lumbar = ADD, RF, and TA; and Sacral = MG). Pink boxes represent a 6.3 years-old male

with SCI (AIS A, motor level T1). Black boxes denote data from P38, typically developing twin sister of P34, assessed 10 months after her brother. **B.** Bar plot comparing the probabilities of EMG activation of the primary agonist muscle during volitional motor tasks between the SCI and TD group. UT, upper trapezius; BB, biceps brachii; TB, triceps brachii; RA, rectus abdominis; ADD, adductor magnus; RF, rectus femoris; TA, tibialis anterior; and MG, medial gastrocnemius muscles. Boxes bound the interquartile range (IQR) and are transected by a line representing the median. Whiskers extend to 1.5 times the IQR. RMS data were analyzed using independent samples Kruskal–Wallis test for nonparametric data with Benjamini-Hochberg corrections for multiple comparisons. Probability data was analyzed using the Z-test for proportions with Benjamini-Hochberg corrections for multiple comparisons. (* $P < .05$; ** $P < .01$; *** $P < .001$; **** $P < .0001$).

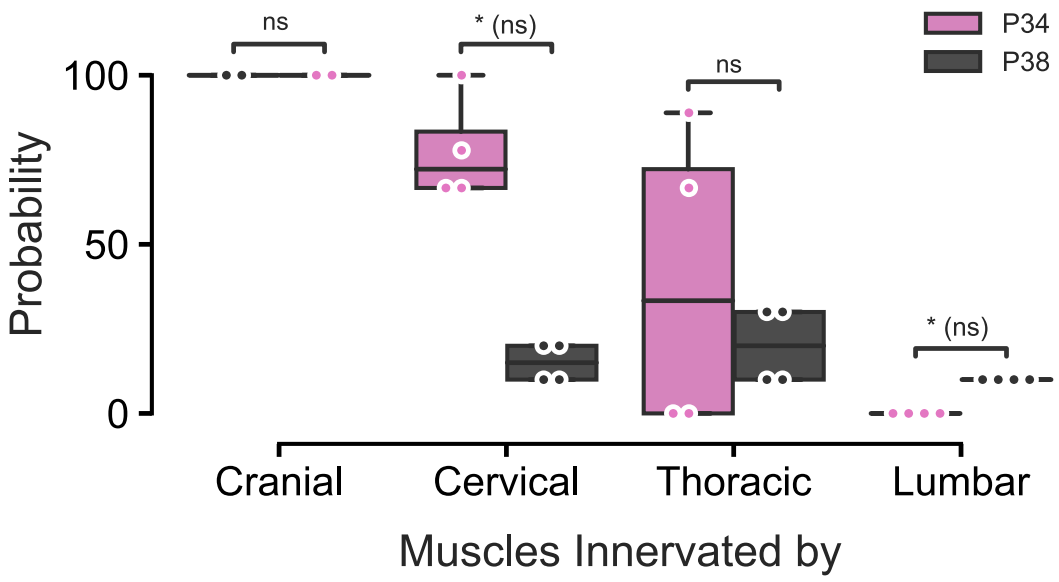


**Figure D-0.2: ASR results for twin participants**

Bar plot comparing ASR probability patterns of the two fraternal twins (*) enrolled in this study. Pink bars represent a 6.3-year-old male with SCI (AIS A, motor level T1). Black bars denote data from P38, typically developing twin sister of P34, assessed 10 months after her brother. OOC, orbicularis oculi; DEL, deltoid; APB, abductor pollicis brevis; PS, paraspinal; RA, rectus abdominis; RF, rectus femoris; TA, tibialis anterior.

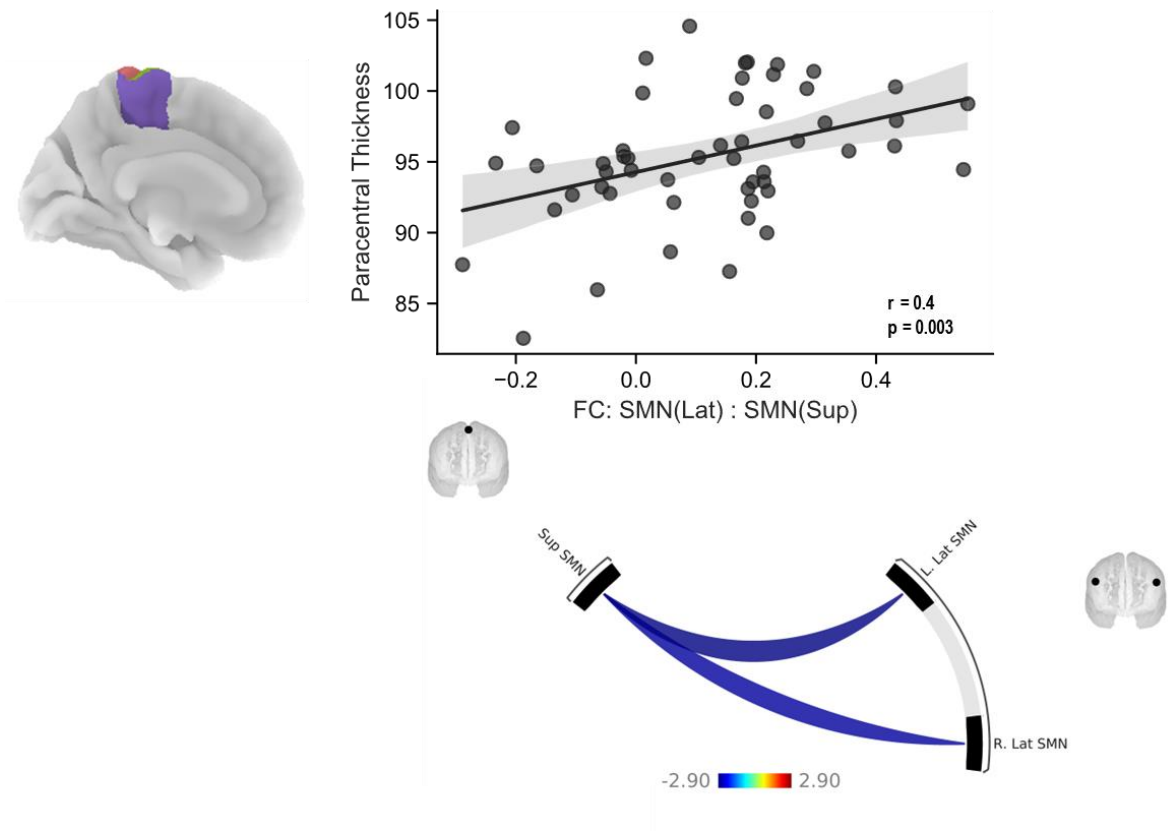


**Figure D-0.3: Normalized Thickness of Paracentral Gyri correlates to SMN FC**

This figure displays the correlation between the normalized thickness of the paracentral gyri and the functional connectivity values of the superior SMN to the lateral SMN. The scatter plot depicts the relationship between the two variables, with each data point representing a single participant. The correlation coefficient (r) and significance level (p) are displayed in the upper right corner of the plot. The positive correlation between the two variables is shown, with higher thickness of the paracentral gyri corresponding to higher functional connectivity values of the superior SMN to the lateral SMN. The results suggest an association between the structural and functional changes in the motor network, which may play a critical role in motor function. Subpanels show the anatomical location of the paracentral gyri (reported in Chapter 3) and the functional connectivity (FC) of the superior SMN to the lateral SMN (reported in Chapter 4).

# CURRICULUM VITAE


# Luis R. Alvarado

☎ +I 714.874.5106
Kentucky Spinal Cord Injury Research Center
220 Abraham Flexner Way, Suite 1500
@ Luis.Alvarado@Louisville.edu


## |EDUCATION

**University of Louisville, School of Medicine** March 2023

- **Ph.D.** in Anatomical Science and Neurobiology
- Dissertation: "Supraspinal Reorganization After Pediatric-Onset Spinal Cord Injury"
- Mentor: Andrea Behrman, Ph.D., PT, FAPTA

**University of Louisville, School of Medicine** December 2017

- **M.S.** in Anatomical Science and Neurobiology

**University of California, Los Angeles** December 2005

- **B.S.** in Neuroscience

## | EXTRAMURAL TRAINING

**Massachusetts Institute of Technology** November 15-18, 2021
**Massachusetts General Hospital**
Martinos Center for Biomedical Imaging
Spinal Cord Workshop

- Learned challenges and techniques specific to human spinal cord MRI imaging.
- Developed an understanding of best practices to avoid pitfalls and failures in spinal cord research.

**Massachusetts Institute of Technology** October 23 -27, 2017
**Massachusetts General Hospital**
Martinos Center for Biomedical Imaging
Structural and Functional Brain Connectivity via MRI and fMRI

- Acquired knowledge of technical aspects involved in brain network visualization using functional MRI data.

- Gained expertise in diffusion-sensitive MRI for anatomical structure analysis of white matter tracts.

## | RESEARCH EXPERIENCE

Research Graduate Fellow 2015-2023
**University of Louisville, School of Medicine**
Anatomical Science and Neurobiology Department
Kentucky Spinal Cord Injury Research Center
Kosair Center for Pediatric NeuroRecovery

Investigated the supraspinal neural changes in children with spinal cord injury (SCI) using multimodal electrophysiology and neuroimaging techniques to elucidate the effects of SCI on the brain and motor pathways activity.

Principal Investigator: Andrea Behrman, Ph.D., P.T., FAPTA

Research Technologist II 2015
**University of Louisville, School of Medicine**
Kentucky Spinal Cord Injury Research Center
Kosair Center for Pediatric NeuroRecovery

Research technologist for multiple research projects focusing on developing and testing therapeutic interventions promoting recovery after spinal cord injury in children.

Principal Investigator: Andrea Behrman, Ph.D., P.T., FAPTA

Research Study Coordinator 2014-2015
**Northwestern University, Feinberg School of Medicine**
Department of Medical Social Sciences
Biobehavioral Mechanisms and Health Outcomes Lab

Research coordinator for a study focusing on the impact of cancer-related stress on the psychological and physiological health of colorectal cancer patients and their caregivers.

Principal Investigator: Frank J. Penedo, Ph.D.

HCOE Research Fellow 2010-2011
**University of Illinois at Chicago, College of Medicine**
Hispanic Center of Excellence
Epidemiology and Biostatistics

Research intern for a study focusing on the Hispanic longevity paradox.

Principal Investigator: S. Jay Olshansky, Ph.D.

Research Associate 2006-2008
**Children's Hospital of Orange County**
Hemostasis and Thrombosis Research Laboratory

Research associate for various studies focusing on congenital factor XIII deficiency and the pharmacology and safety of recombinant Factor XIII replacement therapy.

Principal Investigator: Diane Nugent, M.D.

Student Research Assistant 2002-2005
**University of California, Los Angeles**
Brain Research Institute
Human Locomotion Research Center

Research assistant for a study focusing on the human musculoskeletal and neural responses to locomotor training after spinal cord injury.

Principal Investigator: Susan J. Harkema, Ph.D.

## | ABSTRACTS and PRESENTATIONS

A.L. Behrman, G. Singh, K. Lucas, **L.R. Alvarado**; "Walking Recovery after Pediatric SCI." *Oral presentation as part of the Kentucky Spinal Cord Injury Research Center Seminar Series. Louisville, Kentucky; March 2023*

**L.R. Alvarado**; "Supraspinal reorganization after pediatric spinal cord injury: A case report." *Oral presentation as part of the Kentucky Spinal Cord Injury Research Center Seminar Series. Louisville, Kentucky; July 2021*

**L.R. Alvarado**; " Pediatric SCI Research in the times of Corona." *Oral presentation as part of the Kentucky Spinal Cord Injury Research Center Seminar Series. Louisville, Kentucky; September 2020*

**L.R. Alvarado**; " Supraspinal Changes after Pediatric SCI." *Oral presentation as part of the Kentucky Spinal Cord Injury Research Center Seminar Series. Louisville, Kentucky; July 2019*

**L.R. Alvarado**, A.L. Behrman, B.E. Depue; "Differences in Resting-State Functional Connectivity between Low and High Levels of Physical Activity in Healthy School-Aged Children." Program No 571.08 / H22. 2019 Neuroscience Meeting Planner. *Poster presented at the annual meeting of the Society for Neuroscience. Chicago, Illinois; October 2019*

A.L. Behrman, S.A. Trimble, **L. Alvarado**, D. Atkinson; "Task-dependent recruitment of spinal motor pools after pediatric spinal cord injury." Program No 158.09/RR16. 2016 Neuroscience Meeting Planner. *Poster presented at the annual meeting of the Society for Neuroscience. San Diego, California; November 2016.*

**Alvarado LR**, Lovejoy AE, Nakagawa P, Hsieh LB, Chediak J, Williams SA, Nugent DJ; "A Novel Mutation in Exon 10 of Factor XIII Subunit B." J Thromb Haemost 2007; 5 Supplement 2: P-T-043. *Poster presented at the XXIst Congress of the International Society on Thrombosis and Haemostasis. Geneva, Switzerland; July 2007.*

**Alvarado LR**, Nakagawa P, Hsieh LB, Nugent DJ; "Factor XIII Pharmacokinetics." J Thromb Haemost 2007; 5 Supplement 2: P-T-044. *Poster presented at the XXIst Congress of the International Society on Thrombosis and Haemostasis. Geneva, Switzerland; July 2007.*

**Alvarado LR**, Timmins JE, Beres-Jones JA, Ferreira CK, Harkema SJ; "Activity Dependent Plasticity after Human Spinal Cord Injury: Locomotor Training Interventions Positively Alter the Pattern of Bone Mineral Density Loss after Spinal Cord Injury." *Poster presented at the UCLA Neuroscience Poster Day. Los Angeles, California; May 2005.*

## |PUBLICATIONS

Avecillas-Chasin JM, Gomez G, Jorquera M, **Alvarado LR**, Barcia JA; "Delayed posterior reversible encephalopathy syndrome (PRES) after posterior fossa surgery." *Acta Neurochir (Wien). 2013 Jun;155(6):1045-7.*

## |UNIVERSITY and PUBLIC SERVICE

**Society for Neuroscience, Louisville** Spring 2018, 2019, and 2020*
Kentucky Science Center
Brain Days: Coordinator

- Coordinated annual events aimed at educating the public on the brain and neuroscience through interactive exhibits, talks by experts, and hands-on activities.
- Managed logistics, recruited volunteers, and coordinated with other organizations and sponsors.
- Promoted the event and engaged with attendees to ensure their needs were met.
- Successfully attracted thousands of children and their families to the events.
- * Completed the organization works for 2020 before cancellation due to COVID-19.

**Society for Neuroscience, Louisville** Spring 2019 and 2020*
University of Louisville
Neuroscience Day: Coordinator

- Organized a symposium focused on the dissemination of the latest developments and research from the local neuroscience community.
- Recruited speakers, managed logistics, and coordinated with vendors.
- Collaborated with other organizers and engaged with attendees to ensure their needs were met.
- * Completed the organization works for 2020 before cancellation due to COVID-19.

**University of Louisville, School of Medicine** Spring 2016 to 2019
Anatomical Science and Neurobiology
Interview Day: Student Liaison

- Served as a point of contact for prospective students interested in applying to the department's graduate programs.
- Organized and led campus tours, answered questions about the programs and application process, and helped coordinate interviews with faculty and staff.

**Advocate Illinois Masonic Medical Center** Fall 2010 and 2011
HispanoCare
Health Fairs: Coordinator

- Organized events that provided free primary care screenings to members of the Hispanic community in Chicago.
- Cultivated partnerships with healthcare providers, community organizations, and local businesses to promote the event and provide services to attendees.
- Managed logistics, recruited volunteers, and ensured the event ran smoothly.
- Coordinated fundraising efforts, including soliciting donations from local businesses and individuals, while developing and managing fundraising events.

**University of Illinois at Chicago, College of Medicine** Fall 2010 and 2011
Student National Medical Association
Pre-Medical Student Forum: Organizer

- Coordinated a workshop aimed at providing guidance and support to pre-medical students from underrepresented backgrounds.
- Recruited speakers, managed logistics, and coordinated with vendors.
- Collaborated with other organizers and engaged with attendees to ensure their needs were met.

**University of Illinois at Chicago, College of Medicine** Spring 2010 and 2011
Latino Medical Student Association -LaRaMA
Benito Juarez High School Health Fair: Organizer

- Organized and led an event that provided health education and services to students at a local high school.
- Cultivated partnerships with healthcare providers, community organizations, and local businesses to promote the event and provide services to attendees.
- Managed logistics, recruited volunteers, and ensured the event ran smoothly.
- Coordinated fundraising efforts, including soliciting donations from local businesses and individuals, while developing and managing fundraising events.

## | TEACHING and MENTORSHIP EXPERIENCE

**Galen College of Nursing** 2018-Present
Department of Arts and Sciences
Adjunct Faculty

- Teach Human Anatomy and Physiology to a diverse population of nursing students.
- Create an inclusive learning environment that supports students of all backgrounds and experiences.
- Develop and deliver engaging lectures, create and grade assignments and exams, and provide feedback and support to students.
- Collaborate with other faculty members to ensure consistent course content and student learning outcomes.

**Louisville Regional Science & Engineering Fair** 2020
Mentor

- Mentored a local middle school student on her science fair project titled "Exploring Neurotoxin Shed in Child Products."
- Fostered her curiosity and passion for science by encouraging her to ask questions, explore new ideas, and develop her critical thinking skills.
- Provided mentorship and support to develop the skills to analyze and interpret results, encouraging her interest in neuroscience.
- Her project earned 2nd place statewide and a Broadcom MASTERS Nomination, which allowed her to apply for the national science fair.

**Bellarmine University** 2019-2020
Department of Biology
Adjunct Faculty

- Taught Human Anatomy and Physiology to a diverse population of undergraduate students.

- Created an inclusive learning environment that supported students of all backgrounds and experiences.
- Developed and delivered engaging lectures, created and graded assignments and exams, and provided feedback and support to students.
- Collaborated with other faculty members to ensure course content was culturally responsive and relevant to diverse student populations.

University of Louisville, School of Medicine 2015-2016
Anatomical Science and Neurobiology
Teaching Assistant

- Assisted in teaching Fundamentals of Neuroscience and Medical Neuroanatomy to graduate students at the University of Louisville School of Medicine.
- Worked to create an inclusive learning environment that supported students of all backgrounds and experiences.
- Helped develop course materials, conducted review sessions, and provided one-on-one support to students.

Chicago City Colleges
General Educational Development (GED) Program 2014
Adult Education Instructor

- Taught Mathematics and Science to a diverse population of adult learners.
- Created an inclusive learning environment that supported students of all backgrounds and experiences.
- Worked to develop culturally responsive teaching practices and materials to meet the needs of diverse student populations.
- Developed lesson plans and materials, delivered engaging instruction, and provided individualized support to students.

University of Illinois at Chicago, College of Medicine 2010-2011
Post-Baccalaureate Admission Program
Teaching Assistant

- Assisted in teaching Gross Anatomy and Embryology to a diverse population of post-baccalaureate students in the College of Medicine at the University of Illinois at Chicago.
- Worked to create an inclusive learning environment that supported students of all backgrounds and experiences.
- Helped develop course materials, conducted review sessions, and provided one-on-one support to students.
- Graded assignments and exams and provided feedback to students and faculty.

University of Illinois at Chicago, College of Medicine 2010-2011
Latino Medical Student Association Medical Spanish Course
Peer Educator

- Assisted in teaching Medical Spanish to medical students at the University of Illinois at Chicago.
- Created an inclusive learning environment that supported students of all backgrounds and experiences.
- Developed lesson plans and materials, facilitated group discussions and activities, and provided individualized support to students.

## |PROFESSIONAL MEMBERSHIPS

| | |
|---|---|
| Society for Neuroscience (SfN) | 2015-Present |
| SfN, Louisville Chapter | 2015-Present |
| American Association for the Advancement of Science | 2016-Present |
| The Academy of Spinal Cord Injury Professionals | 2016-Present |
| International Society for Magnetic Resonance in Medicine | 2016-Present |
| UofL Science Policy and Outreach Group | 2015-2020 |

## |HONORS and AWARDS

| | |
|---|---|
| Todd Crawford Foundation Scholar | 2017, 2018 |
| UofL Health Science Center Office of Diversity Travel Award | 2017 |
| UofL Integrated Program in Biomedical Sciences Travel Award | 2017 |
| Hispanic Scholarship Fund Scholar | 1998-2001, 2016 |
| Illinois General Assembly Scholar - 26th district | 2010-2012 |
| HispanoCare Scholar | 2010 |
| UIC-COM Hispanic Center for Excellence Fellow | 2010 |